CENTER ARMAND-FRAPPIER HEALTH BIOTECHNOLOGY

SYNTHESIS OF POTENTIAL INHIBITORS AND SIDEROPHORE CONJUGATES OF KDO-PROCESSING ENZYMES

By

Gokulakrishnan Ravicoularamin

A THESIS
SUBMITTED TO THE FACULTY OF
GRADUATE STUDIES
IN PARTIAL FULFILMENT OF THE
REQUIREMENTS FOR THE
DEGREE OF MASTER OF SCIENCE

GRADUATE PROGRAM IN EXPERIMENTAL
HEALTH SCIENCES

LAVAL, QUEBEC

DECEMBER 2019

INRS
Institut national de la recherche scientifique

Acknowledgements

My immense gratitude goes towards my supervisor Prof. Charles Gauthier for the opportunity to work in his lab and to be part of his research group. I thank him whole heartedly for his guidance, patience and knowledge input during the course of the master's. It would not be an exaggeration to state that I learnt stellar number of things starting right from the scratch.

I would like to acknowledge all my fellow lab mates with whom I have worked over the last two years. Some names in particular: Oscar, Eric, Kevin, Maude, Emmanilo, Shawn, Paul, Gayetri and Seynabou. I am grateful for all their help, support and cooperation as well as for sustaining a healthy research environment. I would like to thank Prof. Annie Castonguay and Dr Janelle Sauvageau for accepting to be the jury members. I would also like to thank Marie-Christine Groleau of lab of Prof. Eric Deziel for her guidance and involvement in the collaboration work. I am also grateful to the funding bodies – RQRM and NSERC – for providing me with the opportunity to carry out my masters and stay in Canada. Finally, I thank all the people who were directly or indirectly involved in helping me.

Abstract

There is an important need for new types of antibacterial agents in present days because of the increased resistance of pathogenic bacteria. Inhibiting enzymes involved in the biosynthesis of polysaccharides from Gram-negative bacteria (GNB), such as lipopolysaccharides (LPS) and exopolysaccharides (EPS), stands as an underexploited approach to pursue. Such inhibition could ultimately lead to damaging of the outer membrane of GNB, which would pave the way for the development of broad spectrum-antibiotics, as LPS is a major structural backbone of outer membrane as well as a virulence factor. Cytidine monophosphate 3-deoxy-D-*manno*-oct-2-ulosonic acid (CMP-Kdo) synthase (CKS) is a crucial enzyme for LPS biosynthesis as it catalyses the rate-determining step for the formation of lipid A-Kdo_2, which is responsible of membrane integrity. In order to tackle the obstacle of bacterial membrane diffusion, the "Trojan horse" strategy of covalently linking iron(III)-chelating siderophore to the LPS inhibitor has been pursued. Since iron is crucial for the metabolism of GNB, we have hypothesized that the "Trojan horse" strategy will enhance the delivery of inhibitors of Kdo-processing enzymes across the bacterial membranes. Kdo residues are also found in the EPS of *Burkholderia* spp., which is an important component of bacterial biofilm and is involved in the pathogenesis of *Burkholderia*-related infections.

Therefore, the objectives of the research project are: 1) to synthesize Kdo mimics that could act as potential inhibitors of Kdo-processing enzymes involved in the biosynthesis of Kdo-containing LPS and EPS from pathogenic GNB; and 2) to couple the former set of inhibitors with siderophores bearing either releasable or non-releasable linkers, leading to siderophore conjugates. The releasable linker will ensure the enzymatic cleavage of conjugates releasing the inhibitor in its free form within the cytoplasm for improved binding affinity with the cytoplasmic target. 2-Deoxy and 8-amino-2,8-deoxy Kdo derivatives were synthesized *via* two different routes starting from D-mannose and D-arabinose. While the former was synthesized in both α- and β-forms, the latter was designed to deliver exclusively the β-form. Compounds were also prepared under their acetylated forms in order to improve their penetration to the cytoplasm owing to bacterial esterases. The commercially available xenosiderophore desferrioxamine B will subsequently be covalently linked to Kdo derivatives through a

synthetic releasable linker, consisting of disulphide bond that could be cleaved under the reducing conditions of cytoplasm.

Kdo glycosides in both α- and β-anomeric forms were synthesized through multi-step synthesis starting from D-arabinose. As a preliminary assay, Kdo derivatives were evaluated for their ability to inhibit the formation of EPS from *Burkholderia* spp. in collaboration with the group of Prof. Éric Déziel from INRS-Institut Armand-Frappier. We showed that 2-adamantane glycosides of Kdo are able to prevent the formation of mucoid bacteria and that only the β-forms are active. In order to quantify the inhibition, 8-d-azido-Kdo were prepared and will be used to label the EPS of bacteria through strain-promoted alkyne-azide cycloaddition with a dibenzylcyclooctyne derivative covalently linked to a fluorescent dye. Another Kdo analogue, 7-d-azido-Kdo was also synthesized through a synthetic pathway starting from L-xylose for similar purpose.

The siderophore conjugates will be tested for their *in vitro* antibacterial activity against several GNB, including *Burkholderia cepacia* complex species and *Pseudomonas aeruginosa.* Ultimately, the research project could generate novel sugar-based chemical entities, which could be used as antibiotic agents or antibiotic adjuvants against pathogenic GNB.

Abstract (in French)

Un besoin important de nouveaux types d'agents antibactériens peut être identifié de nos jours en raison de la résistance accrue des bactéries pathogènes. L'inhibition des enzymes impliquées dans la biosynthèse des polysaccharides des bactéries à Gram négatif (BGN), comme les lipopolysaccharides (LPS) et les exopolysaccharides (EPS), constitue une approche sous-exploitée à approfondir. Une telle inhibition pourrait finalement endommager la membrane externe du GNB, ce qui ouvrirait la voie au développement d'antibiotiques à large spectre car le LPS est un squelette structurel majeur de la membrane externe ainsi qu'un facteur de virulence. Cytidine monophospate 3-désoxy-D-*manno*-oct-2-ulosonique (CMP-Kdo) synthase (CKS) est une enzyme cruciale pour la biosynthèse du LPS, du fait qu'elle catalyse l'étape de détermination du taux de formation du lipide A-Kdo_2, qui est responsable de l'intégrité de la membrane. Afin de surmonter l'obstacle de la diffusion de la membrane bactérienne, la stratégie du « cheval de Troie », consistant à lier de manière covalente un sidérophore chélatant de fer (III) à l'inhibiteur de LPS, a été poursuivie. Étant donné que le fer est crucial pour le métabolisme du BGN, nous avons émis l'hypothèse que la stratégie du « cheval de Troie » améliorera la distribution d'inhibiteurs des enzymes de traitement du Kdo à travers les membranes bactériennes. Des résidus de Kdo sont également trouvés dans l'EPS de *Burkholderia* spp., Il s'agit d'un composant important du biofilm bactérien, impliqué dans la pathogenèse des infections liées à *Burkholderia*.

Par conséquent, les objectifs du projet de recherche sont les suivants : 1) synthétiser des analogues de Kdo qui pourraient agir comme inhibiteurs potentiels des enzymes de traitement de Kdo impliquées dans la biosynthèse de LPS et EPS contenant du Kdo dans les BGN pathogènes; et 2) coupler ces inhibiteurs avec des sidérophores portant des lieurs libérables ou non libérables, conduisant à des conjugués sidérophores. Le lieur libérable assurera le clivage enzymatique des conjugués libérant l'inhibiteur sous sa forme libre dans le cytoplasme pour améliorer son affinité avec la cible cytoplasmique. Les dérivés 2-désoxy et 8-amino-2,8-désoxy Kdo ont été synthétisés par deux voies différentes à partir du D-mannose et du D-arabinose. Alors que le premier a été synthétisé sous les formes α- et β-, le deuxième a été conçu pour obtenir exclusivement la forme β. Des composés ont également été préparés sous leurs formes acétylées afin d'améliorer leur pénétration dans le cytoplasme grâce aux

estérases bactériennes. Le xénosidérophore desferrioxamine B disponible dans le commerce sera ensuite lié de manière covalente aux dérivés de Kdo par le biais d'un lieur synthétique libérable, constitué d'une liaison disulfure qui pourrait être clivée dans les conditions réductrices du cytoplasme.

Les Kdo glycosides sous les formes anomères α- et β- ont été synthétisés par synthèse en plusieurs étapes à partir du D-arabinose. À titre d'essai préliminaire, les dérivés de Kdo ont été évalués pour leur capacité à inhiber la formation d'EPS dans *Burkholderia* spp. En collaboration avec le laboratoire du Prof. Éric Déziel de l'INRS-Institut Armand-Frappier, nous avons montré que les glycosides 2-adamantane de Kdo sont capables d'empêcher la formation de bactéries mucoïdes et que seules les formes β sont actives. Afin de quantifier l'inhibition, le 8-d-azido-Kdo a été préparé et sera utilisé pour marquer l'EPS des bactéries par cycloaddition d'alcyne-azoture favorisée par une souche avec un dérivé de dibenzylcyclooctyne lié de manière covalente à un colorant fluorescent. Un autre analogue de Kdo, le 7-d-azido-Kdo a également été synthétisé par une voie de synthèse à partir du L-xylose dans un but similaire.

Les conjugués de sidérophore seront testés pour leur activité antibactérienne in vitro contre plusieurs BGN, y compris les espèces du complexe *Burkholderia cepacia* et *Pseudomonas aeruginosa.* En fin de compte, le projet de recherche pourrait générer de nouvelles entités chimiques à base de sucre, qui pourraient être utilisées comme agents antibiotiques ou adjuvants antibiotiques contre les BGN pathogènes.

Table of Contents

1. Introduction 1
1.1. Bacteria and brief history of antibiotics 1
1.2. Antimicrobial resistance crisis and superbugs 3
1.3. Gram-negative and Gram-positive bacteria 5
1.4. Membrane of GNB 6
1.5. Lipopolysaccharide (LPS) of GNB 8
1.5.1. *O*-Antigen 9
1.5.2. Core oligosaccharides 10
1.5.3. Lipid A 11
1.5.4. 3-Deoxy-D-*manno*-oct-2-ulosonic acid (Kdo) 12
1.5.5. LPS biosynthesis 15
1.5.6. Biosynthetic pathway of Kdo 16
1.6. CKS inhibitors 17
1.7. Siderophores 19
1.7.1. Transportation of iron-siderophore complex across bacterial membrane 21
1.8. 'Trojan-horse strategy' for delivering drug across bacterial membrane 23
1.8.1. Criteria for siderophore 24
1.8.2. Criteria for linker 26
1.9. Peracetylated Kdo to overcome the membrane diffusion barrier 27
1.10. Kdo EPS 28
1.10.1. Kdo glycosides - as potential inhibitor of Kdo-EPS processing enzymes 30
1.11. Glycan labelling 31
1.11.1. Click-mediated glycan labelling for Kdo EPS visualization 32
1.12. Hypothesis and objectives 34
2. Results and discussion 37
2.1. Synthesis of CKS inhibitors 37
2.1.1. Retrosynthetic analysis 37
2.1.2. Synthesis of 2,8-d-NH_2-Kdo from D-arabinose 38
2.1.3. Synthesis of 2,8-d-NH_2-Kdo from D-mannose 45
2.1.4. Comparison of overall yield of the two synthetic routes 53
2.1.5. Peracetylated derivatives of 2-d-Kdo 54
2.2. Synthesis of Kdo glycosides 55

2.2.1. Synthesis of Kdo thioglycosyl donor **39** 55
2.2.2. Glycosylation step 56
2.2.3 Deprotection of the Kdo glycosides 57
2.3. Synthesis of azido-Kdo 58
2.3.1. Retrosynthetic analysis 59
2.3.2. Synthesis of 8-d-N_3-Kdo 59
2.3.3. Synthesis of 7-d-N_3-Kdo 61
2.4. Synthesis of siderophore conjugates (*work in progress*) 65
2.4.1. Retrosynthetic analysis 65
2.4.2. Synthesis of potential linkers 66
2.4.3. Assembly of DFO-Kdo conjugates 67
3. Conclusion and Perspectives 70
4. Experimental Procedures 72
4.1. General methods 72
4.2. General Procedures 72
4.2.1. For peracetylation 72
4.2.2. For glycosylation 73
4.2.3. For hydrogenolysis of benzyl ester 73
4.2.4. For Zemplén deprotection 73
4.3. Synthetic procedures 74
4.3.1. Ammonium 3-deoxy-D-*manno*-oct-2-ulopyranosylonate (2) 74
4.3.2. Methyl 3-deoxy-4,5:7,8-di-*O*-isopylidene-α-D-*manno*-oct-2-ulopyranosylonate (4) 74
4.3.3. Methyl 3-deoxy-4,5:7,8-di-*O*-isopropylidene-D-*manno*-oct-2-enosonate (5) 75
4.3.4 Methyl 2,3-dideoxy-4,5:7,8-di-O-isopylidene-α-D-*manno*-oct-2-ulopyranosonate (6) 76
4.3.5. Methyl 2,3-dideoxy-4,5:7,8-di-*O*-isopylidene-β-D-*manno*-oct-2-ulopyranosonate (7) 77
4.3.6. Methyl 2,3-dideoxy-4,5-*O*-isopropylidene-β-D-*manno*-oct-2-ulosonate (9) 77
4.3.7. Methyl 2,3-dideoxy-8-*O*-*p*-toluenesulfonyl-4,5-*O*-isopropylidene-β-D-*manno*-oct-2-ulosonate (10) 78
4.3.8. Methyl 2,3,8-trideoxy-8-azido-4,5-*O*-isopropylidene-β-D-*manno*-oct-2-ulosonate (11) 79
4.3.9. 1,2;5,6-di-*O*-isopropylidine-D-mannofuranoside (14) 79
4.3.10. (Carbethoxymethylene)triphenylphosphorane (15) 80

4.3.11. Ethyl (4*R*,5*S*,6*R*,7*R*)-6-hydroxy-4,5:7,8-di-*O*-isopropylidene-oct-2-enoate (16) ..80

4.3.12. Ethyl (4*R*,5*S*,6*R*,7*R*)-6-[(*tert*-butyldimethylsilyl)oxy]-4,5:7,8-di-*O*-isopropylidene-oct-2-enoate (17) 81

4.3.13. Ethyl (4*R*,5*S*,6*R*,7*R*)-6-[(*tert*-butyldimethylsilyl)oxy]-4,5:7,8-di-*O*-isopropylidene-octonate (18) 81

4.3.14. Ethyl (4*R*,5*S*,6*R*,7*R*)-6-hydroxy-4,5:7,8-di-*O*-isopropylidene-octonoate (19)..... 82

4.3.15. Ethyl (4*R*,5*S*,6*R*,7*R*)-6-[trimethylsilyl)oxy]-4,5:7,8-di-*O*-isopropylidene-octonate (20) 83

4.3.16. Ethyl (4*R*,5*S*,6*R*,7*R*)-2-bromo-6-[trimethylsilyl)oxy]-4,5:7,8-di-*O*-isopropylidene-octonate (21) 83

4.3.17. Ethyl 2,3-dideoxy-4,5:7,8-di-*O*-isopropylidene-α,β-D-*manno*-oct-2-ulopyranosonate (22) 84

4.3.18. Ethyl 2,3-dideoxy-4,5-*O*-isopropylidene-β-D-*manno*-oct-2-ulopyranosonate (23) 84

4.3.19. Ethyl 2,3-dideoxy-8-*O*-*p*-toluenesulfonate-4,5-*O*-isopropylidene-β-D-*manno*-oct-2-ulopyranosonate (24) 85

4.3.20. Ethyl 2,3,8-trideoxy-8-azido-4,5-*O*-isopropylidene-β-D-*manno*-oct-2-ulopyranosonate (25) 86

4.3.21. Ethyl 2,3,8-trideoxy-8-azido-β-D-*manno*-oct-2-ulopyranosonate (26) 87

4.3.22. Ethyl 2,3,8-trideoxy-8-amino-β-D-*manno*-oct-2-ulopyranosonate (27)..... 87

4.3.23. 2,3,8-trideoxy-8-amino-β-D-*manno*-oct-2-ulopyranosonic acid (28)..... 88

4.3.24. Methyl 2,8-Dideoxy-8-amino-β-D-*manno*-oct-2-ulopyranosonate (29)..... 88

4.3.25. Ethyl 2,8-Dideoxy-8-amino-β-D-*manno*-oct-2-ulopyranosonate (30) 89

4.3.26. Methyl 4,5,7,8-tetra-*O*-acetyl-2,3-dideoxy-β-D-*manno*-oct-2-ulopyranosonate (31) 89

4.3.27. Ethyl 4,5,7,8-tetra-*O*-acetyl-2,3-dideoxy-β-D-*manno*-oct-2-ulopyranosonate (32) 90

4.3.28. 2,3-dideoxy-β-D-*manno*-oct-2-ulopyranosonic acid (33) 90

4.3.29. Ammonium 2,4,5,7,8-penta-*O*-acetyl-3-deoxy-α-D-*manno*-oct-2-ulopyranosylonate (37) 91

4.3.30. Benzyl 2,4,5,7,8-Penta-*O*-acetyl-3-deoxy-α-D-*manno*-oct-2-ulopyranosonate (38) 91

4.3.31. Benzyl (Ethyl 4,5,7,8-tetra-O-acetyl-3-deoxy-2-thio-α,β-D-*manno*-oct-2-ulopyranosid)onate (39) 92

4.3.32. Benzyl [2-(2'-Adamantyl) 4,5,7,8-tetra-*O*-acetyl-3-deoxy-α,β-D-*manno*-oct-2-ulopyranosid]onate (40) 93

4.3.33. Benzyl [2-(1'-Adamantanemethyl) 4,5,7,8-tetra-*O*-acetyl-3-deoxy-β-D-*manno*-oct-2-ulopyranosid]onate (41) 93
4.3.34. Benzyl [2-(1'-Adamantaneethyl) 4,5,7,8-Tetra-O-acetyl-3-deoxy-β-D-*manno*-oct-2-ulopyranosid]onate (42) 94
4.3.35. 2-(2'-Adamantyl) (4,5,7,8-tetra-*O*-acetyl-3-deoxy-β-D-*manno*-oct-2-ulopyranosid)onic acid (46) 95
4.3.36. 2-(1'-Adamantanemethyl) (4,5,7,8-tetra-*O*-acetyl-3-deoxy-β-D-*manno*-oct-2-ulopyranosid)onic Acid (47) 95
4.3.37. 2-(1'-Adamantaneethyl) (4,5,7,8-Tetra-*O*-acetyl-3-deoxy-β-D-manno-oct-2-ulopyranosid)onic acid (48) 96
4.3.38. 2-(2'-Adamantyl) (3-deoxy-β-D-*manno*-oct-2-ulopyranosid)onic acid (49) 97
4.3.39. 2-(1'-Adamantanemethyl) (3-Deoxy-β-D-*manno*-oct-2-ulopyranosid)onic Acid (50) 97
4.3.40. 2-(2'-Adamantaneethyl) (3-Deoxy-β-D-manno-oct-2-ulopyranosid)onic Acid (51) 98
4.3.41. Ammonium 8-Azido-3,8-dideoxy-D-*manno*-oct-2-ulopyranosylonate (58) 98
4.3.42. Methyl-α,β-L-xylopyranoside (60) 99
4.3.43. Methyl 4-*O*-*p*-toluenesulfonyl-α-L-xylopyranoside (61) 100
4.3.44. Methyl 2,3-di-*O*-benzoyl-4-*O*-*P*-toluenesulfonyl-α,β-L-xylopyranoside (62) 100
4.3.45. Methyl 4-azido-2,3-di-*O*-benzoyl-4-deoxy-α,β-D-arabinopyranoside (63) 101
4.3.46. Methyl 4-azido-4-deoxy-α-D-arabinopyranoside (64) 102
4.3.47. Methyl 4-azido-2,3-di-*O*-acetyl-4-deoxy-α,β-D-arabinopyranoside (65) 102
4.3.48. 4-Azido-4-deoxy-α,β-D-arabinopyranose (66) 103
4.3.49. Ammonium 7-Azido-3,8-dideoxy-D-*manno*-oct-2-ulopyranosylonate (67) 103
4.3.50. Disulfide-*N*,*N*'-disuccinimidyl-ethane-carbonate (72) 104
5. References 171

List of Figures

Figure 1. Structure of Penicillin. 2
Figure 2. Timeline of the antibacterial evolution 3
Figure 3. Image adapted from: Review on antimicrobial resistance, 2016. 4
Figure 4. WHO priority pathogens list. Source: WHO, 2017. 5
Figure 5. Representation of membrane of GNB. Image adapted from: www.dreamstime.com. 6
Figure 6. Structural comparison between GNB and GPB. Image adapted from www.technologynetworks.com 7
Figure 7. Chemical representation of lipopolysaccharide of *S. typhimurium* LT2.[20] 9
Figure 8. Structure of lipid A-Kdo_2 12
Figure 9. Sialic acid structures 14
Figure 10. Chemical structure of Kdo (Fischer projection and chair form). 15
Figure 11. Biosynthetic pathway of Lipid A-Kdo_2 as part of LPS biosynthesis 16
Figure 12. Structure of CMP-Kdo and some of the known inhibitors of CKS with their relative stability 18
Figure 13. Simple representation of role of siderophore. 20
Figure 14. Schematic representation of Fe(III)-siderophore complex across bacterial OM. Scheme adopted from[61] 23
Figure 15. Desferrioxamine B (DFOB) - xenosiderophore 26
Figure 16. Structure of Kdo EPS. 28
Figure 17. *B. pseudomallei* that cause melioidosis are found in the soils of tropical countries such as Vietnam, Thailand. 29
Figure 18. Click-mediated live labelling using 8-d-N_3-Kdo.[13] 32
Figure 19. The targeted Kdo analogues that serve as inhibitors of CKS, along with the peracetylated analogues. 37
Figure 20. Retrosynthetic pathway for the synthesis of 2,8-d-NH_2-Kdo. 38
Figure 21. Global yield comparison for the synthesis of 2-d-β-Kdo residue starting from D-mannose or D-arabinose. 53
Figure 22. Kdo glycosides with adamantane derivatives. 55
Figure 23. Structures of 8-d-N_3-Kdo and 7-d-N_3-Kdo. 58
Figure 24. Retrosynthetic pathway for the synthesis of N_3-Kdo. 59
Figure 25. Click-labelling of *M. xanthus* in presence of 8-d-N_3-Kdo 63
Figure 26. Kdo-tetrazine residue 64
Figure 27. DFO-Kdo analogue conjugate; R = S (releasable) or C (non-releasable). 65
Figure 28. Retrosynthetic analysis of DFO-Kdo conjugate. 66

List of Schemes

Scheme 1. Synthesis of Kdo.NH_3 from D-arabinose. 39
Scheme 2. Synthesis of Kdo glycal **5** from Kdo.NH_3. 40
Scheme 3. Epimerization of **6** to obtain 2-d-β-Kdo methyl ester. 41
Scheme 4. Deprotection of isopropylidene group of Kdo derivative **7**. 42
Scheme 5. Insertion of azide moiety in tetraol **8**. 44
Scheme 6. Azide insertion in diol derivative **9**. 44
Scheme 7. Synthesis of Wittig ester **16** from D-mannose. 45
Scheme 8. Synthesis of stable phosphonium ylide **15**. 45
Scheme 9. Reduction of the olefinic compound **16**. 46
Scheme 10. Synthesis of the alcohol compound **19** through TBS protection and deprotection. 46
Scheme 11. Synthesis of 2-d-Kdo ethyl ester **22**. 48
Scheme 12. Regioselective tosylation catalyzed by Me_2SnCl_2. 50
Scheme 13. Azide insertion on 2-d-β-Kdo ethyl ester. 50
Scheme 14. Synthesis of 2,8-d-β-amino Kdo from **26**. 52
Scheme 15. Synthesis of peracetylated 2-d-Kdo derivatives. 54
Scheme 16. Synthesis of Kdo thioglycosyl donor **39** from Kdo.NH_3. 56
Scheme 17. Glycosylation of **39** with adamantane acceptors. 57
Scheme 18. Deprotection of benzyl and acetyl moieties. 58
Scheme 19. Synthesis of 5-d-N_3-arabinofuranose (**57**). 60
Scheme 20. Synthesis of 8-d-N_3-Kdo **58**. 61
Scheme 21. Synthesis of 4-d-N_3-arabinose **66**. 62
Scheme 22. Synthesis of 7-d-N_3-Kdo **67**. 62
Scheme 23. Synthesis of potential linkers. 66

List of Tables

Table 1. Attempts at reduction of Kdo glycal. 41
Table 2. Regioselective deprotection of terminal isopropylidene groups in compound **7**. 43
Table 3. Attempts at the selective isopropylidene deprotection of **22b**..... 49
Table 4. Isopropylidene deprotection of azide compound **25**. 52
Table 5. Attempts at conjugation of DFO and linker. 68

List of supplementary figures

Supplementary Figure 1. ^{1}H NMR spectrum (D_2O, 600 MHz) of compound 28 106
Supplementary Figure 2. ^{13}C NMR spectrum (D_2O, 100 MHz) of compound 28 107
Supplementary Figure 3. HSQC NMR spectrum (D_2O, 100 MHz) of compound 28 108
Supplementary Figure 4. ^{1}H NMR spectrum ($CDCl_3$, 600 MHz) of compound 31 109
Supplementary Figure 5. ^{13}C NMR spectrum ($CDCl_3$, 100 MHz) of compound 31 110
Supplementary Figure 6. COSY NMR spectrum ($CDCl_3$, 600 MHz) of compound 31 111
Supplementary Figure 7. HSQC NMR spectrum ($CDCl_3$, 600 MHz) of compound 31 112
Supplementary Figure 8. ^{1}H NMR spectrum ($CDCl_3$, 600 MHz) of compound 32 113
Supplementary Figure 9. ^{13}C NMR spectrum (CDCl3, 100 MHz) of compound 32 114
Supplementary Figure 10. COSY NMR spectrum ($CDCl_3$, 600 MHz) of compound 32 115
Supplementary Figure 11. HSQC NMR spectrum ($CDCl_3$, 600 MHz) of compound 32 116
Supplementary Figure 12. ^{1}H NMR spectrum (Acetone-d6, 600 MHz) of compound 41 117
Supplementary Figure 13. ^{13}C NMR spectrum (Acetone-d6, 100 MHz) of compound 41 118
Supplementary Figure 14. COSY NMR spectrum (Acetone-d6, 600 MHz) of compound 41 119
Supplementary Figure 15. HSQC NMR spectrum (Acetone-d6, 600 MHz) of compound 41 120
Supplementary Figure 16. ^{1}H NMR spectrum (Acetone-d6, 600 MHz) of compound 42 121
Supplementary Figure 17. ^{13}C NMR spectrum (Acetone-d6, 100 MHz) of compound 42 122
Supplementary Figure 18. COSY NMR spectrum (Acetone-d6, 600 MHz) of compound 42 123
Supplementary Figure 19. HSQC NMR spectrum (Acetone-d6, 600 MHz) of compound 42 124
Supplementary Figure 20. ^{1}H NMR spectrum ($CDCl_3$, 600 MHz) of compound 46 125
Supplementary Figure 21. ^{13}C NMR spectrum (CDCl3, 100 MHz) of compound 46 126
Supplementary Figure 22. COSY NMR spectrum (Acetone-d6, 600 MHz) of compound 46 127
Supplementary Figure 23. HSQC NMR spectrum (Acetone-d6, 600 MHz) of compound 46 128
Supplementary Figure 24. ^{1}H NMR spectrum (Acetone-d6, 600 MHz) of compound 47 129
Supplementary Figure 25. ^{13}C NMR spectrum (Acetone-d6, 100 MHz) of compound 47 130
Supplementary Figure 26. COSY NMR spectrum (Acetone-d6, 600 MHz) of compound 47 131
Supplementary Figure 27. HSQC NMR spectrum (Acetone-d6, 600 MHz) of compound 47 132
Supplementary Figure 28. ^{1}H NMR spectrum (Acetone-d6, 600 MHz) of compound 48 133
Supplementary Figure 29. ^{13}C NMR spectrum (Acetone-d6, 100 MHz) of compound 48 134
Supplementary Figure 30. COSY NMR spectrum (Acetone-d6, 600 MHz) of compound 48 135
Supplementary Figure 31. HSQC NMR spectrum (Acetone-d6, 600 MHz) of compound 48 136
Supplementary Figure 32. ^{1}H NMR spectrum (MeOH-d4, 600 MHz) of compound 49 137
Supplementary Figure 33. ^{13}C NMR spectrum (MeOH-d4, 100 MHz) of compound 49 138
Supplementary Figure 34. COSY NMR spectrum (MeOH-d4, 600 MHz) of compound 49 139
Supplementary Figure 35. HSQC NMR spectrum (MeOH-d4, 600 MHz) of compound 49 140
Supplementary Figure 36. ^{1}H NMR spectrum (MeOH-d4, 600 MHz) of compound 50 141
Supplementary Figure 37. ^{13}C NMR spectrum (MeOH-d4, 100 MHz) of compound 50 142
Supplementary Figure 38. COSY NMR spectrum (MeOH-d4, 600 MHz) of compound 50 143
Supplementary Figure 39. HSQC NMR spectrum (MeOH-d4, 600 MHz) of compound 50 144
Supplementary Figure 40. ^{1}H NMR spectrum (MeOH-d4, 600 MHz) of compound 51 145
Supplementary Figure 41. ^{13}C NMR spectrum (MeOH-d4, 100 MHz) of compound 51 146
Supplementary Figure 42. COSY NMR spectrum (MeOH-d4, 600 MHz) of compound 51 147
Supplementary Figure 43. HSQC NMR spectrum (MeOH-d4, 600 MHz) of compound 51 148
Supplementary Figure 44. ^{1}H NMR spectrum ($CDCl_3$, 600 MHz) of compound 62 149
Supplementary Figure 45. ^{13}C NMR spectrum ($CDCl_3$, 100 MHz) of compound 62 150

Supplementary Figure 46. COSY NMR spectrum ($CDCl_3$, 600 MHz) of compound 62 151
Supplementary Figure 47. HSQC NMR spectrum ($CDCl_3$, 600 MHz) of compound 62 152
Supplementary Figure 48. ^1H NMR spectrum ($CDCl_3$, 600 MHz) of compound 63 153
Supplementary Figure 49. ^{13}C NMR spectrum ($CDCl_3$, 100 MHz) of compound 63 154
Supplementary Figure 50. COSY NMR spectrum ($CDCl_3$, 600 MHz) of compound 63 155
Supplementary Figure 51. HSQC NMR spectrum ($CDCl_3$, 600 MHz) of compound 63 156
Supplementary Figure 52. ^1H NMR spectrum (D_2O, 600 MHz) of compound 64 157
Supplementary Figure 53. ^{13}C NMR spectrum (D_2O, 100 MHz) of compound 64 158
Supplementary Figure 54. COSY NMR spectrum (D_2O, 600 MHz) of compound 64 159
Supplementary Figure 55. HSQC NMR spectrum (D_2O, 600 MHz) of compound 64 160
Supplementary Figure 56. ^1H NMR spectrum ($CDCl_3$, 600 MHz) of compound 65 161
Supplementary Figure 57. ^{13}C NMR spectrum ($CDCl_3$, 100 MHz) of compound 65 162
Supplementary Figure 58. COSY NMR spectrum ($CDCl_3$, 600 MHz) of compound 65 163
Supplementary Figure 59. HSQC NMR spectrum ($CDCl_3$, 600 MHz) of compound 65 164
Supplementary Figure 60. ^1H NMR spectrum (D_2O, 600 MHz) of compound 66 165
Supplementary Figure 61. ^{13}C NMR spectrum (D_2O, 100 MHz) of compound 66 166
Supplementary Figure 62. COSY NMR spectrum (D_2O, 600 MHz) of compound 66 167
Supplementary Figure 63. HSQC NMR spectrum (D_2O, 600 MHz) of compound 66 168
Supplementary Figure 64. ^1H NMR spectrum (D_2O, 600 MHz) of compound 67 169
Supplementary Figure 65. ^{13}C NMR spectra (D_2O, 100 MHz) of compound 67 170

List of Abbreviations

A5P	D-Arabinose-5-phosphate
ABR	Antibiotic resistance
AcOH	Acetic acid
AMR	Anti-microbial resistance
Aq.	Aqueous
Bn	Benzyl
brsm	based on reaction starting material
Bu	Butyl
Bz	Benzoyl
CAM	Ceric ammonium molybdate
CKS	CMP-Kdo synthase
CMP	Cytidine monophosphate
CPS	Capsular polysaccharide
DBCO	Dibenzyl cyclooctyne
DCM	Dichloromethane
DDQ	2,3-Dichloro-5,6-dicyano-1,4-benzoquinone
DFOB	Desferrioxamine-B
DIPEA	*N*,*N*-Diisopropylethylamine
DMAP	*N*,*N*-4-(Dimethylamino)pyridine
DMF	Dimethylformamide
DMP	2,2-Dimethoxypropane
DMSO	Dimethylsulfoxide
EPS	Exopolysaccharide
EtOAc	Ethyl acetate
EtOH	Ethanol
GNB	Gram-negative bacteria
GPB	Gram-positive bacteria
Hex	Hexanes
IM	Inner membrane

Kdo	3-Deoxy-D-*manno*-oct-2-ulosonic acid
Kdo8P	Kdo-8-phosphate
Kdo.NH_3	Ammonium Kdo
Ko	D-*Glycero*-D-*talo*-oct-2-ulosonic acid
LDA	Lithium diisopropylamide
LOS	Lipooligosaccharide
LPS	Lipopolysaccharide
Lpt	LPS transport proteins
MeCN	Acetonitrile
MeOH	Methanol
MS	Mass spectrometry
NBS	*N*-Bromosuccinimide
NHS	*N*-Hydroxysuccinimde
NIS	*N*-Iodosuccinimide
OM	Outer membrane
OMRs	Outer Membrane Receptors
PBPs	Periplasmic binding proteins
PEP	Phosphoenol pyruvate
Phen	Phenacyl
PTSA	*p*-Toluenesulfonic acid
rt	room temperature
Ru5P	D-ribulose-5-phosphate
SPAAC	Strain-promoted alkyne-azide cycloaddition
TBS	*tertiary*-Butyldimethylsilyl
t-BuOH	*tertiary*-Butanol
TEA	Triethylamine
THF	Tetrahydrofuran
TLC	Thin layer chromatography
TMS	Trimethylsilyl
Ts	Tosyl
WHO	World Health Organization

1. Introduction

1.1. Bacteria and brief history of antibiotics

Bacteria belong to the prokaryotes, which are recognized as the first forms of living organisms that started their life, around 3.8 billion years ago, according to the current model.[1] The eukaryotes, the class which humans belong to, came much later in the history of life on earth, but along with both the evolution of life and humans, they started to build the ecosystem together and started to integrate together. The human body is an ecosystem in itself as it serves as home for millions of bacteria, most of them aid and help in the metabolism of the body.[2] Likewise, bacteria help in improving the biological lifestyle of the human body, but there are also plenty of other bacteria outside of the body. They are present almost everywhere in the environment, like plants, soil, air, and even in extreme conditions such as high temperatures, glacial deserts, hot springs and ocean bottoms.[3] Most of these bacteria possess their own risks for humans in one way or another because of their ability to damage, the organs and/or the metabolisms. It was confirmed with their discovery in the 19th century, that bacteria can have substantial contribution in damaging of the human system. After their discovery, it became evident that they turned out to be one of the major 'infectious agents' along with some of other microorganisms such as fungi, plasmodium.[4] Even simple infections like diarrhea, which are quite simple to treat now, had no treatments at that time and often resulted in death.[5] When scientists were in wide search of a way to find a remedy against several bacterial infections, it was late in the 19th century that scientists started to believe chemicals could be effective antibacterial agents.[6] The pioneer in this regard was Paul Ehrlich, who is credited for the discovery of the 'first modern antibiotic' based on chemicals to inhibit bacterial growth.[7] During that time scientists were able to stain bacteria with dyes that led to the basis of their classification namely Gram-positive or Gram-negative bacteria. Paul Ehrlich also made his share of substantial contributions which include staining several tissues and differentiating between several blood cell types.[8]

He made a conclusion based on the observation that chemical dyes can be used to colour the bacteria specifically. He concluded that chemicals could be used as selective therapeutics against bacteria without damaging other cells. After setting out to find the treatment of the malaria pathogen, a compound named arsphenamine was found to be effective against

spirochaetes bacteria, which caused syphilis, thus becoming the first chemical to treat bacterial infections. But it was not until Alexander Fleming discovered penicillin (**Fig. 1**) that the true inception of chemicals as antibiotics began.[9]

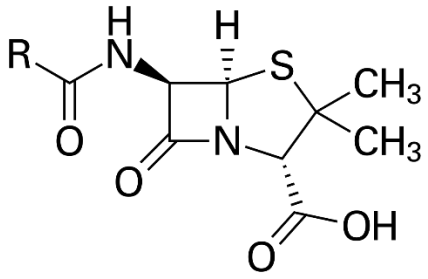

Figure 1. Structure of Penicillin

This was followed by the period of continuous breakthroughs in the field of antibiotics. The number of researches to be carried out and the sheer quantity of compounds to be synthesized, against a wide range of bacterial infections. This led to antibiotics revolutionizing the field of medicine during the period from the 1940s to 1960s (**Fig. 2**). They helped in saving millions of lives every year in due course of time as a result of which the global life expectancy of humans started to increase tremendously, thereby shifting the nature of lifestyle. As the norms with most breakthroughs, this golden phase was short-lived when the bacteria started to undergo mutations to develop resistance against these antibiotics, called antimicrobial resistance (AMR) [also referred as antibiotic resistance (ABR)]. The end of the 1960s also marked the end of the golden period of antibiotics, with the inception of AMR, which only saw the upfield ascending.[10]

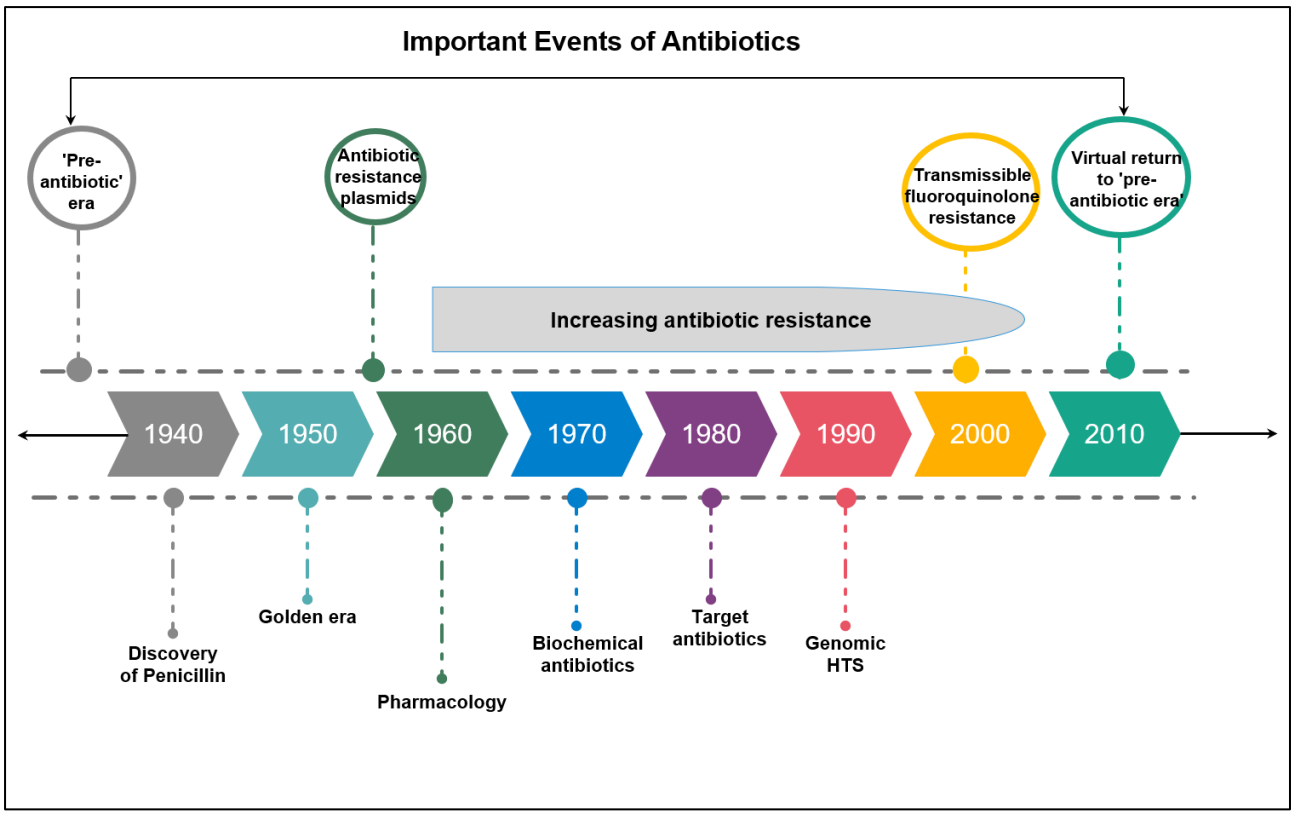

Figure 2. Timeline of the antibacterial evolution

1.2. Antimicrobial resistance crisis and superbugs

With the constant exposure to antibiotics, after a time, the bacteria overcame the medicinal inhibition to develop resistance. In this regard, several classes of human-associated pathogens have developed multidrug-resistance against antibiotics. The bacteria then become immune to the drugs, as a result of mutations, and are able to keep growing in spite of the exposure and are generally named "superbugs".[11] Technically, these superbugs are highly difficult to treat and, in some cases, even impossible. For instance, the tuberculosis-causing bacteria *Burkholderia cepacia, Escherichia coli*, and *Pseudomonas aeruginosa* are all some of the superbugs that currently do not have any practical treatments. With the exponential increase of AMR, the number of effective antibiotics is diminishing, and the need to treat infections caused by superbugs is increasing, so much so that we are in the danger to virtually return back to the 'pre-antibiotic era'.[10]

This crisis is reflected more deeply through some of the morbidity statistics. There are approximately 17 million reported victims to infectious diseases annually worldwide making

infectious diseases the second leading killer. As per the reports of 2014, 700,000 people died of AMR resulting from these deadly bacterial infections. This number will likely increase, as it is projected that the mortality rate due to AMR will reach approximately to 10 million by 2050 (**Fig. 3**). This number could be far higher, if other not-so-common infections would be taken into account.

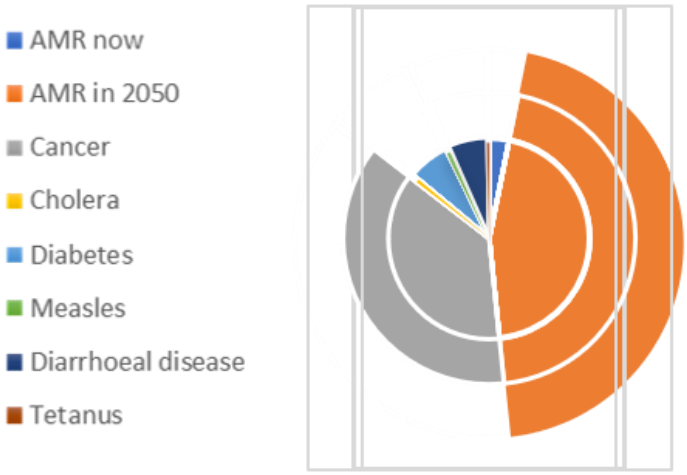

Figure 3. Image adapted from: Review on antimicrobial resistance, 2016

Recently, the World Health Organization (WHO) published a "priority pathogens" list (**Fig. 4**), comprising of twelve antibiotic-resistant superbugs. These are some of the well-known notorious bacteria against which an immediate solution is needed. The nine Gram-negative bacteria (GNB) (that are highlighted), clearly dominate this list compared to the three Gram-positive bacteria (GPB).

PRIORITY: CRITICAL	PRIORITY: HIGH	PRIORITY: MEDIUM
▪ *Acinetobacter baumannii*	▪ *Staphylococcus aureus*	▪ *Streptococcus pneumoniae*
▪ *Pseudomonas aeruginosa*	▪ *Enterococcus faecium*	▪ *Haemophillius influenza*
▪ *Enterobacteriacae*	▪ *Helicobacter pylori*	▪ *Shigella spp.*
	▪ *Campylobacter spp.*	
	▪ *Salmonellae*	
	▪ *Neisseria gonorrhoeae*	

Figure 4. WHO priority pathogens list. Source: WHO, 2017

Thus, the key inference from this list is that it showcases the threat of GNB in particular, compared to Gram-positive bacteria. As quoted by Prof. Evelina Tacconeli, head of the division of Infectious Diseases at the University of Tübingen, who was a major contributor in developing this list: "New antibiotics targeting this priority list of pathogens will help to reduce deaths due to resistant infections around the world. Waiting any longer will cause further public health problems and dramatically impact on patient care". Owing to their high level of resistance and well-built cell structures to tackle the antibiotics much more effectively. Therefore, we are concerned about the GNB that evidently possess more threat to humans than the GPB. The reason behind the high-level resistance of GNB will be discussed in the following section.

1.3. Gram-negative and Gram-positive bacteria

It has been speculated that there are at least one million different species of bacteria but only one hundredth of that has been discovered. Despite this low discovery rate, the number of known bacterial species is approximately 10,000. With such an imperial family of species that has been known and studied, they are classified based on a binary 'Gram staining' method.

The key structural differences in the cell wall composition between Gram-negative and Gram-positive bacteria influences substantially a number of important characteristics. Those

parameters include the membrane properties, permeability and the overall picture of resistance towards antibiotics and chemical inhibitors. GNB are protected by an asymmetric bilayer of phospholipids and another lipid layer, called lipopolysaccharide (LPS). This is yet another structural difference shared by GNB in comparison with GPB. Though, invariably the 'complex multi-layered' cell envelope helps in protecting bacteria in surviving in extreme conditions and most importantly difficult hostile environments and fighting against them. The GNB envelope is supposedly far more impenetrable by antibiotics due to this effective asymmetric bilayer compared to the more susceptible peptidoglycan layers covering of the membrane of GPB.[12]

1.4. Membrane of GNB

The cell-envelope of GNB (membrane) consists of three major layers, *i.e.*, the outer membrane (OM), the monolayer of peptidoglycan, and the inner membrane (IM). As represented in **Fig. 5**, GNB are barricaded by an OM that perimeters the peptidoglycan. As a result, it provides a high level of resistance in fighting against the host immune system. This specific type of distinct OM organelle lack in GPB.[13]

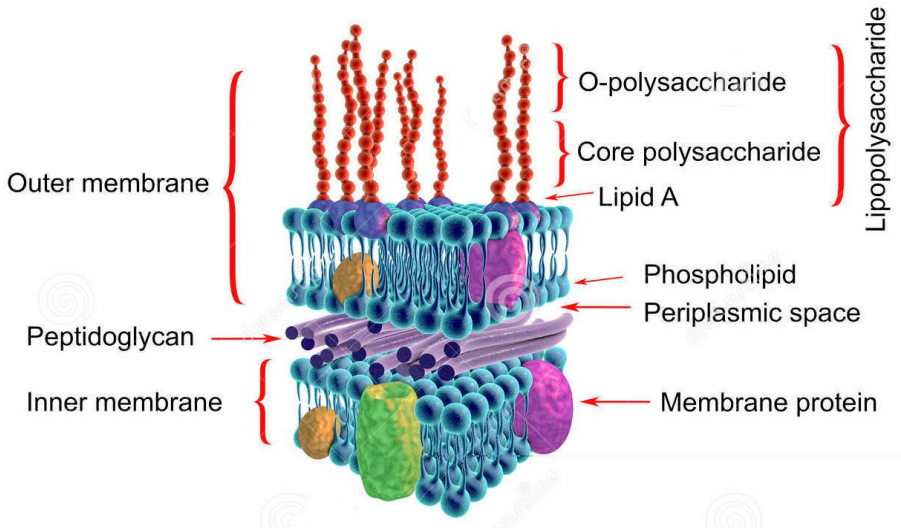

Figure 5. Representation of membrane of GNB. Image adapted from: www.dreamstime.com

The OM of GNB consists of an elaborate asymmetrical lipid bilayer of phospholipids and lipopolysaccharides, the latter being present in the outermost layer. While the phospholipids are restricted to the inner leaflet, the outer leaflet LPS is composed of complex glycolipids.[12] According to the data for certain bacteria, LPS takes up to almost 75% of cell envelope

compared to phospholipids.[14] Under these layers the inner membrane, which is the site of several essential processes including their metabolism that keeps the bacteria functioning. Other than that, all the organelles and mentioned components are biosynthesized in the IM. The synthesized components are transported across the bacterial membrane from the cytoplasm. In a similar fashion, the components of LPS are also biosynthesized in inner membrane of cytoplasm and transported by ABC transporters.[15]

The OM and IM are separated by the aqueous periplasm, to which a peptidoglycan layer is embedded.[16] This is not in the case for GPB, as the peptidoglycan is on the surface and exposed to the extracellular medium. Once the peptidoglycan surrounding is penetrated, the cytoplasm is contactable as seen in **Fig. 6**. In GNB, the elaborate OM ensure that the immune cells or antibiotics do not come into contact with the peptidoglycan and the crucial IM, as it is an improbable task for the drugs to penetrate OM.

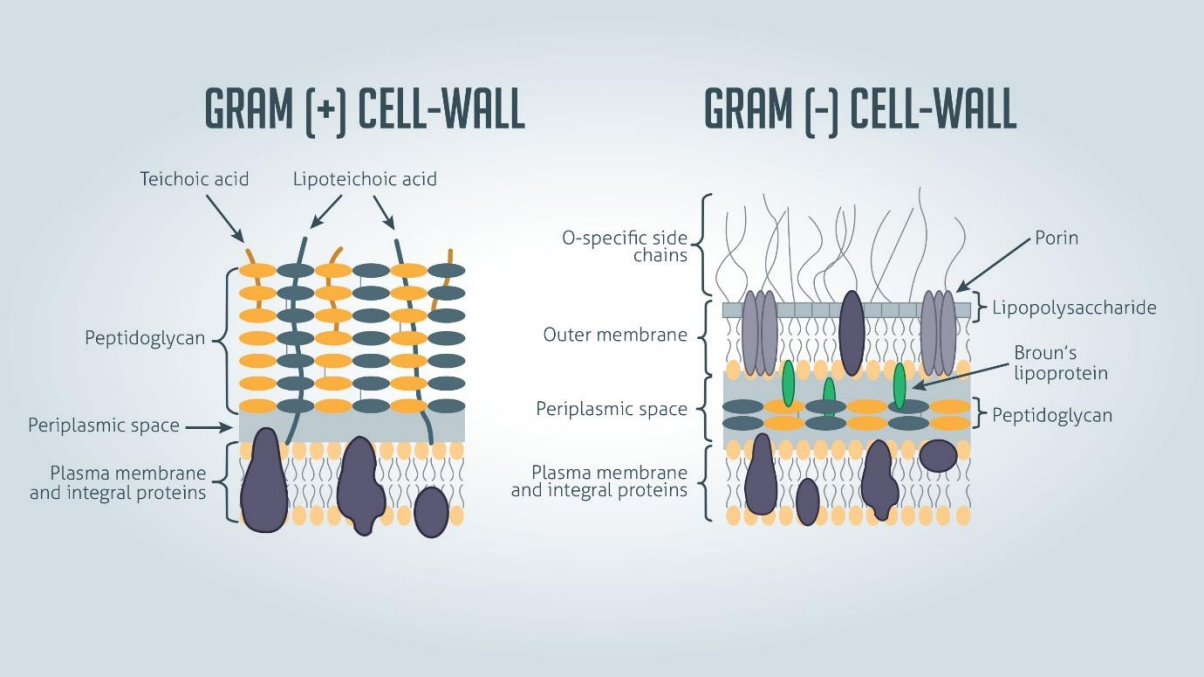

Figure 6. Structural comparison between GNB and GPB. Image adapted from www.technologynetworks.com

Some more experimental data on the corresponding cell envelopes of GNB and GPB reveal that the thickness of the peptidoglycan multilayers in GNB, ranges between 20-80 nm and constitutes the bulk of the bacteria (almost 90%). In the case of GNB, the peptidoglycan constitutes only a 10% of proportion and the thickness ranges between 7-8 nm.[14] But the

main proportion of the cell wall is constituted by LPS, whose thickness is measured in µm. Despite possessing the bulk of peptidoglycan residues, GPB still remain more susceptible to antibiotics compared to GNB. Since, the peptidoglycan covering is not rigid enough to provide high resistance, the foreign bodies are able to interact with the cytoplasm.

1.5. Lipopolysaccharide (LPS) of GNB

As mentioned previously, the complex LPS is on the outer layer interacting directly with the extracellular medium. It is virtually present in all GNB. Due to its abundance, it is one of the major virulence and integral part of the defence system of OM. Its contribution to the toxicity of the OM is so substantial that human innate immune system readily responds to these amphiphilic glycolipids. The unique composition of LPS (**Fig. 7**)[17], as part of the asymmetric bilayer of OM on one hand, limits the entry of hydrophobic compounds through passive diffusion, while on the other hand, the narrow pores prevents the by-size penetration of hydrophilic compounds.[12, 18] Apart from this, there are other cytoplasmic efflux transporters that further slowdown the influx of antibacterial agents across membranes, even if they manage to penetrate the rigid LPS. The mode of actions used by multidrug efflux transporters include effusion of the drug across the IM, consequently reducing the concentration of drug that reaches the inner leaflet of cytoplasm. They also pump out the antibiotics into the extracellular medium completely, by trapping them in the periplasm. Thus, the endotoxin nature of LPS and its contribution to OM in several ways cannot be emphasized enough, and hence it is necessary to explore deeper and understand it.[19]

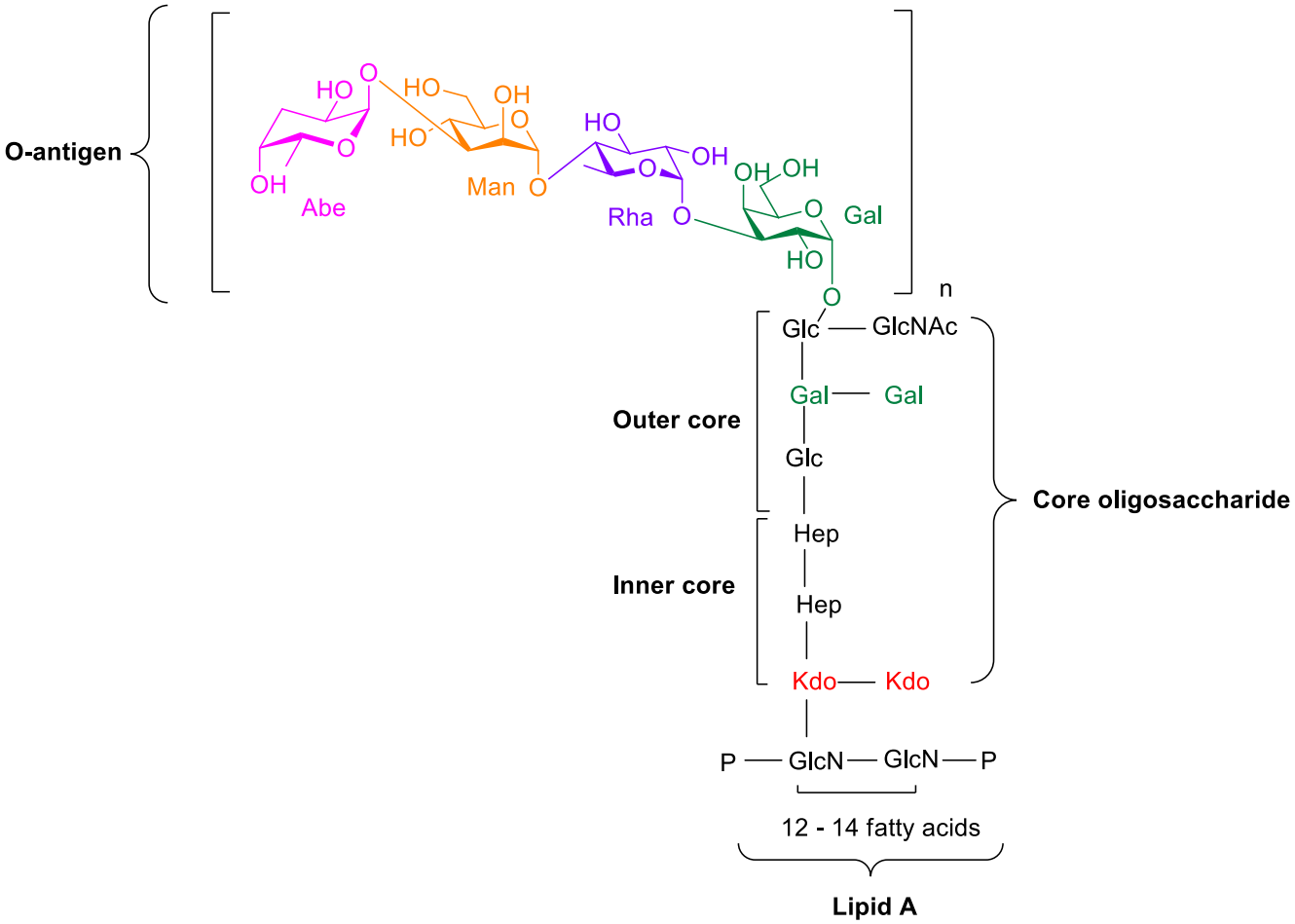

Figure 7. Chemical representation of lipopolysaccharide of *S. typhimurium* LT2[20]

Dissecting the layers of LPS chemically, they consists of three distinct components, starting from inner side of OM – a) **Lipid A**, a hydrophobic structure that is anchored to OM; b) **Core oligosaccharide**, further subdivided into inner core and outer core; and c) the terminal ***O*-antigen**, strain specific polymer chain.[21]

1.5.1. *O*-Antigen

O-Antigens are polymeric chains consisting of repeating oligosaccharide units that are specific to the bacteria strain (serospecific). They are attached to the cell surface as outermost components, separating bacteria and extra-cellular medium. Though this generalized threefold building block of LPS is considered valid for all the characterized GNB, there are exceptions in case of bacteria belonging to genera such as *Haemophilius, Chlamydia*, and *Neisseria*. They lack this type of antigenic polymer structure made up of repeating

oligosaccharides (*O*-antigen), which are replaced by shorter strain-specific oligosaccharides, extending from core oligosaccharides. Thus, referring to them as lipooligosaccharide (LOS).[21]

Being the outermost component of LPS, one of the functions of the *O*-antigen is to provide cover for 'immunostimulatory effects' of the endotoxin lipid-A, which is present further inside the OM.[22]

1.5.2. Core oligosaccharides

As mentioned before, core oligosaccharides are further subdivided into the inner and outer cores. This division was established mainly to distinguish the core region based on its two different patterns of carbohydrate composition.[23] The outer core, linked to *O*-antigen contains mostly hexose sugars like D-glucose, D-galactose as well as hexosamines such as D-glucosamine and *N*-acetyl galactosamine. Whereas, the inner core consists of heptopyranose sugars (Hep*p*) such as D-*glycero*-D-*manno*-heptose and an eight-membered unique sugar acid called 3-deoxy-D-*manno*-oct-2-ulosonic acid (Kdo). Kdo is a characteristic monosaccharide for all core regions, covalently linking the inner core to lipid A. The heptose sugar of inner core may also possess phosphoryl-anionic substituents attached to it.[23-24] However, there are exceptions with this generalization as hexose and hexosamine saccharides are found in the inner core of some strains of bacterial species such as *E. coli* EH100 and *E. coli* K-12 (D-Gal*p* and L-Rha*p*, respectively) to name a couple, and the other way around, heptose saccharides are identified in the outer core in *E. coli* K-12 (Hep*p*). [25]

In terms of the diversity and scope for modification of monosaccharides, unlike *O*-antigen, it is limited comparatively in composition of core regions. But even with this limited modification, the variation mostly occurs in the outer core that is proximal to the *O*-antigen than in the inner core, proximal to endotoxin lipid A. Barring the exception of interchange of hexose and heptose, already mentioned before, it is the sugar fragment Kdo that has been identified in every core region of all the characterized GNB until now and proving to be essential component of not only core region, but ultimately LPS too.[26] There is an exception, though, with the marine bacteria of *Shewanella* species. The derivative 8-amino-8-deoxy-Kdo has been identified in *Shewanella oneidensis*.[27] Generally, there are two molecules (disaccharide) of Kdo that are present in LPS, but in some cases like *Haemophilius influenza*

there is only one Kdo residue. Also, there are exceptions here as well. For instance, in strains of *Acinetobacter,* one of the two Kdo residues is replaced by a similar 8-membered sugar acid called D-*glycero*-D-*talo*-oct-2-ulosonic acid (Ko), to form the Kdo-Ko linkage.[22c, 28] Ultimately, there is at least one Kdo residue in every inner core of bacterial LPS. Due to the omnipresence and characteristic representation of LPS, Kdo is targeted for its potential as a pharmacological hotspot in order to develop novel antibacterials, which will be discussed in detail in the next sections. One important thing to be mentioned here is that, in spite of its key role in LPS biosynthesis, the Kdo targeting has been underexploited.

1.5.3. Lipid A

The hydrophobic anchor of LPS, *i.e.*, lipid A, is linked to the inner core through α-(2→6)-ketosidic linkage with Kdo, which is actually acid labile. Generally, they are composed of two residues of β-1→6 linked phosphorylated glucosamine (phosphorylated at both 1- and 4'-positions), acylated with fatty acid chains.[25a] This acylation with fatty acids, typically 4 to 7 in numbers, may occur at hydroxyl and amino positions either symmetrically or asymmetrically. Lipid A is identified to be the major contributor for toxicity of LPS and hence is considered as endotoxin.[29] The structure of lipid A of *E. coli* is represented in **Fig. 8**. It can be seen that (*R*)-3-hydroxy fatty acids, esterified at the 3-hydroxy position by other fatty acids, are distributed asymmetrically over two GlcN residues. The non-reducing GlcN has two fatty acid chains linked to it at 3-OH position and at amino position. While the fatty acid itself is ester linked to another fatty acid, the reducing GlcN is also acylated with two fatty acids at two similar positions.[30] However, they are not ester-linked at 3-OH. There are approximately 10^6 residues of lipid A in an *E. coli* LPS. An example for symmetrically distributed fatty acids over GlcN can be found in the case of *Chrombacterium violaceum.* The 3-OH ester linked fatty acids are acylated with hydroxyl and amino positions of both the GlcN residues. These variations are substantially recognized during the host LPS recognition.[31]

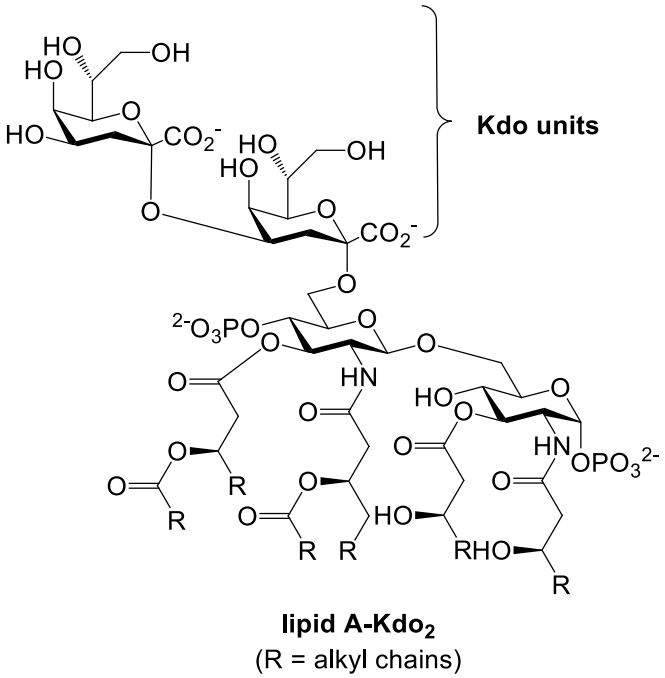

Figure 8. Structure of lipid A-Kdo_2

With the lipid-A-Kdo_2 residues contributing substantially to the permeability barrier of bi-layered OM, the contribution of lipid A, in particular, is enhanced in the way it reduces fluidity of the LPS monolayer. The contribution of co-layer glycerophospholipids is comparatively lesser in this regard. The fluidity of the monolayer is inversely proportional to the number of alkyl chains, *i.e*, the greater is the number of alkyl chains per head group, lesser the fluidity. In general, there are four to seven fatty acid chains attached to lipid A, compared to two fatty acid chains attached to a single glycerophospholipid residue. GlcN fatty acid chains are packed more compactly because of the presence of saturated alkyl chains. The hydrophobic compounds have been demonstrated to diffuse passively across the less fluid OM bilayers at a rate half slower than the glycerophospholipid bilayers.[32] Another important point to be mentioned here is that lipid A and Kdo residues are fundamentally required for the growth of *E. coli* cells. That is how crucial the components lipid A and Kdo are to the membrane viability of the OM.

1.5.4. 3-Deoxy-D-*manno*-oct-2-ulosonic acid (Kdo)

Kdo is not a usual, commercially available sugar fragment like glucose, galactose or mannose. From a chemical point of view, Kdo possesses an unusual nature, being the most conserved sugar residue of LPS.[28] From the biological side of the spectrum, because of its involvement

with lipid A (lipid A-Kdo_2) in providing cell viability and other important contributions in innate immune response, this sugar warrants to be explored in detail.

Kdo was first isolated from a strain of *E. coli* in 1959.[33] The structure of Kdo, composed of a ketose sugar (at position 2), deoxygenated at position 3 and bearing a carboxylic acid functional group linked to the anomeric carbon, is present in the bacterial LPS in the α-form of a pyranose ring. Kdo is a typical example of 2-keto-3-deoxy-sugar acids family, an important family of biologically occurring and functioning carbohydrates (**Fig. 9**). Some of the other examples of sugar acids belonging to this vast family are *N*-acetylneuraminic acid (Neu5Ac) (**A**), 2-keto-3-deoxy-D-*glycero*-D-*galacto*-nonulosonic acid (Kdn) (**B**), *N*-glycosylneuraminic acid (Neu5Gc), 2-keto-3-deoxygalactonic acid, pseudaminic acid (**C**), and legionaminic acid (**D**). All of these mentioned carbohydrates are amino functional bearing 9-membered carbon ring structures, also called as sialic acids, unlike the 8-membered nature of Kdo, once again making it unique even within its own class of carbohydrates.[34] One of the first identified, isolated, synthesized, and well-known sialic acid is Neu5Ac (**A**), found mostly in the mammalian cells glycoproteins, as terminal residue. Comparatively lesser well-known Kdn (**B**) is mostly found in bacterial cell wall and also in a wide range of vertebrates, which also include human cells.[35] In general, sialic acids are not expressed by most of the bacterial carbohydrates or LOS.[36] In exceptional cases, it is mostly the Neu5A and Kdn residues present as internal residues that are linked covalently, unlike as terminal residues present in the animal glycoproteins.[37]

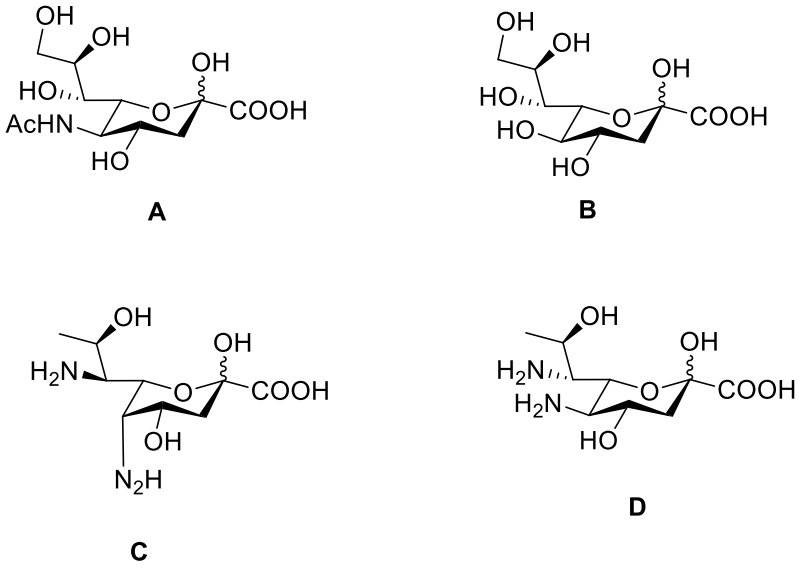

Figure 9. Sialic acid structures

However, those rare bacteria that express these sialic acids are pathogenic, such as *Neisseria meningitidis* that causes meningitis and *Campylobacter jejuni* that causes gastroenteritis. Capsular polysaccharides (CPS) may also contain these sialic acids.[38] Neu5Gc bears similar structure as Neu5Ac barring one oxygen moiety and is found only in glycoproteins of mammalian cells. The rarely known sialic acids of the lot, *i.e*, pseudaminic acid (**C**) is elongated as 5,7-diamino-3,5,7,9-tetradeoxy-L-*glycero*-L-*manno*-nonulosonic acid and legionaminic acid (**D**) is elongated as 5,7-diamino-3,5,7,9-tetradeoxy-D-*glycero*-D-*galacto*-nonulosonic acid. 2-Keto-3-deoxygalactonic acid is known to be expressed in exopolysaccharides (EPS) of *Azotobacter vinelandii*.[39]

Turning towards the chemistry of Kdo sugar (**Fig. 10**), the term ulosonic acid denotes the keto carbonyl linked to the carboxylic acid moiety of the carbohydrate backbone. Upon cyclization, the C-6 hydroxyl group links with the keto moiety at the C-2 position to form the pyranose ring. Due to the configuration of stereocentre carbons barring C-3, the pyranose ring resembles to the D-*manno* backbone. The anomer centre present at the C-2 position, found as a pyranosyl form, is one of the most important aspects with respect to the influence on biological properties. Both the anomers cannot be taken for granted as they impose substantial differences in stability and chemical properties but, more importantly, they make distinct differences in naturally occurring carbohydrates of bacteria. Typically, in an LPS, Kdo

always exists in the α-form of a pyranose backbone. Although the β-anomeric form of Kdo are expressed by the EPS in the biofilm of *Burkholderia* species, which will be discussed later.

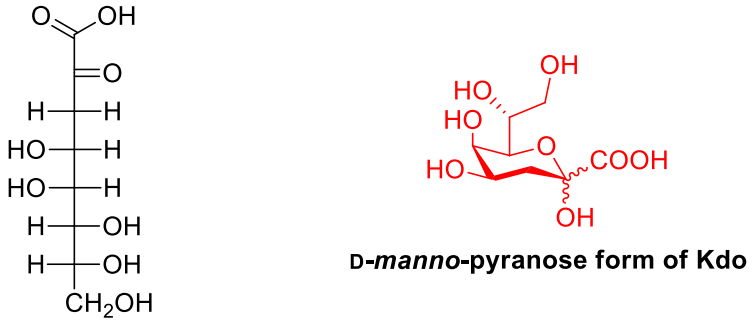

Figure 10. Chemical structure of Kdo (Fischer projection and chair form)

1.5.5. LPS biosynthesis

Fig. 11 provides the overall picture of reaction steps involving several sugar fragments and enzymes that leads to the formation and assembly of LPS. In general, two molecules of Kdo are attached with acylated lipid A through the Kdo donor residue, cytidine monophosphate-Kdo (CMP-Kdo).[15] The site of lipid A-Kdo_2 biosynthesis, catalysed by Kdo transferases (WaaA) enzymes, is the cytoplasm. With the inner core attached to lipid A, it is elongated to the outer core at the cytoplasmic surface of inner membrane catalysed by glycosyltransferases. The next component of LPS, O-antigen, is also synthesized at the same location. With all three-fold components of LPS synthesized in the inner membrane, they are flipped across to the periplasm and are assembled there.[40] While ABC transporters facilitate the lipid A-core transportation from the cytoplasm to the periplasm, the *O*-antigen transportation occurs *via* by Wzx, where it is polymerised by Wzy and Wzz. After the polymerization, WaaL brings the *O*-antigen to the site of core-lipid A.[41] Finally, the LPS assembly takes place by the action of seven LPS transport proteins (Lpt).[42]

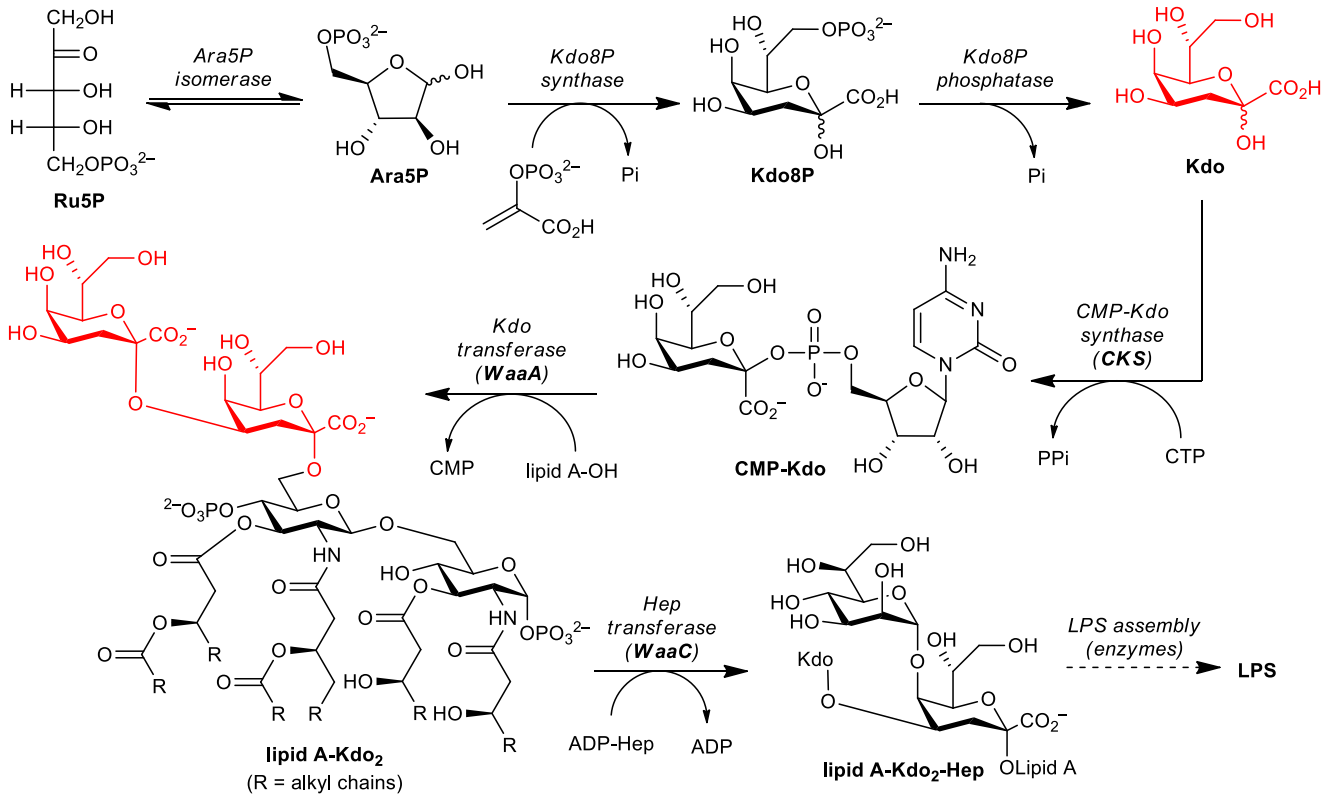

Figure 11. Biosynthetic pathway of Lipid A-Kdo2 as part of LPS biosynthesis

Though as a whole, this is how the biosynthesis of LPS occurs. We are interested in exploring in greater detail about important steps, components and enzymes that take part in the biosynthesis of LPS. This includes the residue lipid A-Kdo_2 and the enzymes involved in this biosynthesis, because of the role it plays in the membrane integrity and cell viability.[43] As already mentioned, lipid A is the toxic substance of LPS, and Kdo is the fragment that links the inner core to lipid A, thereby giving access to the toxic lipid A-Kdo_2. The approach of inhibiting enzymes that are crucial for the biosynthesis of lipid A-Kdo_2 would trigger disruption in LPS assembly, damaging the membrane integrity and ultimately weakening the OM.[44] The weakened OM theoretically makes the GNB spineless, thereby enhancing the entry of antibiotics.

1.5.6. Biosynthetic pathway of Kdo

In the previous section, it was mentioned that the major step involved in the LPS biosynthesis is the formation of lipid-A-Kdo_2 facilitated by the residue CMP-Kdo. The Kdo biosynthetic pathway commences from the pentose, D-ribulose-5-phosphate (Ru5P) and ends with the formation of CMP-Kdo through four enzymatic steps (**Fig. 11**).[34]

D-Arabinose-5-phosphate (A5P) is the precursor aldose sugar that is involved in the synthesis of Kdo-8-phosphate (Kdo8P), which in turn is a precursor for the formation of the free molecule of Kdo. But this A5P is not available in the cytoplasm. Hence, naturally occurring ketose sugar, D-ribulose-5-phosphate, possessing similar structure to A5P, undergoes keto-aldol isomerisation driven by the enzyme A5P isomerase (API). Thus, the pathway is kicked off by the isomerization of RuP to A5P.[45] The second step involves the condensation of A5P with phosphenolpyruvate (PEP) to form Kdo-8-phosphate (Kdo8P). This reaction is catalysed by the enzyme Kdo-8-phosphate synthase (Kdo8PS).[46] The third step is the formation of Kdo by cleaving the residue Kdo 8-phosphate, catalysed by Kdo8P phosphatase (KdsC) along with the formation of inorganic phosphate.[47] Finally, the donor residue CMP-Kdo is formed by attaching a molecule of free Kdo, with the phosphoryl ester cytidine monophosphate at the anomeric position. This step, catalysed by the enzyme CMP-Kdo synthase (CKS), is of particular focus because it is the rate-determining step of LPS biosynthesis.[48] During this course, simultaneously lipid A is also formed and once the activated sugar CMP-Kdo is synthesized, they both converge driven by specific membrane-bound transferases.[49] Inhibiting the enzymes involved in the rate determining step of LPS biosynthesis (CKS) places us in the right direction towards our idea of disrupting LPS biosynthesis and ultimately triggering the membrane perturbation and integrity damage.[34, 50]

In the literature, there have been previous efforts aimed at synthesizing the inhibitors of rate-determining CKS enzyme. The inhibitors were designed with the idea of mimicking and modifying the Kdo residues.

1.6. CKS inhibitors

As one of the earliest works in 1980s, Claesson *et al*. synthesized four Kdo analogues and tested them for their inhibitory activity against CMP-Kdo synthetase isolated from *Salmonella typhimurium* SL 1102 and *E.* coli D21. These compounds were based on a 2-d-Kdo backbone, in which the anomeric hydroxyl group is deoxygenated, with acetylated and free hydroxyl groups in both of its anomeric form, separately. Out of the four compounds, 2-d-β-Kdo was the only compound to show potent inhibitory action with a K_i value of 3.9 µM (**Fig. 12**).[51] In

spite of inhibiting the enzyme CKS, it was unable to kill the bacteria due to its inability to penetrate the cytoplasmic barrier in substantial inhibitory concentrations. In order to overcome this issue, this compound was modified at its C-8 position by an amino group substitution. They hypothesized that the amino-bearing group could manipulate the bacterial peptide permeases by forming an amino acid or peptide linkage thereby enabling the transportation of the inhibitor across the cytoplasm. 8-Amino-2,8-dideoxy-β-Kdo exhibited similar inhibitory action. With this observation, to exploit a similar ideology, several dipeptide derivatives of 8-amino-2,8-dideoxy-β-Kdo were synthesized. When tested, they were successfully shown as potent *in vitro* antibacterial activity. But this soon backfired as bacteria used the aminopeptidases to develop mutation, which ultimately led to resistance from bacteria. Thus, this compound too was unsuccessful to be used further in clinics.[52]

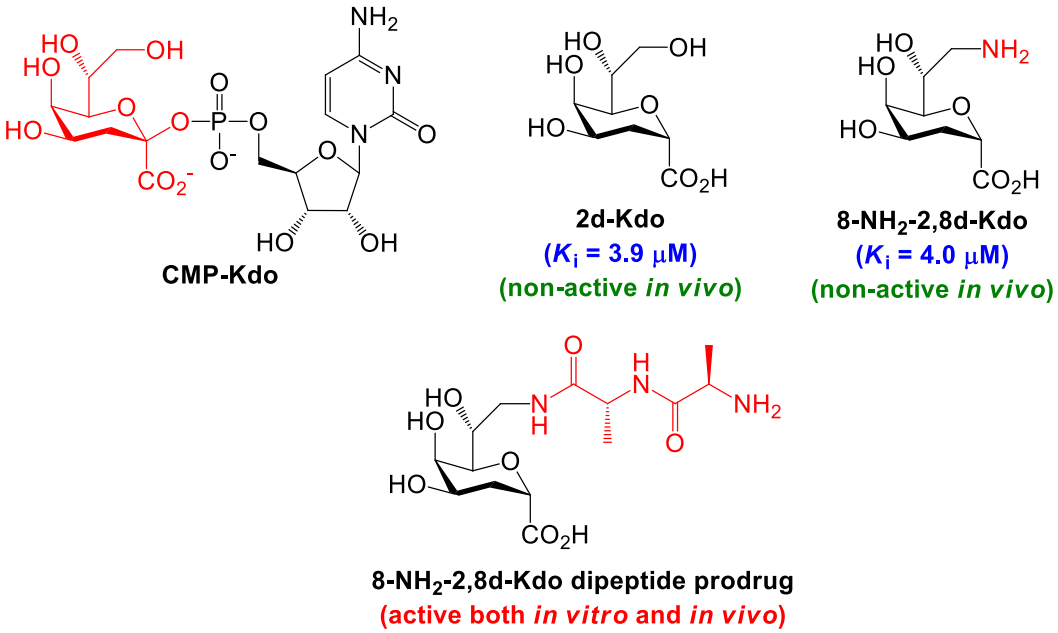

Figure 12. Structure of CMP-Kdo and some of the known inhibitors of CKS with their relative stability

The complex defence system of bacteria given by the bilayer of OM has already been discussed. There is thus a need for different approaches involving the inhibition of Kdo-processing enzymes using the analogues of Kdo. The delivery of the inhibitor is hampered by two problems, the main one being the permeability barrier for the drug to be able to reach cytoplasm in inhibitory concentration, as well as to avoid the backfiring, when bacteria would develop the resistance. Though, the former is a major challenge, and thus in this regard, we

hypothesize that conjugation of the inhibitor to a specific chelating agent called siderophore should help us overcome this issue. This approach of covalently linking the potent Kdo-processing enzyme inhibitor with the siderophore is unprecedented and could potentially help us in overcoming the membrane diffusion barrier.

1.7. Siderophores

The element iron has its own special place in the biological functions of every microorganisms, plants and animals, and bacteria are no exception. Iron is crucial for the metabolism and survival of GNB.[53] The reason for this type of demand for the iron element is its unique d-orbital bearing electronic configuration. Because of the vacant d-orbital subshells, it can vary its oxidation state, resulting in electron transport. Combined with its ability to form coordination linkage making it highly beneficial in cell processes. But iron is not available freely in extracellular medium of a host systems, as much as it is abundant in the earth's crust.[54] The reason for this is the low solubility of iron(III) ions,[55] a characteristic property of transition metals in general.[56] Thus, provided its value in bacterial metabolism, bacteria need to develop a strategy to bind iron and harvest it from the biological medium. This is a challenge for bacteria as iron assimilation does not come without its demerits. First, the concentration has to be monitored since excess of accumulation is leading to the toxic effects and secondly the mentioned low-solubility. Bacteria have been successful in developing strategies for iron accumulation - one of the most common and interesting strategy is the active transportation of iron ions into the cytoplasm by chelating them with a special secondary metabolite, the so-called siderophores.

The term is coined from the Greek word, *siderophores,* which means iron bearers. They are low molecular weight structures, for a naturally expressed residue, typically less than one kDa. They are able to form, high spin, kinetically altered, octahedral complex with Fe(III) ions, that are highly stable and thermodynamically favoured.[57] They show a high affinity towards residues containing three bidentate ligands with formation constant (K_f) of approximately 10^{30} and for this reason they show a virtually specific affinity exclusively towards Fe(III).[58] Siderophores aid in increasing the solubilization and the formation of Fe(III)-siderophore complex, which is actively transported to the cytoplasmic inner membrane facilitated by

several transporters and membrane receptors (**Fig. 13**)[59]. This type of 'scavenging' mechanism of Fe(III) assimilation is referred to as the 'high-affinity system'. This mechanism is regulated under stress conditions caused by iron deficiency in the bacterial cell environment, which is mostly the case. In contrast, other types of systems referred to as the 'low-affinity system' are activated during circumstances of higher concentration of iron availability. When concentration of iron is greater than 10^{-5} M, the Fe(III) ions are transported through diffusion across cell membranes.[60] There are more than 500 structures of siderophores that have been identified and characterized in microorganisms, which makes siderophore a diverse group of compounds.[61]

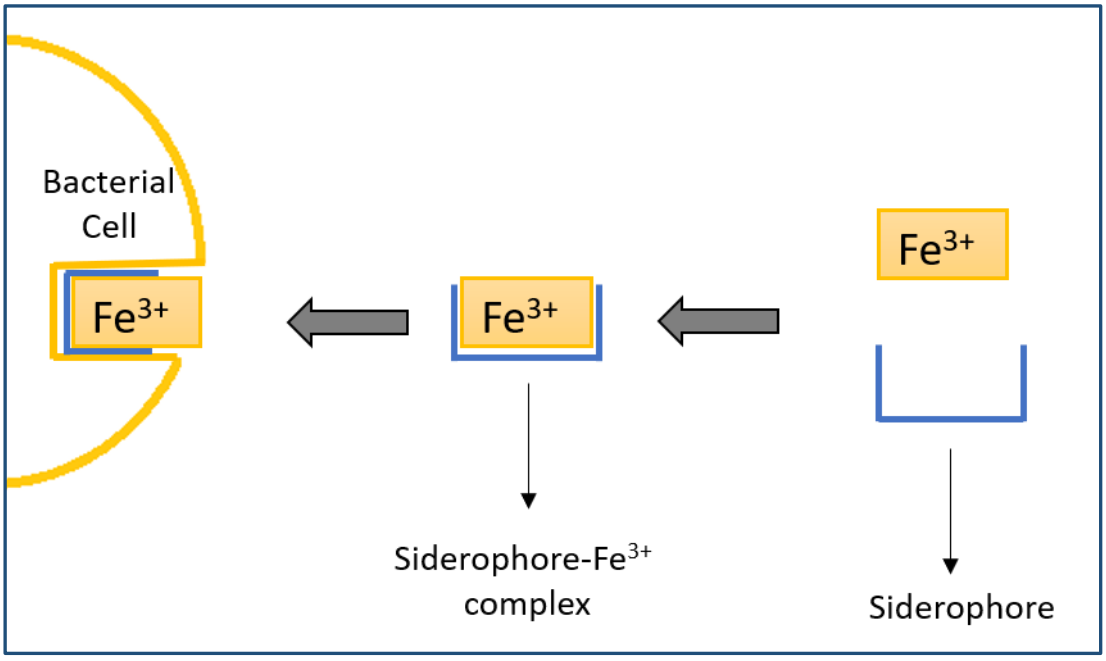

Figure 13. Simple representation of role of siderophore

In general, the siderophores are oxygen-donating, hexadentate ligands. They are classified into three main classes: catecholates, hydroxamates, and α-hydroxycarboxylates, based on the chemical nature of binding sites (oxygen ligands) of chelation of Fe^{3+} cations.[62] In some instances, the oxygen ligand may be replaced by nitrogen or sulphur ligands, distorting the octahedral field. But these are not common occurrences and examples of such unusual cases are hydroxyphenyloxazolone, α-amino-carboxylate, and α-hydroxyimidazole moieties.[61] Coming back to the ideal hexadentate coordinating siderophores, they are synthesised by special domains of enzymes called 'nonribosomal peptide synthases' (NRPSs). The siderophore biosynthesis involves the elongation of peptide chain, formed through a linkage

of amino acids facilitated by thioester residues, in whole coordinated by NRPs. Then, the formation of chelating sites that are able to coordinate iron occurs. For instance, in the case of hydroxamate group formations, the functional groups are provided by ornithine or lysine side chains. The amino acids are acylated *via* formate, acetate or the C-terminal side of peptide catalyzed by monoxygenases.

1.7.1. Transportation of iron-siderophore complex across bacterial membrane

After the release of siderophores by bacteria in extra-cellular medium to coordinate with the Fe(III) ions, a Fe(III)-siderophore complex is formed, that is actively transported to the cytoplasm. But owing to the highly rigid defence barrier of OM of GNB provided by bilayers of complex LPS and peptidoglycans, this transportation comes as a challenge for bacteria itself. OM prevents the entry of bulky molecules, only permitting the small hydrophilic molecules.[53] Fe(III)-siderophore complex especially finds it difficult to diffuse past the outer membrane because of its higher molecular weight, making it bigger than the size compatibility of pores. Thus this Fe(III)-siderophore complex uptake is coordinated through a system of energy-dependent processes facilitated by specific carrier proteins such as periplasmic binding proteins (PBPs), the TONB protein complex, outer-membrane receptors (OMRs) and the ABC-type transporters.[56, 61] The pathway discussed here is a generalized idea based on the two well-studied, characterized and identified siderophores of GNBs, *E. coli* and *P. aeruginosa.*

Due to the inability of a siderophore complex to penetrate the OM, it is recognized by OMRs, which have high affinity towards these complexes. So, they bind to the complexes and are transported inside the bacterial membrane directly to the periplasmic space from the extracellular medium.[60] The homologous proteins of OMRs of *E. coli* and *P. aeruginosa* are FepA, FhuA, FecA, and FpvA. Their domains have been shown to possess structural similarities, proved through characterization by X-ray crystallography.[63] Though this step is comparatively straightforward and made easy by affinity of the OMR proteins towards siderophore complexes, it gets energy-dependent from here onward to transport to the cytoplasm across the periplasmic space.[64] In order to promote the transportation of the complexes actively to the cytoplasm across the OM, metabolic energy is required which is not available with OM receptors. The required energy is provided by the cytoplasmic membrane

"proton motive force", facilitated by the transducing ability of proteins of TonB complex (**Fig. 14**).[65] TonB protein complex is a group of cytoplasmic membrane complex consisting of proteins, TonB, ExbB, and ExbD. They are more like transmembrane proteins, as they also cover the periplasm. Precisely, they serve as an energy transducer, in transferring the energy from cytoplasmic membrane to the required OM inner surface.[66] In order to facilitate this energy transduction, the N-terminal of TonB conjugates with domains of ExbN and ExbD. The C-terminal domain of Ton B then binds with N-terminal domain of OMRs, to which the siderophore complex is already bound, thereby forming the bridge to facilitate the transfer of energy.[67] This results in the cleavage of the Fe(III) siderophore from the surface of OMRs, to reach the cytoplasmic membrane, where they are in turn bound by PBP upon recognition, resulting in a Fe(III)-siderophore-PBP complex. ABC-type transporters are present in this membrane. These transporters facilitate the ultimate active transportation of the Fe(III)-siderophore-PBP complex across the cytoplasmic membrane into the cytoplasm.[65] They are also involved in the elimination of PBP substrates through pumping energy provided by ATP hydrolysis. Upon entry in the cytoplasm, Fe is freed from the siderophore complex through a reductive mechanism. The enzyme iron reductase enables the reduction of Fe(III) of Fe(III)-siderophore complex into Fe(II) ions, which are now available to be involved in the metabolism of components of cytoplasmic membrane.[68] The free siderophore, upon iron release, is eliminated through the efflux pump gradients. The alternate pathway for iron release is through a Fe(III)-siderophore complex hydrolysis catalysed by the same particular enzymes.

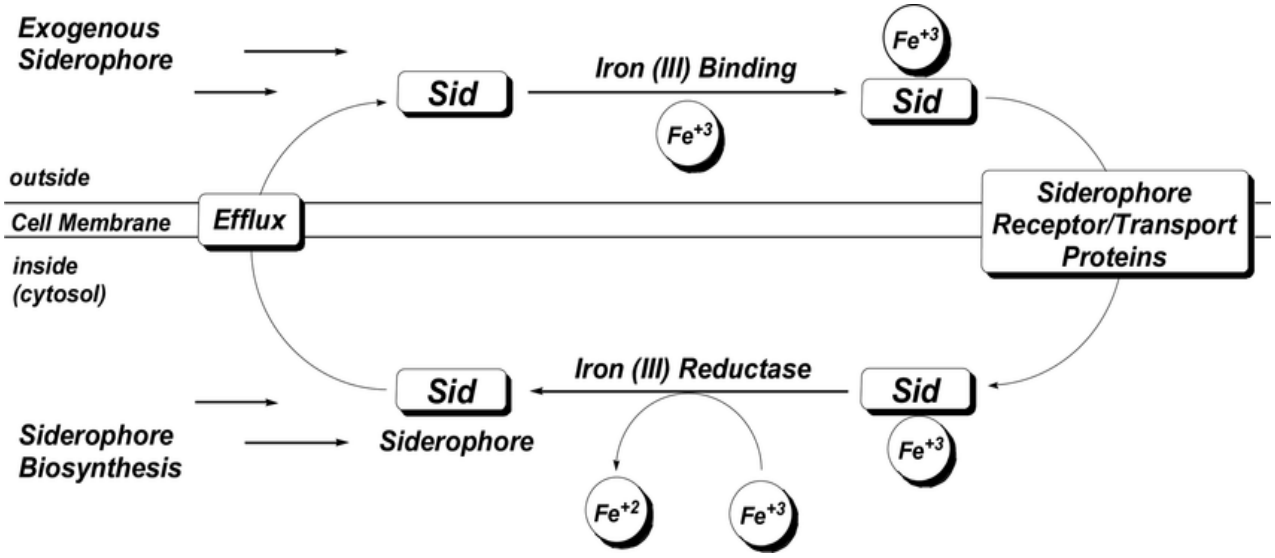

Figure 14. Schematic representation of Fe(III)-siderophore complex across bacterial OM. Scheme adopted from[61]

1.8. 'Trojan-horse strategy' for delivering drug across bacterial membrane

As described extensively in the previous section, the fact that, upon chelating, the iron-siderophore complexes are transported actively to the cytoplasm is facilitated by several proteins and transporters. The trojan horse strategy is an analogy of exploiting this iron uptake pathway for the sake of drugs.[69] By conjugating the antibiotic with the siderophore, the drug is theoretically transported actively across the OM, directly to the cytoplasm. In our case, we hypothesize that the conjugation of siderophore with the Kdo-inhibitor could deliver the inhibitor actively into the cytoplasm. The Kdo residues are primarily unable to penetrate the OM, due to its impeccable defence barrier, and even if they are able to diffuse this, they are not able to reach the cytoplasm in substantial inhibitory concentrations. The efflux receptors pump out the inhibitor to ensure the cytoplasm is protected. The Kdo mimics has to reach the cytoplasm to be involved in the lipid A-Kdo_2 biosynthesis in order to be able to effectively inhibit the rate-determining CKS enzyme. As mentioned before, after the processes in cytoplasm, lipid A-Kdo_2 is flipped across the periplasmic space to OM, to participate in the LPS bioassembly. Thus, these are the main challenges involving the inhibitory target of cytoplasmic enzyme CKS, even if the Kdo residues are active *in vitro* against the enzyme.

The hypothesis of the trojan-horse strategy involves covalent linking of the siderophore to the Kdo-inhibitor. This enables us to potentially overcome the major membrane permeability barrier of OM, along with its LPS and peptidoglycan bilayer soldiers, to smuggle the Kdo inhibitor inside the bacteria. The possibility of the undesired contact with the efflux receptors would also be tackled, to successfully transport the inhibitor in desired concentrations across the cytoplasmic membrane. Consequently, the LPS biosynthesis would be damaged upon the targeted enzymatic inhibition, leading to the weakening of the OM. Thus, the entry of antibiotics is increased, thereby making the bacteria highly vulnerable. Studies have indeed demonstrated the potential of synthesized siderophore-drug conjugates and their manipulation of iron uptake pathways to deliver the drug for treating GNB infections. For instance, the drug cefiderocol, a conjugate with cephalosporin siderophore, is used for the treatment of urinary tract infections. The infection is caused by multidrug resistant *P. aeruginosa* and *Acinetobacter baumannii.*[70] In fact, it has been clinically approved.

Generally, the siderophore-drug conjugates are built upon three components, *i.e.*, a siderophore processed by the target bacteria, a linker, and the drug or an antibacterial compound.[69b] In our research project, the potential antibacterial agent will be the synthesized Kdo-inhibitor compound. The mimics of Kdo, *i.e*, 2-d-β-Kdo and 8-amino-2,8-dideoxy-β-Kdo, are two of the known effective CKS inhibitors. These Kdo residues, that are desired to reach the cytoplasm with the aim of targeting the cytoplasmic enzymes, have to be conjugated with the siderophore *via* a linker residue. The linker residue, apart from providing a bridge to the siderophore and the Kdo compound, could also be used to control the release of the Kdo-inhibitor, providing it in free form from the siderophore complex. With the inhibitor in hand, the aspect of the siderophore and linker has to be considered based on several parameters.

1.8.1. Criteria for siderophore

The role of the siderophore component is apparent, *i.e.*, to be able to chelate with the Fe(III) ions. But apart from that, there are other important factors to be taken into consideration. We saw that bacteria have their own orchestrated mechanisms and criteria based on which they biosynthesize specific siderophores. These naturally biosynthesized siderophores are referred to as “native” siderophores. But, it is not exclusive that bacteria need to exploit only

the native siderophores for iron scavenging. They are able to uptake Fe(III) complexes formed with non-native siderophores or siderophores produced by other species. These type of siderophores are referred to as "xenosiderophores".[71] Thus, for the simplicity and sake of our synthesis of siderophore conjugates, commercially available and affordable xenosiderophores will be exploited. However, even with the commercially available siderophores, there are further parameters to be taken into account. The aim is to conjugate the linker and Kdo mimic with the siderophore. For this purpose, it is convenient if the siderophores bear suitable functional groups, such as primary amine, which can readily undergo conjugation with the functional group of linker or Kdo mimic, upon activation. The important thing to note here is that during this reaction, the overall structural block of siderophore should not undergo change, or participate in the reaction, which could potentially lead to stripping-off its iron-chelating properties, thereby placing itself in a compromising position of non-contactable by the bacterial receptors. Having checked all these boxes, the qualified siderophore has to be exploited by several pathogenic multidrug resistant GNB.

One such xenosiderophore that fits the aforementioned criteria, important for the synthesis of siderophore-drug conjugate, is desferrioxamine B (DFOB). DFOB (**Fig. 15**) is a native siderophore released by several species of bacteria but was first isolated and characterized from the actinomycete *Streptomyces pilosus* in 1958. It is a trihydroxamic acid siderophore with linear alkyl backbone. Since then, it has been widely exploited for its suitable properties in biological and chemical manipulations. From a biological perspective, it is able to chelate with Fe(III) ions present in the extracellular medium and is able to take part in the iron-uptake pathway. It is exploited by several pathogenic GNB that possess multi-drug resistance, such as, *E. coli, P. aeruginosa* and *A. baumannii*.[72] From a chemical point of view, DFOB bears one terminal primary amino group that can be used for coupling with the synthesized compounds, without being involved in iron chelation. It is commercially available as the mesylate salt of DFOB at an affordable cost. Thus, the properties of DFOB are in accordance with the expected criteria, making it suitable for our experimental purposes during the siderophore conjugates synthesis. Apart from the threshold parameters, they also have other advantages like, solubility in water and highly polar organic solvents to carry out reactions. But the experimental trails are not restricted to DFOB exclusively, as there are other possible

commercially available siderophores that are also under our consideration. Ornibactin is another commercially available siderophore with a terminal amino group, which is in fact a native siderophore of *Burkholderia* species.[73]

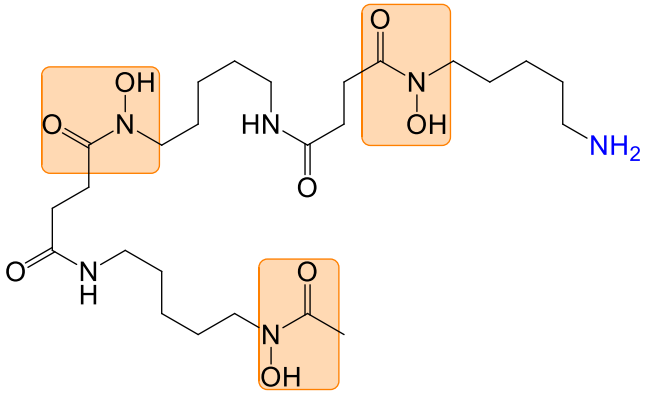

Figure 15. Desferrioxamine B (DFOB) - xenosiderophore

1.8.2. Criteria for linker

The fundamental function of a linker is to bridge the siderophore and Kdo-inhibitor. But the ability to control the toggle of the Kdo inhibitor, whether to release or not release it from the siderophore complex, plays an important role in the antibacterial activity. The drugs have proven to be fully potent in their free forms as their activity is known to be slowed down upon conjugation with siderophore, owing to the decrease in affinity of antibiotics toward the enzymatic target in cytoplasm.[69b] Thus, the linker that is able to free the inhibitor from the siderophore conjugates is preferred and is called a “releasable linker”. In recent studies by Nolan[74] and Chmielewski[75], they demonstrated that disulphide linkers are susceptible to cleavage due to reducing conditions provided by the cytoplasmic membrane. They showed that antibiotic prodrug was actively transported inside the cytoplasm *via* the iron uptake pathway. Upon its entry, the antibiotic was released inside the cytoplasm by the action of glutathione (GSH) and followed by the intramolecular conjugation to form thiol bearing carbamate ester.[76] This strategy can be used for the synthesis of releasable linker in case of the siderophore-Kdo conjugate. The potential releasable linker, thus, could consist of disulphide linkage in its alkyl chain, to be able to be cleaved, in theory, *via* reductive conditions. Along with the disulphide linkage, it needs to bear carbamate moieties, to form the thioester through intramolecular attack.[77] For this purpose, the type of functional group that can facilitate the formation of carbamate ester upon covalent linking with primary amine functional group of siderophore and Kdo residue would be bis-*N*-hydrosuccinimide (NHS)

carbonates. The NHS carbonate readily undergoes condensation with a primary amine catalysed by a base to yield the carbamate ester conjugation.[78] The terminal NHS carbonate moieties, in theory, will help in conjugation with the siderophore on one end, while with Kdo-inhibitor on the other end, thereby facilitating the bridging network. This will be the idea of the potential releasable linker. For comparison purposes, the contrary, *i.e.*, non-releasable linker must be synthesized too. The absence of a disulfide linkage with normal alkyl chain, which cannot be cleaved by the cytoplasmic condition, is called the 'non-releasable linker'. It is supposedly lesser potent than the releasable linker, making it suitable for comparison. There are other alternate type of linkers to explore. For instance, *p*-nitrophenyl carbonate bearing alkyl chain can be a valuable back-up plan, considering the stability of aromatic groups during the conjugation reaction.[79] On the other hand, the non-releasable linker does not specifically need to bear the carbamate ester moiety, since it is not subjected to cleavage. Instead the more stable and simpler amide linkage can be formed with the siderophore and the inhibitor.[80]

1.9. Peracetylated Kdo to overcome the membrane diffusion barrier

Indeed, the Trojan horse strategy of exploiting the iron uptake pathway using siderophores conceptually provides us with the solution of overcoming the membrane diffusion barrier, but as an alternate hypothesis, through simple structural modification of the Kdo inhibitor, the membrane penetration via passive diffusion could be enabled. The peracetylated sugars have been demonstrated to diffuse across the OM pores into the cystosol more efficiently, in fact 900-times more, than the unacetylated sugars.[81] The main reason for this phenomenon is that the OM prevents the entry of hydrophilic sugars, but protecting the polar hydroxyl groups with acetyl moieties, which are hydrophobic in nature, could activate the passive diffusion.[32, 82] The advantage through structural modification does not end here, as, after the diffusion across the membrane, the non-specific cystolic esterases deprotect the acetyl groups *in situ*, resulting in a free form of sugar, which is now ready in its potent form to be able to take part in its enzymatic targets.[81] Employing a similar approach, the free hydroxyl groups of synthesized Kdo-inhibitor residues can be peracetylated in order to activate the membrane diffusion passively, which in turn upon its entry inside the bacterial membrane

returns back to its original form, as a result of cystolic esterases action. Now the free Kdo-analogue is available to interact with its cytoplasmic enzymatic target.

1.10. Kdo EPS

Just like the unique sugar Kdo is present in the α-form as a member of the complex polysaccharide network of bacterial LPS, likewise, the β-form of Kdo is found in another polysaccharide called exoplysaccharide (EPS).[83] EPS is expressed in the biofilm of GNB belonging to the genus *Burkholderia*, such as *B. pseudomallei, B. mallei* and *B. cepacia* complex (**Fig. 16**).[84] Similar to LPS, being a key 'surface-exposed' polysaccharide that serves as backbone of OM of GNB, EPS is a key polysaccharide for the biofilm of GNB.[85]

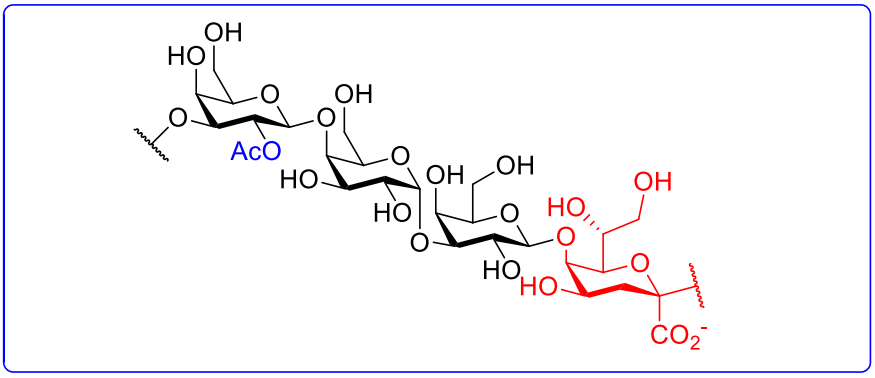

EXOPOLYSACCHARIDE (EPS)
→3)-2-*O*-Ac-β-D-Gal*p*-(1→4)-α-D-Gal*p*-(1→3)-β-D-Gal*p*-(1→5)-β-D-Kdo*p*-(2→

(EPS is expressed by: *B. pseudomallei*, *B. oklahomensis*
B. ambifaria, B. cepacia, B. dolosa, B. stabilis)

Figure 16. Structure of Kdo EPS

These are some of the most notorious human pathogenic bacteria. Specifically, *B. pseudomallei* and *B. mallei* are classified as Tier 1 select agents and toxins by the US Centres for Disease Control and Prevention (CDC),[86] which is a top-priority list that includes other notorious pathogens like Ebola virus, *Yersinia pesitis*, and *Bacillus anthracis*. *B. pseudomallei* is a pathogenic bacterium that is found in the soil of tropical countries of the southeastern part of Asia such as Thailand, India and is associated with the deadly infectious disease that is melioidosis (**Fig. 17**).[87] Similarly, *B. mallei* is the causative agent of glanders. These are not infections to be taken lightly, as some of the symptoms may include pneumonia or septicaemia. With a mortality estimated to 89,000/year (recorded data as of 2015), which is

higher than several infectious diseases for instance dengue, high level of resistance to antibiotics, they are also considered as potential bioterrorism agents (category B).[88]

Figure 17. *B. pseudomallei* that cause melioidosis are found in the soils of tropical countries such as Vietnam, Thailand

Though *B. mallei* is found to infect mostly horses, they still possess a threat to humans, and have been exploited as biological warfare agents during World Wars I and II. *B. pseudomallei* has also been experimented as a biological warfare agent.[86] They bear similarity in damaging the respiratory tract. Likewise, the species belonging to *B. cepacia* complex are the causative agents of fatal infections of the respiratory tract in people affected by cystic fibrosis (CF) called 'Cepacia syndrome'.[89] Just like the other notorious members of *Burkholderia* spp., *B. cepacia* complex also pose a problem of high resistance against antibiotics. Unfortunately, there are no therapeutics or vaccines available to treat these major infections.[90]

During the bacterial invasion in the host system, biofilms are produced by the bacteria as a survival tool as well as providing defence and necessary hydrophilic conditions.[90a] This can be analogized with the LPS of asymmetrical bilayer of OM that provides defence barrier and helping the bacteria in surviving the immune attack of a host system in the extracellular medium. The acidic β-Kdo containting EPS (Kdo-EPS) constitutes the major portions of these biofilms specifically in *B. pseudomallei* and *B. cepacia* complex (that include but not limited to *B. ambifaria, B. dolosa, B. stabilis* and *B. cepacia*).[85, 91] Though, the area of Kdo-EPS and its biosynthesis, the enzymes involved, are still being studied and explored, but it has been found that Kdo transferase enzymes do play roles in Kdo-EPS biosynthesis. Similar to the development of inhibitors of CKS associated with virulence LPS, gaining access to the β-Kdo residues and developing inhibitors of Kdo transferase enzymes involved in the biosynthesis of

virulence Kdo-EPS would provide us with potential antibiotic adjuvants or antibacterial agents against these deadly bacteria. EPS inhibition would consequently lead to the biofilm inhibition, which ultimately ignites the weakening of the bacterial defence against antibiotics and/or its surviving ability against the immune cells of the host system.

1.10.1. Kdo glycosides - as potential inhibitor of Kdo-EPS processing enzymes

In connection to this β-Kdo containing Kdo-EPS, Gauthier *et al.* recently developed a sequential methodology for the stereoselective synthesis of β-Kdo glycosides.[92] To overcome the challenges associated with β-Kdo glycosylation, they exploited the presence of a participating 4'-methoxyphenacyl (Phen) auxiliary group at C1 position of peracetylated β-Kdo thioglycoside donors. Having tried several conditions and solvents, with the glycosylation reactions promoted by NIS/AgOTf in acetonitrile as the solvent, it afforded the products in good yields and β-selectivity. They reacted the synthesized phenacyl containing thioglycoside donors with a series of acceptors consisting of several types of alcohols ranging from primary to secondary and to tertiary alcohols to obtain a series of Kdo glycosides. For comparison purposes, the glycosylation reaction was also carried out with glycoside donors containing non-participating benzyl ester groups at C1 carbonyl position.

The synthesized Kdo glycosides, as part of the stereoselective synthesis, were tested for their inhibition activity against biofilm containing Kdo-EPS of *B. cepacia complex* and *B. ambifaria,* in collaboration with Prof. Éric Déziel, (INRS) with the anticipation that these glycosides could serve as Kdo mimics inhibiting the Kdo transferases enzymes involved in the biosynthesis of Kdo-EPS.

For this assay, the bacterial strains containing Kdo-EPS were grown as mucoidal colonies. These shiny mucoid colonies of the strain were incubated in the presence of synthesized Kdo glycosides compounds dissolved in DMSO. They were also incubated, for comparison purposes, without DMSO. The takeaway from this experiment was that the growth and shiny texture of mucoid colonies were inhibited in dishes containing some of the Kdo-compounds (active compounds) which turned out to be in coherence with the formulated hypothesis. Out of all the tested compounds, the compound consisting of mixtures of anomers of Kdo-glycosides containing benzyl ester of 2-adamantyl moiety were the most active, showcasing

their ability to inhibit mucoidy compared to other Kdo analogues. However, since the compounds were tested as mixtures of anomers, a better picture of the influence of anomers was required. As we have seen the influence of anomeric effect in biological functions, it is highly important to test these compounds separately as particular forms of anomers of Kdo-adamantyl derivative (α and β) to explore more on this inhibition activity and find out more information of the parameters influencing the inhibition activity.

But even with the data of testing the specific anomers of compounds individually, it would not provide us with sufficient proof that the Kdo-analogues are actually inhibiting the Kdo transferase enzymes involved in the biosynthesis of Kdo-EPS. There is a possibility that the mucoid-inhibition activity caused by the Kdo-analogues can be due to the inhibition of other enzymes. In order to provide us with desired quantitative data and evidence that the bacterial strain expresses the expected Kdo-EPS in their mucoid forms and that the tested Kdo-analogue compounds inhibit the enzymes responsible for this Kdo-EPS formation, we will attempt to make use of the click-labelling of live bacteria using kdo-azide.

1.11. Glycan labelling

The molecular imaging or labelling of biological molecules is a key tool to visualise and study the cells and their structures. Biomolecules such as DNA, RNA, and other proteins are visualized using 'fluorescent protein fusion'.[93] But this technique of visualisation is limited to proteins and does not extend to a wide range of biomolecules such as glycans because of the inability to manipulate their genetic sequences or genomic coding, unlike DNA and proteins. It is important to visualize and study glycans in their wide range of participation in biological activities.[94] For example, cell-surface glycans are involved in the metastasis of cancerous cells. This mechanism can be visualized through the incorporation of a chemical reporter using biorthogonal chemistry and covalently activating the receptor with an imaging probe which enables the labelling.[95]

Biorthogonal chemistry involves the concept of carrying out chemical reactions in living cells, without disturbing the biological environment.[94b, 96] One of the most effective and efficient tools that facilitates the biorthogonal chemistry is 'click chemistry'. 'A chemical reporter' is a

ready-to-react molecule that is incorporated into the glycan. This is based on the biosynthesis of an 'unnatural monosaccharide' that is assimilated during the modified cellular process. Once the chemical reporter is assimilated *via* metabolic labelling, it can be 'clicked' with an imaging probe such as fluorescent probes containing chemically suitable functional groups, which enables the visualisation of glycan. One of the most suitable functional groups has been determined to be the azide-bearing reporter that can be reacted with an imaging probe containing a cyclooctyne functional group. This type of biorthogonal chemicals, which do not interfere with the cell metabolism, is termed as strain-promoted azide-alkyne cycloaddition (SPAAC). Using this type of click chemistry, several surface-glycans have been visualized.[93a, 97]

1.11.1. Click-mediated glycan labelling for Kdo EPS visualization

Further stretching this technique of metabolic modification in bacterial lipopolysaccharides, Dumont *et al.* demonstrated the click-mediated labelling of LPS of *E. coli*.[13] Having explained enough about the role of Kdo and its important role in LPS biosynthesis and providing access to the inner core, Kdo was again targeted here for the labelling of LPS through modification of polysaccharides. As discussed in the LPS biosynthesis, the free Kdo is formed via Kdo pathway, starting from arabinose-5-phosphate. The free Kdo goes on to attach with CMP to form CMP-Kdo, which is essential for LPS biosynthesis. When the modified Kdo mimic, containing the biorthogonal azide functional group (8-azido-8-deoxy-Kdo), is incorporated into the LPS of *E. coli*, it was assumed to be involved in the LPS biosynthesis, replacing the naturally formed free Kdo. Through the azide-alkyne chemistry, the Kdo was reacted through treating with a fluorophore under Copper-catalysed Alkyne Azide Cycloaddition (CuAAC). The bacteria, in presence of 8-azido-8-deoxy-Kdo (8-d-N_3-Kdo) was found to be visualized by fluorescence, thereby labelling the LPS of *E. coli*, as well as other pathogenic GNB (**Fig. 18**).

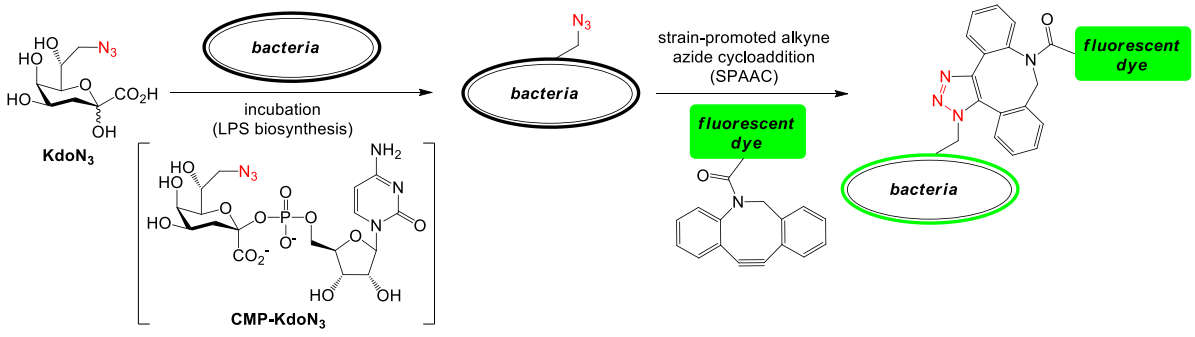

Figure 18. Click-mediated live labelling using 8-d-N_3-Kdo[13]

A similar labelling technique could be exploited with the Kdo-EPS of *B. cepacia* complex, by metabolically assimilating the Kdo-azide and incorporating it into the bacterial membrane and activating it. The plate coated with the *B. cepacia* strain could be incubated in the presence of synthesized Kdo-azide. By taking part in the surface polysaccharide biosynthesis, the Kdo azide would be assimilated in the Kdo EPS of bacterial OM, replacing the native free Kdo. Upon incubation, the colonies would contain the chemical receptor Kdo-azide residue. The latter could be activated by carrying out click chemistry, coupling the dibutyl cyclooctyne (DBCO) fluorescence dye with the azide moiety of Kdo via SPAAC. Upon activation, the OM could now be visualized, by proxy, Kdo-EPS could also be visualised. Carrying out extraction procedures to isolate the EPS from the bacterial colony could yield the labelled EPS. When the labelled Kdo EPS is incubated in the presence of the Kdo analogues, the mucoidy inhibition activity will commence. After activation and visualisation, conceptually, we are supposed to see less fluorescence as a result of inhibition. Through this way, by comparing the Kdo-EPS fluorescence, we can calculate the percentage inhibition of Kdo EPS, potentially giving us the data with evidence. Once incorporated and activated through click chemistry, they can potentially give a number of inferences, including the proof that Kdo analogues are inhibiting the enzymes involved in the biosynthesis of Kdo-EPS and also the quantitative data, of how much of the inhibition takes place.

1.12. Hypothesis and objectives

The core theme of the MSc project is to develop (or improve) sequential methodologies for the synthesis of analogues of Kdo derivatives. These novel derivatives, which are in turn mimics of naturally occurring Kdo, are sought as potential inhibitors of Kdo processing-enzymes involved in the biosynthesis of α- and β-containing surface polysaccharides (LPS and EPS, respectively) expressed by human pathogenic GNB.

The Kdo-processing enzymes targeted in case of endotoxin LPS is the CKS, which plays a major role in their biosynthesis. Hence the aim is to synthesize potential inhibitors of this particular enzyme. There are known analogues of Kdo, for instance 2-d-β-Kdo that have been synthesized to inhibit CKS and they turned out to be a highly short-term solution, with their own limitations that include mainly membrane diffusion barriers. That is why we hypothesize that the conjugation of this Kdo-inhibitor to a siderophore molecule would enable the exploitation of the iron uptake pathway of siderophore complex via the Trojan-horse strategy. The complex would be processed by bacterial transporters, thereby overcoming the membrane diffusion barrier and consequently enhancing the delivery of novel Kdo derivatives. Although the CKS inhibitors that are going to be synthesized are known derivatives in literature, they come with their own set of challenges, as these synthetic pathways go way back, and there are no proper known pathways in recent times. Having mentioned that, the development of synthetic pathways is not completely reminiscent of the ones of literature, as new pathways with modifications in most of the steps were carried out. The siderophore-Kdo conjugate targets consists of assembling three components, *i.e*, the Kdo inhibitor, the potential releasable or non-releasable linker, and the siderophore. With Kdo residues being synthesized through the developed pathway and siderophore being commercially available, the carbamate bearing potentially releasable linkers will be synthesized in two steps starting from commercially available diol compounds. The ultimate conjugation of these compounds leading to the synthesis of siderophore-Kdo conjugates has not been developed yet as far as we know.

An alternate hypothesis to overcome the challenging membrane diffusion barrier is to synthesize peracetylated analogues of 2-d-Kdo. This is based on the hypothesis of taking

advantage of passive diffusion of comparatively hydrophobic acetyl moiety, thereby increasing the efficiency of the diffusion of inhibitor compounds.

The enzymes involved in the biosynthesis of β-Kdo containing EPS, expressed in certain bacterial biofilms, are the inhibitory targets. They are again mimics of Kdo, but unlike the 2-d-Kdo and specifically β-anomeric form in case of CKS enzyme of LPS, here they are Kdo glycoside derivatives. Kdo bearing donor moiety at its anomeric position were synthesized to carry out the glycosylation with different adamantane derivatives in order to generate a mini-library of Kdo-adamantane analogues. These synthesized compounds were tested for their EPS inhibition activity against particular strains of pathogenic GNB in collaboration with Prof Éric Déziel's group.

The final objective of synthesizing Kdo mimics is to incorporate them in the bacterial LPS in order to enable the live-labelling of OM upon click-activation. The compounds for this purpose are the known 8-azido-Kdo with a slightly modified pathway as well as the 7-azido-Kdo, which was unknown and was synthesized through a developed sequential methodology. These compounds will enable the quantitative evaluation of inhibitory activity of Kdo compounds against Kdo-EPS. They have also been tested for their glycan assimilation and labelling in collaboration with Prof. Salim Islam (INRS).

Summarizing the whole three-fold objectives of the project, more precisely and specifically:

1) To develop a sequential methodology for the synthesis of:
   A. 2-d-β-Amino-Kdo, which is a CKS inhibitor, and its corresponding siderophore conjugate.

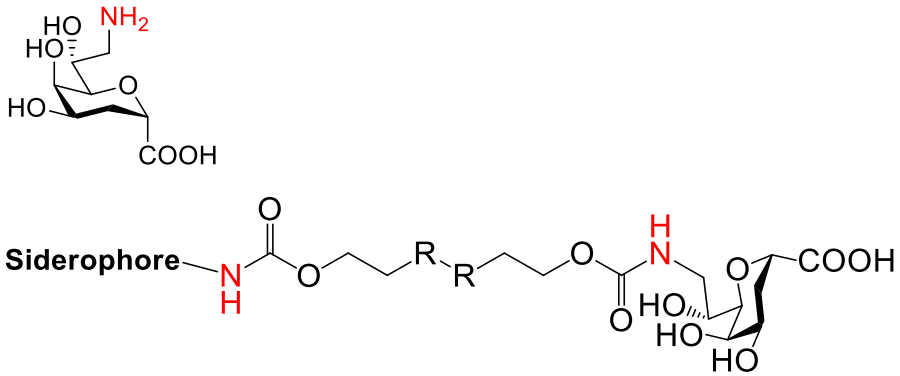

   B. Peracetylated analogues of 2-d-Kdo in both their anomeric forms.

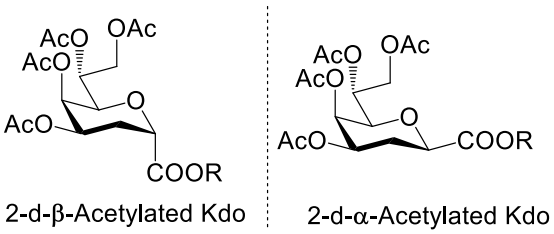

2) To develop a sequential methodology for the synthesis of analogues of Kdo-adamantane glycosides in both of their anomeric forms and to evaluate their mucoidy-inhibition activity against Kdo-EPS expressing *B. cepacia* strains.

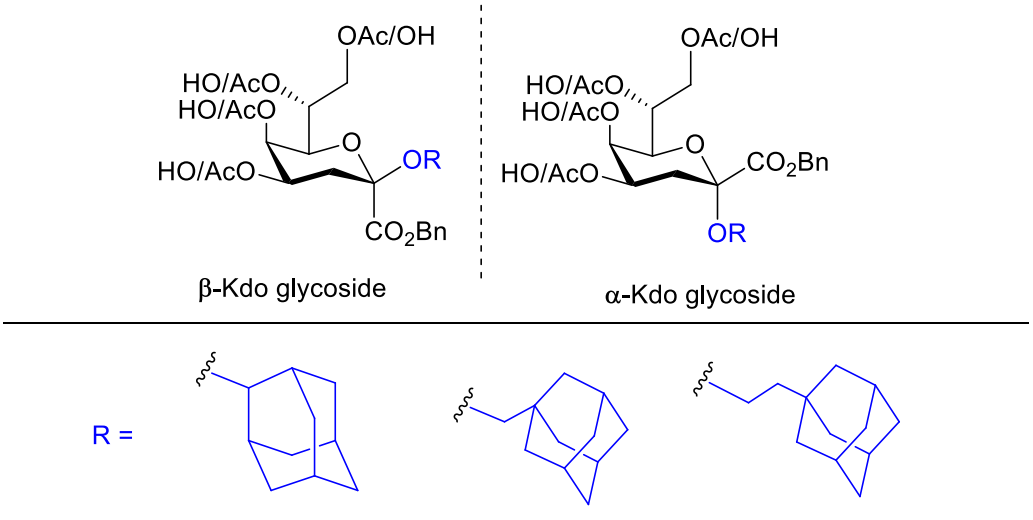

3) To develop a sequential methodology for the synthesis of 8-d-N_3-Kdo and 7-d-N_3-Kdo as potential biorthogonal 'chemical reporter' for glycan-labelling.

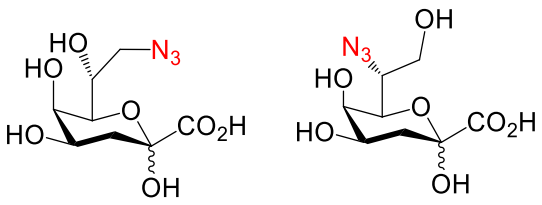

KdoN$_3$

2. Results and discussion

2.1. Synthesis of CKS inhibitors

Two analogues of Kdo, *i.e.*, 2-d-β-Kdo and 2,8-d-β-NH_2-Kdo, have been shown to inhibit the target enzyme CKS, *in vitro* (**Fig. 19**). The latter compounds are considered as the Kdo-inhibitor component of the targeted siderophore conjugates. The peracetylated derivatives of 2-d-Kdo will also be synthesized with the idea of improving the membrane diffusion of Kdo-inhibitor.

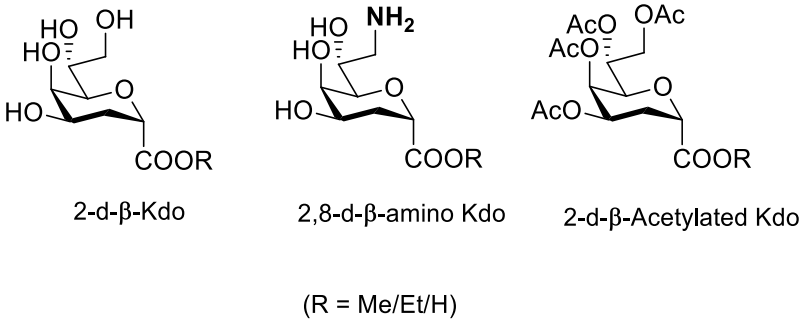

Figure 19. The targeted Kdo analogues that serve as inhibitors of CKS, along with the peracetylated analogues

2.1.1. Retrosynthetic analysis

The synthesis of 2-d-β-Kdo would guide us in the pathway of reaching the target compound 8-amino-2,8-d-β-Kdo. The reason being the structural similarity of both of the compounds, as the only difference is the functional group found at the C-8 position of 2-d-β-Kdo chain. The synthesis of protected 2-d-β-Kdo was achieved through two synthetic pathways starting from a pentose and hexose sugar, correspondingly (**Fig. 20**). In the first pathway, the starting material would be ammonium Kdo (Kdo.NH_3, **2**). Since Kdo.NH_3 is too expensive to be obtained through commercial sources, it would be synthesized *via* the Cornforth procedure, involving aldolization of commercially available and affordable D-arabinose with oxaloacetic acid. The second pathway is a lesser conventional route, commencing from commercially available D-mannose. The [6 + 2] approach of building the 8-membered Kdo skeleton from the hexose sugar mannose will be employed. The open chain structure of mannose will be elongated to 8-membered chain through a Wittig reaction. The subsequent bromide substitution would enable cyclization of the open chain to form a 2-d-Kdo pyranose ring.

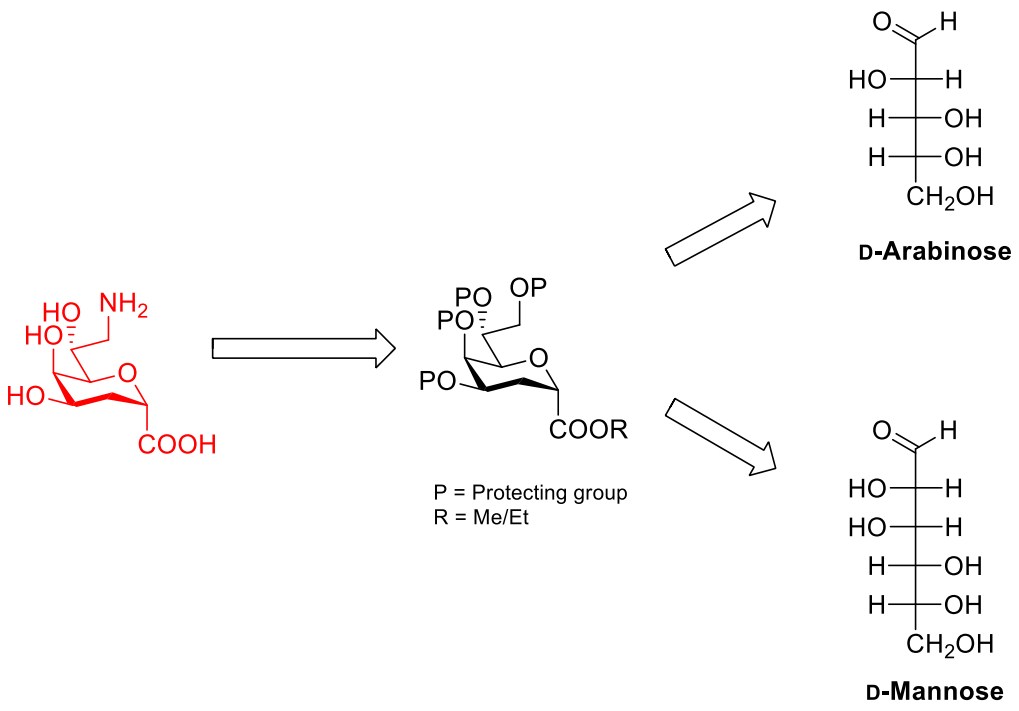

Figure 20. Retrosynthetic pathway for the synthesis of 2,8-d-NH_2-Kdo

2.1.2. Synthesis of 2,8-d-NH_2-Kdo from D-arabinose

Crystalline Kdo.NH_3 (**2**) was synthesized from D-arabinose *via* the Cornforth procedure with slight modifications (**Scheme 1**). The Cornforth procedure involved aldolization between an excess of arabinose and oxaloacetic acid under alkaline conditions.[98] That was followed by the modified decarboxylation step under slightly acidic conditions (pH = 5.7) in the presence of $NiCl_2.6H_2O$ as catalyst.[99] This is a classic example of synthesizing Kdo by a [5 + 3] approach from a carbohydrate building block. The crude product containing unreacted arabinose and both the C-4 epimeric forms of Kdo, was subjected to purification through an anion-exchange resin column. The column was performed with increasing concentrations of aqueous solution of ammonium bicarbonate as eluent, the desired *manno*-configured ammonium Kdo was obtained. The reason for the elimination of the other epimer (*gluco*-form) was the possibility of its interference in the crystallization process. The fractions with the desired form of Kdo, as verified through TLC, were pooled, freeze dried, and crystallized using absolute ethanol to obtain target compound **2** in 40% overall yield.

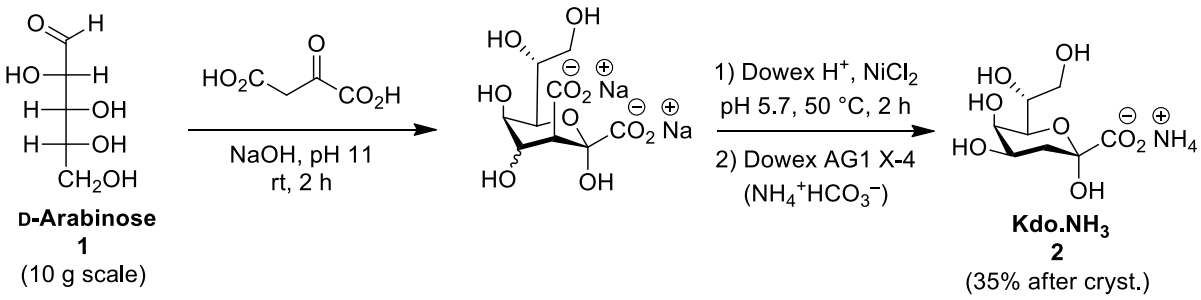

Scheme 1. Synthesis of Kdo.NH_3 from D-arabinose

Even though the α-form of Kdo featuring a pyranose backbone was obtained as the major product, in aqueous solution, approximately 30% of Kdo was present in the furanose form.[100] For the purpose of retrieving the pyranose form while protecting the hydroxyl groups, the isopropylation of Kdo.NH_3 (**2**) was performed under slightly acidic conditions provided by TsOH and in the presence of 2,2-DMP to yield the isopropylidene protected Kdo **3** in free acid form (**Scheme 2**). Due to the steric effect rendered by isopropylidene functional group at the C-3 and C-4 positions on the ring, the existing chair form of Kdo pyranose ring ($^4C_1$) is converted to boat form ($B_{2,5}$). The C-1 carboxylic acid of hemiketal **3** was transformed into a methyl ester *via* an S_N2 reaction with methyl iodide in DMF in the presence of Cs_2CO_3.[101] The methyl ester product **4** was obtained in both its anomeric forms, with the α-form being the major product. Compound **3** was used as mixture of anomers for the glycal formation step as only the major α-form can be transformed into the glycal while the β-form neither interferes nor participates in the reaction. The *trans*-configuration of OH moiety at the anomeric position of the α-form with H-3_{axial} favours the elimination to form the alkene.[102]

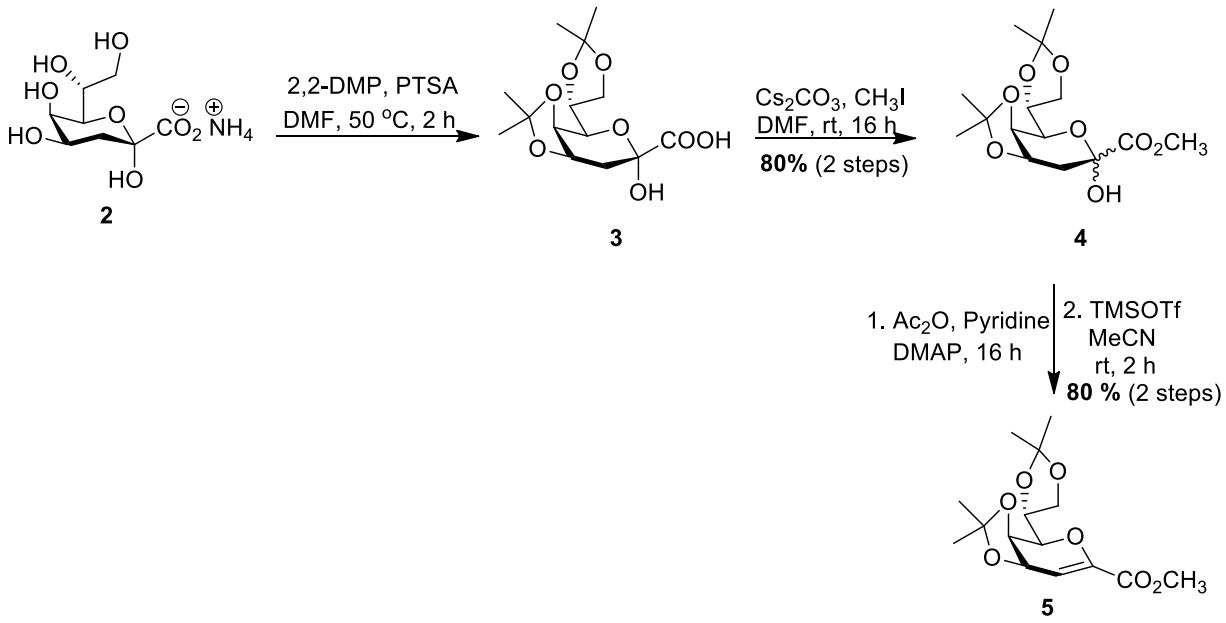

Scheme 2. Synthesis of Kdo glycal 5 from Kdo.NH3

The elimination of hemiketal **4** to form glycal **5** was performed *via* two different procedures. The first procedure involved activation by MsCl in the presence of an excess of TEA in DCM. Though it was a single-step reaction, it was moderately efficient with 65% yield. The yield was eventually improved to 80% by an alternate two-step reaction. Initially, the hydroxyl group at the anomeric position was acetylated and then subjected to elimination catalysed by TMSOTf in acetonitrile.

According to literature, reduction of Kdo glycal **5** would yield 2-d-α-Kdo derivative **6**.[103] However the olefinic bond of glycal **5** proved to be difficult to reduce using the classical Pd-catalysed conditions for hydrogenolysis (**Table 1**). Heating the reaction mixture to promote the catalysis led to degradation. However, as reported by Norbeck *et al*.,[101] hydrogenolysis of Kdo glycal **5** catalysed by Raney Ni provided the desired compound **6** in 95% yield.

Table 1. Attempts at reduction of Kdo glycal

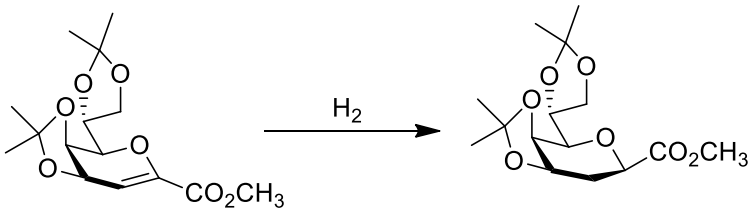

5 **6**

entry	catalyst	solvent	temp., time	yield (%)
1	Pd/C	EtOAc	rt, overnight	no reaction
2	Pd Black	MeOH	40 °C, overnight	degradation
3	Raney Ni	EtOH	rt, overnight	95[a]

[a] Isolated yield.

The α-form of 2-d-Kdo methyl ester **6** was epimerized to the β-form using LDA as a base (**Scheme 3**). The starting material was treated with LDA for 30 min at a cryogenic temperature of –78 °C. With subsequent protonation by *t*-BuOH, desired β-anomeric product **7** was obtained in 60% yield after purification. The α-form was also isolated from the reaction mixture.

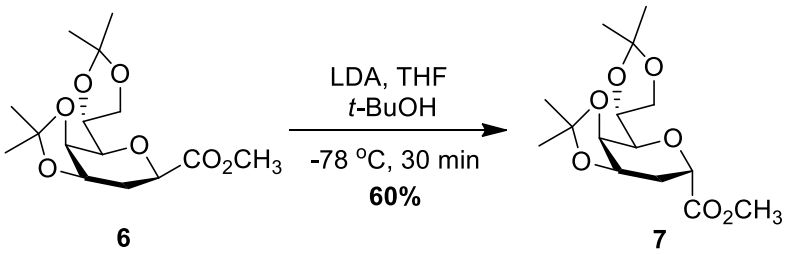

6 **7**

Scheme 3. Epimerization of 6 to obtain 2-d-β-Kdo methyl ester

With the formation of 2-d-β-Kdo, cleavage of isopropylidene protecting groups would provide an access to hydroxyl group at C-8 enabling the further insertion of desired azide moiety. Complete cleavage of both the isopropylidene groups via hydrolysis with 90% aqueous acetic acid yielded tetraol **8** in excellent yield (**Scheme 4**). The regioselective deprotection of terminal isopropylidene group yielding diol **9** turned out to be either a low yielding process or without any reaction. Hence, attempts were made to carry out the reaction in order to substantially enhance the yield.

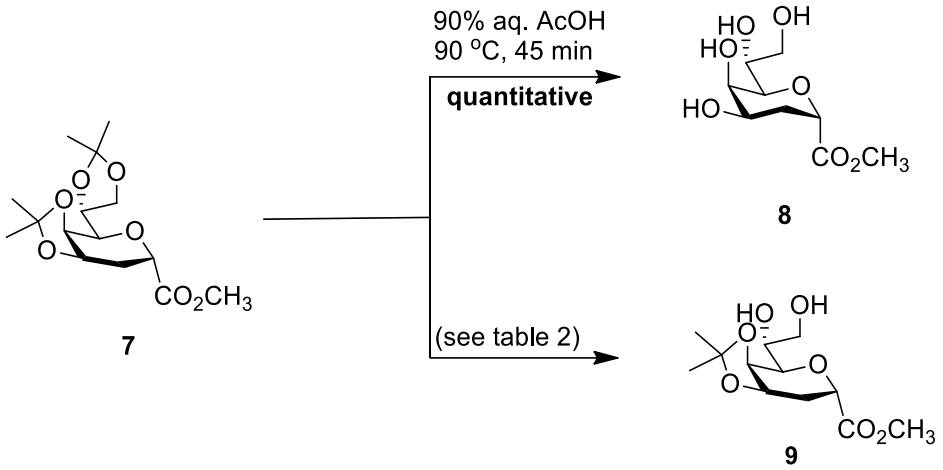

Scheme 4. Deprotection of isopropylidene group of Kdo derivative **7**

Compound **7** was treated with the reagent $Zn(NO_3)_2.6H_2O$ and the mixture was heated to 50 °C (**Table 2**, entry 1).[104] The reaction resulted in degradation of the reactant along with the slight formation of tetraol **8**. Bronsted acid reagents such as AcOH have been previously used for selective terminal hydrolysis of sugars.[105] When diisopropylidene compound **7** was treated with 60% aq. AcOH at rt, diol product **9** was obtained in 40% yield, along with hydrolysed tetraol product **8** in 60% yield (entry 2). Other subsequent attempts made with several Lewis acid reagents like $Yb(OTf)_3$, $CeCl_3.7H_2O$ either resulted in the degradation of the starting materials or low yield (entries 3 and 4). Other reagents like $CoCl_2.H_2O$ and catalytic amount of DDQ gave similar results (entries 5 and 6). The other acids such as trifluoroacetic acid and PTSA are much stronger than the 60% aq. acetic acid, which means they are not suitable for the selective deprotection of isopropylidene. Thus, the reaction with 60% aq. AcOH, though not highly efficient, was the best of the lot. To prevent the formation of tetraol in substantial amounts, the reaction was stopped after 3 h at rt, irrespective of the conversion of the starting material. The reactant compound **7** (13%), diol compound **9** (60%), and tetraol compound **8** (20%), showing marked differences in their polarity, were separated using flash chromatography and isolated individually. Based on recovery starting material, desired mono-isopropylidene compound **7** was obtained in 93% yield.

Table 2. Regioselective deprotection of terminal isopropylidene groups in compound **7**

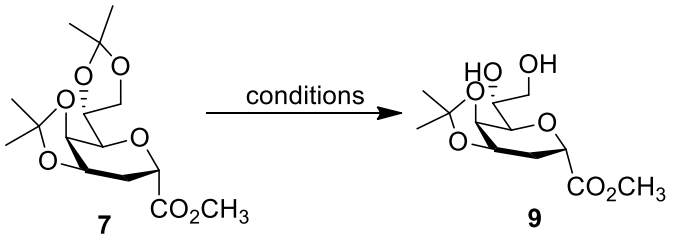

7 **9**

entry	reagent	solvent	yield (%)[a]
1	$Zn(NO_3)_2 \cdot 6H_2O$	MeCN	degradation
2	60% aq. AcOH	-	40[b]
3	$Yb(OTf)_3$	MeCN	degradation
4	$CeCl_3 \cdot 7H_2O$/ $(COOH)_2 \cdot H_2O$	rt	degradation
5	DDQ	$MeCN/H_2O$	20
6	$CoCl_2$	MeCN	no reaction
7	60% aq. AcOH	-	60[c] (93 *brsm*)

[a] Isolated yield;

[b] Overnight reaction;

[c] Three-hour reaction.

The next step was the insertion of azide functional group at the C-8 position of 2-d-Kdo as a precursor of the primary amine functionality. According to the literature, the azide moiety was introduced in the Kdo structure through a one-pot S_N2 reaction (**Scheme 5**).[106] The reagent LiN_3 along with PPh_3 and CBr_4 were treated with Kdo tetraol derivative **8** in DMF. However, due to its potentially explosive nature, LiN_3 has been ceased to be available commercially. Hence, we attempted the azide insertion reaction through currently available NaN_3, which turned out to be unsuccessful. The introduction of 15-crown-5 ether to improve the availability of azide anions did not help the process either.

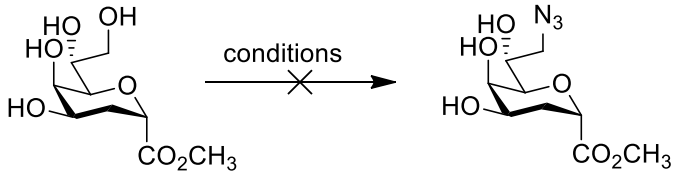

8 12

Scheme 5. Insertion of azide moiety in tetraol 8

Toluene sulphonic ester (tosyl) has been demonstrated to be a more suitable aromatic leaving group to facilitate the azide substitution. Combined with the fact that tosyl moieties show better selectivity towards attack on a primary alcohol, a two-step reaction of azide introduction was explored with tetraol compound **8.** Attempts to carry out the reaction by treating compound **8** with different number of equivalents of tosyl chloride under varying temperature and time resulted in failure as the starting material remained unreactive. A reaction with Bu_2SnO was also performed to form the tin acetal derivative. Subsequent treatment with TsCl *in situ* yielded several undesired degradation products. Tetraol compound **8** was also subjected to Tf_2O/TEA in an unsuccessful attempt to introduce triflate moiety at C-8, which is also a potentially effective leaving group.

Another possibility was to introduce the azide functionality starting from diol **9** (**Scheme 6**). Therefore, diol derivative **9** was subjected to a Dean-Stark-aided reaction with Bu_2SnO in refluxing toluene to form a 2-d-Kdo dibutyl acetal intermediate. This residue on treatment with TsCl in THF in the presence of catalytic DMAP yielded desired tosylated compound **10** in 70% yield over two steps. With tosyl substituted compound in hand, an S_N2 reaction with the known conditions of NaN_3 in DMSO heated to 90 ^oC was carried out successfully to obtain compound **11** in 90% yield.

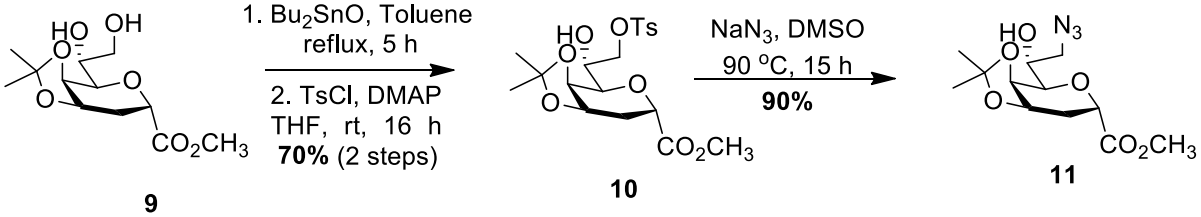

9 10 11

Scheme 6. Azide insertion in diol derivative 9

2.1.3. Synthesis of 2,8-d-NH_2-Kdo from D-mannose

The hydroxyl moieties of D-mannose were protected by isopropylidene functional groups via treatment with iodine in acetone to form derivative **14** (**Scheme 7**, represented as open-chain form). The reagent (ethoxycarbonlymethylene)-triphenylphosphorane needed for subsequent Wittig reaction was synthesized by condensing commercially available (ethoxycarbonylmethyl)-triphenylphosphonium bromide with 1 M aq. NaOH solution in DCM (**Scheme 8**).[107] The Wittig reaction of compound **14** with a stable 2C ylide unit was performed in refluxing toluene in the presence of a catalytic amount of benzoic acid.[108] Benzoic acid was added to prevent the cyclisation of the open chain into tetrahydrofuran.[109] The desired 8-membered Wittig product **16** was obtained in 98% yield accordingly.

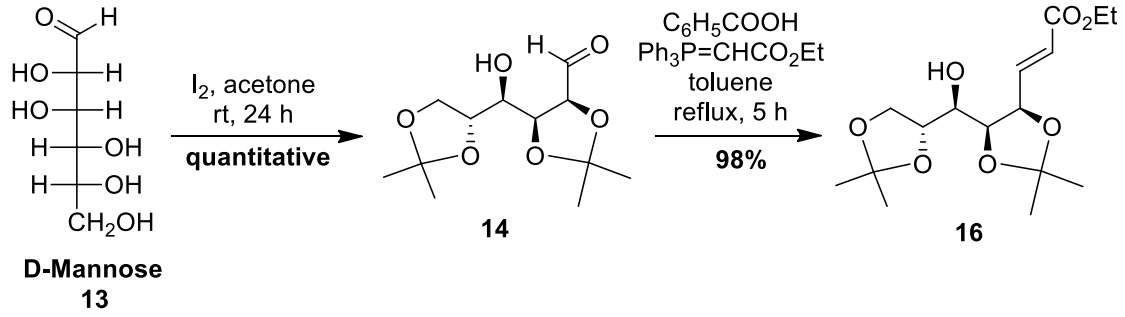

Scheme 7. Synthesis of Wittig ester 16 from D-mannose

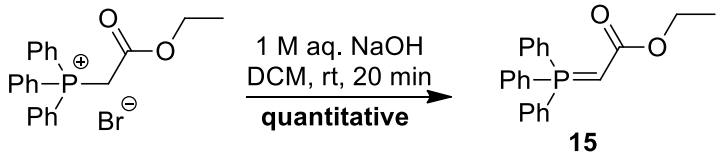

Scheme 8. Synthesis of stable phosphonium ylide **15**

The reduction of olefinic bond of ester **16** would enable the substitution of a bromide moiety at the C-2 position (**Scheme 9**). In our hands, initial attempts to reduce through conventional hydrogenolysis in the presence of Pd-based catalysts (Pd/C and Pd black) in EtOAc were unsuccessful. Changing charges of catalyst, solvent systems (to methanol and ethanol) and/or reaction temperatures all failed to promote the double bond reduction. The catalyst was then changed to more reactive Raney Nickel. When the reaction was flushed with hydrogen in ethanol overnight, it resulted in the degradation of the starting material.

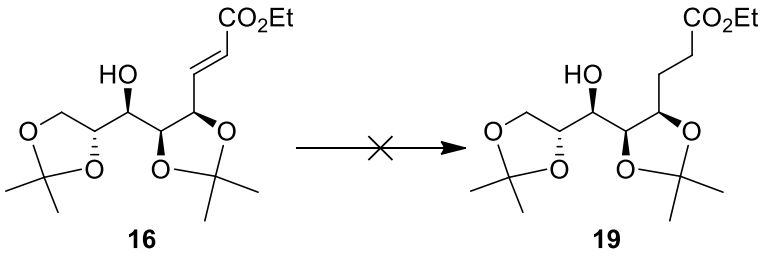

Scheme 9. Reduction of the olefinic compound **16**

The inability to reduce the double bond could be attributed to the presence of a free hydroxyl moiety. To prevent the possible interference of this moiety, it was protected with a bulky TBS group, thereby also stabilizing the compound (**Scheme 10**). TBS-protected compound **17** was subjected to hydrogenolysis in the presence of Raney Ni catalyst. The reaction at the milligram scale went on to proceed to give desired product **18** after 48 h at room temperature. But, when the reaction was performed on a multi-gram scale (15.0 g), the same conditions failed to yield the target product. The reaction was thus performed twice separately, at small scale (~8.0 g) along with heating to 40 °C. After 16 h, the starting material was consumed completely providing the expected product **18** in 95% yield. The TBS ether was deprotected using an 1.0 M TBAF solution in THF to free the C-6 hydroxyl moiety leading to compound **19** in 90% after two steps.

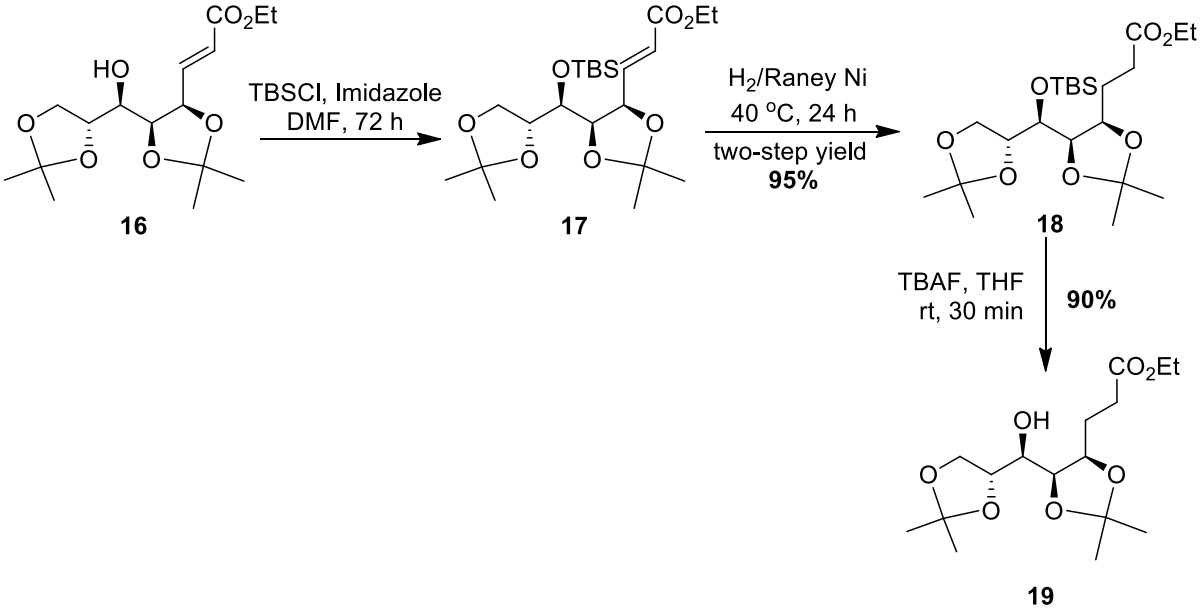

Scheme 10. Synthesis of the alcohol compound **19** through TBS protection and deprotection

The classical way of introducing TMS ether in compound **19** through the treatment of TMSCl in DMF in the presence of imidazole was a low yielding reaction. The reaction performed with hexamethyldisilazane, catalysed by TMSCl in acetonitrile, provided desired product **20** that was used for the next step without further purification (**Scheme 11**).[110] The subsequent step was the bromide substitution using NBS as bromide donor. Initially, compound **20** was treated with the base LDA at –78 ^{o}C in THF to form the enolate of lithium, *in situ.* TMSCl was also added simultaneously to counter the possible attack by LDA on the susceptible TMS moiety of the compound. After an hour of stirring, the NBS reagent was added to the mixture. A mixture of compounds was formed, as monitored by TLC, suggesting the possible formation of the bromide diastereomers. The obtained crude product **21** was utilized for next step without isolating each of the diastereomers although the crude product was subjected to a flash chromatography to eliminate the reactants and other by-products.

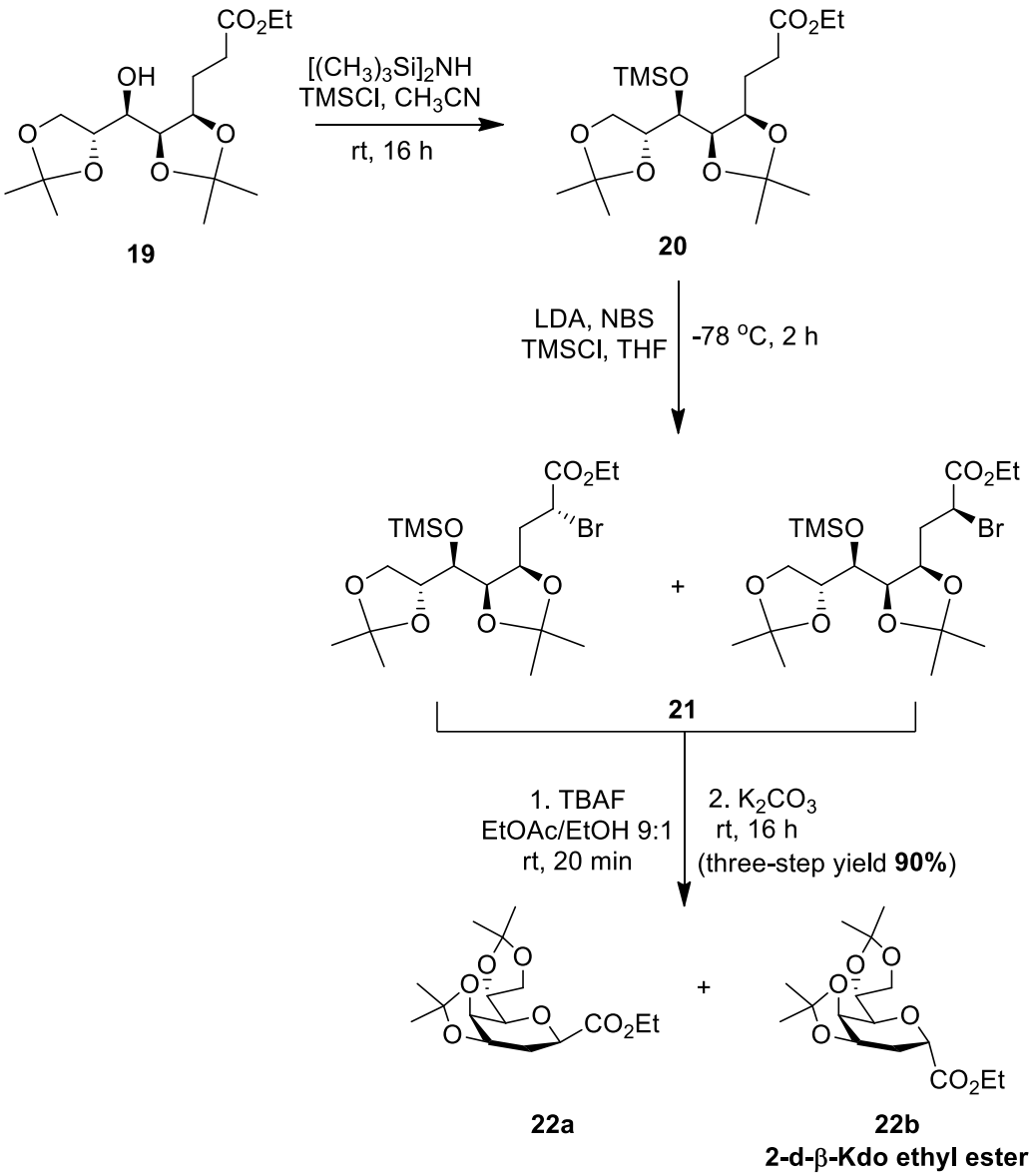

Scheme 11. Synthesis of 2-d-Kdo ethyl ester **22**

The deprotection of the TMS moiety was performed on a mixture of compound **21** using the TBAF solution. The resulting formation of bromoalcohol triggered the cyclization that was facilitated *in situ* by the addition of excess of K_2CO_3. By serving as the bromide abstractor, K_2CO_3 facilitated in unmasking the bromide anion. The two-step, one-pot reaction was performed in a mixture of solvent system, *i.e.*, EtOAc/EtOH 9:1. The presence of EtOH helped in countering the attack of the fluoride anions that could be released from the TBAF solution and thereby preventing the potential formation of undesired 5-membered furanose ring. The obtained crude product was separated through silica gel flash chromatography. The mixture

contained anomers of 2-d-Kdo, as confirmed by NMR analysis. The desired β-form of the 2-d-Kdo compound **22b** was the major product with 57% yield, while the α-form of 2-d-Kdo compound **22a** was isolated in 27% yield, with the overall yield of the two-step reaction being 94%.

Having synthesized one of the target compound, *i.e.*, 2-d-β-Kdo, the subsequent aim was to insert the azide moiety at position C-8 of the Kdo ring. The first step towards this aim was to selectively cleave the terminal isopropylidene group. As discussed in section **2.1.2**, this can be readily performed through hydrolysis in 60% aq. acetic acid solution. Since this reaction provided a moderate yield of 60%, additional conditions were experimented with compound **22b** (bearing an ethyl ester instead of a methyl ester as compared to similar derivative **7**) to improve the yield (**Table 3**).

Table 3. Attempts at the selective isopropylidene deprotection of **22b**

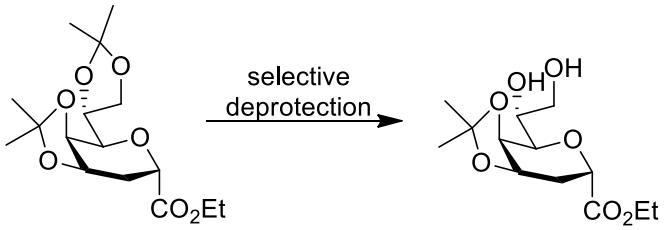

22b **23**

entry	reagent	solvent	yield[a]
1	$Zn(NO_3)_2.6H_2O$	MeCN	degradation
2	60% aq. AcOH (20 mL·mmol^{-1})	-	45
3	Dowex H^+ resin	MeCN/MeOH	30
4	60% aq. AcOH (15 mL·mmol^{-1})		57

[a] Isolated yield.

Compound **22b** was treated with a Bronsted acid reagent Dowex H^+ resin in methanol/water (9:1) mixture. The starting material was unable to convert completely. Hence, the amount of resin was increased along with the temperature of the reaction mixture. With these different conditions, the major product turned out to be the tetraol (35%) while the yield of the desired

diol was not optimal (30%). Other reagents like $Zn(NO_3)_2 \cdot 6H_2O$ showed similar results to the methyl ester of 2-d-Kdo. Finally, 60% aq. acetic acid was used to selectively deprotect **22b** with a yield of 60% for the desired diol product **23**.

A one-pot, single step, regioselective protection of the C-8 hydroxyl moiety by tosyl group was attempted on diol compound **23** (**Scheme 12**). The starting material was treated with TsCl in the presence of catalytic amounts of Me_2SnCl_2, DIPEA, and DMAP. However, the reaction did not yield the expected product.

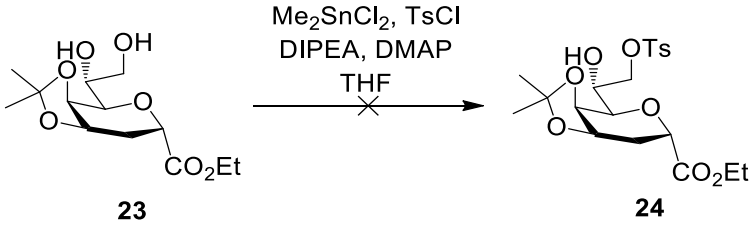

Scheme 12. Regioselective tosylation catalyzed by Me_2SnCl_2

The tosyl moiety was substituted at the C-8 position of the diol derivative **23** using Bu_2SnO chemistry such as for the methyl ester of 2-d-Kdo (**Scheme 13**). Compound **23** was refluxed in toluene with Bu_2SnO to form the dibutyl acetal intermediate. This crude residue was treated with TsCl in presence of catalytic amounts of DMAP in THF to obtain the tosyl derivative **24** in 70% yield. The reaction of the tosyl-substituted derivative with NaN_3 in DMSO yielded the target azide compound **25** in excellent yield (90%).

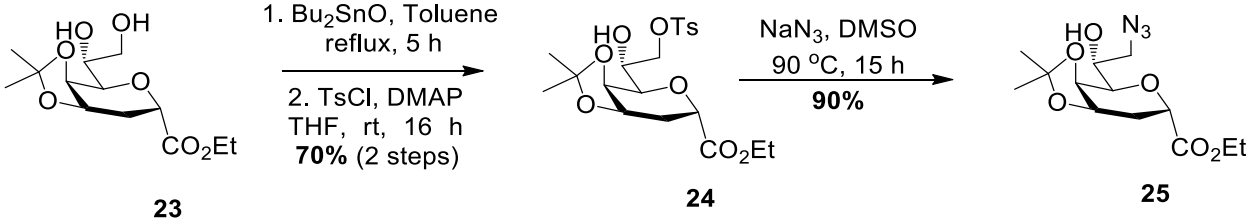

Scheme 13. Azide insertion on 2-d-β-Kdo ethyl ester

The conventional way of hydrolysing the isopropylidene ketal using an aqueous solution of acetic acid was carried out (**Table 4**). The solution of compound **25** in 90% aq. acetic acid was heated to 90 °C. It resulted in the degradation of starting material, possibly due to the unstable nature of azide moiety attached to the 2-d-Kdo ring. Hence, further conditions were experimented to obtain the product without any degradation. Treatment with Dowex H^+ resin

reagent in a methanol/water (9:1) mixture resulted in a partial conversion of the starting material. When the reaction mixture was gradually heated from 50 to 90 ^{o}C, the starting material started to undergo degradation. The conditions involving 60% aq. acetic acid in a comparatively concentrated reaction mixture (20 mL·mmol^{-1}) resulted in partial consumption of starting material. Upon gradual heating to 90 ^{o}C, complete conversion was witnessed without any visible degradation (as indicated by TLC) leading to the quantitative formation of triol compound **26**.

Table 4. Isopropylidene deprotection of azide compound **25**

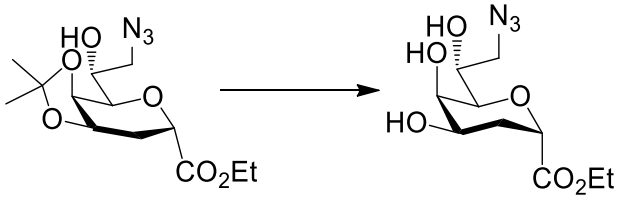

25 **26**

entry	conditions	temp., time	yield
1	90% aq. AcOH (300 mL·mmol^{-1})	90 °C, 20 min	degradation
2	Dowex H$^+$, MeOH/H_2O 9:1, 110% *wt*	rt, overnight	unable to complete
3	Dowex H$^+$, MeOH/H_2O 9:1, 110% *wt*	50 °C, overnight	unable to complete
4	Dowex H$^+$, MeOH/H_2O 9:1, 110% *wt*	90 °C, overnight	degradation
5	60% aq. AcOH (20 mL·mmol^{-1})	rt, overnight	unable to complete
6	60% aq. AcOH (20 mL·mmol^{-1})	60 °C, overnight	unable to complete
7	60% aq. AcOH (20 mL·mmol^{-1})	90 °C, overnight	quantitative

The azide moiety of compound **26** was reduced by standard hydrogenolysis procedure involving a $Pd(OH)_2/C$ catalyst (**Scheme 14**). The crude product obtained after overnight stirring and was purified by C_{18} reverse-phase flash chromatography. The final step involved the saponification of the ethyl ester moiety of amino compound **27** to obtain acid **28**. The ester was saponified using LiOH as the base in a THF/H_2O (3:1) mixture. The obtained Li-salt product was protonated by adding 2.0 M aq. solution of HCl. The target compound **28** was obtained in quantitative yield.

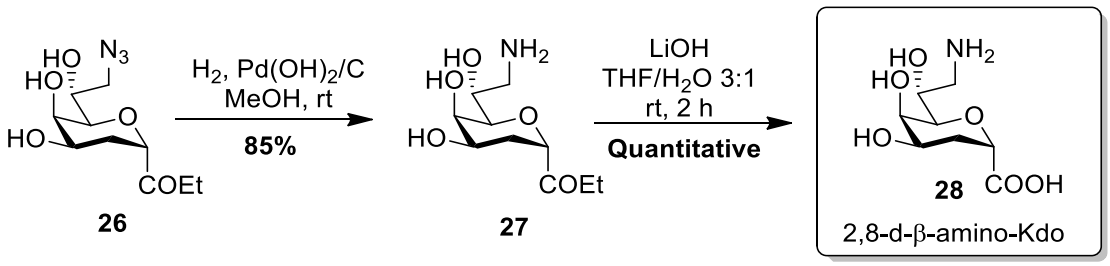

26 **27**

Scheme 14. Synthesis of 2,8-d-β-amino Kdo from **26**

2.1.4. Comparison of overall yield of the two synthetic routes

The first synthetic route commencing from D-arabinose, based on the [5 + 3] approach, led to the desired compound 2-d-β-Kdo methyl ester **7** through seven steps with an overall yield of approximately 22% (**Fig. 21**). But it was not suitably efficient to reach the target compound in substantial amounts. Moreover, the feasibility aspect of the reactions involved prevented scaling up of this scheme. These limitations were overcome by the second sequence. Starting from D-mannose, the 2-d-β-Kdo ethyl ester compound **22b** was obtained through nine steps with an overall yield of approximately 50%. Apart from the double efficiency of this scheme, the feasibility of the [6 + 2] approach made the scale-up possible leading to the target product in substantial amounts. As a result, 3.1 g of 2-d-β-Kdo ethyl ester **22b** was obtained, while currently 40.0 mg of the final compound **28** is currently available.

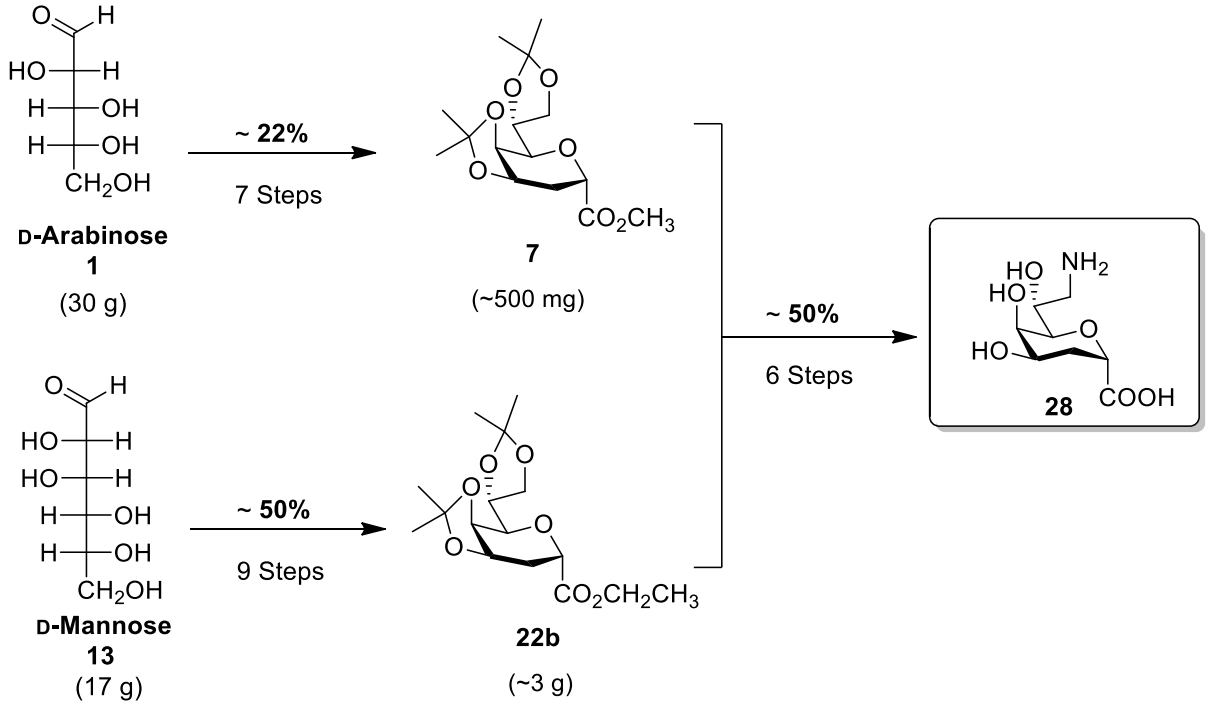

Figure 21. Global yield comparison for the synthesis of 2-d-β-Kdo residue starting from D-mannose or D-arabinose

2.1.5. Peracetylated derivatives of 2-d-Kdo

As depicted in **Scheme 15**, the isopropylidene ketals were completely deprotected to obtain tetraol compounds **29** and **30**. The latter compounds were peracetylated using standard conditions of acetic anhydride and pyridine to provide peracetylated-2-d-Kdo ester derivatives (**31** and **32**). In order to synthesize peracetylated Kdo with free carboxylic acid, esters of tetraol were initially saponified and then acetylated. The reaction conditions to transform both the synthesized isopropylidene protected 2-d-Kdo residues, with methyl ester **7** (β-form) and **6** (α-form) with ethyl esters **22a** (α-form) and **22b** (β-form) were standard, as all of the four compounds showed similar chemical behaviours towards these reactions.

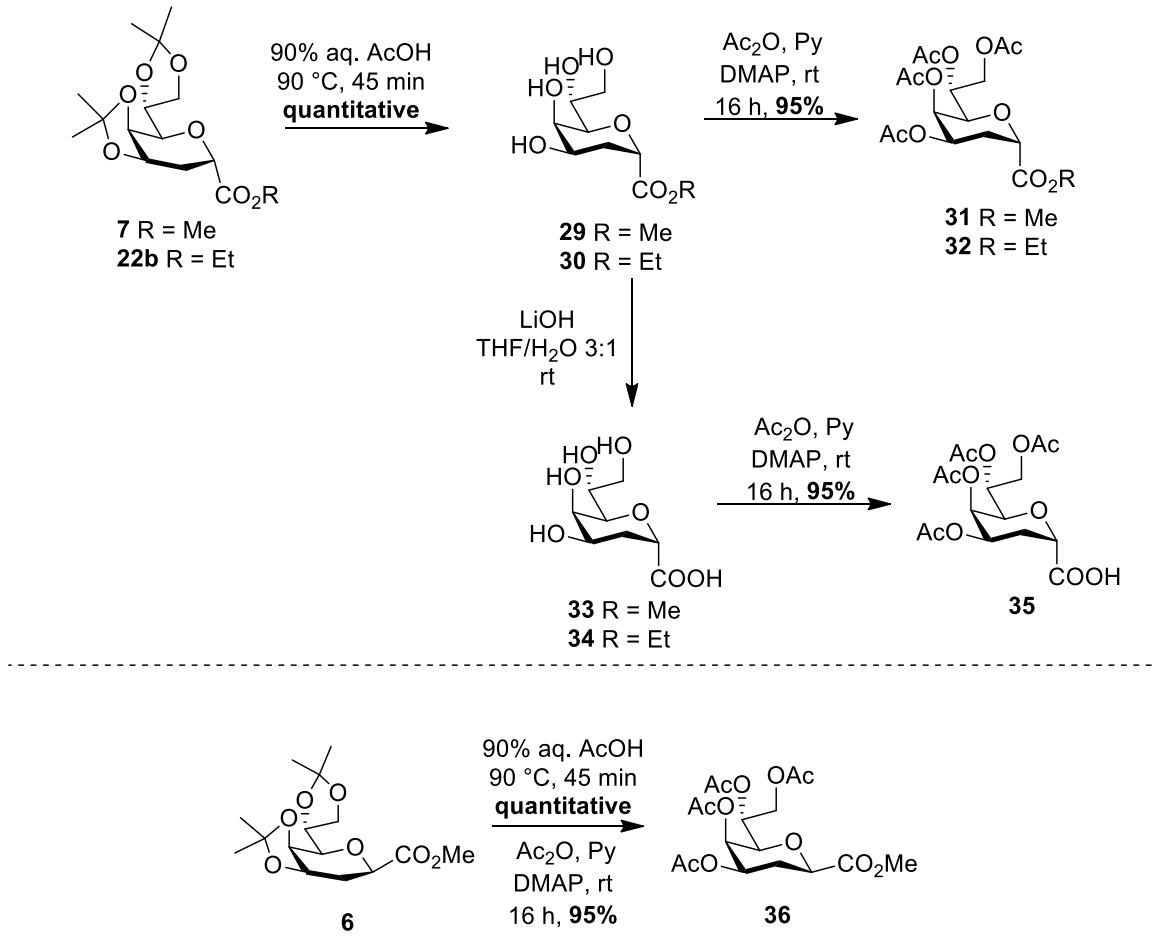

Scheme 15. Synthesis of peracetylated 2-d-Kdo derivatives

The compounds were tested for their antibacterial activity in collaboration with the lab of Prof. Eric Deziel of INRS. They used the microdilution method with ranging concentrations of the compound in DMSO, from 0.0975 µM to 100 µM in Mueller Hinton broth. The tests were done against several multidrug resistant GNB such as *P. aeruginosa* PA14, *E. coli* O157:H7, *B.*

cepacia K56-2, *Serratia marcescens* ATCC145756 and *Klebsiella pneumonia* ATCC4352. However, there was no antibacterial activity observed after shaking at 37 ^{o}C. This draws two inferences - either the Kdo residues were unable to diffuse past the OM or they were able to cross the OM and periplasmic space but unable to inhibit the target enzymes.

2.2. Synthesis of Kdo glycosides

The analogues of Kdo glycosides with three different adamantane derivatives were synthesized and isolated in both their anomeric forms separately (**Fig. 22**). These analogues were synthesized with the aim of testing them for their mucoid-inhibition activity against pathogenic strains of *B. cepacia*. As part of this, the compounds were primarily obtained in acetylated forms. Further deprotection were also carried out to explore the influence of functional groups on biological activity.

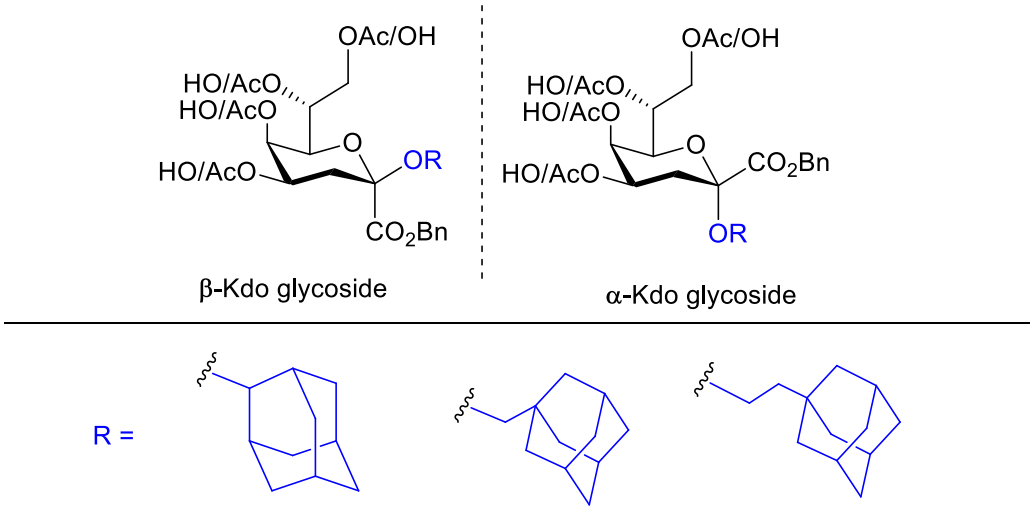

Figure 22. Kdo glycosides with adamantane derivatives

2.2.1. Synthesis of Kdo thioglycosyl donor 39

The primary precursor for this synthetic pathway was Kdo.NH_3 (**2**), which was synthesized through the modified Cornforth procedure. It was subsequently peracetylated using standard conditions involving Ac_2O and pyridine in the presence of a catalytic amount of DMAP (**Scheme 16**). The ammonium form of the carboxylic acid moiety of product **37** was converted to a non-participating benzyl ester. This was achieved using reagents BnBr and Cs_2CO_3 in DMF. The anomeric position of compound **38** was transformed into a thioglycosyl moiety by

treatment with ethanethiol in the presence of BF_3.OEt. Kdo donor product **39** was obtained as a mixture of anomers.

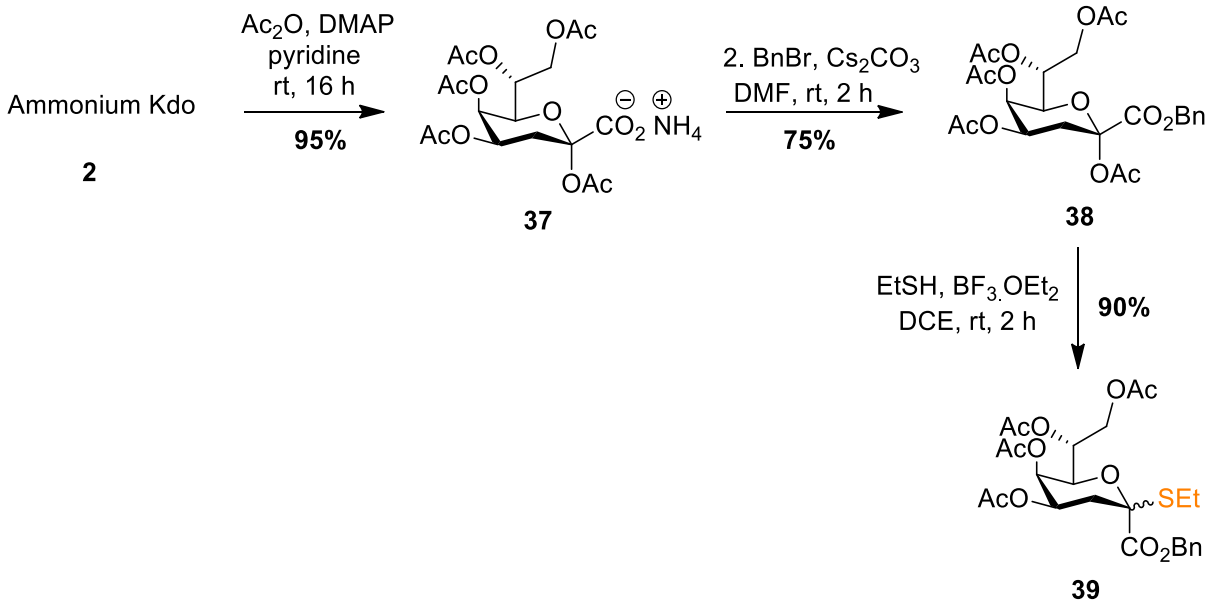

Scheme 16. Synthesis of Kdo thioglycosyl donor **39** from Kdo.NH_3

2.2.2. Glycosylation step

The first glycosylation attempt was carried out with 2-adamantanol (**43**) as an acceptor promoted by NIS/AgOTf (**Scheme 17**). The reaction was performed in the presence of powdered, activated 4 Å molecular sieves in anhydrous acetonitrile. The Kdo glycoside product **40** was obtained in a moderate yield of 50%. The yield could have been hampered by the possible interference with water molecules, either from reagents or solvent since water molecules are competitor in the glycosylation reaction. In order to improve the efficiency of the glycosylation reaction, the reagents consisting of the starting material, NIS, and 2-adamantanol were pre-dried *in vacuo*. Then, the reaction was carried out after the addition of solvent and activated powdered 4 Å molecular sieves. As a result, compound **43** was obtained in reasonable 74% yield. Similar glycosylation reactions were carried out with other acceptors, *i.e.*, 1-adamantanemethanol **44** and 1-adamantaneethanol **45**, with similar yields.

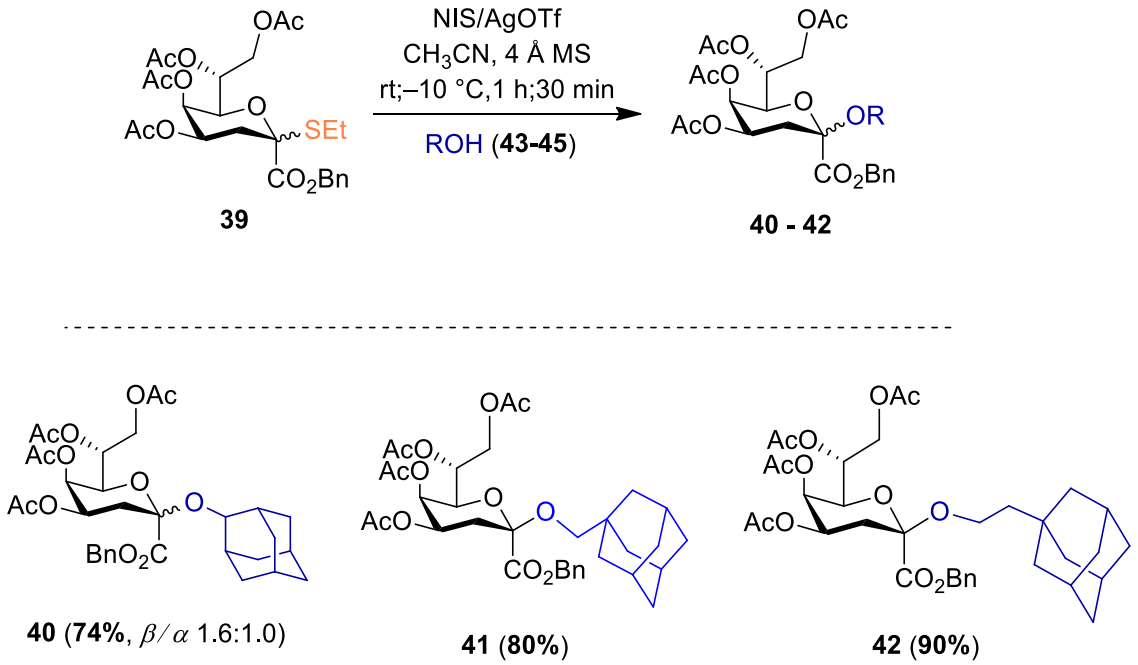

Scheme 17. Glycosylation of **39** with adamantane acceptors

For the purpose of biological evaluation, it is pertinent to isolate both the α- and β-form of Kdo glycosides separately. It was achieved through column chromatography, though the difference in polarity of the anomers were subtle. The β-form constituted majority of the crude product.

2.2.3 Deprotection of the Kdo glycosides

Kdo glycosides **40**–**42** were subjected to catalytic hydrogenolysis in order to reduce the benzyl ester (**Scheme 18**). The reaction was carried out with the mixture of the α- and β-forms in the presence of Pd/C as catalyst for 24 h yielding the free carboxylic acid compounds. There was an enhanced polarity between the anomers of the obtained crude carboxylic acid product (**46**–**48**), which were separated through column chromatography. Zemplén deprotection was utilized to deprotect the acetyl moieties. Treatment of carboxylic acid residues **46**–**48** with NaOMe gave free Kdo glycosides **49–51** in β-form exclusively. These two deprotection reactions enabled us to obtain further Kdo derivatives.

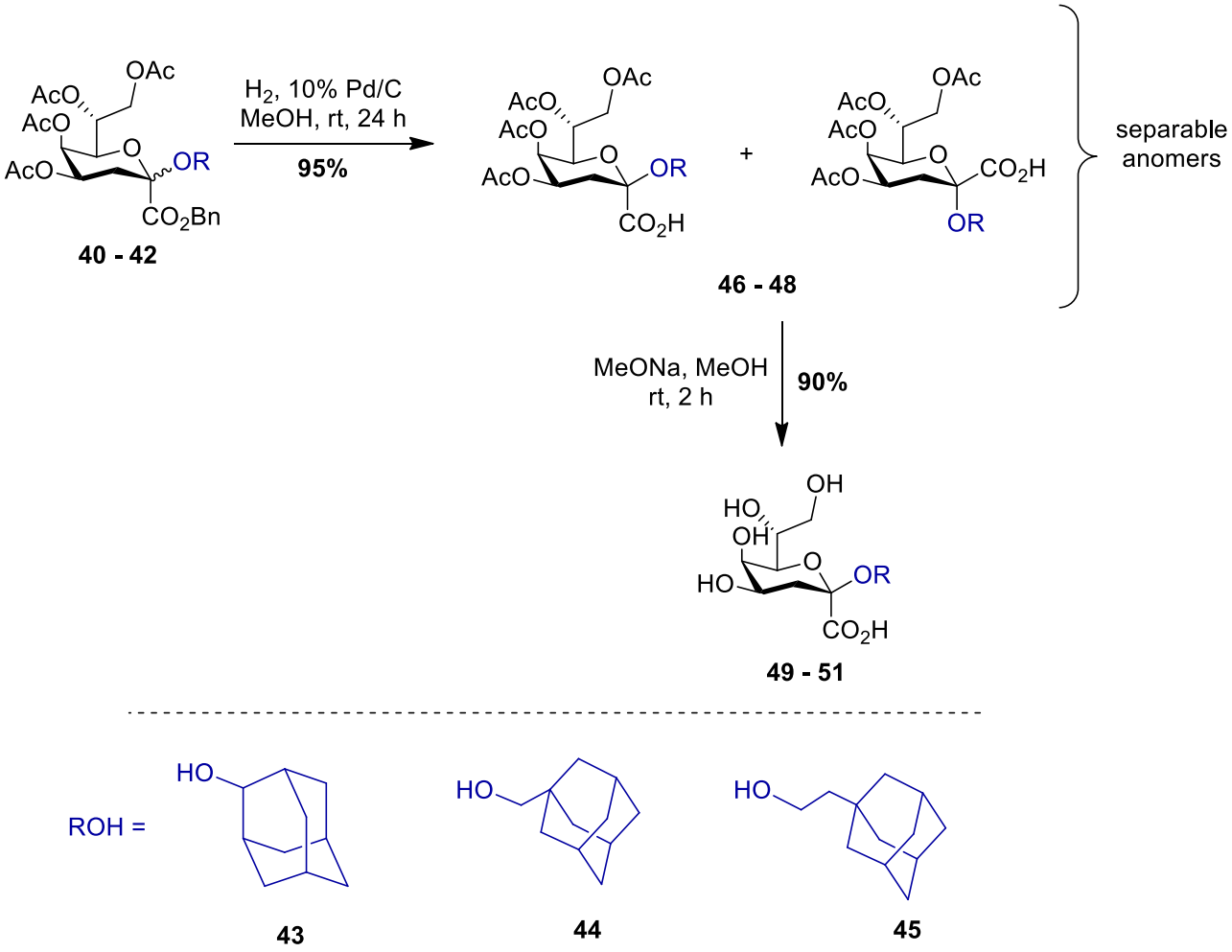

Scheme 18. Deprotection of benzyl and acetyl moieties

2.3. Synthesis of azido-Kdo

Kdo analogue (8-d-N_3-Kdo), a biorthogonal receptor, has been demonstrated to be assimilated in LPS of bacterial OM.[13] This enables the visualisation of the bacteria upon activation via click-mediated conjugation with a fluorescence dye. For the purpose of possibly exploiting a similar strategy of visualisation in Kdo-EPS of *B. cepacia*, 8-d-N_3-Kdo and 7-d-N_3-Kdo were synthesized (**Fig. 23**).

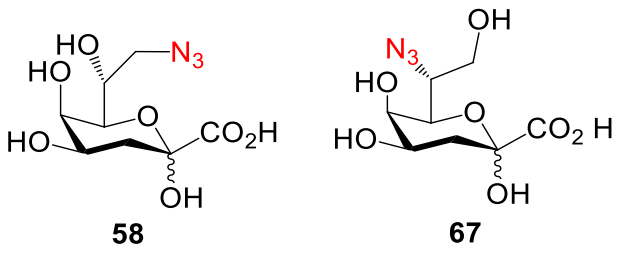

Figure 23. Structures of 8-d-N_3-Kdo and 7-d-N_3-Kdo

2.3.1. Retrosynthetic analysis

Similar to the Cornforth procedure, the Kdo scaffold would be constructed from the D-arabinose sugar (**Fig. 24**). As this is a modified analogue of Kdo with a substitution of an azide functional group at the C-8 position, consequently, the modification would be made at the arabinose level. The fact that the C-5 position of arabinose is concurrent to the primary carbon, the C-8 position of Kdo means that the modified arabinose would be synthesized with an azide substitution at its C-5 position.

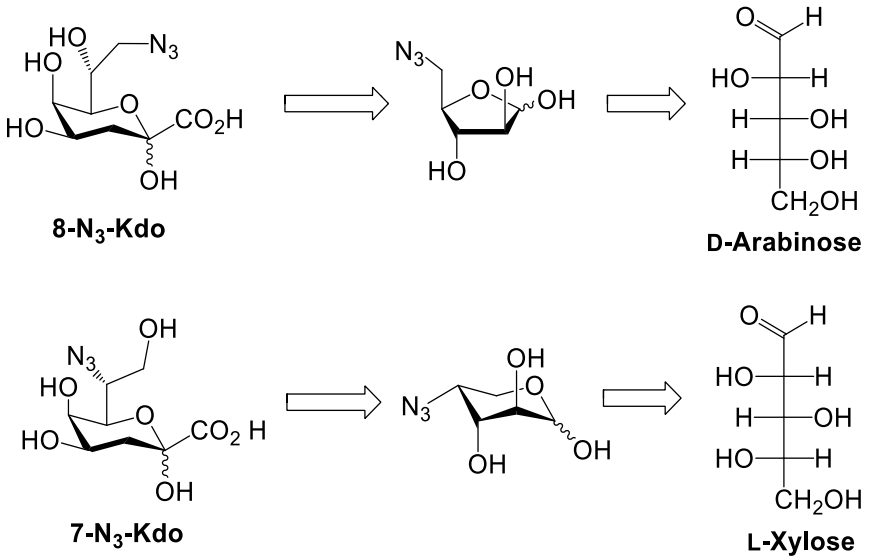

Figure 24. Retrosynthetic pathway for the synthesis of N_3-Kdo

Likewise, in the case of 7-d-N_3-Kdo, the C-4 position of arabinose is concurrent to the C-7 position of Kdo ring. The C-4 carbon is part of the ring skeleton. A change in this ring configuration changes the nature of sugar. L-Xylose is a commercially available pentose sugar and an epimer of D-arabinose. These two sugars share structural similarity overall, except the hydroxyl group at C-4 that is inverse of arabinose. With the azide substitution in L-xylose, the inversion of configuration leads to the structure of D-arabinose. This 5-d-N_3-arabinose and 4-d-N_3-arabinose will subsequently yield to the corresponding Kdo azide, when they are subjected to the modified Cornforth condensation with oxaloacetic acid.

2.3.2. Synthesis of 8-d-N_3-Kdo

The first step of this synthetic pathway commenced with the introduction of a primary-selective trityl moiety (trimethylphenyl). As a result, formation of the furanose ring was enabled, thereby accessing the C-5 primary hydroxyl moiety. The crude trityl product **52** was

directly treated with Ac_2O and pyridine in order to acetylate the other hydroxyl moieties. A carefully monitored selective trityl deprotection reaction was carried out on compound **53** by heating in a solution of 80% aq. AcOH. The obtained primary alcohol product **54** was tosylated by standard conditions of TsCl in pyridine. The tosyl product **55** was then heated with NaN_3 at a temperature of 80 °C to eventually insert the azide moiety. Zemplén deprotection of acetate groups of compound **56** ultimately led to the formation of 5-d-N_3-arabinopyranose (**57**).

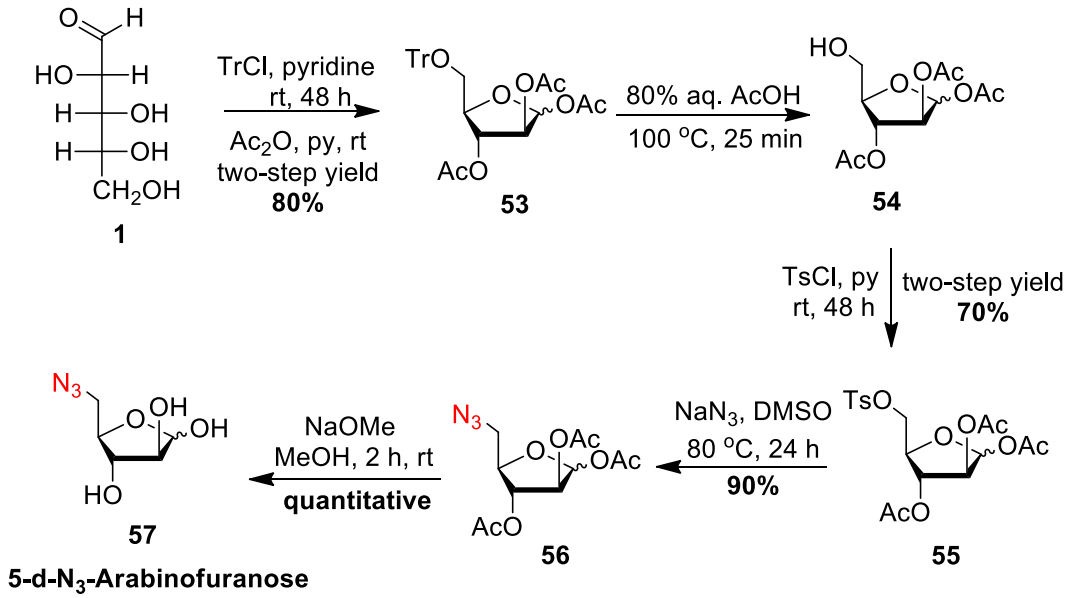

Scheme 19. Synthesis of 5-d-N_3-arabinofuranose (**57**)

Unlike the previously mentioned Cornforth procedure, which involves an excess of arabinose and oxaloacetic acid, this time in contrary an excess of oxaloacetic acid was used.[111] In this regard, the modified Cornforth procedure was carried out by treating starting material **57** with 2.5 equiv of oxaloacetic acid in H_2O. The solvent environment was maintained at pH 11 using an aq. solution of NaOH. It was followed by a $NiCl_2 \cdot 6H_2O$-catalysed decarboxylation step under acidic pH maintained by concentrated AcOH. The crude mixture was subjected to anion-exchange resin column, eluted with a linear gradient solution of aqueous NH_4HCO_3. The desired Kdo-azide compound **58** was obtained in 65% yield. This yield is considerably good for a Kdo synthesis *via* Cornforth procedure.

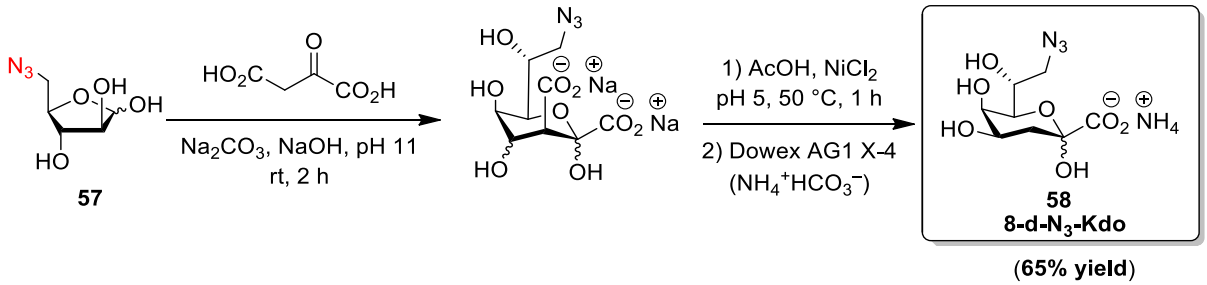

Scheme 20. Synthesis of 8-d-N_3-Kdo **58**

2.3.3. Synthesis of 7-d-N_3-Kdo

With L-xylose as the precursor sugar, the synthesis commenced with Fischer glycosylation reaction, with the aim of obtaining the methyl glycoside of xylopyranose. It was carried out using Fischer-Helferich conditions (**Scheme 21**). L-Xylose was refluxed in methanol in the presence of Dowex H^+ resin.[112] Though the overall yield was low (42%), the major product was obtained as methyl xylopyranoside **60**. A nosyl leaving group was regioselectively introduced through 3,4-*O*-stannylene acetal intermediate.[113] But the attempts made to carry out subsequent azide substitution on the nosyl compound using sodium azide failed. Hence, the tosyl moiety was substituted at the C-4 position using the same tin acetal derivative to obtain tosylated xylopyranoside derivative **61**. The other hydroxyl groups were protected with benzyl ethers prior to attempting the azide substitution. Eventually the reaction of tosyl compound **62** with NaN_3 heated to 90 °C in DMSO yielded desired 4-d-N_3-arabinopyranoside compound **63**. The benzyl ethers were deprotected using Zemplén conditions. In order to deprotect the methyl glycoside, the hydroxyl moieties including the anomeric group of diol compound **64** were first acetylated. The corresponding acetolysis reaction on compound triacetate **65** was carried out using Ac_2O and H_2SO_4. The final Zemplén deprotection resulted in 4-d-N_3-arabinopyranose **66**.

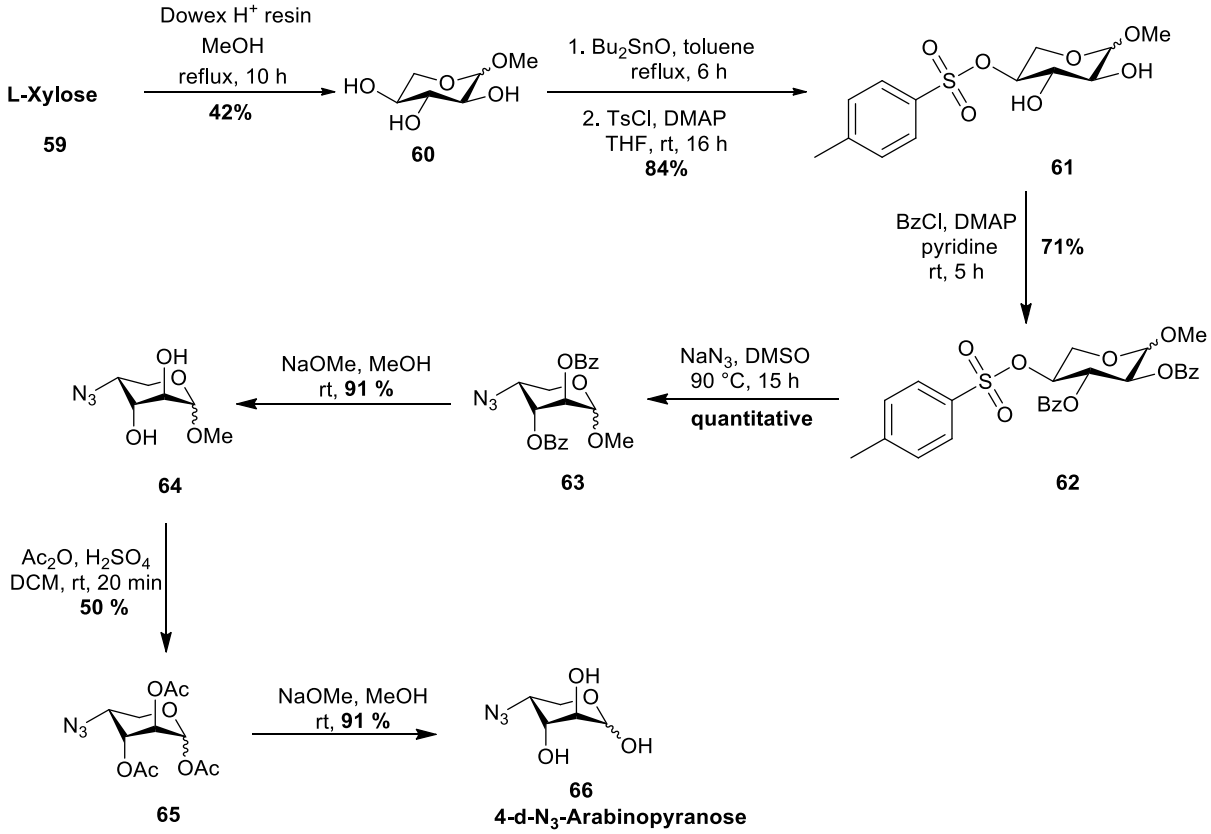

Scheme 21. Synthesis of 4-d-N_3-arabinose **66**

Similar conditions of modified Cornforth procedure involving condensation of arabinose with excess of oxaloacetic acid yielded desired 7-d-N_3-Kdo (**67**) in 65% yield (**Scheme 22**). The structure of the product was confirmed based on ^{1}H and ^{13}C NMR characterization. The spectra were complicated with mixture of different forms such as pyranose, furanose but the α-form of pyranose ring was the major one. The product was also confirmed by MS-ESI experiment.

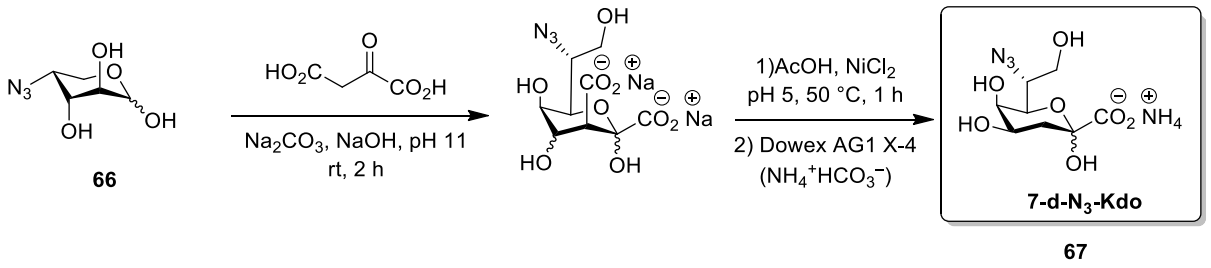

Scheme 22. Synthesis of 7-d-N_3-Kdo **67**

The synthesized N_3-Kdo residues were manipulated by the lab of Prof. Salim Islam for the labelling tests. They incorporated **58** and **67** in the LPS of GNB *Myxococcus xanthus* and

coupled it with a DBCO-sulforhodamine B dye. The compound **58** (8-d-N_3-Kdo) was successfully labelled and visualized through the electron microscope (**Fig. 25**). The compound **67** (7-d-N_3-Kdo) was unable to be labelled, as the red colour visualization was not seen. This could be due to the fact that either 7-d-N_3-Kdo residue was unable to incorporate into the bacterial LPS, or the failure of coupling with the DBCO dye with the azide moiety.

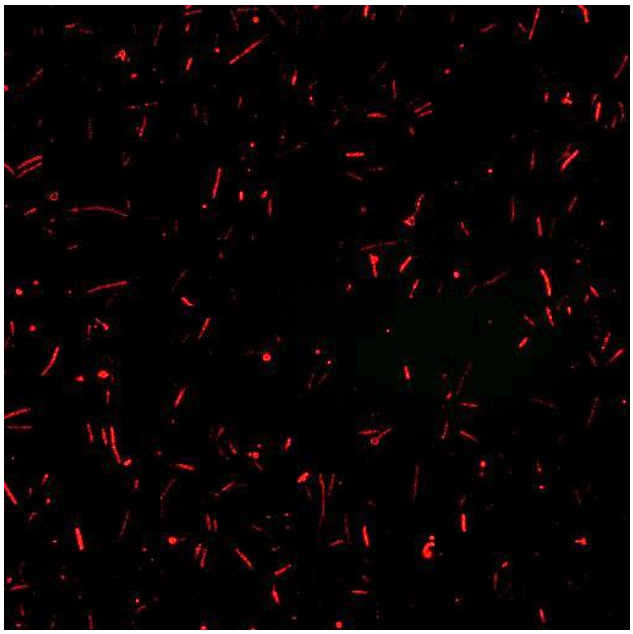

Figure 25. Click-labelling of *M. xanthus* in presence of 8-d-N_3-Kdo

Since the compound **67** was unsuccessful in the labelling, another analogue of Kdo could prove to be an interesting tool to be tested. The tetrazine Kdo residue (**Fig. 26**) can be synthesized via two-steps from 7-d-N_3-Kdo. The reduction of the azide moiety of **67** will yield the primary amine, which can be coupled with the tetrazine-NHS-ester. A more defined tetrazine moiety could potentially be incorporated in the bacterial LPS.

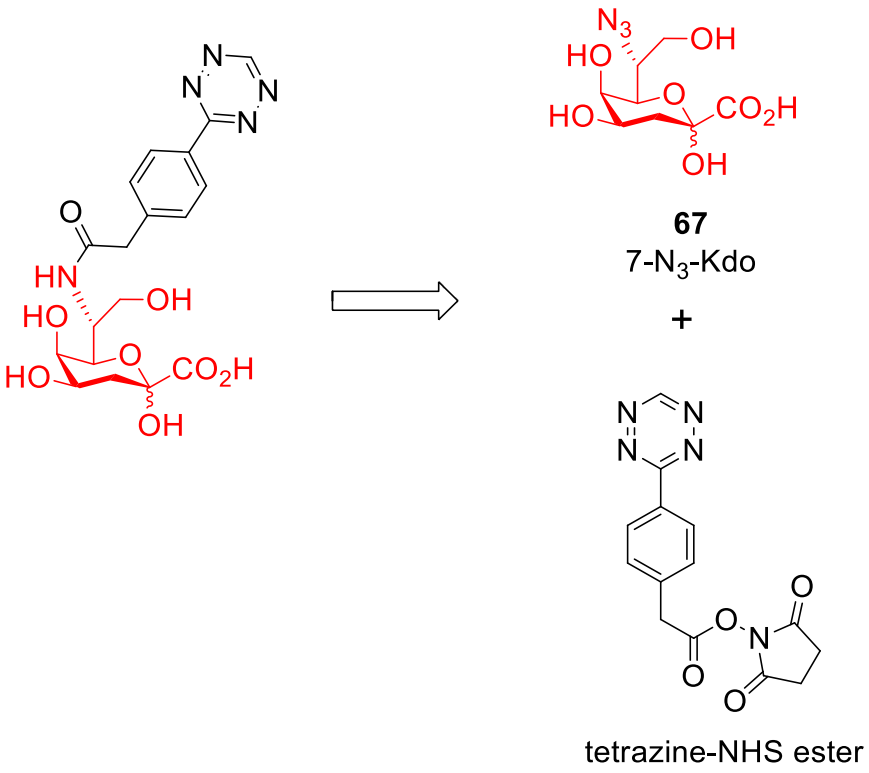

Figure 26. Kdo-tetrazine residue

2.4. Synthesis of siderophore conjugates (*work in progress*)

The siderophore conjugate consists of desferrioxamine, potential releasable or non-releasable linkers, and the Kdo inhibitor molecule (**Fig. 25**). It will be synthesized with the idea of emulating the "Trojan-horse" strategy of exploiting the iron-uptake pathway of GNB.[61, 69b] By this way, we hypothesize to overcome the different barriers of OM, by potentially delivering the inhibitor into the cytoplasm.

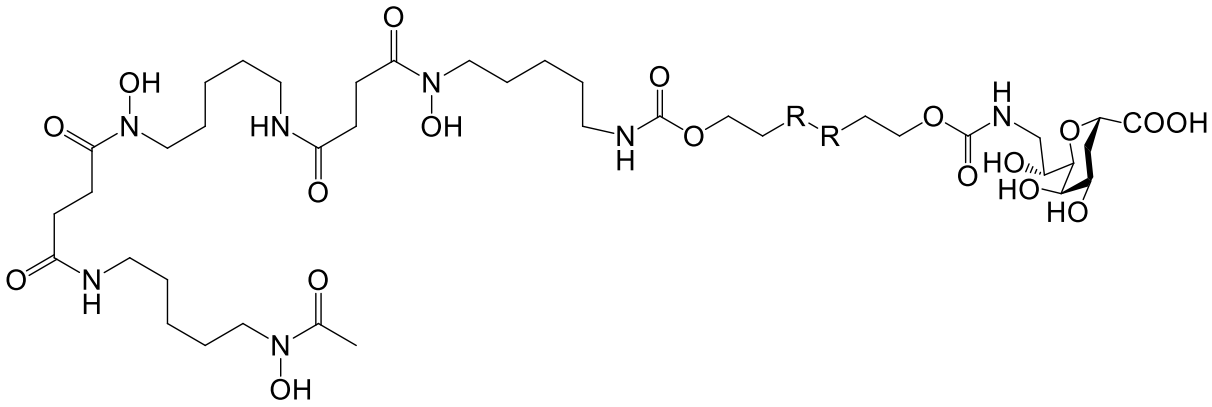

Figure 27. DFO-Kdo analogue conjugate; R = S (releasable) or C (non-releasable)

2.4.1. Retrosynthetic analysis

The commercially available xenosiderophore DFO would be primarily conjugated with the synthesized linker, which further facilitates the conjugation with the Kdo residue (**Fig. 26**). The potential releasable linker would consist of an alkyl chain bearing a disulphide linkage and an NHS carbonate ester moiety at both of its terminal ends. The NHS carbonate ester moiety would facilitate the coupling with the primary amine group of the DFO and Kdo residue, upon activation by a base. On the other hand, the potential non-releasable linker would be based on the absence of disulphide linkage.

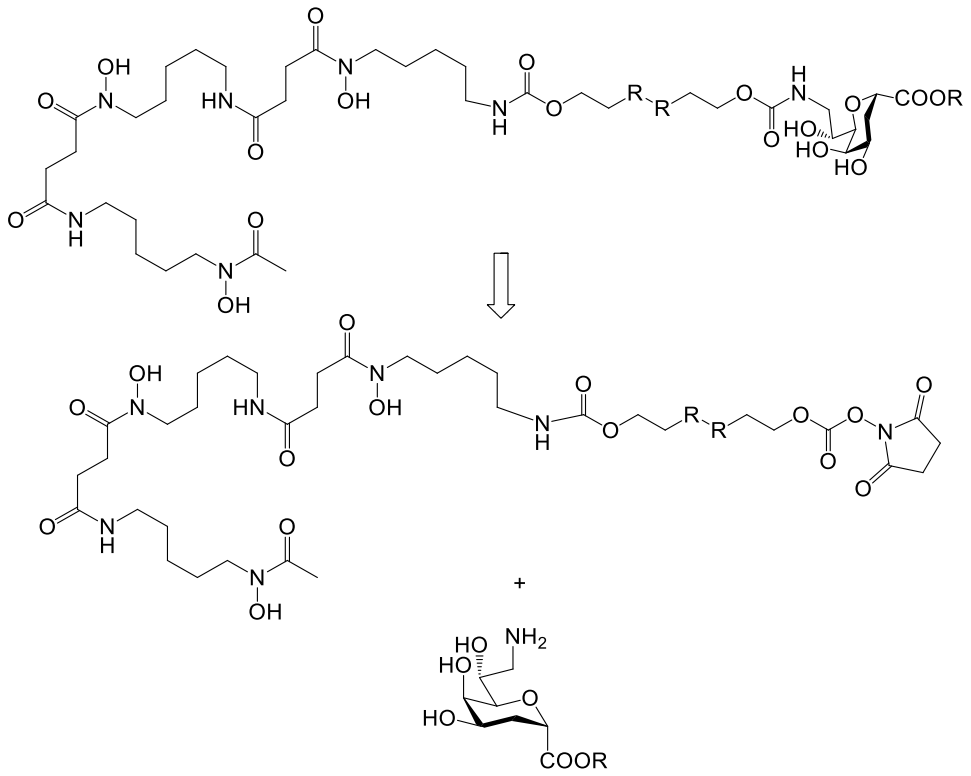

Figure 28. Retrosynthetic analysis of DFO-Kdo conjugate

2.4.2. Synthesis of potential linkers

The commercially available reagent dithioethanol was transformed to dithiochloroformate on treatment with triphosgene (**Scheme 23**). This chloroformate crude compound was condensed with the reagent *N*-hydroxysuccinimide (NHS) in the presence of pyridine. Desired disulphide compound **72** was obtained in 65% overall yield of the two-step reactions. Alkyl chain compound **73** was obtained from 1,6-hexanediol in similar a two-step fashion.

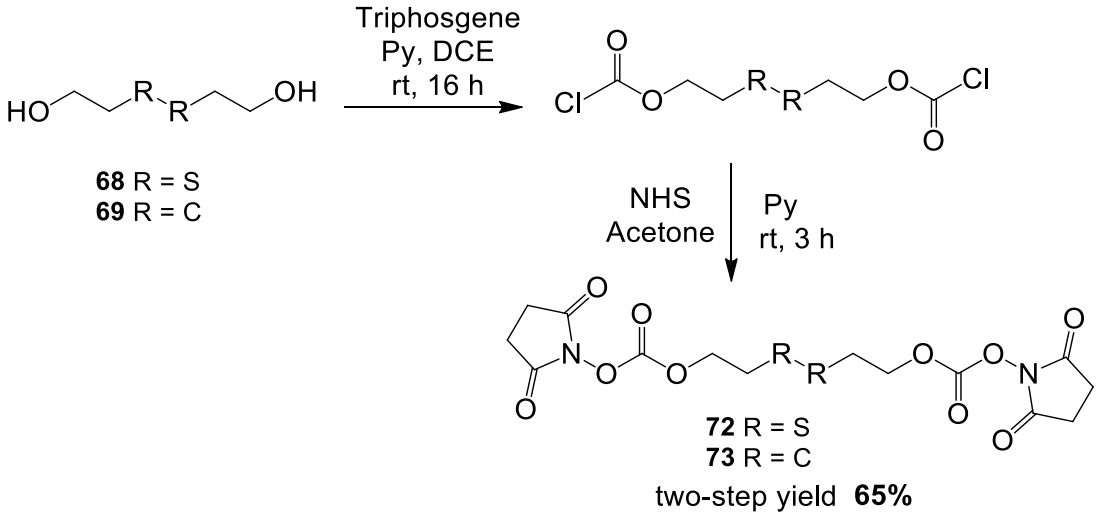

Scheme 23. Synthesis of potential linkers

2.4.3. Assembly of DFO-Kdo conjugates

The attempts were made to conjugate the synthesized potential linkers (**72** & **73**) with the DFO primarily. The strategy was to conjugate the resulting DFO-linker residue subsequently with the Kdo residue, to ultimately obtain the DFO-linker-Kdo conjugate. The DFO residue was treated with the disulphide bearing NHS carbonate residue **72** in presence of the base TEA. The obtained crude was purified through silica gel flash chromatography and characterized by ^{1}H NMR. The resulting spectra was not clear to be able to characterize the expected residue distinctly. The first attempt led to important observations regarding the reaction involving DFO. Though, the reaction was monitored through TLC by staining with $FeCl_3$ solution in ethanol, we were unable to draw a clear picture of progression of the starting material. The substantial differences in polarity of the starting materials (DFO and **72/73**) and product contributes to the dilemma of mode of purification through flash chromatography. Considering the challenges involved, further conditions were experimented with change in solvent and/or base (**Table 5**).

The DFO was treated with both the residues **72** and **73** in presence of the base DIPEA and TEA. Apart from DMF, the reaction was also carried out in acetonitrile. Instead of the organic base, sodium phosphate buffer mixture was added to activate the reactant in THF. All of these attempts were unsuccessful as it failed to yield the desired product. A one-pot reaction involving the DFO, **72** and Kdo residue were attempted to similar result. Since, the purification of the crude was complicated, the crude obtained after the reaction was subjected to MALDI-TOF mass spectrometry directly.

Table 5. Attempts at conjugation of DFO and linker

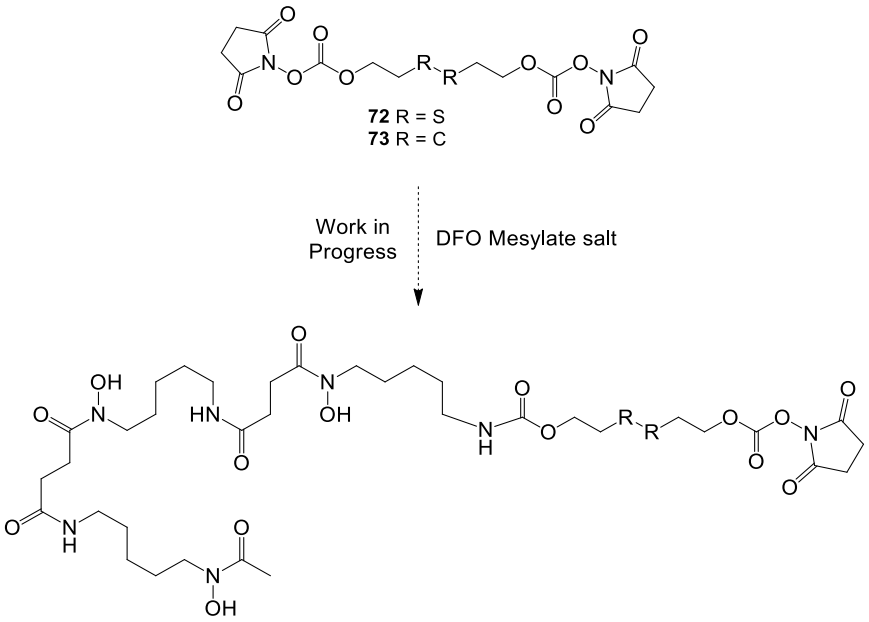

entry	reagents	solvent
1	DFO (1.0 equiv.), **72** (2.0 equiv.), TEA (2.0 equiv.)	DMF
2	DFO (1.0 equiv.), **72** (1.0 equiv.), TEA (2.0 equiv.)	ACN
3	DFO (1.0 equiv.), **73** (1.0 equiv.), TEA (2.0 equiv.)	DMF
4	DFO (1.0 equiv.), **72** (1.0 equiv.), Sodium Phosphate buffer	THF
5	DFO (1.0 equiv.), **73** (1.0 equiv.), DIPEA (2.0 equiv)	DMF

Theoretically, there are two factors that could contribute to the unsuccessful nature of the reaction. The first one being the nucleophilic nature of hydroxylamine moiety present in the DFO structure. The three hydroxylamine moieties per molecule could interfere with the reaction, thereby resulting in undesired products. As a probable solution to tackle this

potential issue would be to protect the hydroxyl amine groups with a protecting group, prior the reaction with the linker residue. The protecting groups limits the interference of these moieties to enable the smooth coupling, which could later be deprotected. The other factor could be the unstable nature disulphide bearing NHS carbonate. The product obtained after coupling with **72** possess an NHS carbonate ester moiety, that could undergo degradation. As an alternate for this, the potential linker with more stable aromatic *p*-nitrophenyl ester could be synthesized. Also, the carbamate ester linkage is more complicated to form compared to a simpler amide linkage, which could also be experimented.

3. Conclusion and Perspectives

As mentioned in the objectives section, the core theme of the project was to develop sequential methodologies for the synthesis of Kdo derivatives analogues. Accordingly, the Kdo derivatives were synthesized with the idea of potentially inhibiting the Kdo-processing enzymes. These target enzymes play key role in the biosynthesis of surface polysaccharides, such as LPS and EPS, expressed by human pathogenic GNB.

First, the target enzyme was CKS, that catalyses the rate-determining step in the biosynthesis of endotoxin LPS. The inhibitor of this important enzyme, 2,8-d-β-amino Kdo was synthesized through two synthetic pathways starting from D-mannose and D-arabinose. The synthetic pathway starting from D-arabinose was more conventional. But the pathway starting from D-arabinose was lesser conventional. Many modifications were employed for certain reaction steps to obtain the final target product in substantial and efficient yield. Having synthesized the Kdo-analogue inhibitor as part of the siderophore conjugates, the potential releasable and non-releasable linker were synthesized. The conjugation of all three components - siderophore, linker and Kdo-inhibitor – should result in the formation of siderophore conjugate. But there were lot of challenges involved in this conjugation which led to changes in the original strategy. Hence, this is still work in progress.

An alternate hypothesis where peracetylated Kdo analogues were synthesized. The idea of improving the efficiency of membrane penetration of the inhibitor through passive diffusion was also investigated. The peracetylated analogues were synthesized from 2-d-Kdo methyl/ethyl ester to inhibit the enzyme CKS. When these analogues were tested for their antibacterial activity against several multi-drug resistant GNB, they failed to show any activity.

The Kdo glycoside analogues were synthesized as potential enzyme inhibitors involved in the biosynthesis of β-Kdo containing Kdo-EPS. The desired Kdo glycosides were synthesized starting from D-arabinose. The adamantane derivatives were utilized as glycosyl acceptors to form mini-library of Kdo-adamantane glycosidic compounds.

Other analogues of Kdo, 8-d-N_3-Kdo and 7-d-N_3-Kdo were synthesized, as part of assimilating them in the bacterial LPS, to enable the click-mediating labelling of the OM. The known 8-d-N_3-Kdo was synthesized from D-arabinose through six-step synthetic pathway. The new 7-d--N_3-Kdo was synthesized starting from L-xylose. The Kdo analogues were tested in collaboration with Prof. Salim Islam for their role in labelling GNB *Myxococcus xanthus.* When the tests were carried out in the presence of 8-d-N_3-Kdo, the labelling was achieved with the help of DBCO-suforhodamine dye. But the same test resulted in failure in presence of 7-d-N_3-Kdo.

The completion of synthesis of the siderophore conjugates will be an interesting tool because of their potential to smuggle the Kdo-inhibitor across the OM, thereby overcoming the barrier. In the process they will theoretically exploit the iron-uptake pathway of the bacteria via "Trojan-horse strategy'. The conjugate will be tested for its *in vitro* antibacterial activity against several multidrug-resistant GNB, including, but not restricted to *P. aeruginosa*, *A. baumannii*, and *B. cepacia* complex species. The inhibitory activity of the siderophore conjugates will be compared with that of free Kdo mimics, which will pave new pathways for more such conjugates.

The quantification of Kdo EPS mucoid inhibition using the click-mediated labelling will be crucial. As it will provide confirmation for the presence of Kdo-processing enzymes in Kdo-EPS and their inhibition via Kdo-adamantane glycosides. Through this several opportunities will arise to improve inhibition and thereby guiding in developing a novel therapeutic agent against *Burkholderia* spp.

The Kdo analogue consisting of tetrazine moiety will be synthesized in quest to overcome the limitations of 7-d-N_3-Kdo in LPS labelling.

4. Experimental Procedures

4.1. General methods

All the starting materials and reagents were purchased from commercial sources and utilized as it is, without further processes. Air and water sensitive reactions were conducted in oven-dried glassware under inert atmosphere in anhydrous solvents, which were prepared by supplying the solvents over heat-gun activated 4 Å molecular sieves. These solvents were introduced to the reaction through a dried, argon-filled syringe. Reactions were monitored by thin-layer chromatography (TLC) with silica gel 60 F_{254} 0.25 mm pre-coated aluminium foil plates. The staining agents utilized to visualize the TLC plates were UV_{254} and/or orcinol (1 $mg{\cdot}mL^{-1}$) in a 10% aq. solution of H_2SO_4 and/or Hanessian's stain (ceric ammonium molybdate) with heating. The iron-associated compounds were visualized using 60 mM of $FeCl_3$ solution in ethanol. Flash chromatography was performed on silica gel 60 Å (15-40 µm). Reverse-phased flash column chromatography was performed on C_{18} silica gel (fully capped, 25-40 µm). Anion exchange chromatography was performed on Serdolit CG-400 I (Cl^- form). NMR spectra was recorded at 297 K in the mentioned solvents with 400 or 600 MHz instruments, employing standard softwares given by the manufacturer. ^1H and ^{13}C NMR spectra were referenced to TMS ($\delta_H = \delta_C = 0.00$ ppm) and acetone ($\delta_H = 2.22$ ppm; $\delta_C = 30.9$ ppm) for spectra in D_2O. Assignments were based on ^1H, ^{13}C, HSQC, and COSY experiments. All the ^{13}C NMR experiments are ^1H-decoupled. High resolution mass spectra (HRMS) were recorded on an ESI-Q-TOF mass spectrometer.

4.2. General Procedures

4.2.1. For peracetylation

The corresponding tetraol residues are dissolved in anhydrous pyridine (10.0 $mL{\cdot}mmol^{-1}$) and treated with acetic anhydride (10.0 $mL{\cdot}mmol^{-1}$) in the presence of DMAP (0.01 equiv). After stirring the reaction mixture under Ar for 16 h, the solvents were co-evaporated with toluene (3×) under reduced pressure. The crude residue was purified with silica gel flash chromatography to obtain the desired products.

4.2.2. For glycosylation

Thioglycoside **33** (1.0 equiv), NIS (2.0 equiv), and adamantyl-derivatives (1.3 equiv) were taken collectively in a clean reaction flask and co-evaporated with toluene (3×) under reduced pressure. They were dissolved in anhydrous MeCN (20 mL·mmol^{-1}). After adding freshly activated 4 Å powdered molecular sieves, the solution was stirred at rt for 1 h under Ar. The mixture was then cooled to -10 ^{o}C, protected from light, and AgOTf (1.0 equiv) was added, and the reaction was stirred at this temperature for 30 min under Ar. It was then quenched with TEA (2.0 equiv), filtered over celite, rinsed with DCM, and concentrated under reduced pressure. The residue was purified by silica gel flash chromatography to obtain target glycoside as a mixture of anomers.

4.2.3. For hydrogenolysis of benzyl ester

Kdo glycoside (1.0 equiv) was dissolved in MeOH (20 mL·mmol^{-1}) and the solution was stirred under the atmosphere of H_2 at rt in presence of 10% Pd/C catalyst (1 mg.mg^{-1}) overnight. Then the catalyst was filtered over celite, rinsed with MeOH, and the solvents were evaporated under reduced pressure. The residue was purified by silica gel flash chromatography to separate the two anomers of the Kdo glycoside.

4.2.4. For Zemplén deprotection

To a solution of acid **37-39** (1.0 equiv) dissolved in anhydrous MeOH (10 mL·mmol^{-1}), NaOMe (25% wt. MeOH, 1.0 equiv) was added and the solution was stirred at rt for 2 h under Ar. It was neutralized by adding Dowex H^+ resin, filtered over celite, and concentrated under reduced pressure to obtain tetraol glycoside.

4.3. Synthetic procedures

4.3.1. Ammonium 3-deoxy-D-*manno*-oct-2-ulopyranosylonate (2)

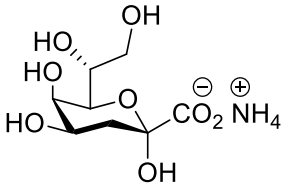

2

$NaHCO_3$ (0.1 g, 1.2 mmol) was dissolved in distilled water (30 mL) with a pH meter setup. It was cooled to 0 ^oC and 10 M aq. NaOH solution was added dropwise until pH 10.0 was reached. Oxaloacetic acid (3.17 g, 24.0 mmol) was added portion wise over 60 min. To maintain the pH approximately at 10.0, simultaneously a 10 M aq. NaOH solution was added, accompanying the acid. After the complete addition of oxaloacetic acid, a solution of D-arabinose (10 g, 66.6 mmol) in distilled water (30 mL) was added at once. The ice bath was then removed, 10 M aq. NaOH was added to adjust the pH to 11.0 and the reaction mixture was stirred for 2 h at rt. After 2 h, the mixture was heated to 50 ^oC and a solution of $NiCl_2.6H_2O$ (47 mg, 0.2 mmol) in distilled water (0.5 mL) was added. It was followed by the addition of Dowex H^+ resin in small portions to adjust the pH to 5.7 and stirred for 2 h at this temperature. The pH increases slightly during this decarboxylation step. Hence small amount of Dowex H^+ resin was added to maintain the pH at 5.7. The resin was filtered off using celite and the crude was directly passed on to the anion exchange resin column. The column was first eluted with water (500 mL) to eliminate the unreacted arabinose. Then the column was eluted with increasing linear gradient of aq. NH_4HCO_3 (0 to 0.25 M). The fractions containing the desired form of Kdo epimer were pooled, freeze dried and crystallized using ethanol. The crystalline Kdo.NH_3 was obtained as white crystals (2.7 g, 40%). NMR spectral data correspond to the one reported in the literature.[114]

4.3.2. Methyl 3-deoxy-4,5:7,8-di-*O*-isopylidene-α-D-*manno*-oct-2-ulopyranosylonate (4)

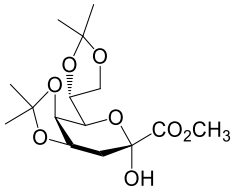

4

A solution of Kdo.NH_3 (4.7 g, 18.46 mmol, 1.0 equiv) in anhydrous DMF (185 mL) was prepared under Ar. After adding 2,2-DMP (18.0 mL, 147.7 mmol, 8.0 equiv) and crystals of PTSA in small portions (3.5 g, 18.5 mmol, 1.0 equiv, until slightly acidic pH was attained) to the solution, it was heated to 50 °C and stirred for 2 h. After completion [R_f 0.4 (DCM/MeOH 8:2)], the reaction mixture was quenched by TEA (1.0 equiv, until the pH of solution was neutral) and solvents were co-evaporated with toluene (3×) under reduced pressure to obtain a yellow crude residue **3**, that was used directly for next step without further purification. This crude (5.1 g, 16.1 mmol, 1.0 equiv) was then dissolved in anhydrous DMF (130 mL), followed by Cs_2CO_3 (6.5 g, 19.9 mmol, 1.2 equiv) and MeI (2.3 mL, 36.6 mmol, 2.2 equiv). The reaction mixture was stirred at rt under Ar for 16 h. After filtering off the Cs salts over celite, the solution was diluted with EtOAc (130 mL). The organic phase was first washed with saturated solution of aq. NH_4Cl (65 mL), then with H_2O (65 mL). The combined aqueous phase was extracted with EtOAc (2 × 65 mL). The combined organic phase were dried over $MgSO_4$ and concentrated under reduced pressure. The residue was purified by silica gel flash chromatography (Hex/EtOAc 7:3 to 1:1) to obtain ester **4** (4.1 g, 80% over two steps) as a pale yellow solid: R_f 0.3 (Hex/EtOAc 6:4); ^{1}H NMR (600 MHz, $CDCl_3$) δ 4.51 (dd, ^3J = 11.4, 6.4 Hz, 1H, H-4), 4.35 (ddd, ^3J = 8.2, 6.1, 4.5 Hz, 1H, H-7), 4.26 (dd, ^3J = 6.4, 2.0 Hz, 1H, H5), 4.08 (dd, ^3J = 7.1, 4.6 Hz, 1H, H-8b), 4.02 – 3.98 (m, 1H, H-8a), 3.89 (dd, ^3J = 8.2, 2.1 Hz, 1H, H-6), 3.82 (s, 1H, O*H*), 3.81 (s, 3H, O-C*H*$_3$), 2.52 (dd, ^3J = 14.5, 6.5 Hz, 1H, H-3a), 1.90 (dd, ^3J = 14.5, 4.8 Hz, 1H, H-3b), 1.46 (s, 3H, C*H*$_3$), 1.43 (s, 3H, C*H*$_3$), 1.37 (s, 3H, C*H*$_3$), 1.36 (s, 3H, C*H*$_3$). NMR spectral data correspond to the one reported in the literature.[101]

4.3.3. Methyl 3-deoxy-4,5:7,8-di-*O*-isopropylidene-D-*manno*-oct-2-enosonate (5)

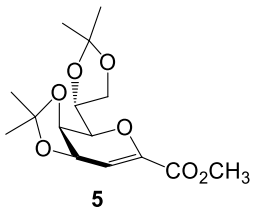

5

To the solution of ester **4** (4.1 g, 12.3 mmol, 1.0 equiv) dissolved in anhydrous pyridine (60 mL), Ac_2O (60 mL) followed by DMAP (15 mg, 0.12 mmol, 0.01 equiv) and the solution was stirred overnight under Ar at rt. After completion [R_f 0.35 (Hex/EtOAc 6:4)], the solvents were co-evaporated with toluene (3×) under reduced pressure to yield a yellow crude residue which was used directly for next step without further purification. This crude was dissolved in

anhydrous MeCN (240 mL) under Ar, to which catalytic amount of TMSOTf (446 µL, 2.47 mmol, 0.2 equiv) was added and stirred at rt for 2 h. It was quenched by TEA and concentrated under reduced pressure. The residue was purified by silica gel flash chromatography (Hex/EtOAc 9:1 to 7:3) to obtain Kdo glycal **5** (2.7 g, 80% over two steps) as a yellow oil: R_f 0.4 (Hex/EtOAc 7:3); ^{1}H NMR (600 MHz, $CDCl_3$) δ 6.00 (dd, ^3J = 3.2, 1.2 Hz, 1H, H-3), 4.78 (dd, ^3J = 6.0, 3.3 Hz, 1H, H-4), 4.47 (dd, ^3J = 5.5, 4.3 Hz, 1H, H-5), 4.45 (dd, ^3J = 4.9, 3.4 Hz, 1H, H-7), 4.20 (dd, ^3J = 9.1, 4.4 Hz, 1H, H-8a), 4.17 (dd, ^3J = 9.1, 6.1 Hz, 1H, H-8b), 3.85 – 3.82 (m, 1H,H-6), 3.79 (s, 3H, OCH_3), 1.45 (s, 3H, CH_3), 1.39 (s, 9H, 3 X CH_3). NMR spectral data correspond to the one reported in the literature.[101]

Alternative method

Ester **4** (25 mg, 75 µmol, 1.0 equiv) was dissolved in anhydrous DCM (500 µL). After cooling to 0 °C, TEA (53 µL, 375 µmol, 5.0 equiv), MsCl (7.0 µL, 90 µmol, 1.2 equiv) was added dropwise and stirred for 2 h at 0 °C under Ar. The reaction mixture was diluted with DCM (5 mL), washed with a saturated aq. solution of $NaHCO_3$ (2 × 2.5 mL) and dried over $MgSO_4$. The solvents were evaporated under reduced pressure and purified by silica gel flash chromatography (Hex/EtOAc 8:2 to 6:4) to obtain glycal **5** (15 mg, 65%) as yellow oil.

4.3.4 Methyl 2,3-dideoxy-4,5:7,8-di-O-isopylidene-α-D-*manno*-oct-2-ulopyranosonate (6)

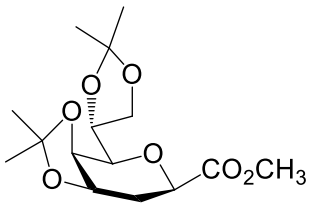

6

The solution of glycal **5** (450 mg, 1.43 mmol, 1.0 equiv) in absolute EtOH (20 mL) was stirred overnight under an H_2 atmosphere at rt in the presence of a Raney Ni catalyst (1.0 g). The catalyst was filtered off over celite by rinsing with EtOH and the solvents were evaporated under pressure to get the product ester **6** (370 mg, 82%) as yellow oil: R_f 0.2 (Hex/EtOAc 7:3); ^{1}H NMR (600 MHz, $CDCl_3$) δ 4.41 – 4.37 (m, 2H, H-4, H-2), 4.22 (dd, ^3J = 6.0, 1.8 Hz, 1H, H-5), 4.14 – 4.09 (m, 3H, CH_2, H-7), 3.77 (s, 3H, OCH_3), 3.54 (dd, ^3J = 8.0, 1.9 Hz, 1H, H-6), 2.19 (ddd, appearing as br. dt, ^3J = 14.0, 4.9 Hz, 1H, H-3a), 2.05 (ddd, appearing as br. dt, ^3J = 14.1, 8.1

Hz, 1H, H-3b), 1.50 (s, 3H, CH_3), 1.45 (s, 3H, CH_3), 1.39 (s, 3H, CH_3), 1.37 (s, 3H, CH_3). NMR spectral data correspond to the one reported in the literature.[101]

4.3.5. Methyl 2,3-dideoxy-4,5:7,8-di-*O*-isopylidene-β-D-*manno*-oct-2-ulopyranosonate (7)

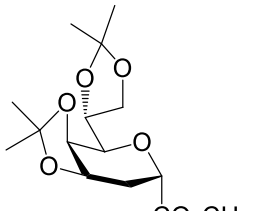

7

Ester **6** (2.2 g, 7.1 mmol, 1.0 equiv) was dissolved in anhydrous THF (7 mL) under Ar. Separately, solution of LDA in 1.0 M THF/Hex (17.8 mL, 17.8 mmol, 2.5 equiv) was taken in a flask under Ar and cooled down to –78 °C. To this the former solution was added dropwise. After stirring for 30 min at –78 °C under Ar, a solution of *t*-BuOH (1.7 mL, 17.78 mmol, 2.5 equiv) in dry THF (3 mL) was added, stirred for 5 min and quickly poured over a cold saturated solution of aq. $NaHCO_3$ (40 mL). The reaction mixture was extracted with EtOAc (3 × 40 mL), dried over $MgSO_4$ and concentrated under reduced pressure. The residue was purified by silica gel flash chromatography (Hex/EtOAc 8:2 to 6:4) to obtain ester **7** (850 mg, 60%) as pale-yellow oil: R_f 0.5 (Hex/EtOAc 6:4); ^{1}H NMR (600 MHz, $CDCl_3$) δ 4.59 (ddd, appearing as dt, ^3J 7.9, 2.8, 1H, H-4), 4.56 (dd, ^3J = 11.5, 5.9 Hz, 1H, H-2), 4.35 (dd, ^3J = 8.0, 1.6 Hz, 1H, H-5), 4.24 – 4.20 (m, 2H, CH_2), 4.14 – 4.09 (m, 1H, H-7), 3.75 (s, 3H, OCH_3), 3.51 (dd, ^3J = 8.0, 1.5 Hz, 1H, H-6), 2.30 (ddd, ^3J = 15.0, 5.9, 3.3 Hz, 1H, H-3a), 1.87 (ddd, 14.8, 11.4, 2.6, 1H, H-3b), 1.49 (s, 3H, CH_3), 1.43 (s, 3H, CH_3), 1.38 (s, 3H, CH_3), 1.37 (s, 3H, CH_3). NMR spectral data correspond to the one reported in the literature.[101]

4.3.6. Methyl 2,3-dideoxy-4,5-*O*-isopropylidene-β-D-*manno*-oct-2-ulosonate (9)

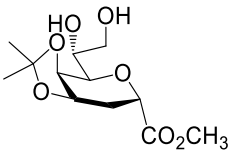

9

The solution of compound **7** (500 mg, 1.6 mmol, 1.0 equiv) in 60% aq. AcOH (30 mL) was stirred at rt. The reaction was stopped after 3 h even if it was not totally complete (since longer time led to tetraol formation) and concentrated under reduced pressure. The lesser

polar diol was isolated by silica gel flash chromatography (Hex/EtOAc 8:2 to 0:1) as a pale-yellow oil **9** (160 mg, 40%): R_f 0.15 (Hex/EtOAc 3:7); ^{1}H NMR (600 MHz, $CDCl_3$) δ 4.64 (ddd, appearing as dt, ^3J = 7.9, 2.9 Hz, 1H, H-4), 4.60 (dd, ^3J = 11.2, 6.7 Hz, 1H, H-2), 4.45 (dd, ^3J = 7.9, 1.6 Hz, 1H, H-5), 4.05 (dd, appearing as br.d, ^3J = 12.5 Hz, 1H, H-8), 3.88 (m, 1H, H-7), 3.79 (s, 3H, OC*H*$_3$), 3.78 – 3.73 (m, 1H, H-8b), 3.64 (dd, ^3J = 8.7, 1.6 Hz, 1H, H-6), 3.31 (d, ^3J = 8.2 Hz, 1H, O*H*), 2.41 (ddd, ^3J = 14.9, 6.6, 3.2 Hz, 1H, H-3a), 2.31 (d, ^3J = 7.2 Hz, 1H, O*H*), 1.82 (ddd, ^3J = 15.0, 11.2, 2.6 Hz, 1H, H-3b), 1.51 (s, 3H, C*H*$_3$), 1.40 (s, 3H, C*H*$_3$); HRMS (ESI-TOF) *m/z* [M + Na]$^+$ cald for $C_{12}H_{20}O_7$ 299.1091; found 299.11.012.

4.3.7. Methyl 2,3-dideoxy-8-*O*-*p*-toluenesulfonyl-4,5-*O*-isopropylidene-β-D-*manno*-oct-2-ulosonate (10)

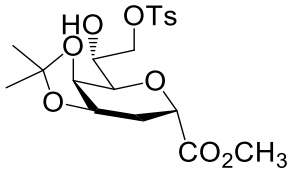

10

To the flask attached with a Dean-stark apparatus, diol **9** (40 mg, 0.14 mmol, 1.0 equiv) and Bu_2SnO (54 mg, 0.22 mmol, 1.5 equiv) were suspended in anhydrous toluene (2 mL) and refluxed for 3 h. After cooling the reaction mixture to rt, the solvents were evaporated under reduced pressure to obtain a yellow crude residue. This crude residue was dissolved in anhydrous THF (1 mL) followed by DMAP (0.2 mg, 20 µmol, 0.01 equiv) and the solution cooled to 12–15 ^{o}C. A solution of TsCl (41 mg, 0.22 mmol, 1.5 equiv) in anhydrous THF (1 mL) was prepared separately and added to the crude solution dropwise and stirred overnight under Ar at rt. The mixture was concentrated under reduced pressure and purified by silica gel flash chromatography (Hex/EtOAC 8:2 to 3:7) to obtain alcohol **10** (43 mg, 70% over two steps) as yellow oil: R_f 0.4 (Hex/EtOAc 3.5:6.5); ^{1}H NMR (600 MHz, $CDCl_3$) δ 7.82 (d, ^3J = 8.3 Hz, 2H, C*H*-Ar), 7.35 (d, ^3J = 8.1 Hz, 2H, C*H*-Ar), 4.57 (ddd, appearing as dt, ^3J = 7.6, 3.0 Hz, 1H, H-4), 4.52 (dd, ^3J = 11.1, 6.0 Hz, 1H, H-2), 4.41 (dd, ^3J = 2.7, 10.5 Hz, 1H, H-8a), 4.37 (dd, ^3J = 7.9, 1.7 Hz, 1H, H-5), 4.20 (dd, ^3J = 10.5, 6.6 Hz, 1H, H-8b), 4.04 – 3.99 (m, 1H, H-7), 3.73 (s, 3H, OC*H*$_3$), 3.62 (dd, ^3J = 8.3, 1.7 Hz, 1H, H-6), 2.75 (br. s, 1H, O*H*) 2.45 (s, 3H, C*H*$_3$-Ar), 2.28 (ddd, ^3J = 15.0, 6.0, 3.5 Hz, 1H, H-3b), 1.87 – 1.82 (m, 1H, H-3a), 1.45 (s, 3H, C*H*$_3$), 1.35 (s, 3H, C*H*$_3$); ^{13}C NMR (100 MHz, CDCl3) δ 173.43 (C-1), 145.23 (C-Ar), 133.13 (C-Ar), 130.20 (*C*H-Ar), 128.36 (*C*H-Ar), 109.76 (*C*$(CH_3)_2$), 72.36 (C-8), 72.19 (C-5), 71.18 (C-6), 70.18 (C-4), 69.09 (C-

7), 68.82 (C-2), 52.41 (C-9), 26.96 (C-3), 26.54 (*C*H_3), 25.29 (*C*H_3), 21.99 (*C*H_3-Ar); HRMS (ESI-TOF) *m/z* [M + Na]$^+$ cald for $C_{19}H_{26}O_9S$ 453.1189; found 453.1194; *m/z* [M + NH_4]$^+$ cald for $C_{19}H_{26}O_9S$ 448.1636; found 448.1639.

4.3.8. Methyl 2,3,8-trideoxy-8-azido-4,5-*O*-isopropylidene-β-D-*manno*-oct-2-ulosonate (11)

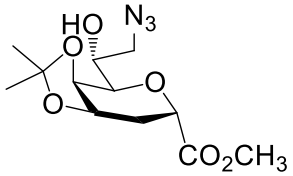

11

The solution of tosyl compound **10** (24 mg, 0.042 mmol, 1.0 equiv) dissolved in anhydrous DMSO (400 µL), was heated to 90 °C in the presence of sodium azide (7 mg, 0.11 mmol, 2.5 equiv) and stirred at this temperature for 15 h. The mixture was, diluted with DCM (5 mL), washed first with H_2O (2 × 5 mL) and then with a saturated solution of aq. $NaHCO_3$ (5 mL), dried over $MgSO_4$ and concentrated under reduced pressure. The residue was purified by silica gel flash chromatography (Hex/EtOAc 1:1 to 3:7) to obtain azide product **11** (11 mg, 90%) as pale-yellow oil: R_f 0.45 (Hex/EtOAc 3.5:6.5); ^{1}H NMR (400 MHz, $CDCl_3$) δ 4.61 – 4.51 (m, 2H, H-2, H-4), 4.40 (dd, ^3J = 7.9, 1.6 Hz, 1H, H-5), 4.24 – 4.09 (m, 1H, H-7), 3.75 (s, 3H, OCH_3), 3.72 (dd, ^3J = 12.6, 2.8 Hz, 1H, H-8a), 3.63 (dd, ^3J = 8.3, 1.5 Hz, 1H, H-6), 3.53 (dd, ^3J = 12.7, 6.4 Hz, 1H, H-8b), 2.31 (ddd, ^3J = 15.0, 6.1, 3.5 Hz, 1H, H-3a), 1.89 – 1.81 (m, 1H, H-3b), 1.49 (s, 3H, CH_3), 1.38 (s, 3H, CH_3); *m/z* [M + Na]$^+$ cald for $C12H19N_3O_6$ 324.11595; found 324.11661.

4.3.9. 1,2;5,6-di-*O*-isopropylidine-D-mannofuranoside (14)

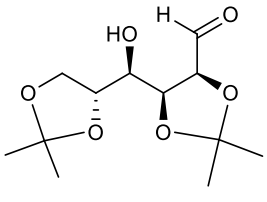

14

After dissolving D-mannose (40.0 g, 222.0 mmol, 1.0 equiv) in anhydrous acetone (1.5 L), followed by the addition of iodine (11.3 g, 44.4 mmol, 0.2 equiv), the mixture was stirred at rt under Ar overnight. The excess of I_2 was quenched by saturated solution of aq. $Na_2S_2O_3$ (500 mL) until the solution turned brown to pale-yellow visibly and then acetone was

evaporated under reduced pressure. The remaining aqueous phase was extracted with EtOAc (3 × 600 mL), dried over $MgSO_4$ and evaporated under reduced pressure to provide aldehyde **14** (58.0 g, quantitative) as white amorphous solid residue, which was used directly for the next step without further purification: R_f(DCM/MeOH 9:1).

4.3.10. (Carbethoxymethylene)triphenylphosphorane (15)

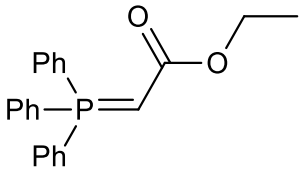

15

(Ethoxycarbonylmethyl)triphenylphosphonium bromide (40.0 g, 93.17 mmol, 1.0 equiv) was dissolved in DCM (200 mL). It was stirred at rt for 20 min in presence of aq. NaOH (1.0 M, 150 mL). After separating the layers, the aqueous phase was extracted with DCM (2 × 75 mL). The combined organic phase was washed with brine (100 mL), dried over $MgSO_4$ and concentrated under reduced pressure to get the stable phosphonium ylide **15** (32.4 g, quantitative) as white amorphous solid which is used for Wittig reaction without further purification.

4.3.11. Ethyl (4*R*,5*S*,6*R*,7*R*)-6-hydroxy-4,5:7,8-di-*O*-isopropylidene-oct-2-enoate (16)

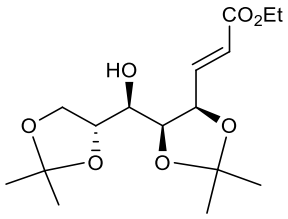

16

The previously obtained stable ylide **15** (32.4 g, 93.13 mmol, 1.2 equiv) was suspended in anhydrous toluene (465 mL) along with compound **13** (20.2 g, 77.6 mmol, 1.0 equiv). It was refluxed for 5 h after adding catalytic amount of benzoic acid (948 mg, 7.8 mmol, 0.1 equiv). The reaction mixture was passed over silica gel, rinsed with EtOAc (500 mL) and concentrated under reduced pressure. The residue was purified by silica gel flash chromatography (Hex/EtOAc 9:1 to 6:4) to obtain Wittig product **16** (25 g, 98%) as a pale yellow oil: R_f 0.4 (Hex/EtOAc 7:3)**;** ^{1}H NMR (600 MHz, $CDCl_3$) δ 7.07 (dd, ^3J = 15.7, 6.2 Hz, 1H, H-2), 6.10 (dd, ^3J = 15.7, 1.4 Hz, 1H, H-1), 4.83 (ddd, ^3J = 7.5, 6.3, 1.4 Hz, 1H, H-3), 4.46 (dd, ^3J = 7.4, 2.2 Hz, 1H,

H-4, 4.21 (qd, ^3J = 7.1, 3.6 Hz, 2H, CH_2-9), 4.13 – 4.08 (m, 1H, H-7a), 4.03 – 3.96 (m, 2H, H-6, H-7b), 3.45 (td, ^3J = 7.9, 2.1 Hz, 1H, H-5), 2.20 (d, ^3J = 7.7 Hz, 1H, O*H*), 1.55 (s, 3H, CH_3-10), 1.42 (s, 3H, CH_3), 1.40 (s, 3H, CH_3), 1.35 (s, 3H, CH_3), 1.30 (t, ^3J = 7.1 Hz, 3H, CH_2CH_3) ppm. NMR spectral data correspond to the one reported in the literature.[108]

4.3.12. Ethyl (4*R*,5*S*,6*R*,7*R*)-6-[(*tert*-butyldimethylsilyl)oxy]-4,5:7,8-di-*O*-isopropylidene-oct-2-enoate (17)

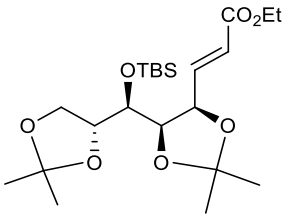

17

To a solution of Wittig compound **16** (14.5 g, 43.95 mmol, 1.0 equiv) in anhydrous DMF (31 mL), imidazole (6.0 g, 87.9 mmol, 2.0 equiv) and TBSCl (16.6 g, 109.9 mmol, 2.5 equiv) were added sequentially. The reaction mixture was stirred at rt under Ar for 72 h. It was taken up in a separatory funnel and partitioned between ice water (250 mL) and diethyl ether (250 mL). The aqueous layer was extracted with diethyl ether (2 × 250 mL), dried over $MgSO_4$ and concentrated under reduced pressure. The residue was purified by silica gel flash chromatography (Hex/EtOAc 8:2) to obtain ester **17** (19.51 g, quantitative) as yellow oil: R_f0.7 (Hex/EtOAC 8:2). NMR spectral data correspond to the one reported in the literature.[108]

4.3.13. Ethyl (4*R*,5*S*,6*R*,7*R*)-6-[(*tert*-butyldimethylsilyl)oxy]-4,5:7,8-di-*O*-isopropylidene-octonate (18)

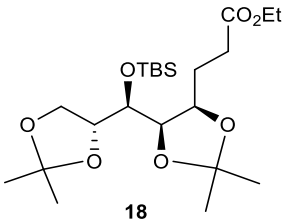

18

A solution of ester **17** (900 mg, 2.0 mmol, 1.0 equiv) in absolute EtOH (20 mL) was heated to 40 °C in the presence of Raney Ni catalyst (900 mg) and stirred overnight under H_2 (solution taken up in a 250 mL flask to create a H_2 atmosphere). The catalyst was filtered off over celite and washed thoroughly with EtOH (60 mL). The solvents were evaporated under reduced

pressure to obtain ester **18** (770 mg, 90%) as a colourless oil, which was used directly for next step without further purification: R_f 0.57 (Hex/EtOAc 9:1)); ^{1}H NMR (600 MHz, $CDCl_3$) δ 4.15 – 4.10 (m, 2H, CH_2-9), 4.09 – 4.04 (m, 2H, H-8a, H-4), 3.96 – 3.93 (m, 1H, H-7), 3.91 – 3.85 (m, 3H, H-8b, H-5, H-6), 2.52 (ddd, ^3J = 15.8, 9.2, 5.3 Hz, 1H, H-2a), 2.35 (ddd, ^3J = 16.0, 9.1, 6.9 Hz, 1H, H-b2), 1.96 – 1.89 (m, 1H, H-3a), 1.73 – 1.67 (m, 1H, H-3b), 1.44 (s, 3H, CH_3), 1.40 (s, 3H, CH_3), 1.33 (s, 3H, CH_3-10), 1.31 (s, 3H, CH_3), 1.25 (t, ^3J = 7.1 Hz, 3H, CH_2CH_3), 0.88 (s, 9H, 3 X CH_3), 0.12 (s, 3H, CH_3), 0.11 (s, 3H, CH_3); ^{13}C NMR (100 MHz, CDCl3) δ 173.94 (C-1), 109.78 ($C(CH_3)_2$), 107.88 ($C(CH_3)_2$), 80.63 (C-5), 77.30 (C-7), 77.0 (C-4), 72.17 (C-6), 67.78 (C-8), 60.65 (CH_2-9), 30.89 (C-2), 28.83 (CH_3), 26.53 (2 x CH_3), 26.49 (C-3), 26.31 ($C(CH_3)_3$), 25.61 (CH_3), 18.81 ($C(CH_3)_3$), 14.58 (CH_3-10), -3.50 (CH_3-Si), -4.19 (CH_3-Si); HRMS (ESI-TOF) *m/z* $[M + H]^+$ cald for $C_{22}H_{42}O_7Si$ 447.2772; found 447.2775; *m/z* $[M + Na]^+$ cald for $C_{22}H_{42}O_7Si$ 469.2592; found 469.2599.

4.3.14. Ethyl (4*R*,5*S*,6*R*,7*R*)-6-hydroxy-4,5:7,8-di-*O*-isopropylidene-octonoate (19)

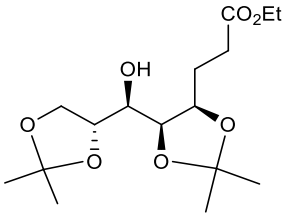

19

Ester compound **18** (14.0 g, 31.3 mmol, 1.0 equiv) was dissolved in THF anhydrous (300 mL) and cooled to 0 °C. A 1.0 M TBAF in THF solution (31.3 mL, 31.3 mmol, 1.0 equiv) was added and stirred at this temperature for 10 min. The ice bath was then removed, and the mixture was stirred at rt for 2 h under Ar. The residue was concentrated under reduced pressure and purified by silica gel flash chromatography (Hex/EtOAc 9:1 to 7:3) to obtain alcohol **19** (9.1 g, 90%) as pale yellow oil; $[\alpha]_D^{20}$ = –7.0 (*c* 0.80, $CHCl_3$); ^{1}H NMR (600 MHz, $CDCl_3$) δ 4.29 (dd, ^3J = 6.9, 1.5 Hz, 1H, H-5), 4.25 (ddd, ^3J = 10.1, 6.9, 3.0 Hz, 1H, H-4), 4.16 – 4.09 (m, 3H, CH_2-9, H-8a), 4.05 – 3.98 (m, 2H, H-8b, H-7), 3.52 (t, ^3J = 6.9 Hz, 1H, H-6), 2.56 (ddd, ^3J = 16.2, 8.6, 5.6 Hz, 1H, H-2a), 2.45 – 2.39 (m, 1H, H-2b), 2.13 – 2.06 (m, 1H, H-3a), 2.02 – 1.96 (m, 1H, H-3b), 1.69 (br. s, 1H, O*H*), 1.48 (s, 3H, CH_3), 1.41 (s, 3H, CH_3), 1.36 (s, 3H, CH_3), 1.35 (s, 3H, CH_3-10), 1.26 (t, ^3J = 7.2 Hz, 3H, CH_2CH_3); $[\alpha]_D^{20}$ = -7.0 (*c* 0.80, $CHCl_3$); ^{13}C NMR (100 MHz, $CDCl_3$) δ 173.32 (C-1), 109.48 ($C(CH_3)_2$), 108.13 ($C(CH_3)_2$), 76.46 (C-7), 76.29 (C-4), 76.20 (C-5), 70.73 (C-6), 67.30 (C-8), 60.58 (CH_2-9), 31.55 (C-2), 27.08 (CH_3), 26.92 (CH_3), 25.54 (C-3), 25.48 (CH_3),

24.83 (*C*H_3), 14.37 (*C*H_3-10); HRMS (ESI-TOF) *m/z* [M + H]$^+$ cald for $C_{16}H_{28}O_7$ 333.19078; found 333.19016; *m/z* [M + Na]$^+$ cald for $C_{16}H_{28}O_7$ 355.17272; found 355.17214.

4.3.15. Ethyl (4*R*,5*S*,6*R*,7*R*)-6-[trimethylsilyl)oxy]-4,5:7,8-di-*O*-isopropylidene-octonate (20)

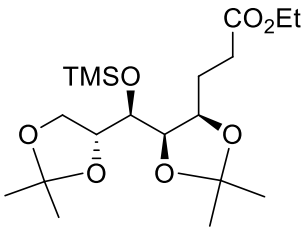

20

To a solution of alcohol **19** (7.8 g, 23.5 mmol, 1.0 equiv) in anhydrous MeCN (120 mL), bis(trimethylsilyl)amine (9.8 mL, 47.0 mmol, 2.0 equiv), and TMSCl (598 µL, 4.7 mmol, 2.0 equiv) were added sequentially and stirred overnight at rt under Ar. The ammonium salts were filtered off over celite and the solvents were evaporated under reduced pressure. The residue was then co-evaporated with toluene (2×) and then dried *in vacuo* to obtain ester **20** (9.5 g, quantitative) as yellow oil, which was used for next reaction without purification: R_f 0.4 (Hex/EtOAc 9:1).

4.3.16. Ethyl (4*R*,5*S*,6*R*,7*R*)-2-bromo-6-[trimethylsilyl)oxy]-4,5:7,8-di-*O*-isopropylidene-octonate (21)

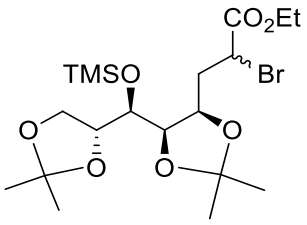

21

Ester **20** (9.5 g, 23.5 mmol, 1.0 equiv) and TMSCl (5.9 mL, 47.0 mmol, 2.0 equiv) were dissolved in anhydrous THF (120 mL) under Ar. This solution was added to a solution of 1.0 M LDA in THF/Hex (47.0 mL, 47.0 mmol, 2.0 equiv) at –78 °C and stirred for 1 h under Ar. NBS (10.1 g, 56.4 mmol, 2.4 equiv) was added slowly in small portions (over 20 min), brought to 0 °C and stirred for 1 h. The reaction was quenched by saturated solution of aq. $NaHCO_3$ (100 mL), diluted with EtOAc (200 mL) and washed with H_2O (200 mL). The aqueous phase was extracted with EtOAc (3 × 200 mL), dried over $MgSO_4$ and concentrated under reduced pressure. The residue was purified by silica gel flash chromatography (Hex/EtOAc/TEA 89:10:1) to obtain a

mixture of isomers **21** (11.3 g, quantitative) as yellow oil, which was used directly for next step: R_f 0.5 & 0.6 (Hex/EtOAc 9:1).

4.3.17. Ethyl 2,3-dideoxy-4,5:7,8-di-*O*-isopropylidene-α,β-D-*manno*-oct-2-ulopyranosonate (22)

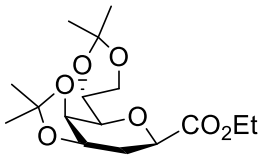

22a

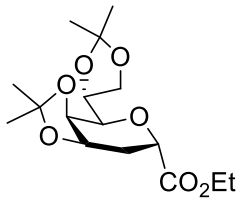

22b

The isomers **21** (11.3 g, 23.5 mmol, 1.0 equiv) were dissolved in mixture of EtOAc/abs. EtOH 9:1 (235 mL). A solution of 1.0 M TBAF in THF (23.5 mL, 23.5 mmol, 1.0 equiv) was added dropwise and stirred for 5 min at rt (until complete deprotection). Then K_2CO_3 (9.7 g, 70.6 mmol, 3.0 equiv) was added and stirred overnight at rt. After the reaction mixture was diluted with EtOAc (400 mL) and washed with H_2O (400 mL), the aqueous layer was extracted with EtOAc (3 x 400 mL). The combined organic phases were dried over $MgSO_4$ and concentrated under reduced pressure. The residue was purified by silica gel flash chromatography (Hex/EtOAc 9:1 to 7:3) to obtain d-Kdo-ester **22b** (4.4 g, 60%) as yellow oil along with anomer **22a** (2.2 g, 30%) as yellow crystal: Analytical data for **22b**: R_f 0.6 (Hex/EtOAc 7:3); $[\alpha]_D^{20}$ = –43.1 (*c* 0.45, $CHCl_3$); ^{1}H NMR (600 MHz, $CDCl_3$) δ 4.59 (ddd, appeared as dt, ^3J = 7.9, 2.9 Hz, 1H, H-4), 4.53 (dd, ^3J = 11.4, 5.9 Hz, 1H, H-2), 4.34 (dd, ^3J = 8.0, 1.6 Hz, 1H, H-5), 4.24 – 4.19 (m, 4H,), 4.13 – 4.09 (m, 1H), 3.51 (dd, ^3J = 8.4, 1.6 Hz, 1H, H-6), 2.31 (ddd, ^3J = 15.0, 5.9, 3.3 Hz, 1H, H-3a), 1.86 (ddd, ^3J = 14.8, 11.4, 2.6 Hz, 1H, H-3b), 1.49 (s, 3H, CH_3), 1.42 (s, 3H, CH_3), 1.38 (s, 3H, CH_3), 1.36 (s, 3H, CH_3), 1.29 (t, ^3J = 7.1 Hz, 3H, CH_3-10). NMR spectral data correspond to the one reported in the literature.[115]

4.3.18. Ethyl 2,3-dideoxy-4,5-*O*-isopropylidene-β-D-*manno*-oct-2-ulopyranosonate (23)

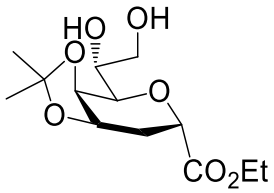

23

The solution of compound **22b** (1.0 g, 3.0 mmol, 1.0 equiv) in 60% aq. AcOH (60 mL) was stirred at rt for 3 h. The solution was concentrated under reduced pressure and purified by silica gel flash chromatography (Hex/EtOAc 7:3 to 0:1 followed by DCM/MeOH 9:1) to obtain diol **23** (502 mg, 57%) as yellow oil along with starting material **22b** (274 mg, 27 %) as yellow oil and tetraol (99 mg, 13%) as white solid: **23** R_f 0.15 (Hex/EtOAc 3:7); $[\alpha]_D^{20}$ = -30.4 (*c* 0.5, $CHCl_3$); ^{1}H NMR (600 MHz, $CDCl_3$) δ 4.61 (dt, ^3J = 7.9, 2.9 Hz, 1H, H-4), 4.55 (dd, ^3J = 11.2, 6.7 Hz, 1H, H-2), 4.43 (dd, ^3J = 8.0, 1.6 Hz, 1H, H-5), 4.22 (qd, ^3J = 7.1, 4.4 Hz, 2H, CH_3-9), 4.01 (dd, ^3J = 12.1, 3.1 Hz, 1H, H-8a), 3.85 (br. d, ^3J = 8.2 Hz, 1H, H-7), 3.74 (br. d, ^3J = 11.8 Hz, 1H, H-8b), 3.62 (dd, ^3J = 8.7, 1.6 Hz, 1H, H-6), 3.48 (br. s, 1H, O*H*), 2.63 (br. s, 1H, O*H*), 2.37 (ddd, ^3J = 15.1, 6.7, 3.3 Hz, 1H, H-3a), 1.80 (ddd, ^3J = 15.0, 11.2, 2.6 Hz, 1H, H-3b), 1.48 (s, 3H, CH_3), 1.38 (s, 3H, CH_3), 1.29 (t, ^3J = 7.1 Hz, 3H, CH_3-10); ^{13}C NMR (100 MHz, $CDCl_3$) δ 174.77 (C-1), 109.67 (*C*$(CH_3)_2$), 72.41 (C-5), 72.07 (C-6), 70.49 (C-4), 70.36 (C-7), 68.61 (C-2), 64.44 (C-8), 61.81 (*C*H_2-9), 26.65 (C-3), 26.54 (*C*H_3), 25.38 (*C*H_3), 14.50 (*C*H_3-10); HRMS (ESI-TOF) *m/z* $[M + NH_4]^+$ cald for $C_{13}H_{22}O_7$ 308.1703; found 308.1692; *m/z* $[M + Na]^+$ cald for $C_{13}H_{22}O_7$ 313.1257; found 313.125.

4.3.19. Ethyl 2,3-dideoxy-8-*O*-*p*-toluenesulfonate-4,5-*O*-isopropylidene-β-D-*manno*-oct-2-ulopyranosonate (24)

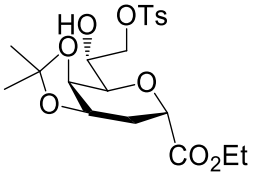

24

A Dean-stark apparatus attached to a flask containing diol **23** (418 mg, 1.44 mmol, 1.0 equiv) and Bu_2SnO (538 mg, 2.16 mmol, 1.5 equiv), suspended in anhydrous toluene (17.3 mL), was refluxed for 3 h. After cooling the mixture to rt, it was concentrated under reduced pressure to obtain a yellow residue. This residue was dissolved in anhydrous THF (8.6 mL) followed by DMAP (1.7 mg, 14.4 µmol, 0.01 equiv). Separately, a solution of TsCl (412 mg, 2.16 mmol, 1.5 equiv) in anhydrous THF (4.0 mL) was prepared and this was added to the former solution dropwise at 12–15 ^{o}C. The ice water bath was then removed and the reaction mixture was stirred overnight at rt under Ar. The solvents were evaporated under reduced pressure. The residue was purified by silica gel flash chromatography (Hex/EtOAc 8:2 to 4:6) to obtain

alcohol **24** (472 mg, 73%) as colourless oil: R_f0.4 (Hex/EtOAc 1:1); $[\alpha]_D^{20}$ = –6.28 (*c* 0.35, $CHCl_3$); ^{1}H NMR (600 MHz, $CDCl_3$) δ 7.82 (d, ^3J = 8.3 Hz, 2H, C*H*-Ar), 7.35 (d, ^3J = 8.1 Hz, 2H, C*H*-Ar), 4.57 (ddd, appeared as dt, ^3J = 7.5, 3.0 Hz, 1H, H-4), 4.49 (dd, ^3J = 11.1, 6.1 Hz, 1H, H-2), 4.45 (dd, ^3J = 10.6, 2.7 Hz, 1H, H-8a), 4.37 (dd, ^3J = 7.9, 1.7 Hz, 1H, H-5), 4.20 – 4.14 (m, 3H, CH_2-9, H-8b), 4.03 (m, 1H, H-7), 3.60 (dd, ^3J = 8.3, 1.7 Hz, 1H, H-6), 2.67 (d, ^3J = 5.4 Hz, 1H, O*H*), 2.45 (s, 3H, CH_3-Ar), 2.28 (ddd, ^3J = 15.0, 6.1, 3.5 Hz, 1H, H-3a), 1.82 (ddd, ^3J = 15.0, 11.2, 2.6 Hz, 1H, H-3b), 1.46 (s, 3H, CH_3), 1.35 (s, 3H, CH_3), 1.26 (t, ^3J = 7.1 Hz, 3H, CH_3-10); ^{13}C NMR (100 MHz, $CDCl_3$) δ 172.95 (C-1), 145.21 (C-Ar), 133.18 (C-Ar), 130.19 (*C*H-Ar), 128.37 (*C*H-Ar), 109.77 (*C*$(CH_3)_2$), 72.54 (C-8), 72.19 (C-5), 71.26 (C-6), 70.22 (C-4), 69.14 (C-7), 68.88 (C-2), 61.37 (*C*H_2-9), 26.93 (C-3), 26.55 (*C*H_3), 25.33 (*C*H_3), 21.99 (*C*H_3-Ph), 14.51 (*C*H_3-10); HRMS (ESI-TOF) *m/z* $[M + NH_4]^+$ cald for $C_{20}H_{28}O_9S$ 462.1792; found 462.1805.

4.3.20. Ethyl 2,3,8-trideoxy-8-azido-4,5-*O*-isopropylidene-β-D-*manno*-oct-2-ulopyranosonate (25)

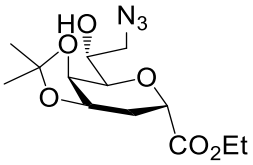

25

A solution of alcohol **24** (300 mg, 0.67 mmol, 1.0 equiv) dissolved in anhydrous DMSO (7.0 mL) and heated to 90 °C in the presence of NaN_3 (110 mg, 1.70 mmol, 2.5 equiv) was stirred overnight. The reaction mixture was diluted with DCM (30 mL), washed with H_2O (2 × 25 mL) and then with a saturated solution of aq. $NaHCO_3$ (20 mL). After drying over $MgSO_4$, the mixture was concentrated under reduced pressure. The residue was purified by silica gel flash chromatography (Hex/EtOAc 7:3 to 1:1) to obtain alcohol **25** (191 mg, 90%) as colourless oil: R_f0.5 (Hex/EtOAc 1:1); $[\alpha]_D^{20}$ = -7.2 (*c* 0.50, $CHCl_3$); ^{1}H NMR (600 MHz, $CDCl_3$) *δ* 4.59 (dt, ^3J = 7.7, 3.1 Hz, 1H, H-4), 4.53 (dd, ^3J = 11.1, 6.1 Hz, 1H, H-2), 4.40 (dd, ^3J = 7.9, 1.8 Hz, 1H, H-5), 4.21 (qd, ^3J = 7.1, 2.4 Hz, 2H, CH_2-9), 3.95 (m, 1H, H-7), 3.72 (dd, ^3J = 12.7, 2.9 Hz, 1H, H-8a), 3.62 (dd, ^3J = 8.4, 1.8 Hz, 1H, H-6), 3.51 (dd, ^3J = 12.7, 6.9 Hz, 1H, H-8b), 2.71 (d, ^3J = 5.2 Hz, 1H, O*H*), 2.31 (ddd, ^3J = 15.0, 6.1, 3.6 Hz, 1H, H-3), 1.85 (ddd, ^3J = 15.0, 11.1, 2.7 Hz, 1H, H-3), 1.49 (s, 3H, CH_3), 1.38 (s, 3H, CH_3), 1.29 (t, ^3J = 7.1 Hz, 3H, CH_3-10); ^{13}C NMR (100 MHz, $CDCl_3$) δ 173.14 (C-1), 109.76 (*C*$(CH_3)_2$), 72.35 (C-5), 72.11 (C-6), 70.26 (C-7, C-4), 68.81 (C-2), 61.14 (*C*H_2-9), 54.44 (C-8), 26.91 (C-3), 26.58 (*C*H_3), 25.35 (*C*H_3), 14.53 (*C*H_3-10); HRMS (ESI-TOF) *m/z*

[M + NH_4]$^+$ cald for $C_{13}H_{21}N_3O_6$ 333.1769; found 333.1771; *m/z* [M + Na]$^+$ cald for $C_{13}H_{22}N_3O_6$ 338.1322; found 338.1324.

4.3.21. Ethyl 2,3,8-trideoxy-8-azido-β-D-*manno*-oct-2-ulopyranosonate (26)

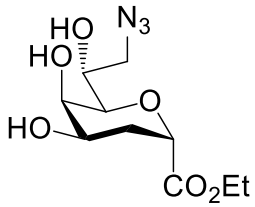

26

Azide **25** (140 mg, 0.44 mmol, 1.0 equiv) was dissolved in 60% aq. AcOH (10 mL), heated at 90 ^oC and stirred for 25 min. The solvents were evaporated under reduced pressure to obtain triol **26** (125 mg, quantitative) as a white amorphous solid, which was used for next step without further purification: R_f 0.4 ($CHCl_3$/MeOH 9:1); $[\alpha]_D^{20}$ = +26.3 (*c* 0.30, MeOH).

4.3.22. Ethyl 2,3,8-trideoxy-8-amino-β-D-*manno*-oct-2-ulopyranosonate (27)

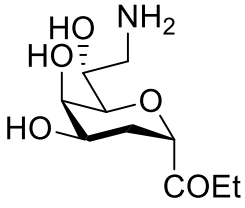

27

A solution of triol **26** (40 mg, 0.145 mmol, 1.0 equiv) dissolved in MeOH (1.5 mL) and flushed with H_2 was stirred overnight in the presence of 20% $Pd(OH)_2$/C (80 mg) at rt. The catalyst was filtered off over celite, rinsed with MeOH and concentrated under reduced pressure. The residue was purified by reversed-phase (C_{18}) silica gel flash chromatography packed with H_2O (H_2O/MeOH 1:0 to 1:1) to obtain amino compound **27** (30 mg, 85%) as white amorphous solid: R_f 0.5 (*i*-PrOH/H_2O/$CHCl_3$ 14:3:3, Ninhydrin stain); $[\alpha]_D^{20}$ = +121.9 (*c* 0.75, MeOH); ^{1}H NMR (600 MHz, D_2O) δ 4.72 (d, ^3J = 6.4 Hz, 1H, H-2), 4.32 – 4.26 (m, 2H, CH_2-9), 4.06 (td, ^3J = 8.1, 3.8 Hz, 1H, H-7), 4.02 (d, ^3J = 2.5 Hz, 1H, H-5), 3.79 (ddd, ^3J = 12.4, 4.9, 2.9 Hz, 1H, H-4), 3.56 (d, ^3J = 8.6 Hz, 1H, H-6), 3.40 (dd, ^3J = 13.2, 3.7 Hz, 1H, H-8a), 3.15 (dd, ^3J = 13.2, 7.9 Hz, 1H, H-8b), 2.26 (m, 1H, H-8a), 2.11 (ddd, J = 18.0, 12.2, 5.8 Hz, 1H, H-3b), 1.31 (t, ^3J = 7.2 Hz, 3H, CH_3-10); ^{13}C NMR (100 MHz, D_2O) δ 173.11 (C-1), 76.08 (C-6), 72.64 (C-2), 65.96 (C-4), 65.87 (C-5),

65.18 (C-7), 62.82 (*C*H_2-9), 42.92 (C-8), 27.38 (C-3), 13.42 (*C*H_3-10); HRMS (ESI-TOF) *m/z* [M + H]$^+$ cald for $C_{10}H_{19}NO_6$ 250.1281; found 250.1285.

4.3.23. 2,3,8-trideoxy-8-amino-β-D-*manno*-oct-2-ulopyranosonic acid (28)

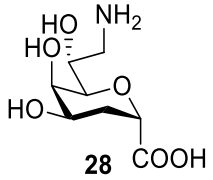

28

Triol **27** (10 mg, 36.0 µmol, 1.0 equiv) was dissolved in a mixture of THF/H_2O 3:1 (1.4 mL) and LiOH (2.0 mg, 72 µmol, 2.0 equiv) was added and stirred at rt for 2 h. The reaction mixture was protonated with 2.0 M aq. HCl until the pH was 1.0 and then evaporated under reduced pressure. The residue was purified by reversed-phase (C_{18}) silica gel flash chromatography (H_2O/MeOH 1:0 to 1:1) to obtain acid product **28** (8 mg, quantitative) as pale yellow solid: R_f 0.45 (MeOH/$CHCl_3$/H_2O 10:10:3); $[\alpha]_D^{20}$ = +13.5 (*c* 0.20, H_2O); ^{1}H NMR (600 MHz, D_2O) δ 4.65 (d, ^3J = 6.0 Hz, 1H, H-2), 4.09 (m, 1H, H-7), 4.02 (br. s, 1H, H-5), 3.81 (br. d, ^3J = 11.3 Hz, 1H, H-4), 3.57 (d, ^3J = 8.4 Hz, 1H, H-6), 3.34 (br. d, ^3J = 13.6 Hz, 1H, H-8a), 3.20 (dd, ^3J = 12.7, 6.5 Hz, 1H, H-8b), 2.24 (dd, ^3J = 9.4 Hz, 1H, H-3a), 2.14 – 2.07 (m, 1H, H-3b); ^{13}C NMR (100 MHz, D_2O) δ 175.77 (C-1), 75.48 (C-6), 72.72 (C-2), 66.14 (C-4), 65.86 (C-5), 64.93 (C-7), 42.97 (C-8), 27.59 (C-3); HRMS (ESI-TOF) *m/z* [M + H]$^+$ cald for $C_8H_{15}NO_6$ 222.09808; found 222.09721; *m/z* [M + K]$^+$ cald for $C_8H_{15}NO_6$ 260.05432; found 260.0531.

4.3.24. Methyl 2,8-Dideoxy-8-amino-β-D-*manno*-oct-2-ulopyranosonate (29)

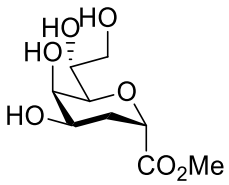

29

β-Compound **7** (135 mg, 0.427 mmol, 1.0 equiv) was heated to 90 °C in a solution of 90% aq. AcOH (100 mL) and stirred for 45 min. The solvents were evaporated under reduced pressure and purified by silica gel flash chromatography (DCM/MeOH 8:2) to obtain **29** (110 mg, quantitative) as a white amorphous solid: R_f 0.3 (DCM/MeOH 9:1); ^{1}H NMR (600 MHz, MeOD) δ 4.59 (d, ^3J = 5.9 Hz, 1H, H-2), 3.98 (d, ^3J = 2.0 Hz, 1H, H-5), 3.86-3.80 (m, 2H, H-7, H-8a), 3.78 (s, 3H, C*H*$_3$-9), 3.68 (dd, ^3J = 11.4, 5.7 Hz, 1H, H-8b), 3.63 (ddd, ^3J = 11.9, 5.1, 2.8 Hz, 1H, H-4),

3.54 (d, ^3J = 8.3 Hz, 1H, H-6), 2.22 – 2.12 (m, 2H, H-3a, H-3b). NMR spectral data correspond to the one reported in the literature.[17]

4.3.25. Ethyl 2,8-Dideoxy-8-amino-β-D-*manno*-oct-2-ulopyranosonate (30)

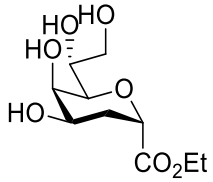

30

β-Compound **22b** (331 mg, 1.0 mmol, 1.0 equiv) was heated to 90 °C in a solution of 90% aq. AcOH (100 mL) and stirred for 45 min. The solvents were evaporated under reduced pressure and purified by silica gel flash chromatography (DCM/MeOH 8:2) to obtain **30** (251 mg, quantitative) as a white solid: R_f 0.3 (DCM/MeOH 9:1); ^{1}H NMR (600 MHz, MeOD) δ 4.58 – 4.55 (m, 1H, H-2), 4.24 (q, ^3J = 7.1 Hz, 2H, CH_2-9), 3.97 (d, ^3J = 2.3 Hz, 1H, H-5), 3.86-3.81 (m, 2H, H-7, H-8a), 3.67 (dd, ^3J = 11.9, 6.2 Hz, 1H, H-8b), 3.62 (ddd, ^3J = 11.4, 5.7, 2.8 Hz, 1H, H-4), 3.52 (d, ^3J = 8.8 Hz, 1H, H-6), 2.21 – 2.11 (m, 2H, H-3a, H-3b), 1.31 (t, ^3J = 7.2, 3H, CH_3-10). NMR spectral data correspond to the one reported in the literature.[116]

4.3.26. Methyl 4,5,7,8-tetra-*O*-acetyl-2,3-dideoxy-β-D-*manno*-oct-2-ulopyranosonate (31)

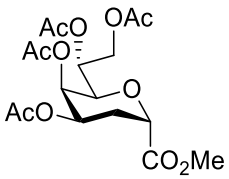

31

Compound **29** (15 mg, 0.085 mmol, 1.0 equiv) was acetylated according to the general procedure for peracetylation to obtain **31** (25 mg, 95%) as yellow oil: R_f 0.5 (Hex/EtOAc 7:3); $[\alpha]_D^{20}$ = +89.6 (*c* 1.0, $CHCl_3$); ^{1}H NMR (600 MHz, $CDCl_3$) δ 5.33 – 5.31 (m, 1H, H-5), 5.09 (ddd, ^3J = 9.5, 4.8, 2.2 Hz, 1H, H-7), 4.96 (ddd, ^3J = 12.7, 4.8, 3.0 Hz, 1H, H-4), 4.66 (d, ^3J = 6.2 Hz, 1H, H-2), 4.43 (dd, ^3J = 12.3, 2.2 Hz, 1H, H-8a), 4.31 – 4.25 (m, 2H, H-6, H-8b), 3.78 (s, 3H, CH_3-9), 2.30 (td, ^3J = 12.9, 6.7 Hz, 1H, H-3a), 2.20 – 2.16 (m, 1H, H-3b), 2.10 (s, 3H, COCH_3), 2.10 (s, 3H, COCH_3), 2.01 (s, 3H, COCH_3), 1.99 (s, 3H, COCH_3); ^{13}C NMR (100 MHz, $CDCl_3$) δ 171.03 (C-1), 170.84, 170.53, 170.07, 169.94 (4 X *C*OCH_3), 72.37 (C-2), 70.58 (C-6), 68.13 (C-7), 66.87 (C-4), 65.03 (C-5), 62.66 (C-8), 52.48 (*C*H_3), 26.38 (C-3), 20.91 – 20.73 (4 X CO*C*H_3); HRMS (ESI-

TOF) *m/z* [M + NH_4]$^+$ cald for $C_{17}H_{24}O_{11}$ 422.1657; found 422.165; *m/z* [M + Na]$^+$ cald for $C_{17}H_{24}O_{11}$ 427.1211; found 427.1205.

4.3.27. Ethyl 4,5,7,8-tetra-*O*-acetyl-2,3-dideoxy-β-D-*manno*-oct-2-ulopyranosonate (32)

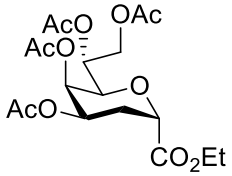

32

Compound **30** (28 mg, 0.112 mmol, 1.0 equiv) was acetylated according to the general procedure for peracetylation to obtain **32** (44 mg, 96%) as pale yellow oil: R_f 0.5 (Hex/EtOAc 7:3); ^{1}H NMR (600 MHz, $CDCl_3$) δ 5.33 – 5.32 (m, 1H, H-5), 5.09 (ddd, ^3J = 9.5, 5.1, 2.3 Hz, 1H,H-7), 4.97 (ddd, ^3J = 12.7, 4.8, 2.9 Hz, 1H, H-4), 4.63 (d, ^3J = 5.9 Hz, 1H, H-2), 4.48 (dd, ^3J = 12.3, 2.3 Hz, 1H, H-8a), 4.29 (d, ^3J = 9.5 Hz, 1H, H-6), 4.26 – 4.22 (m, 3H, H-8b, CH_2-9), 2.29 (td, ^3J = 12.9, 6.6 Hz, 1H, H-3a), 2.18 (dd, ^3J = 13.0, 5.0 Hz, 1H, H-3b), 2.10 (s, 3H, COCH_3), 2.09 (s, 3H, COCH_3), 2.00 (s, 3H, COCH_3), 1.99 (s, 3H, COCH_3), 1.32 (t, ^3J = 7.1 Hz, 3H, CH_3-10); ^{13}C NMR (100 MHz, $CDCl_3$) δ 170.89 (C-1), 170.56, 170.09, 169.98 (4 X *C*OCH_3), 72.43 (C-2), 70.67 (C-6), 68.20 (C-7), 66.91 (C-4), 65.10 (C-5), 62.76 (C-8), 61.67 (*C*H_2), 26.42 (C-3), 20.96 – 20.76 (4 X CO*C*H_3), 14.30 (*C*H_3); HRMS (ESI-TOF) *m/z* [M + NH_4]$^+$ cald for $C_{18}H_{26}O_{11}$ 436.18134; found 436.1814; *m/z* [M + Na]$^+$ cald for $C_{18}H_{26}O_{11}$ 441.13673; found 441.13684.

4.3.28. 2,3-dideoxy-β-D-*manno*-oct-2-ulopyranosonic acid (33)

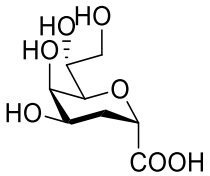

33

Tetraol **30** (60 mg, 0.240 mmol, 1.0 equiv) was dissolved in a mixture of THF/H_2O 3:1 (10 mL), LiOH (11.5 mg, 0.480 mmol, 2.0 equiv) was added and the mixture was stirred at rt for 2 h. The reaction mixture was protonated with 2.0 M aq. HCl until the pH was 1.0 and then evaporated under reduced pressure. The residue was purified by reversed-phase (C_{18}) silica gel flash chromatography (H_2O/MeOH 1:0 to 1:1). The fractions containing the compound were pooled and freeze-dried to obtain acid product **33** (53 mg, quantitative) as a white solid:

R_f 0.5 (MeOH/$CHCl_3$/H_2O 10:10:3); ^{1}H NMR (600 MHz, D_2O) δ 4.64 (d, ^3J = 6.2 Hz, 1H, H-2), 4.01 (d, ^3J = 2.5 Hz, 1H, H-5), 3.87 – 3.79 (m, 3H, H-4, H-8a, H-7), 3.70 (dd, ^3J = 12.0, 6.0 Hz, 1H, H-8b), 3.58 – 3.56 (m, 1H, H-6), 2.22 (dd, ^3J = 13.3, 4.9 Hz, 1H, H-3a), 2.10 (td, ^3J = 12.9, 6.8 Hz, 1H, H-3b); ^{13}C NMR (100 MHz, D_2O) δ 175.35 (C-1), 74.51 (C-6), 72.45 (C-2), 69.24 (C-4), 66.22 (C-5, C-7), 63.45 (C-8), 27.50 (C-3); HRMS (ESI-TOF) *m/z* [M + NH_4]$^+$ cald for $C_8H_{14}O_7$ 240.10778; found 240.10712; *m/z* [M + Na]$^+$ cald for $C_8H_{14}O_7$ 245.06317; found 245.06239.

4.3.29. Ammonium 2,4,5,7,8-penta-*O*-acetyl-3-deoxy-α-D-*manno*-oct-2-ulopyranosylonate (37)

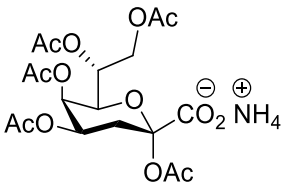

37

Crystalline Kdo.NH_3 **2** (2.0 g, 7.8 mmol, 1.0 equiv) was dissolved in anhydrous pyridine, by adding the crystals portionwise while stirring continuously. Acetic anhydride (80 mL), DMAP (10 mg, 18 µmol, 0.01 equiv) were added to the solution and it was stirred for 16 h at rt under Ar. The reaction mixture was concentrated under reduced pressure by co-evaporating with toluene (3×) and purified by silica gel flash chromatography (DCM/MeOH 1:0 to 8:2) to obtain peracetylated **37** (3.5 g, 95%) as yellow oil: R_f 0.2 (DCM/MeOH 8:2); NMR spectral data correspond to the one reported in the literature.[117]

4.3.30. Benzyl 2,4,5,7,8-Penta-*O*-acetyl-3-deoxy-α-D-*manno*-oct-2-ulopyranosonate (38)

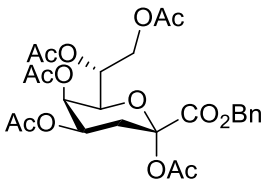

38

To a stirred solution of peracetylated Kdo **37** (2.9 g, 6.4 mmol, 1.0 equiv) in anhydrous DMF (30 mL), BnBr (1.7 mL, 14.0 mmol, 2.2 equiv) followed by Cs_2CO_3 (0.8 g, 2.5 mmol, 0.4 equiv) were added and stirred for 2 h at rt under Ar. The mixture was filtered over celite to eliminate Cs salt and rinsed with EtOAc (75 mL). The solution was washed with a saturated solution of aq. NH_4Cl (50 mL) resulting in a white foam, which later disappeared by washing separated

organic layer with H_2O (50 mL). The aqueous phase was extracted with EtOAc (2 × 50 mL). The combined organic phase was dried over $MgSO_4$ and concentrated under reduced pressure. The residue was purified by silica gel flash chromatography (Hex/EtOAc 8:2 to 1:1) to obtain ester **38** (2.5 g, 75%) as yellow oil; R_f 0.2 (Hex/EtOAc 6:4); NMR spectral data correspond to the one reported in the literature.[118]

4.3.31. Benzyl (Ethyl 4,5,7,8-tetra-O-acetyl-3-deoxy-2-thio-α,β-D-*manno*-oct-2-ulopyranosid)onate (39)

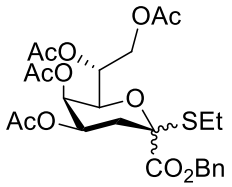

39

Ester **38** (2.5 g, 4.7 mmol, 1.0 equiv) was dissolved in anhydrous DCE (23 mL), EtSH (700 µL, 9.3 mmol, 2.0 equiv) was added and cooled to 0 °C. $BF_3.OEt_2$ (860 µL, 6.9 mmol, 1.5 equiv) was added dropwise to the solution and stirred for 20 min at 0 °C. Ice water bath was then removed and the reaction mixture was stirred at rt for 2 h under Ar. After neutralizing with saturated solution of aq. $NaHCO_3$ (until the CO_2 evolution stopped), it was diluted with DCM (30 mL), followed by addition of iodine (~2.0 equiv) until the colour change from yellow to red was permanent. Iodine was in turn quenched by 10% aq. solution of $Na_2S_2O_3$ until the red colour disappeared. The aqueous layer was extracted with DCM (3 × 20 mL). The combined organic layer was washed with brine (20 mL), dried over $MgSO_4$ and concentrated under reduced pressure. The residue was purified by silica gel flash chromatography (Hex/EtOAc 8:2/6:4) to obtain thioglycoside **39** (2.3 g, 90%) as pale-yellow oil: R_f 0.4 (Hex/EtOAc 6:4); NMR spectral data correspond to the one reported in the literature.[84]

4.3.32. Benzyl [2-(2'-Adamantyl) 4,5,7,8-tetra-*O*-acetyl-3-deoxy-α,β-D-*manno*-oct-2-ulopyranosid]onate (40)

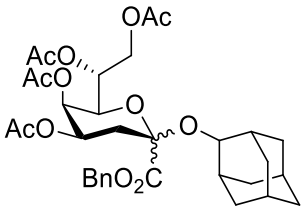

40

Thioglycoside donor **39** (500 mg, 0.925 mmol, 1.0 equiv) was reacted with 2-adamantanol (182 mg, 1.2 mmol, 1.3 equiv) according to the above-mentioned general procedure for glycosylation to obtain glycoside **40** (515 mg, 74%) as yellow oil: R_f 0.3 (Hex/EtOAc 7:3); NMR spectral data correspond to the one reported in the literature.[92]

4.3.33. Benzyl [2-(1'-Adamantanemethyl) 4,5,7,8-tetra-*O*-acetyl-3-deoxy-β-D-*manno*-oct-2-ulopyranosid]onate (41)

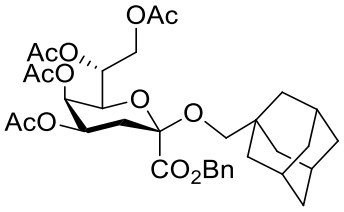

41

Thioglycoside donor **39** (600 mg, 1.11 mmol, 1.0 equiv) was reacted with 1-adamantanemethanol (240 mg, 1.443 mmol, 1.3 equiv) according to the above-mentioned general procedure for glycosylation to obtain glycoside **41** (580 mg, 80%) as brownish yellow solid: R_f 0.3 (Hex/EtOAc 7:3); $[\alpha]_D^{20}$ = +42.0 (*c* 0.50, $CDCl_3$); ^{1}H NMR (600 MHz, acetone-d6) δ 7.49-7.47 (m, 2H, C*H*-Ar), 7.42 – 7.39 (m, 2H, C*H*-Ar), 7.38 – 7.35 (m, 1H, C*H*-Ar), 5.32 (br. s, 2H, CH_2-Ph), 5.26 – 5.24 (m, 1H, H-5), 5.13 (ddd, ^3J = 9.2, 5.8, 2.3 Hz, 1H, H-7), 4.95 (ddd, ^3J = 13.1, 4.6, 3.1 Hz, 1H, H-4), 4.41 (dd, ^3J = 12.2, 2.3 Hz, 1H, H-8a), 4.27-4.21 (m, 2H, H-8b, H-6), 3.33 (d, ^3J = 9.1 Hz, 1H, C*H*H-Ad), 2.89 (d, ^3J = 9.1 Hz, 1H, C*H*H-Ad), 2.42 (dd, ^3J = 12.3, 4.6 Hz, 1H, H-3), 2.06 – 2.02 (m, 1H, H-8b), 2.04 (s, 3H, COCH_3), 2.01 (s, 3H, COCH_3), 1.94 (s, 3H, COCH_3), 1.97 – 1.89 (m, 3H, 3 X C*H*-Ad), 1.92 (s, 3H, COCH_3), 1.74 – 1.60 (m, 6H, 3 X CH_2-Ad), 1.48 – 1.41 (m, 6H, 3 X CH_2-Ad); ^{13}C NMR (100 MHz, acetone-d6) δ 170.95, 170.87, 170.19, 170.08 (4 X *C*OCH$_3$), 168.71 (C-1), 136.76 (C-Ar), 129.80-129.45 (*C*H-Ar), 100.42 (C-2), 75.07 (*C*H$_2$-Ad), 71.92 (C-6), 69.07 (C-7), 68.32 (*C*H$_2$Ph), 68.00 (C-4), 65.06 (C-5), 63.47 (C-8), 40.12

(3 X *C*H_2-Ad), 37.92 (3 X *C*H_2-Ad), 34.09 (*C*-Ad), 33.25 (C-3), 29.20 (3 X *C*H-Ad), 20.95 – 20.75 (4 X CO*C*H_3); HRMS (ESI-TOF) *m/z* [M + NH_4]$^+$ cald for $C_{34}H_{44}O_{12}$ 662.3171; found 662.3182; *m/z* [M + Na]$^+$ cald for $C_{34}H_{44}O_{12}$ 667.2725; found 667.2735.

4.3.34. Benzyl [2-(1'-Adamantaneethyl) 4,5,7,8-Tetra-O-acetyl-3-deoxy-β-D-*manno*-oct-2-ulopyranosid]onate (42)

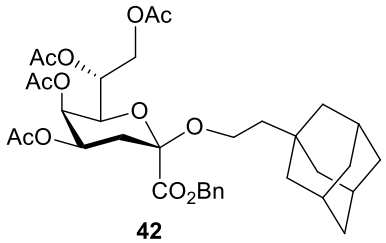

42

Thioglycoside donor **39** (620 mg, 1.15 mmol, 1.0 equiv) was reacted with 1-adamantaneethanol (260 mg, 1.45 mmol, 1.3 equiv) according to the above-mentioned general procedure for glycosylation to obtain glycoside **42** (755 mg, 90%) as brown solid: R_f 0.3 (Hex/EtOAc 7:3); $[\alpha]_D^{20}$ = +130.4 (*c* 0.70, $CDCl_3$); ^{1}H NMR (600 MHz, Acetone-d6) δ 7.50-7.46 (m, 2H, C*H*-Ar), 7.42-7.35 (m, 3H, C*H*-Ar), 5.34 (br. s, 2H, CH_2-Ph), 5.27 – 5.24 (m, 1H, H-5), 5.14 (ddd, ^3J = 9.3, 5.7, 2.2 Hz, 1H, H-7), 4.94 (ddd, ^3J = 13.1, 4.7, 3.1 Hz, 1H, H-4), 4.41 (dd, ^3J = 12.2, 2.2 Hz, 1H, H-8a), 4.29 - 4.25 (m, 2H, H-8b, H-6), 3.83 (td, ^3J = 8.8, 6.3 Hz, 1H, C*H*H-Ad), 3.35 (td, ^3J = 8.8, 6.3 Hz, 1H, C*H*H-Ad), 2.41 (dd, ^3J = 12.4, 4.7 Hz, 1H, H-3a), 2.04 (s, 3H, COCH_3), 2.03 - 2.02 (m, 1H, H-3b) 2.01 (s, 3H, COCH_3), 1.94 (s, 3H, COCH_3), 1.92 (s, 3H, COCH_3), 1.91 – 1.87 (m, 3H, 3 X CH-Ad), 1.72 – 1.59 (m, 6H, 3 X CH_2-Ad), 1.48 – 1.44 (m, 6H, 3 X CH_2-Ad), 1.28 (ddd, ^3J = 21.1, 8.1, 6.1 Hz, 2H, CH_2-Ad); ^{13}C NMR (100 MHz, Acetone-d6) δ 170.93, 170.86, 170.18, 170.10 (4 X *C*OCH_3), 168.81 (C-1), 136.75 (C-Ar), 129.65-129.41 (*C*H-Ph), 100.46 (C-2), 71.92 (C-6), 69.09 (C-7), 68.39 (*C*H_2Ph), 67.97 (C-4), 65.09 (C-5), 63.44 (C-8), 61.28 (*C*H_2-Ad), 44.48 (*C*H_2-Ad), 43.31 (3 X *C*H_2-Ad), 37.87 (3 X *C*H_2-Ad), 33.56 (C-3), 32.55 (*C*-Ad), 30.40 – 29.60 (3 X *C*H-Ad), 20.90 – 20.80 (4 X CO*C*H_3); HRMS (ESI-TOF) *m/z* [M + NH_4]$^+$ cald for $C_{35}H_{46}O_{12}$ 676.3328; found 676.334; *m/z* [M + Na]$^+$ cald for $C_{35}H_{46}O_{12}$ 681.2881; found 681.2894.

4.3.35. 2-(2'-Adamantyl) (4,5,7,8-tetra-*O*-acetyl-3-deoxy-β-D-*manno*-oct-2-ulopyranosid)onic acid (46)

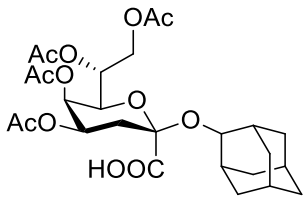

46

Kdo glycoside **40** (240 mg, 0.381 mmol, 1.0 equiv) was reduced according to the general procedure for hydrogenolysis to obtain acid derivative **46** (381 mg, 95%) as yellow solid: R_f (β-form) 0.7 (DCM/MeOH 9:1); R_f (α-form) 0.3 (DCM/MeOH 9:1); $[\alpha]_D^{20}$ = +53.9 (*c* 0.33, $CHCl_3$); ^{1}H NMR (600 MHz, $CDCl_3$, β-anomer) δ 5.31-5.29 (m, 1H, H-5), 5.17 – 5.10 (m, 2H, H-4, H-7), 4.34 – 4.30 (m, 1H, H-8a), 4.27 (dd, ^3J = 12.3, 4.5 Hz, 1H, H-8b), 4.19 (d, ^3J = 9.5 Hz, 1H, H-6), 4.05 (br. s, 1H, C*H*-Ad), 2.31 (dd, ^3J = 12.6, 4.5 Hz, 1H, H-3a), 2.15 (t, ^3J = 12.9 Hz, 1H, H-3b), 2.11 (s, 3H, COCH_3), 2.10-2.03 (m, 2H, CH_2-Ad), 2.07 (s, 3H, COCH_3), 2.01 (s, 3H, COCH_3), 1.99 (s, 3H, COCH_3), 1.98-1.94 (m, 1H, C*H*-Ad), 1.89 – 1.78 (m, 5H, CH_2-Ad, 3 X C*H*-Ad), 1.73 – 1.64 (m, 4H, 2 X CH_2-Ad), 1.56 – 1.49 (m, 2H, CH_2-Ad); ^{13}C NMR (100 MHz, $CDCl_3$) δ 171.02, 170.52, 170.14 (4 X *C*OCH_3), 170.19 (C-1), 99.23 (C-2), 78.23 (*C*H-Ad), 70.86 (C-6), 68.15 (C-4), 67.63 (C-7), 64.29 (C-5), 62.69 (C-8), 37.53, 37.0, 36.88 (3 X *C*H_2-Ad), 34.33, 33.76 (2 X *C*H-Ad), 31.73 (C-3), 31.68 (2 X *C*H_2-Ad), 27.29, 27.03 (2 X *C*H-Ad), 20.95 - 20.72 (4 X CO*C*H_3); HRMS (ESI-TOF) *m/z* $[M + NH_4]^+$ cald for $C_{26}H_{36}O_{12}$ 558.2545; found 558.2562; *m/z* $[M + Na]^+$ cald for $C_{26}H_{36}O_{12}$ 563.2099; found 563.2114.

4.3.36. 2-(1'-Adamantanemethyl) (4,5,7,8-tetra-*O*-acetyl-3-deoxy-β-D-*manno*-oct-2-ulopyranosid)onic Acid (47)

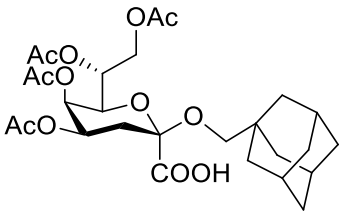

47

Kdo glycoside **40** (550 mg, 0.853 mmol, 1.0 equiv) was reduced according to the general procedure for hydrogenolysis to obtain acid derivative **47** (407 mg, 90%) as white solid: R_f (β-form) 0.7 (DCM/MeOH 9:1); R_f (α-form) 0.3 (DCM/MeOH 9:1); $[\alpha]_D^{20}$ = +41.0 (*c* 0.60, $CDCl_3$);

^{1}H NMR (600 MHz, Acetone-d6) δ 5.29-5.27 (m, 1H, H-5), 5.14 (ddd, ^{3}J = 9.3, 5.0, 2.7 Hz, 1H, H-7), 4.99 (ddd, ^{3}J = 13.1, 4.6, 3.1 Hz, 1H, H-4), 4.38 – 4.31 (m, 2H, H-8a, H-8b), 4.26 (dd, ^{3}J = 9.4, 1.0 Hz, 1H, H-6), 3.40 (d, ^{3}J = 9.1 Hz, 1H, C*H*H-Ad), 3.07 (d, ^{3}J = 9.1 Hz, 1H, C*H*H-Ad), 2.39 (dd, ^{3}J = 12.3, 4.6 Hz, 1H, H-3a), 2.10 – 2.07 (m, 1H, H-3b), 2.06 (s, 3H, COC*H*$_3$), 2.01 (s, 3H, COC*H*$_3$), 1.99-1.92 (m, 3H, C*H*-Ad) 1.96 (s, 3H, COC*H*$_3$), 1.94 (s, 3H, COC*H*$_3$), 1.77 – 1.66 (m, 6H, 3 X C*H*$_2$-Ad), 1.60 – 1.54 (m, 6H, 3 X C*H*$_2$-Ad); ^{13}C NMR (100 MHz, Acetone-d6) δ 170.96, 170.85, 170.22, 170.14 (4 X *C*OCH$_3$), 169.80 (C-1), 100.20 (C-2), 75.05 (*C*H$_2$-Ad), 71.71 (C-6), 69.11 (C-7), 68.20 (C-4), 65.12 (C-5), 63.40 (C-8), 40.26 (3 X *C*H$_2$-Ad), 37.95 (3 X *C*H$_2$-Ad), 34.15 (C-Ad), 33.13 (C-3), 29.23 (3 x *C*H-Ad), 20.90 - 20.74 (4 X CO*C*H$_3$); HRMS (ESI-TOF) *m/z* [M + NH$_4$]$^+$ cald for $C_{27}H_{38}O_{12}$ 572.2702; found 572.2703; *m/z* [M + Na]$^+$ cald for $C_{27}H_{38}O_{12}$ 577.2255; found 577.2254.

4.3.37. 2-(1'-Adamantaneethyl) (4,5,7,8-Tetra-*O*-acetyl-3-deoxy-β-D-manno-oct-2-ulopyranosid)onic acid (48)

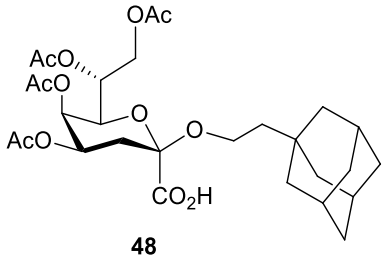

48

Kdo glycoside **42** (700 mg, 1.063 mmol, 1.0 equiv) was reduced according to the general procedure for hydrogenolysis to obtain acid derivative **48** (543 mg, 90%) as white solid: R_f (β-form) 0.7 (DCM/MeOH 9:1); R_f (α-form) 0.3 (DCM/MeOH 9:1); $[\alpha]_D^{20}$ = +24.7 (*c* 0.55, $CDCl_3$); ^{1}H NMR (600 MHz, Acetone-d6) δ 5.28 – 5.26 (m, 1H, H-5), 5.17 – 5.12 (m, 1H, H - 7), 5.01 – 4.96 (m, 1H, H-4), 4.38 – 4.32 (m, 2H, H-8a, H-8b), 4.28 (d, ^{3}J = 9.3 Hz, 1H, H-6), 3.90 (dd, ^{3}J = 16.0, 8.0 Hz, 1H, C*H*H-Ad), 3.54 (dd, ^{3}J = 15.0, 7.5 Hz, 1H, C*H*H-Ad), 2.37 (dd, ^{3}J = 12.3, 4.5 Hz, 1H, H-3a), 2.05 (s, 3H, COC*H*$_3$), 2.05 – 2.01 (m, 1H, H-3b), 2.00 (s, 3H, COC*H*$_3$), 1.95 (s, 3H, COC*H*$_3$), 1.93 (s, 3H, COC*H*$_3$), 1.95 – 1.90 (m, 3H, 3 X C*H*-Ad), 1.74 – 1.64 (m, 6H, 3 X C*H*$_2$-Ad), 1.58 – 1.54 (m, 6H, 3 X C*H*$_2$-Ad), 1.40 – 1.34 (m, 2H, C*H*$_2$-Ad); ^{13}C NMR (100 MHz, Acetone-d6) δ 170.86, 170.78, 170.13, 170.09 (4 X *C*OCH$_3$), 169.73 (C-1), 100.14 (C-2), 71.66 (C-6), 69.05 (C-7), 68.07 (C-4), 65.08 (C-5), 63.30 (C-8), 61.06 (*C*H$_2$-Ad), 44.52 (*C*H$_2$-Ad), 43.31 (3 X *C*H$_2$-Ad), 37.83 (3 X *C*H$_2$-Ad), 33.32 (C-3), 32.59 (C-Ad), 30.40 – 29.50 (3 X *C*H-Ad), 20.85 – 20.70 (4 X

COCH$_3$); HRMS (ESI-TOF) *m/z* [M + NH$_4$]$^+$ cald for $C_{28}H_{40}O_{12}$ 586.2858; found 586.2882; *m/z* [M + Na]$^+$ cald for $C_{28}H_{40}O_{12}$ 591.2412; found 591.2433.

4.3.38. 2-(2'-Adamantyl) (3-deoxy-β-D-*manno*-oct-2-ulopyranosid)onic acid (49)

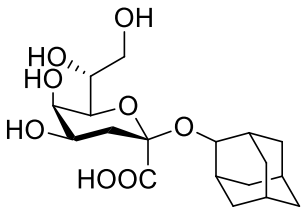

49

Kdo glycoside (102 mg, 0.188 mmol, 1.0 equiv) was treated with NaOMe (25% wt. MeOH, 47 µL, 0.188 mmol, 1.0 equiv) according to the general procedure for Zemplén deprotection to obtain **49** (63 mg, 90%) as yellow oil: R_f 0.2 (DCM/MeOH 6:4); $[\alpha]_D^{20}$ = +11.5 (*c* 0.8, MeOH); ^{1}H NMR (600 MHz, MeOD) δ 4.13-4.11 (m, 1H, H-5), 3.90 – 3.84 (m, 3H, H-7, H-8a, C*H*-Ad), 3.68 – 3.64 (m, 2H, H-8b, H-4), 3.51 (d, ^3J = 9.1 Hz, 1H, H-6), 2.46 (dd, ^3J = 12.2, 4.6 Hz, 1H, H-3a), 2.16 (dd, ^3J = 21.0, 12.3 Hz, 2H, CH_2-Ad), 1.96 – 1.84 (m, 3H, H-3b, 2 X C*H*-Ad), 1.79 – 1.70 (m, 6H, 2 X CH_2-Ad, 2 X C*H*-Ad), 1.48 – 1.45 (m, 2H, CH_2-Ad), 1.31 – 1.28 (m, 2H, CH_2-Ad); ^{13}C NMR (100 MHz, MeOD) δ 78.08 (C-5), 75.15 (C-6), 70.75 (*C*H-Ad), 69.33 (C-4), 67.13 (C-7), 65.95 (C-8), 38.01, 37.95 (2 X *C*H$_2$-Ad), 36.88 (C-3), 35.52, 34.52 (2 X *C*H-Ad), 32.69, 32.63 (2 X *C*H$_2$-Ad), 28.86, 28.61 (2 X *C*H-Ad); HRMS (ESI-TOF) *m/z* [M + NH$_4$]$^+$ cald for $C_{18}H_{28}O_8$ 390.2122; found 390.2124; *m/z* [M + Na]$^+$ cald for $C_{18}H_{28}O_8$ 395.1676; found 395.1679.

4.3.39. 2-(1'-Adamantanemethyl) (3-Deoxy-β-D-*manno*-oct-2-ulopyranosid)onic Acid (50)

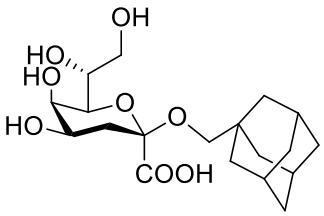

50

Kdo glycoside (320 mg, 0.577 mmol, 1.0 equiv) was treated with NaOMe (25% wt. MeOH, 264 µL, 0.154 mmol, 2.0 equiv) according to the general procedure for Zemplén deprotection to obtain **50** (63 mg, 90%) as white solid: R_f 0.2 (DCM/MeOH 6:4); $[\alpha]_D^{20}$ = +37.8 (*c* 0.60, MeOH); ^{1}H NMR (600 MHz, MeOD) δ 3.92 – 3.89 (m, 2H, H-5, H-7), 3.79 (dd, ^3J = 11.8, 2.6 Hz, 1H, H-8a), 3.74 (dd, ^3J = 11.9, 5.4 Hz, 1H, H-8b), 3.63 (ddd, ^3J = 12.5, 4.5, 3.0 Hz, 1H, H-4), 3.45 (d, ^3J

= 8.9 Hz, 1H, H-6), 3.28 (d, ^3J = 9.1 Hz, 1H, C*H*H-Ad), 2.98 (d, ^3J = 9.1 Hz, 1H, C*H*H-Ad), 2.33 (dd, ^3J = 12.4, 4.5 Hz, 1H, H-3a), 2.00 – 1.96 (m, 1H, H-3b), 1.95-1.92 (m, 3H, 3 X C*H*-Ad), 1.78-1.66 (m, 6H, 3 X CH_2-Ad), 1.55-1.50 (m, 6H, 3 X CH_2-Ad); ^{13}C NMR (100 MHz, Acetone-d6) δ 172.24 (C-1), 100.71 (C-2), 75.80 (C-6), 75.17 (*C*H_2-Ad), 70.82 (C-7), 68.95 (C-4), 67.03 (C-5), 65.77 (C-8), 40.59 (3 X *C*H_2-Ad), 38.26 (3 X *C*H_2-Ad), 35.54 (C-3), 34.33 (C-Ad), 29.68 (3 X *C*H-Ad); HRMS (ESI-TOF) *m/z* [M + NH_4]$^+$ cald for $C_{19}H_{30}O_8$ 404.2279; found 404.2293; *m/z* [M + Na]$^+$ cald for $C_{19}H_{30}O_8$ 409.1833; found 409.1844.

4.3.40. 2-(2'-Adamantaneethyl) (3-Deoxy-β-D-manno-oct-2-ulopyranosid)onic Acid (51)

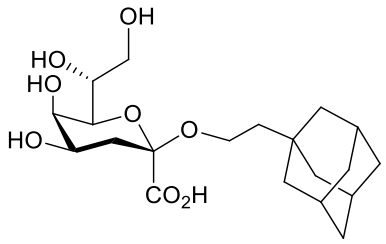

51

Kdo glycoside **48** (330 mg, 0.58 mmol, 1.0 equiv) was treated with NaOMe (25% wt. MeOH, 265 µL, 1.154 mmol, 2.0 equiv) according to the general procedure for Zemplén deprotection to obtain glycoside **51** (230 mg, quantitative) as white solid: R_f 0.2 (DCM/MeOH 6:4); $[\alpha]_D^{20}$ = +39.4 (*c* 0.46, $CDCl_3$); ^{1}H NMR (600 MHz, MeOD) δ 3.90 – 3.87 (m, 3H, H-5, H-7, H-8a), 3.80 (td, ^3J = 8.9, 6.4 Hz, 1H, CH_2-Ad), 3.72 – 3.69 (m, 1H, H-8b), 3.67 – 3.64 (m, 1H, H-4), 3.54 (d, ^3J = 9.0 Hz, 1H, H-6), 3.49 (td, ^3J = 8.8, 6.8 Hz, 1H, CH_2-Ad), 2.40 (dd, ^3J = 12.2, 4.6 Hz, 1H, H-3a), 1.93 – 1.86 (m, 4H, 3 X C*H*-Ad, H-3a), 1.75 – 1.64 (m, 8H, 4 X CH_2-Ad), 1.57 – 1.53 (m, 4H, 2 X CH_2-Ad), 1.34 – 1.31 (m, 2H, CH_2-Ad). ^{13}C NMR (100 MHz, MeOD) δ 173.69 (C-1), 101.57 (C-2), 75.18 (C-6), 70.73 (C-5), 69.24 (C-4), 67.14 (C-7), 65.79 (C-8), 60.97 (*C*H_2-Ad), 44.90 (*C*H_2-Ad), 43.81, 43.75 (2 X *C*H_2-Ad), 38.18 (4 X *C*H_2-Ad), 36.34 (C-3), 32.80 (C-Ad), 30.12 (3 X *C*H-Ad); HRMS (ESI-TOF) *m/z* [M + NH_4]$^+$ cald for $C_{20}H_{32}O_8$ 418.2435; found 418.2455.

4.3.41. Ammonium 8-Azido-3,8-dideoxy-D-*manno*-oct-2-ulopyranosylonate (58)

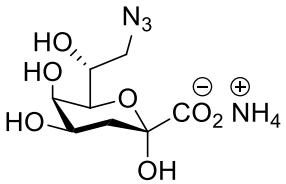

58

4-Azido-arabinose **57** was synthesized through a six-step synthetic sequence starting from D-arabinose.[119] Arabinose-N_3 **57** (350 mg, 2.0 mmol, 1.0 equiv) was dissolved in distilled H_2O (6.0 mL) containing Na_2CO_3 (526 mg, 4.9 mmol, 2.5 equiv). Crystals of oxaloacetic acid (317 mg, 2.4 mmol, 1.2 equiv) were added in small portions over five min. After adding few drops of 10.0 N aq. NaOH solution until the pH of the mixture was increased to 11.0 (checked by pH meter), the reaction mixture was stirred at rt for 2 h. Then, the pH was further brought down to 5.0 using AcOH, followed by adding $NiCl_2.6H_2O$ (0.01 equiv) and stirred at 50 °C for 1 h. After cooling the mixture to rt, it was passed to an anion exchange resin column CG-400 (HCO_3^-). It was first eluted with H_2O to remove the excess of arabinose-N_3, followed by aq. NH_4HCO_3 (0.05–0.30 N). The fractions were pooled after analysing by TLC ($CHCl_3$/MeOH/H_2O 10:10:3; revealed by CAM stain) and lyophilized to obtain desired Kdo product **67** (340 mg, 61%) as white amorphous solid. The presence of several other isomeric forms made the ^{1}H NMR characterization complicated and indistinct. However, the data for selected forms were consistent with the reported data.[13]

4.3.42. Methyl-α,β-L-xylopyranoside (60)

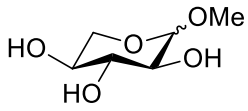

60

L-Xylose (20 g, 133.22 mmol, 1.0 equiv) was dissolved in anhydrous methanol (200 mL) under Ar at rt. Dowex H^+ resin (10 g) was added and the mixture was refluxed for 12 h based on TLC analysis. The reaction mixture was cooled down to rt and then filtered over celite. The solvents were evaporated under reduced pressure. The residue (dry loaded) was purified through silica gel flash chromatography (DCM/MeOH/acetone 15.5:1.5:3 to 14:3:3) to give methyl glycoside **60** (9.4 g, 42%, β/α 5:3) as pale yellowish residue: R_f 0.3 (DCM/MeOH/acetone 7:1.5:1.5); ^{1}H NMR (600 MHz, $CDCl_3$) δ 4.12 (d, ^3J = 7.6 Hz, 1H, H-1), 3.87 (dd, ^3J = 5.36, 11.48 Hz, H-5a), 3.58 – 3.54 (m, 1H, H-4), 3.50 (s, 3H, CH_3), 3.48 – 3.45 (m, 1H, H-5b), 3.23 – 3.19 (m, 1H, H-3), 3.16 (dd, ^3J 9.0, 7.7 Hz, 1H, H-2).

4.3.43. Methyl 4-*O*-*p*-toluenesulfonyl-α-L-xylopyranoside (61)

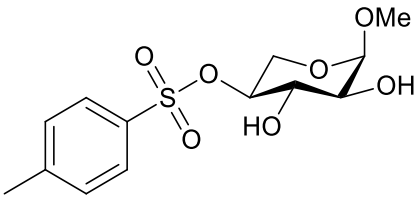

61

A Dean-stark apparatus was attached to a flask in which Bu_2SnO (14.4 g, 57.8 mmol, 1.0 equiv) and triol **60** (9.4 g, 57.2 mmol, 1.0 equiv) were suspended in anhydrous toluene (183 mL). After the mixture was refluxed for 6 h, it was cooled down to rt and the solvents were evaporated under reduced pressure. To the solution of this residue in dry THF (86 mL), a separately prepared solution of TsCl (13.2 g, 69.2 mmol, 1.2 equiv) in dry THF (70 mL) was added dropwise under Ar in presence of DMAP (6 mg, 51 µmol, 0.001 equiv) and left to stir overnight at rt. After the completion, the mixture was concentrated under reduced pressure. The residue was dry loaded and purified using silica gel flash chromatography. First the column was eluted with four column volumes of toluene to remove the excess of dibutyl tin salt and then with the eluent system (EtOAc/Tol 80:20 to 100) to obtain diol **61** (15.2 g, 84%) as a white amorphous solid: R_f 0.4 (EtOAc); ^{1}H NMR (600 MHz, $CDCl_3$) δ 7.83 (d, ^3J = 8.3 Hz, 2H, H-Ar), 7.36 (d, ^3J = 8.2 Hz, 2H, H-Ar), 4.62 (d, ^3J = 3.6 Hz, 1H, H-1), 4.25 (dd, ^3J = 9.6, 3.7 Hz, 1H, H-2), 3.87 (t, ^3J = 8.9 Hz, 1H, H-3) 3.67 – 3.62 (m, 2H, H-4, H-5a), 3.49 (m, 1H, H-5b), 3.27 (s, 3H, CH_3), 2.45 (s, 3H, CH_3-Ph); HRMS (ESI-TOF) *m/z* $[M + NH_4]^+$ cald for $C_{13}H_{18}O_7S$ 336.1111; found 336.1121.

4.3.44. Methyl 2,3-di-*O*-benzoyl-4-*O*-*P*-toluenesulfonyl-α,β-L-xylopyranoside (62)

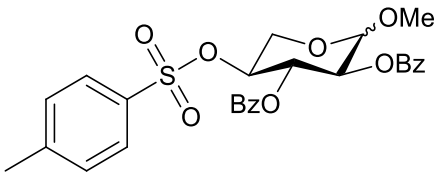

62

Diol **61** (15 g, 47.1 mmol, 1.0 equiv) was dissolved in anhydrous pyridine (42 mL) under Ar. After cooling the mixture to 0 °C, BzCl (13.8 mL, 117.8 mmol, 2.5 equiv) was added dropwise followed by DMAP (5.8 mg, 0.047 mmol, 0.001 equiv). The reaction mixture was warmed to rt and stirred for 5 h. After the completion [TLC: R_f 0.4 (Hex/EtOAc 6:4)], it was diluted with

DCM (100 mL). The organic phase was washed with an 1 M aq. HCl (2 × 100 mL) solution, followed by saturated aq. $NaHCO_3$ (100 mL) and then with brine (100 mL). The organic layers were dried using $MgSO_4$ and then evaporated under reduced pressure. The obtained residue was purified by silica gel flash chromatography (Hex/EtOAc 8:2 to 6:4) to give derivative **62** (17.6 g, 71%, α/β 1:3) as a white amorphous solid; ^{1}H NMR (600 MHz, $CDCl_3$, β-anomer) δ 7.91 – 7.87 (m, 2H, H-Ar), 7.71 – 7.68 (m, 2H, H-Ar), 7.63 – 7.61 (m, 2H, H-Ar), 7.51 – 7.47 (m, 2H, H-Ar), 7.34 – 7.31 (m, 4H, H-Ar), 6.96 (d, ^3J = 8.3 Hz, 2H, H-Ar), 5.56 (t, ^3J = 8.5 Hz, 1H, H-3), 5.23 (dd, ^3J = 8.7, 6.7 Hz, 1H, H-2), 4.66 (ddd, ^3J = 13.5, 6.9, 4.3 Hz, 1H, H-4), 4.58 (d, ^3J = 6.7 Hz, 1H, H-1), 4.38 (dd, ^3J = 12.2, 5.1 Hz, 1H, H-5a), 3.69 (dd, ^3J = 12.2, 8.7 Hz, 1H, H-5b), 3.48 (s, 3H, C*H*$_3$), 2.18 (s, 3H, C*H*$_3$-Ph); ^{13}C NMR (100 MHz, $CDCl_3$) δ 165.19, 164.94 (2 X *C*O), 145.08, 133.41, 133.35, 132.72, 129.93, 129.90, 129.83, 129.14, 128.84, 128.45, 128.30, 127.78 (*C*-Ar), 100.79 (C-1), 75.11 (C-4), 70.93 (C-2, C-3), 63.04 (C-5), 57.08 (*C*H$_3$), 21.69 (*C*H$_2$-Ph); HRMS (ESI-TOF) *m/z* [M + NH_4]$^+$ cald for $C_{27}H_{26}O_9S$ 527.137; found 527.1376; *m/z* [M + Na]$^+$ cald for $C_{27}H_{26}O_9S$ 549.119; found 549.1202.

4.3.45. Methyl 4-azido-2,3-di-*O*-benzoyl-4-deoxy-α,β-D-arabinopyranoside (63)

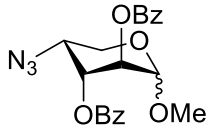

63

To a solution of compound **62** (17.5 g, 33.23 mmol, 1.0 equiv) dissolved in dry DMSO (50 mL), crystals of NaN_3 (8.1 g, 125.2 mmol, 2.5 equiv) were added and the mixture was stirred under Ar at 90 °C overnight. After the reaction mixture was diluted with DCM (200 mL), the organic phase was washed with distilled water (2 × 100 mL) and saturated aq. $NaHCO_3$ (100 mL) solution. The organic layer was dried using $MgSO_4$ and the solvents were removed under reduced pressure. The resulting residue was purified by silica gel flash chromatography (Hex/EtOAc 7:3 to 1:1) to obtain product **63** (14.0 g, quantitative, α/β 3.5:1.5) as a white amorphous solid: R_f 0.3 (Hex/Acetone 6:3).; ^{1}H NMR (600 MHz, $CDCl_3$, α-anomer) δ 8.06 – 7.97 (m, 6H, C*H*-Ar), 7.57 – 7.52 (m, 2H, C*H*-Ar), 7.44 – 7.40 (m, 4H, C*H*-Ar), 5.59 – 5.56 (m, 1H, H-2), 5.51 (dd, ^3J = 7.9, 3.3 Hz, 1H, H-3), 4.60 (d, ^3J = 5.6 Hz, 1H, H-1), 4.20 – 4.16 (m, 2H, H-5a, H-4), 3.80 (m, 1H, H-5b), 3.50 (s, 3H, C*H*$_3$); ^{13}C NMR (100 MHz, $CDCl_3$) δ 165.78, 165.18

(2 X *C*O), 133.73, 133.48, 130.15, 129.94, 129.41, 128.88, 128.63, 128.54 (C-Ar), 101.22 (C-1), 71.64 (C-3), 69.32 (C-2), 61.86 (C-5), 57.73 (C-4), 56.64 (CH$_3$).

4.3.46. Methyl 4-azido-4-deoxy-α-D-arabinopyranoside (64)

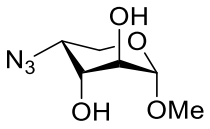

64

To the solution of azide **63** (13 g, 32.71 mmol, 1.0 equiv) dissolved in dry DCM (50 mL), anhydrous methanol (300 mL) was added under Ar at rt. MeONa solution (25 wt. % in methanol, 1.5 mL, 6.5 mmol, 0.2 equiv) was added to this solution and stirred overnight at rt. The reaction mixture was quenched using Dowex H^+ resin until neutral pH was obtained (checked by pH paper). The resin was filtered through celite and the solvents were evaporated under reduced pressure. The residue was purified by silica flash chromatography (DCM/MeOH 1:0 to 92:8) to give diol **64** (5.66 g 91%), as white solid: R_f 0.4 (DCM/MeOH 9:1); ^{1}H NMR (600 MHz, D_2O, β-anomer) δ 4.27 (d, ^3J = 7.7 Hz, 1H, H-1), 4.05 – 4.02 (m, 1H, H-5a), 4.00 – 3.98 (m, 1H, H-4), 3.89 (dd, ^3J = 9.5, 4.0 Hz, 1H, H-3), 3.73 (dd, ^3J = 13.2, 1.5 Hz, 1H, H-5b), 3.54 (s, 3H, CH_3), 3.51 – 3.48 (m, 1H, H-2); ^{13}C NMR (100 MHz, D_2O) δ 103.98 (C-1), 72.32 (C-3), 70.76 (C-2), 63.76 (C-5), 61.48 (C-4), 57.06 (CH$_3$); HRMS (ESI-TOF) *m/z* [M + NH_4]$^+$ cald for $C_6H_{11}N_3O_4$ 207.10878; found 207.10974; *m/z* [M + Na]$^+$ cald for $C_6H_{11}N_3O_4$ 212.06418; found 212.064445.

4.3.47. Methyl 4-azido-2,3-di-*O*-acetyl-4-deoxy-α,β-D-arabinopyranoside (65)

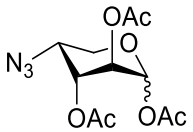

65

To the solution of diol **64** (5.2 g, 27.49 mmol, 1.0 equiv) dissolved in DCM (275 mL), Ac_2O (26 mL, 274.8 mmol, 10.0 equiv) was added and the reaction mixture was cooled down to 0 °C. Solution of conc. H_2SO_4 (1.5 mL, 27.49 mmol, 1.0 equiv) was added, warmed to rt and stirred for 20 min. After diluting the mixture with DCM (50 mL), the organic phase was washed with a saturated solution of aq. $NaHCO_3$ (3 × 100 mL) and brine (100 mL). The combined organic

layers were dried over $MgSO_4$ and the solvents were concentrated under reduced pressure. The residue was purified by silica gel flash chromatography (Hex/EtOAc 8:2 to 1:1) to obtain azide **65** (3.8 g, 50%, α/β 1.5:3.5) as a white amorphous solid: R_f 0.3 (Hex/EtOAc 6:4); ^{1}H NMR (600 MHz, $CDCl_3$, β-anomer) δ 6.31 (d, ^3J = 3.0 Hz, 1H, H-1), 5.41 – 5.36 (m, 2H, H-2, H-3), 4.15 (dt, ^3J = 4.0, 2.0 Hz, 1H, H-4), 4.06 – 4.03 (m, 1H, H-5a), 3.84 – 3.81 (m, 1H, H-5b), 2.15 (s, 3H, COCH_3), 2.14 (s, 3H, COCH_3), 2.04 (s, 3H, COCH_3); ^{13}C NMR (100 MHz, $CDCl_3$) δ 170.41, 169.80, 169.09 (3 X COCH_3), 90.23 (C-2), 69.19, (C-3), 66.71 (C-2), 62.50 (C-5), 59.40 (C-4), 20.97, 20.70, 20.67 (3 X COCH_3); HRMS (ESI-TOF) *m/z* $[M + NH_4]^+$ cald for $C_{11}H_{15}N_3O_7$ 319.1257; found 319.1248; *m/z* $[M + Na]^+$ cald for $C_{11}H_{15}N_3O_7$ 324.0802; found 324.081.

4.3.48. 4-Azido-4-deoxy-α,β-D-arabinopyranose (66)

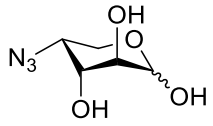

66

Azide **65** (3.8 g, 12.6 mmol, 1.0 equiv) was dissolved in anhydrous DCM (25 mL). Methanol (100 mL) was added followed by MeONa (25 wt. % in methanol, 577 µL, 2.52 mmol, 0.2 equiv) and the reaction was stirred overnight at rt. The reaction mixture was quenched with Dowex H^+ resin until the pH of mixture is neutral which was confirmed by pH paper. The resin was filtered off through celite and solvents were evaporated under reduced pressure. The residue was purified by reversed-phase (C_{18}) silica gel flash chromatography loaded with H_2O (H_2O/ACN 1:0 to 75:25) to obtain arabinose-N_3 **66** (2 g, 91%, α/β 1.5:2.5) as white amorphous solid: R_f 0.2 (DCM/MeOH 9:1); ^{1}H NMR (600 MHz, D_2O, β-anomer) δ 4.52 (br. s, 1H, H-1), 4.05-3.95 (m, 2H, H-5a, H-4), 3.88 (br. s, 1H, H-3), 3.74 (br. s, 1H, H-5b), 3.48 (1H, br. s, H-2); ^{13}C NMR (600 MHz, D_2O) δ 96.77 (C-1), 72.49 (C-3), 71.88 (C-2), 63.90 (C-5), 61.67 (C-4); HRMS (ESI-TOF) *m/z* $[M + Na]^+$ cald for $C_5H_9N_3O_4$ 198.0485; found 198.048.

4.3.49. Ammonium 7-Azido-3,8-dideoxy-D-*manno*-oct-2-ulopyranosylonate (67)

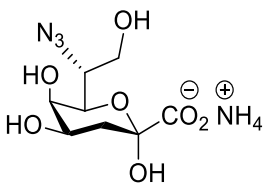

67

Arabinose-N_3 **66** (350 mg, 2.0 mmol, 1.0 equiv) was dissolved in distilled H_2O (6.0 mL) containing Na_2CO_3 (526 mg, 4.9 mmol, 2.5 equiv). Crystals of oxaloacetic acid (317 mg, 2.4 mmol, 1.2 equiv) were added in small portions over five min. After adding few drops of 10.0 N Aq. NaOH solution until the pH of the mixture was increased to 11.0 (checked by pH meter), the reaction mixture was stirred at rt for 2 h. Then, the pH was further brought down to 5.0 using AcOH, followed by $NiCl_2.6H_2O$ (0.01 equiv) and stirred at 50 °C for 1 h. After cooling the mixture to rt, it was passed on an anion exchange resin column CG-400 (HCO_3^-). It was first eluted with H_2O to remove the excess of arabinose-N_3, followed by aq. NH_4HCO_3 (0.05 N to 0.30 N). The fractions were pooled after analysing on TLC ($CHCl_3$/MeOH/H_2O 10:10:3; revealed by CAM stain) and lyophilized to obtain the desired Kdo product **67** (340 mg, 61%) as white amorphous solid. Selected NMR data for the major α-pyranose form; $[\alpha]_D^{20}$ = +0.67 (*c* 0.90, H_2O); ^{1}H NMR (600 MHz, D_2O) δ 4.03 (ddd, ^3J = 12.1, 5.2, 3.1 Hz, 1H, H-4), 3.94 (d, ^3J = 12.1 Hz, 1H, H-8a), 3.79 (dd, ^3J = 9.7, 0.9 Hz, 1H, H-5), 3.76 (ddd, ^3J = 9.5, 4.2, 1.7 Hz, 1H, H-7), 3.69 (d, ^3J = 12.1 Hz, 1H, H-8b), 3.56 (dd, 1H, H-6), 1.95 (d, ^3J = 12.9 Hz, 1H, H-3a), 1.86 (dd, 1H, H-3b); ^{13}C NMR (100 MHz, D_2O) δ 104.28 (C-1 α*p*), 96.47 (C-2 α*f*), 85.90 (C-2 α*p*), 69.92, 66.97, 65.89, 61.88, 61.24 (C-4 α*p*, 5 α*p*, 6 α*p*, 7 α*p*, 8 α*p*), 44.64 (C-3 α*f*), 33.49 (C-3 α*p*); HRMS (ESI-TOF) *m/z* $[M]^-$ cald for $[C_8H_{12}N_3O_7]^-$ 262.06860; found 262.06750.

4.3.50. Disulfide-*N*,*N*'-disuccinimidyl-ethane-carbonate (72)

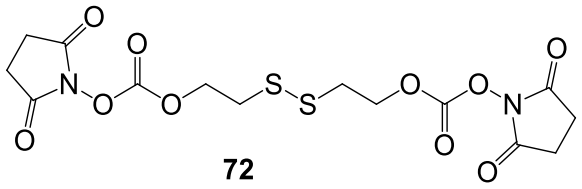

72

Pyridine (13 µL, 0.163 mmol, 0.4 equiv) was added to a solution of phosgene (121 mg, 0.408 mmol, 1.0 equiv) in anhydrous DCE (600 µL). After cooling the reaction to –20 °C and stirring it for 40 min, dithiodiethanol (50 µL, 0.408 mmol, 1.0 equiv) was added at once. The reaction mixture was warmed to rt and stirred overnight under Ar. Phosgene was treated by purging the flask with N_2 and passing this N_2 through 2 M aq. NaOH. The solvents were evaporated under reduced pressure. The residue was dissolved in EtOAc, filtered through celite and evaporated to obtain compound **70** (113 mg, quantitative) as yellow solid. It was used for next step without further purification. Compound **70** (110 mg, 0.394 mmol, 1.0 equiv) was dissolved in acetone (4.0 mL) and NHS (100 mg, 0.867 mmol, 2.2 equiv) was added. After

adding a solution of K_2CO_3 (109 mg, 2.0 mmol, 1.0 equiv) in distilled water (2.0 mL), the reaction mixture was stirred for three hours at rt. Saturated solution of aq. $NaHCO_3$ (5 mL) was added and the layers were separated. The aqueous phase was extracted with EtOAc (3 × 6 mL). The combined organic phase was washed with brine, filtered through $MgSO_4$ and evaporated under reduced pressure. The crude residue was subjected to silica gel flash chromatography (Hex/EtOAc 7:3 to 2:8) to obtain compound **72** (67 mg, 65%) as yellow oil: R_f 0.5 (Hex/EtOAc 3:7); ^{1}H NMR (600 MHz, $CDCl_3$) δ 4.58 (t, ^3J = 6.6 Hz, 4H, 2 X SCH_2), 3.05 (t, ^3J = 6.6 Hz, 4H, 2 X CH_2CH_2), 2.84 (s, 8H, 2 X NCOCH_4); ^{13}C NMR (100 MHz, $CDCl_3$) δ 168.66 (4 X N*C*O), 151.52 (2 X *C*O), 68.75 (2 X S*C*H_2C), 36.62 (2 X *C*H_2O), 25.60 (4 X NCO*C*H_2); HRMS (ESI-TOF) *m/z* [M + NH_4]$^+$ cald for $C_{14}H_{16}N_2O_{10}S_2$ 454.05848; found 454.05846; *m/z* [M + Na]$^+$ cald for $C_{14}H_{16}N_2O_{10}S_2$ 459.0138; found 459.01386.

Supplementary Figure 1. ^{1}H NMR spectrum (D_2O, 600 MHz) of compound 28

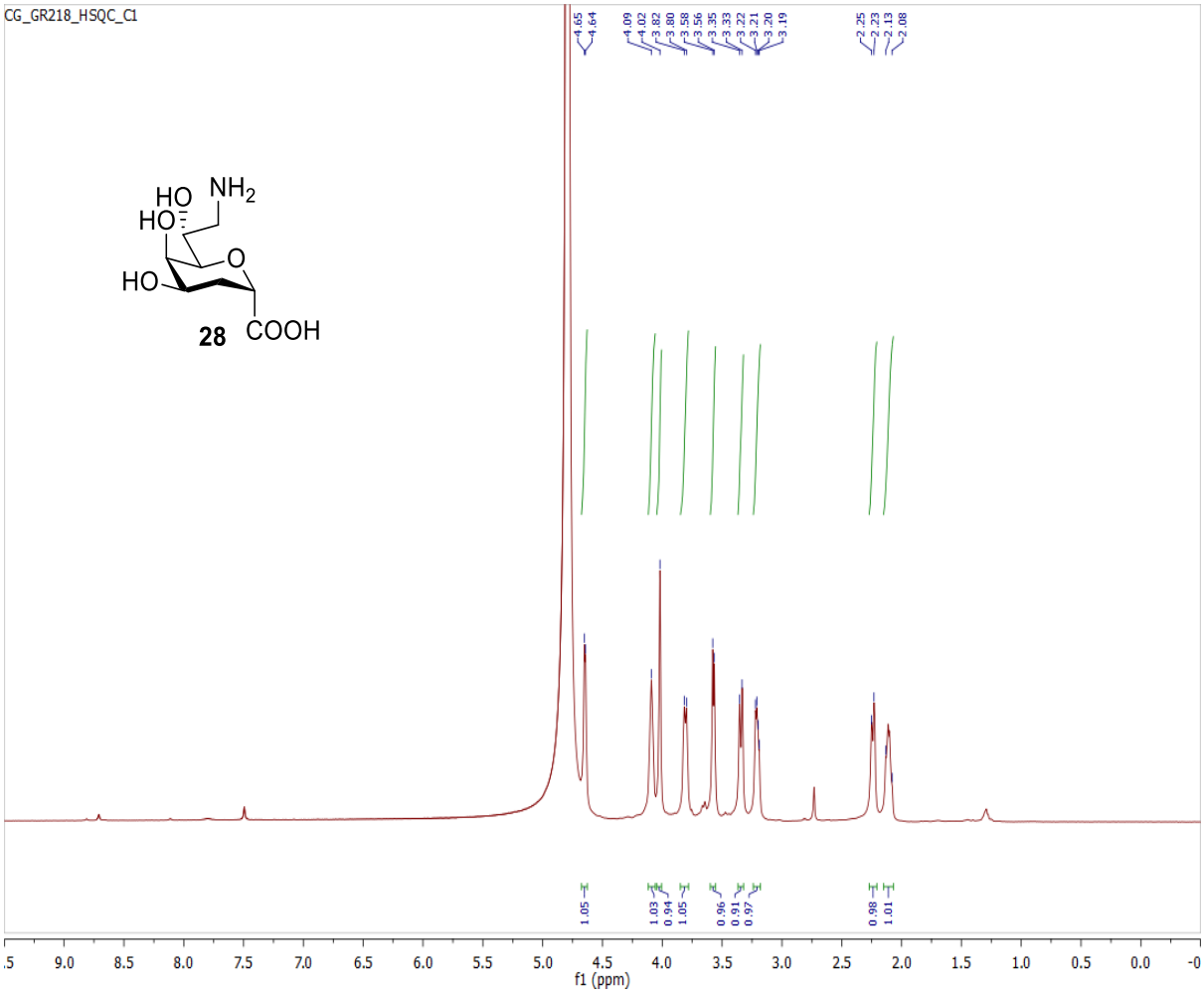

Supplementary Figure 2. ^{13}C NMR spectrum (D_2O, 100 MHz) of compound 28

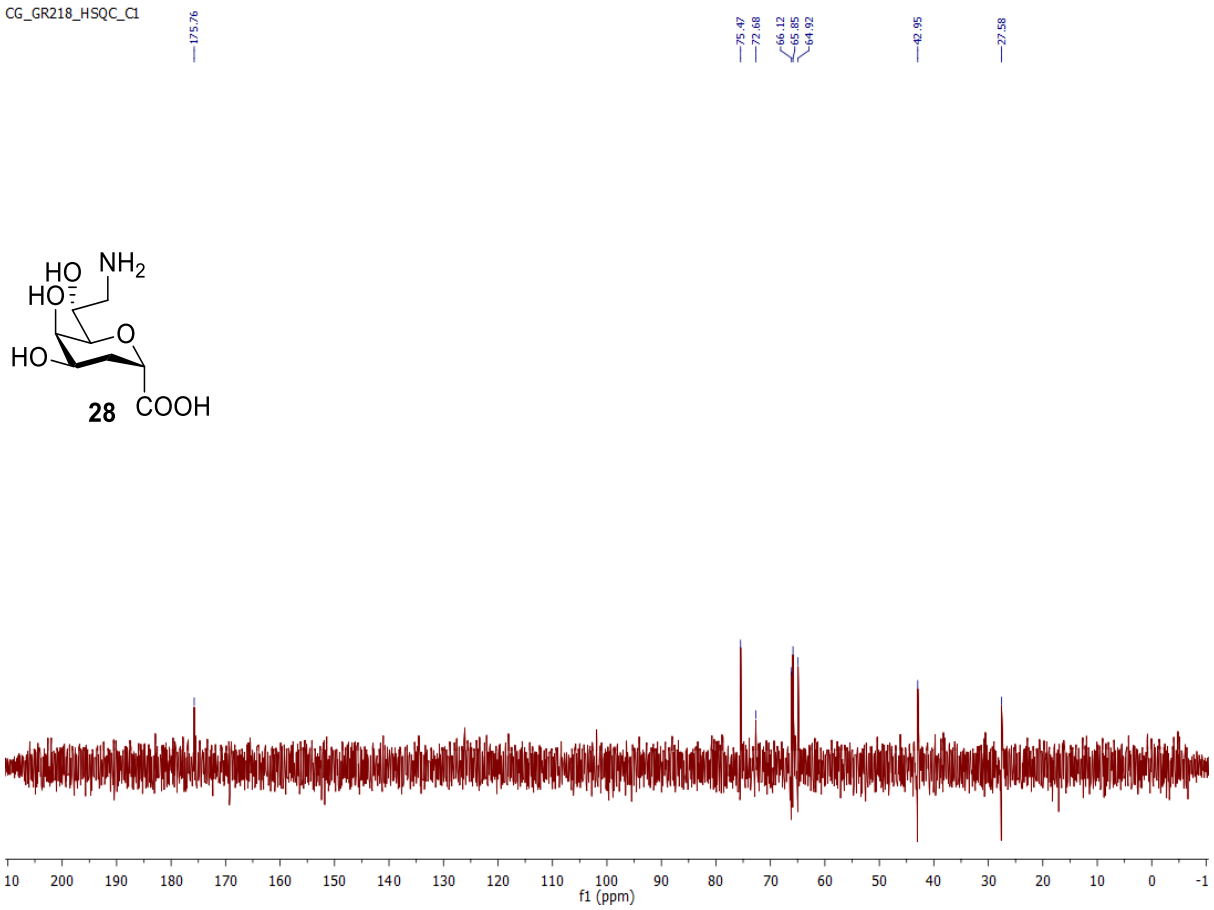

Supplementary Figure 3. HSQC NMR spectrum (D_2O, 100 MHz) of compound 28

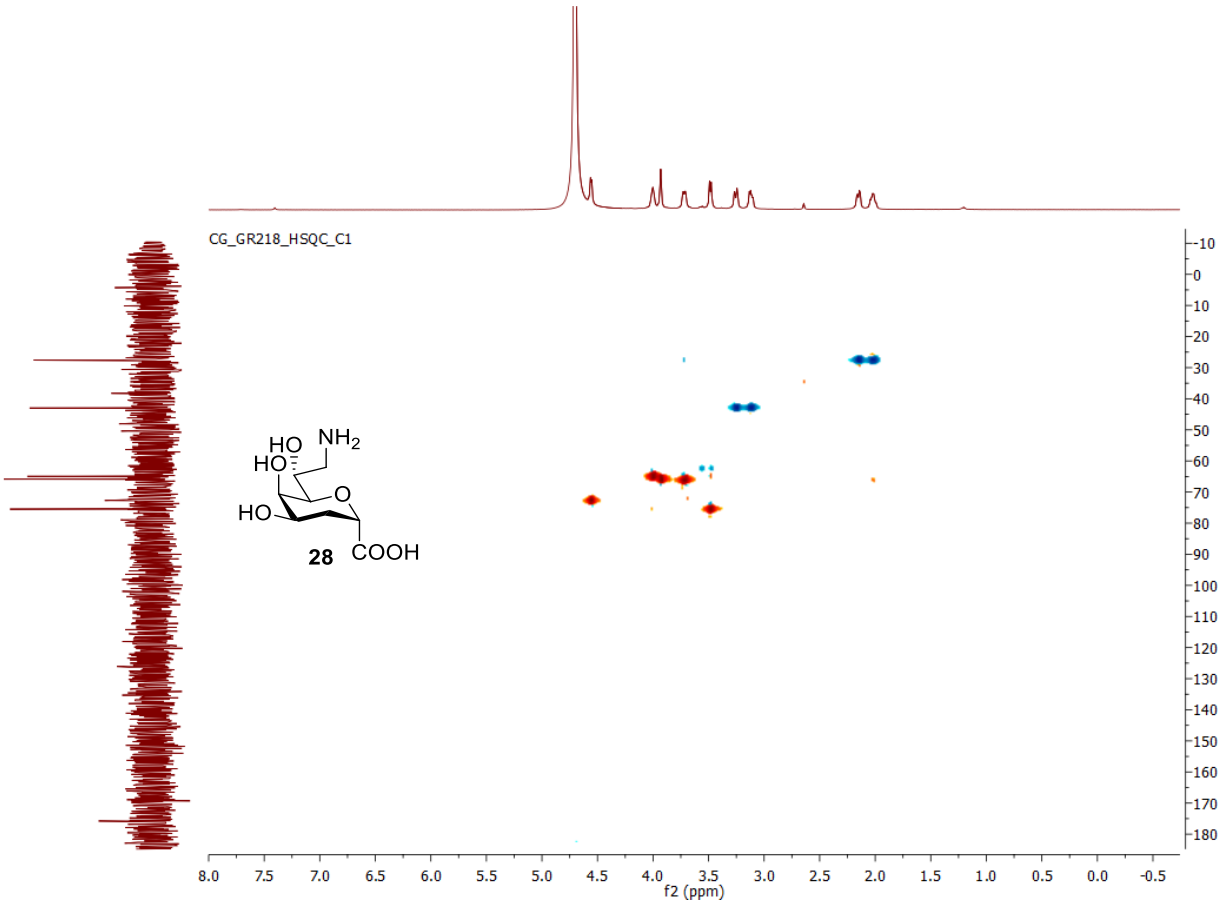

Supplementary Figure 4. ^{1}H NMR spectrum ($CDCl_3$, 600 MHz) of compound 31

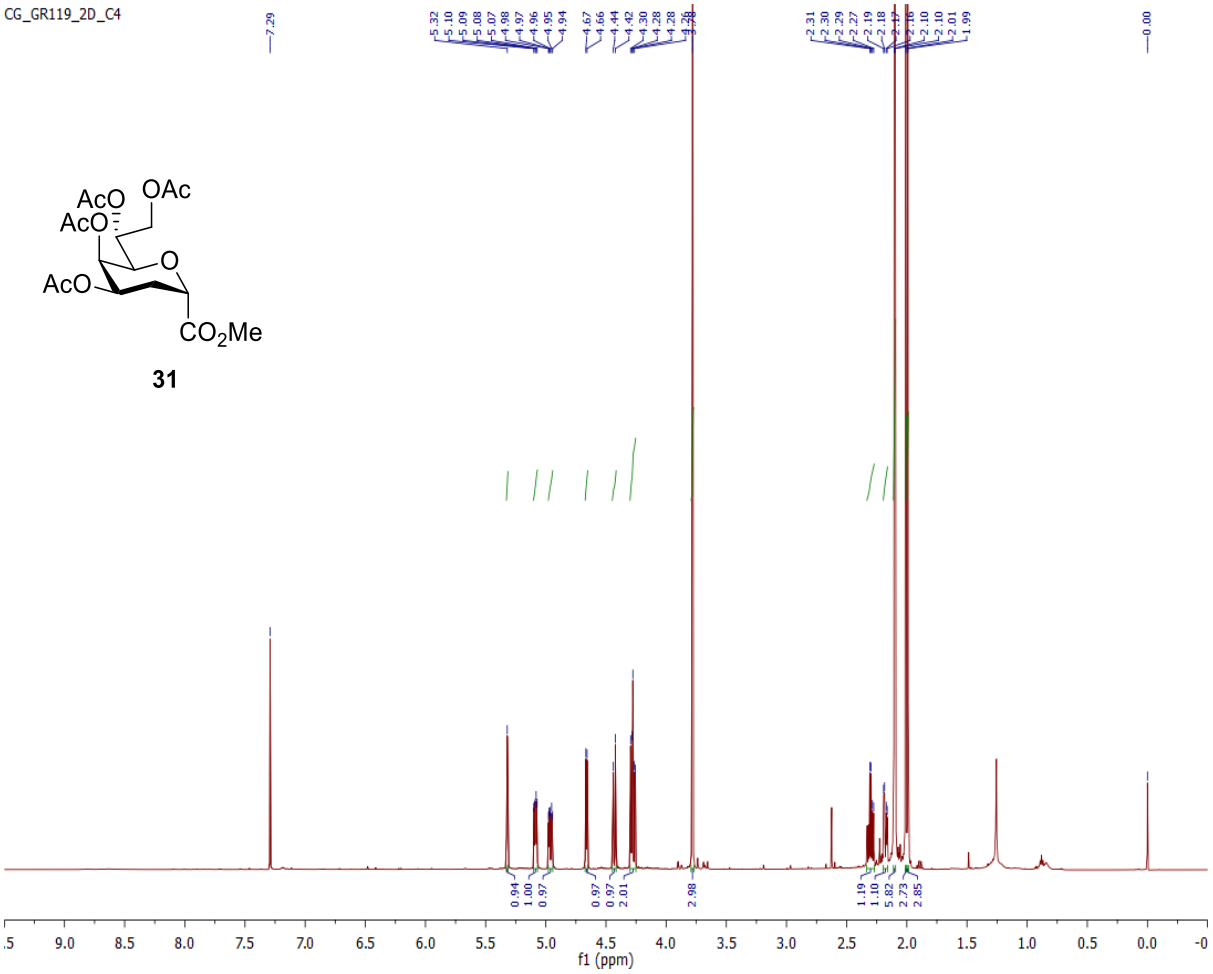

Supplementary Figure 5. ^{13}C NMR spectrum ($CDCl_3$, 100 MHz) of compound 31

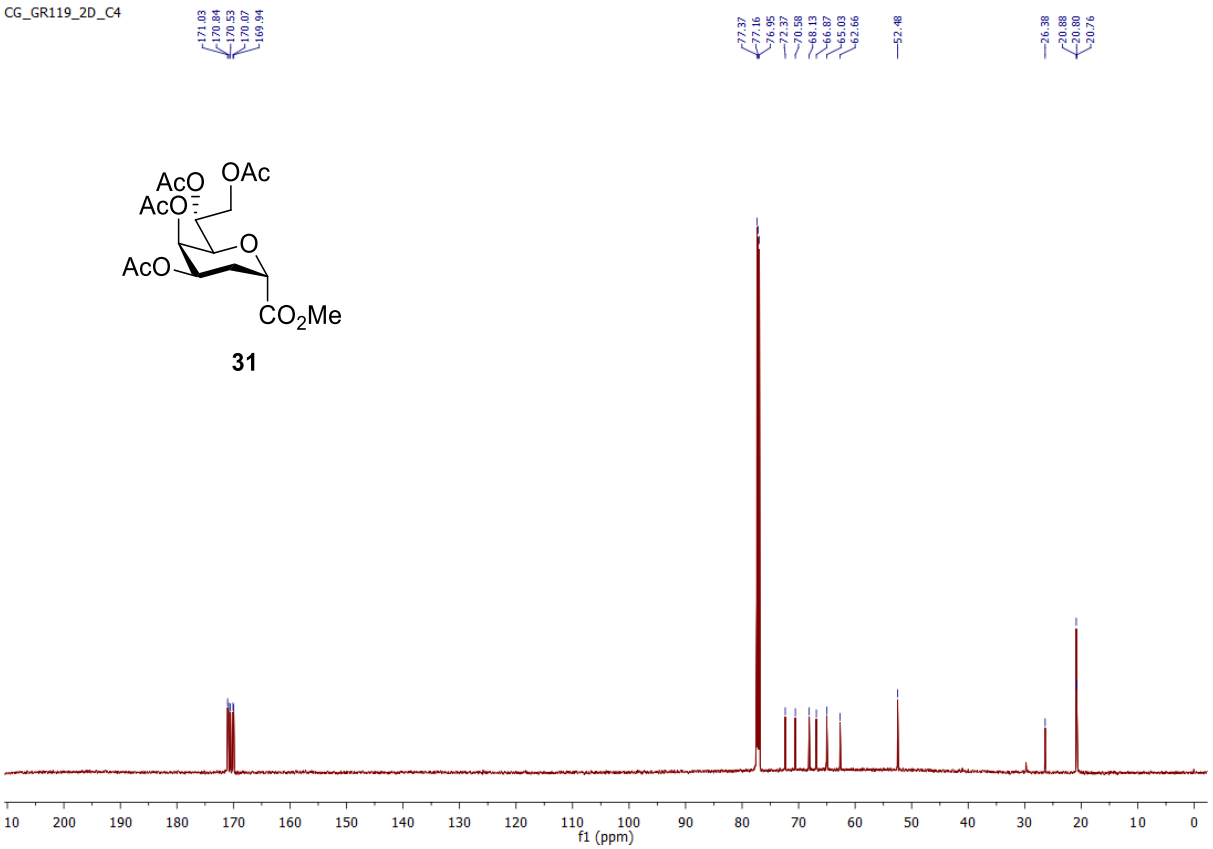

Supplementary Figure 6. COSY NMR spectrum ($CDCl_3$, 600 MHz) of compound 31

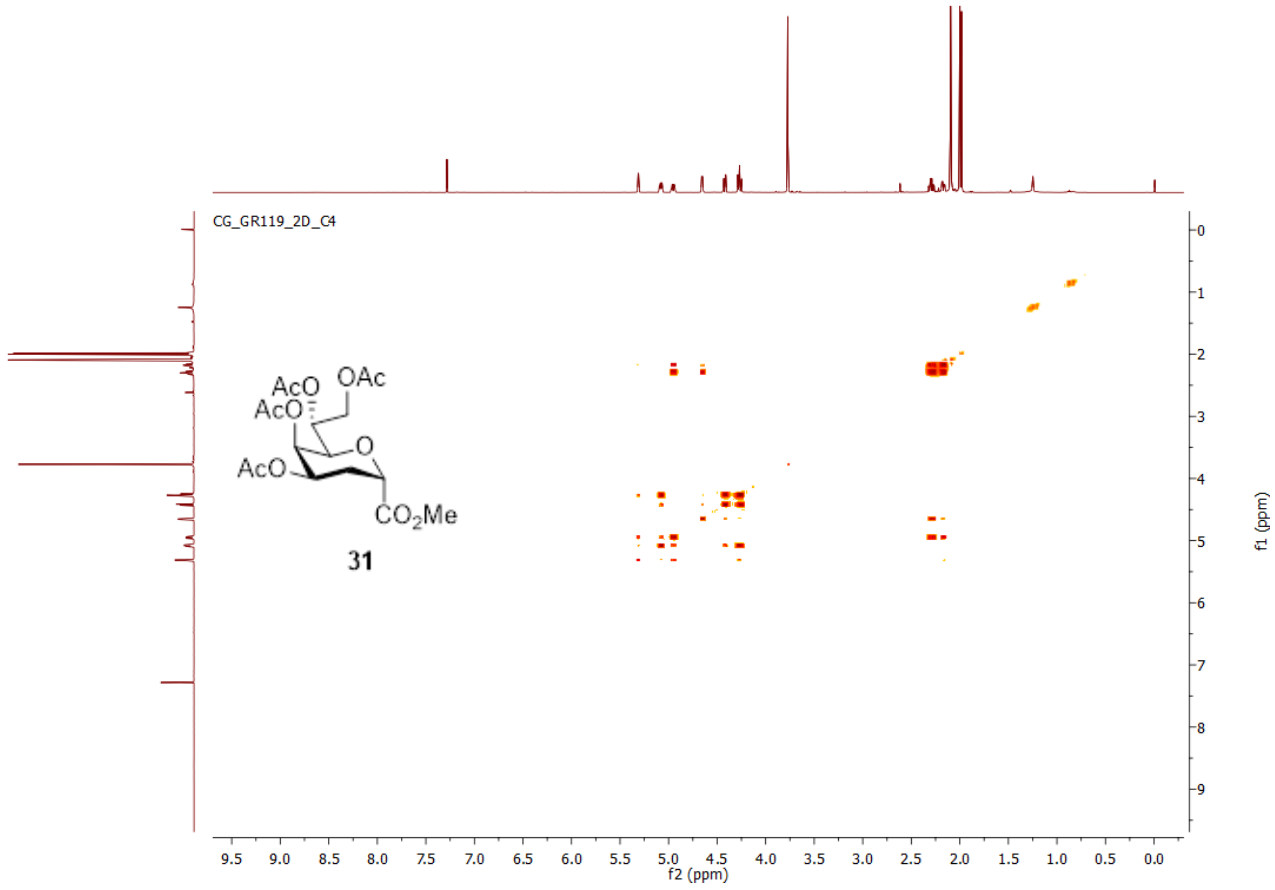

Supplementary Figure 7. HSQC NMR spectrum ($CDCl_3$, 600 MHz) of compound 31

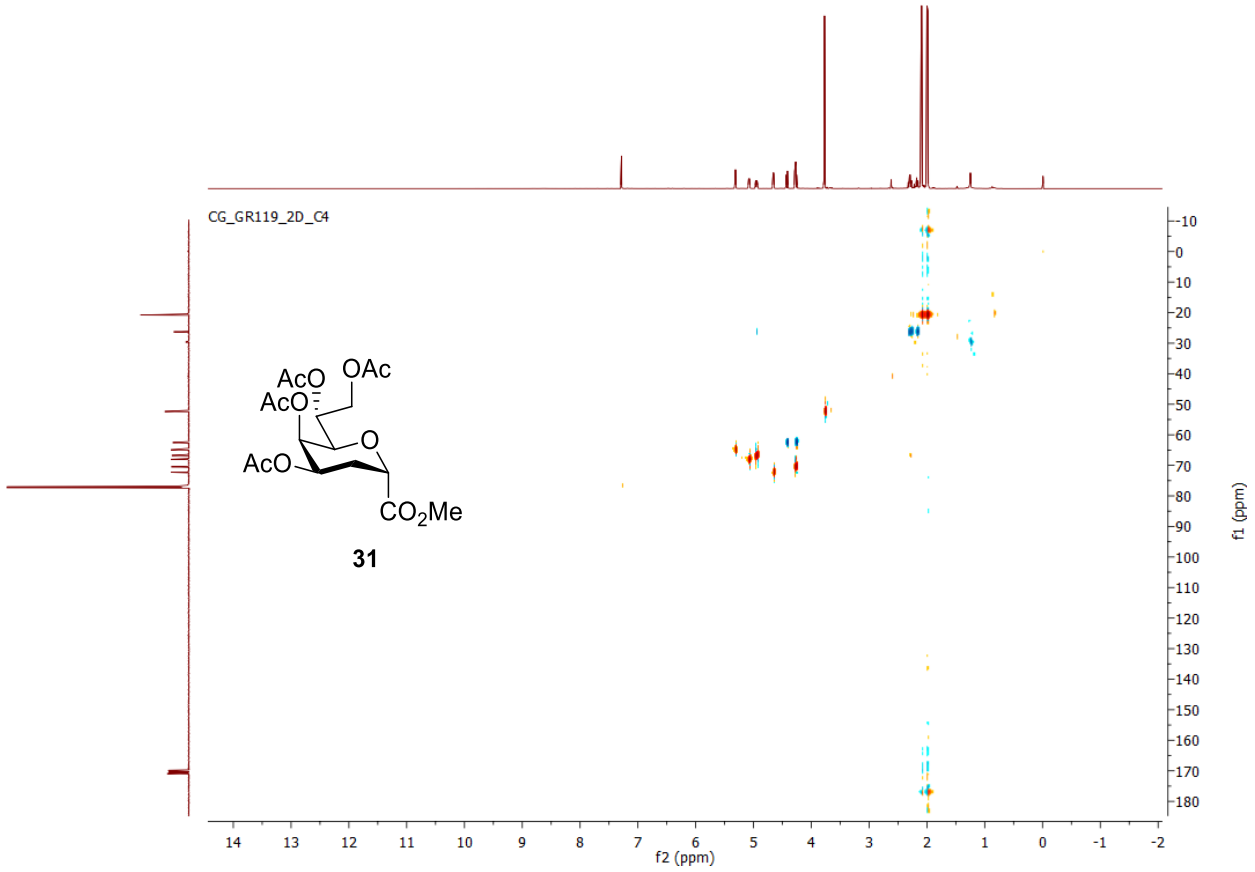

Supplementary Figure 8. ^{1}H NMR spectrum ($CDCl_3$, 600 MHz) of compound 32

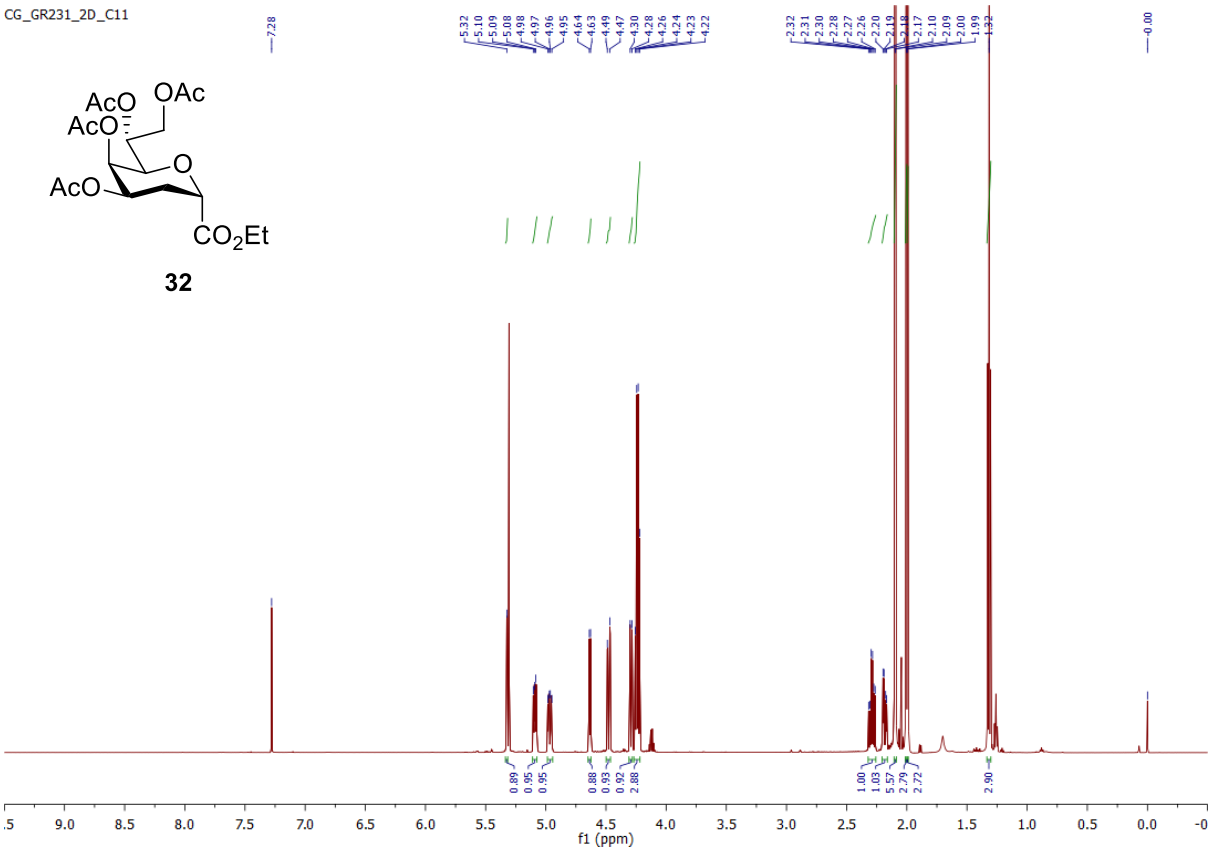

Supplementary Figure 9. ^{13}C NMR spectrum (CDCl3, 100 MHz) of compound 32

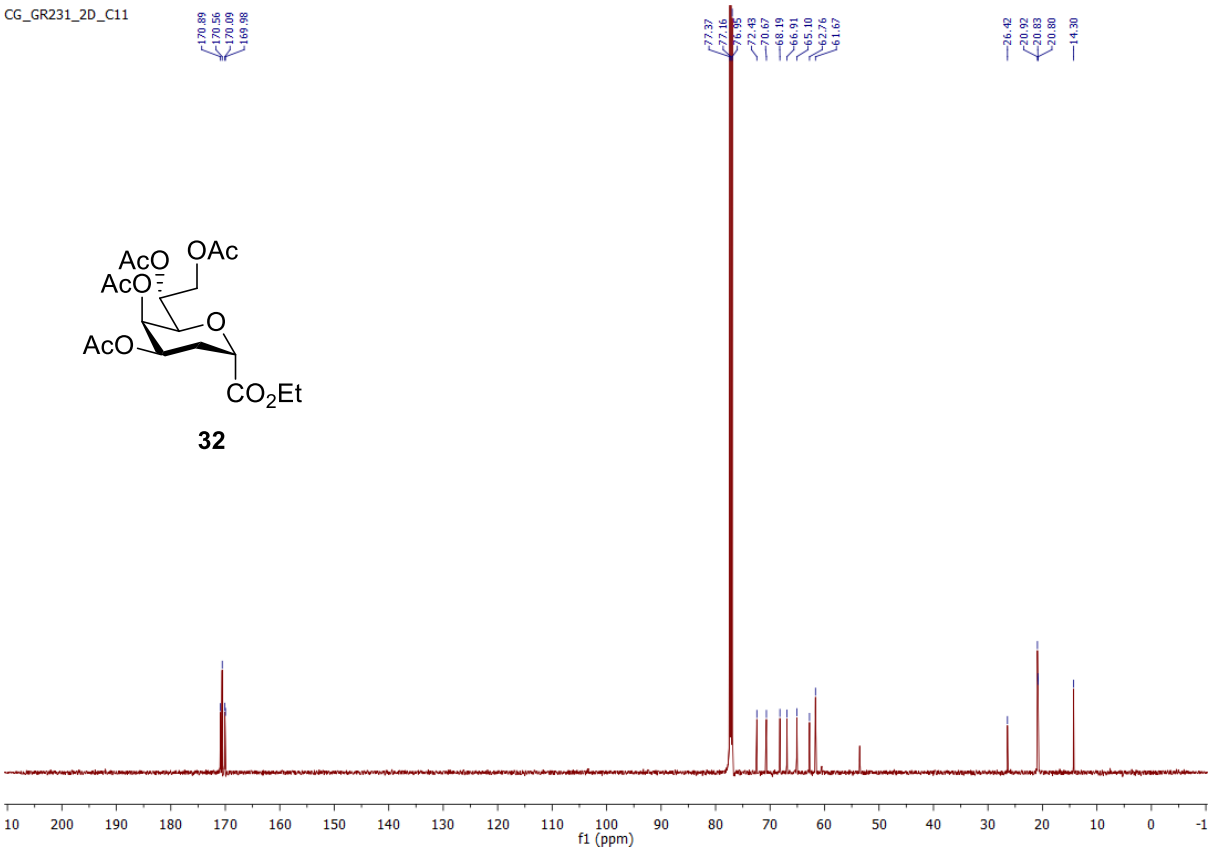

Supplementary Figure 10. COSY NMR spectrum ($CDCl_3$, 600 MHz) of compound 32

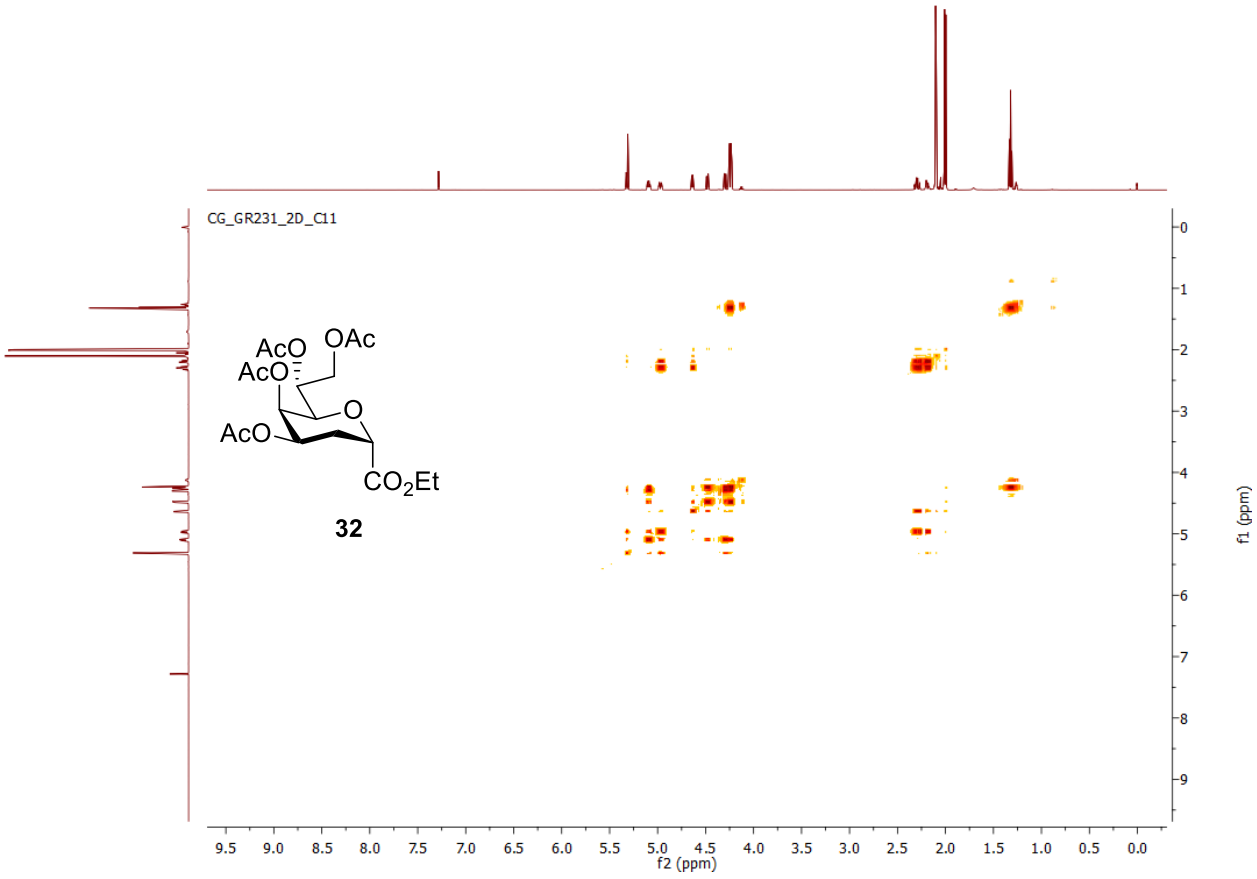

Supplementary Figure 11. HSQC NMR spectrum ($CDCl_3$, 600 MHz) of compound 32

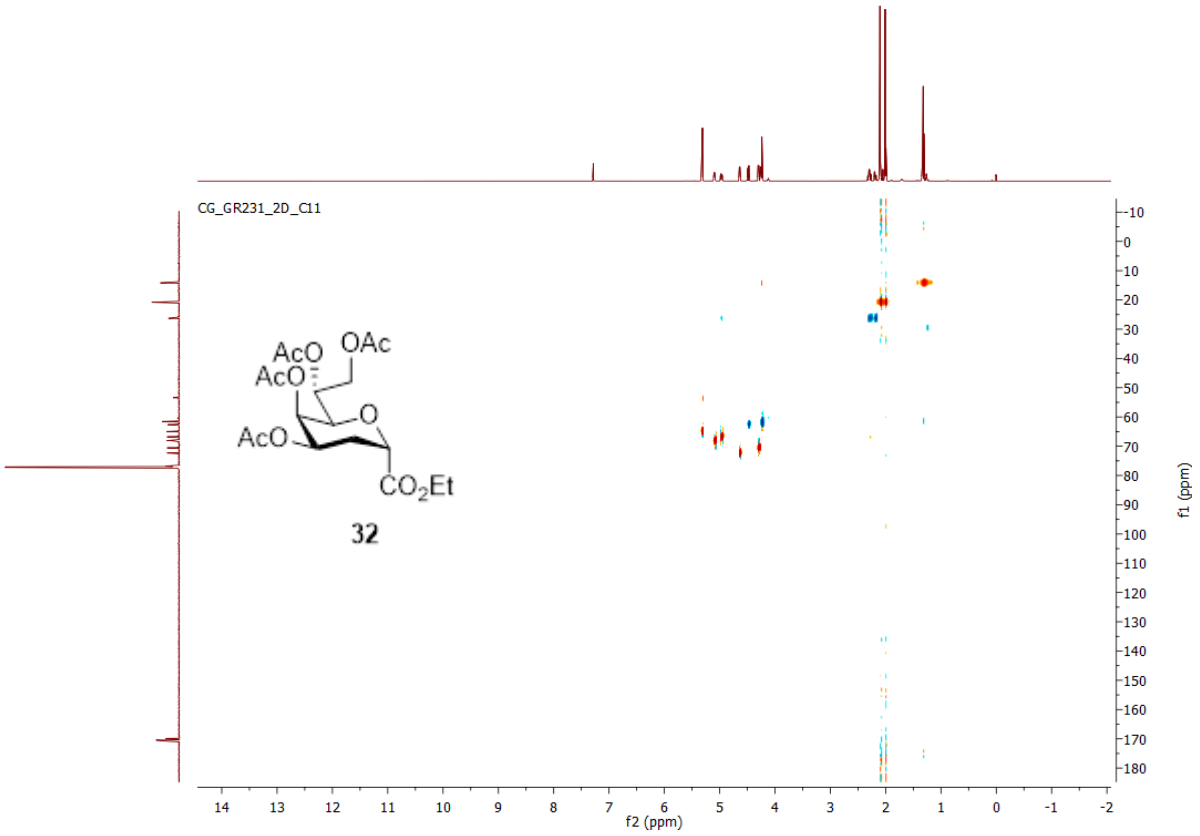

Supplementary Figure 12. ^{1}H NMR spectrum (Acetone-d6, 600 MHz) of compound 41

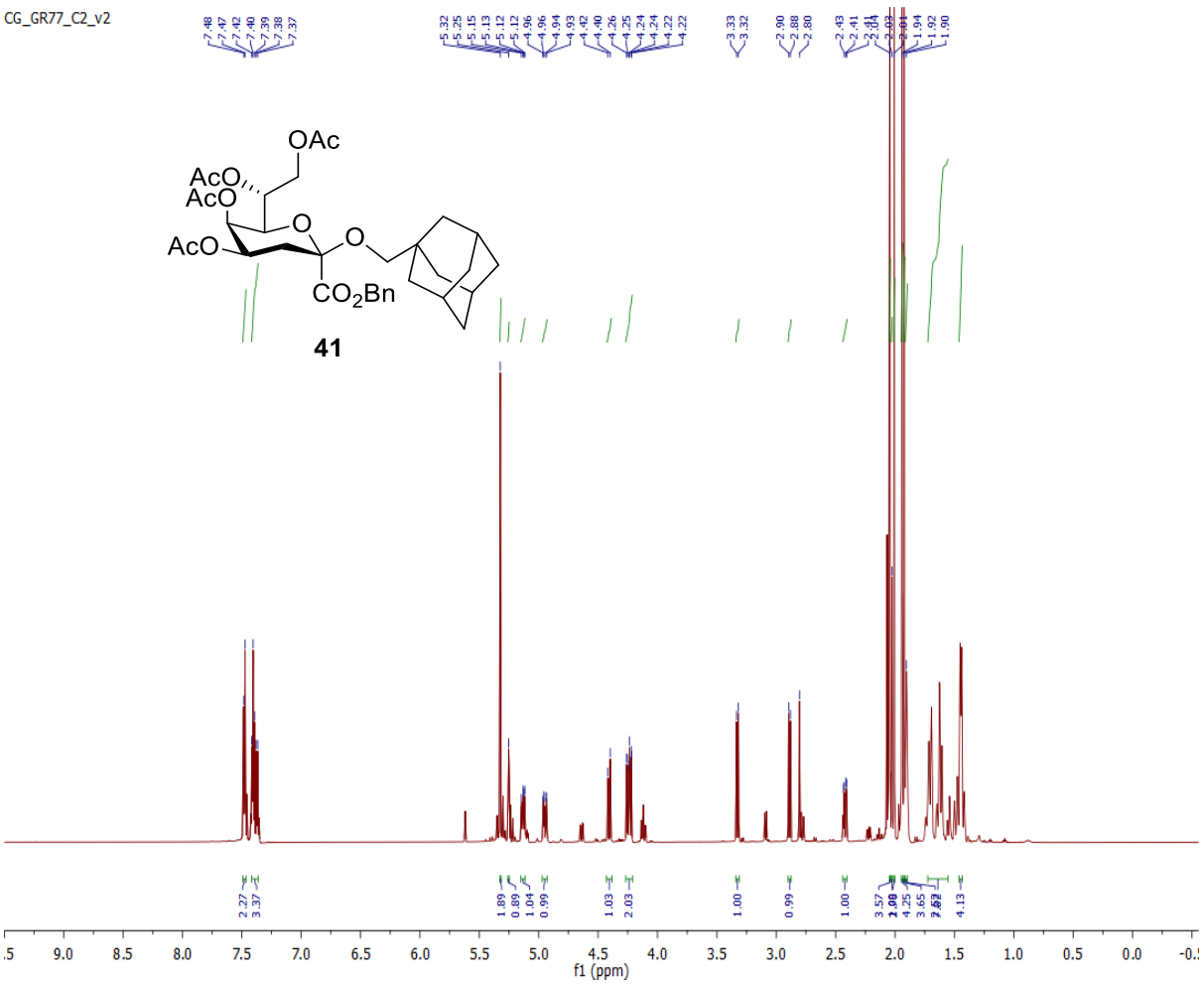

Supplementary Figure 13. ^{13}C NMR spectrum (Acetone-d6, 100 MHz) of compound 41

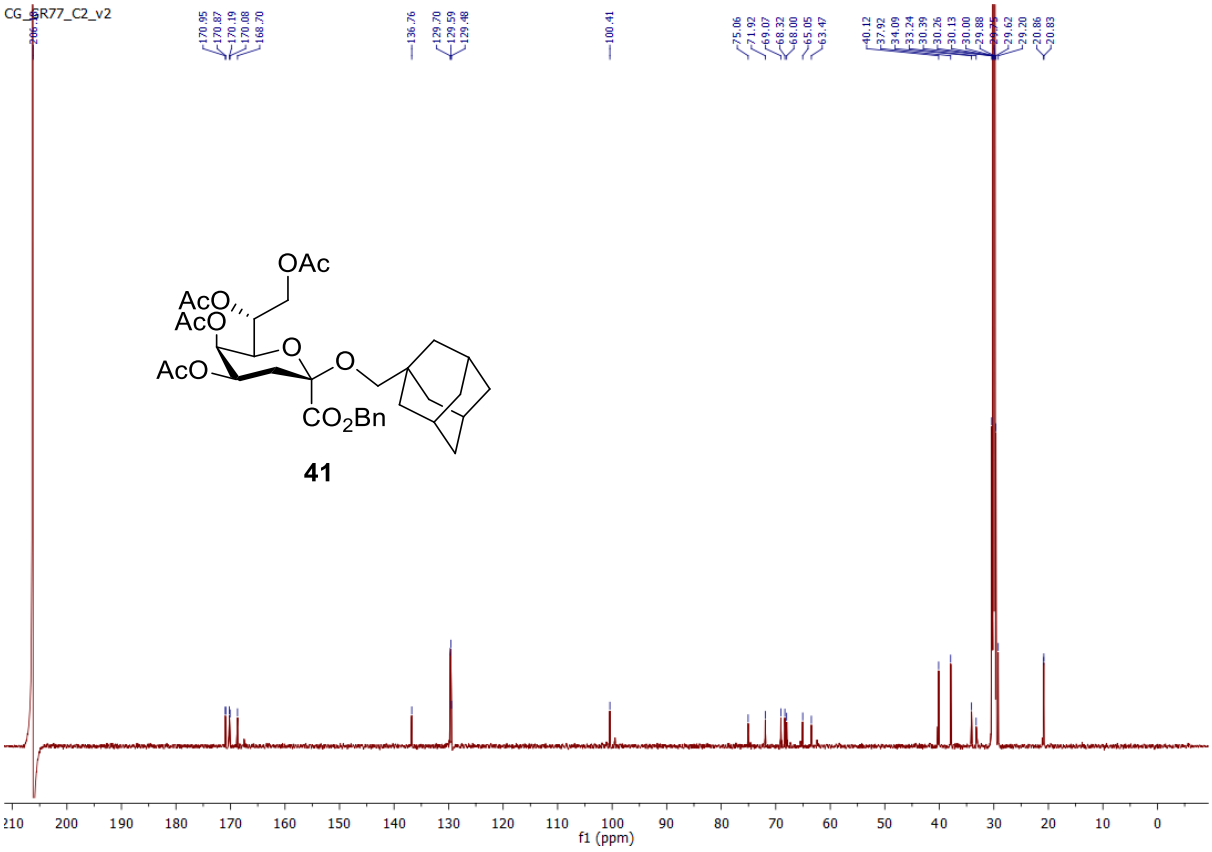

Supplementary Figure 14. COSY NMR spectrum (Acetone-d6, 600 MHz) of compound 41

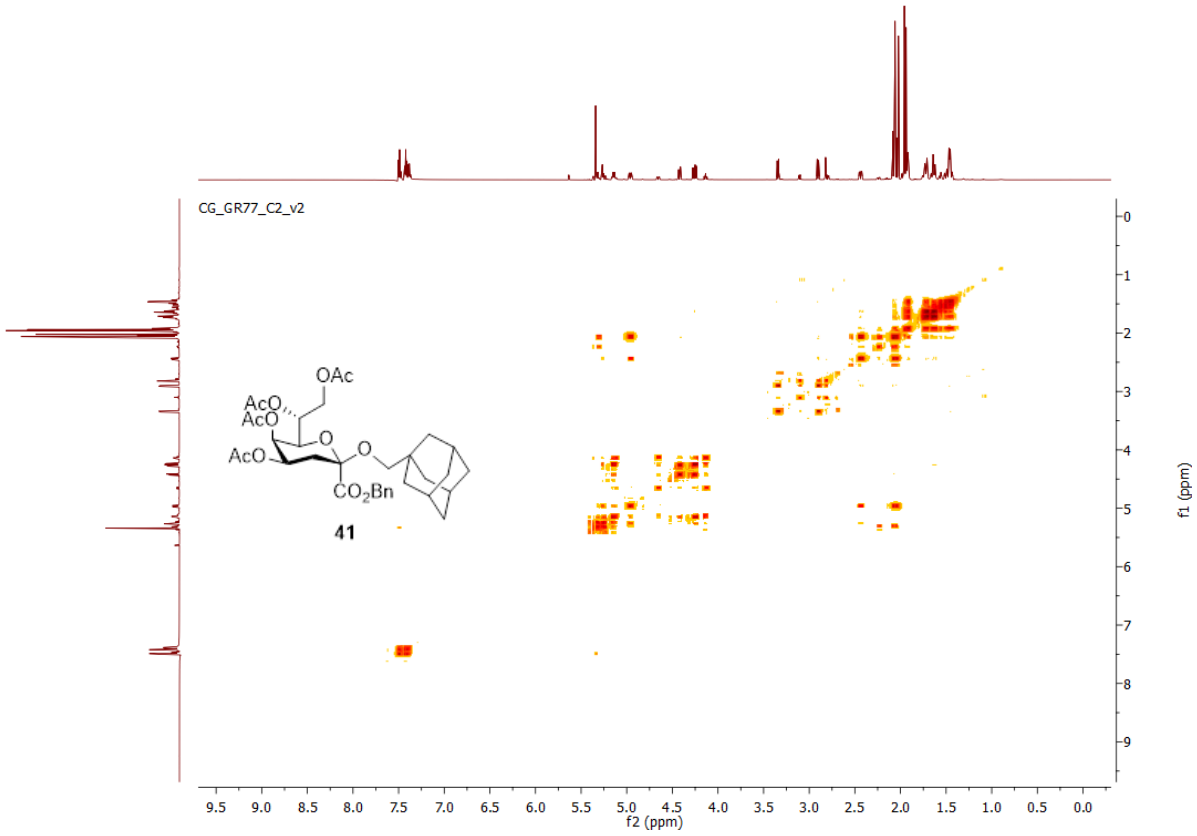

Supplementary Figure 15. HSQC NMR spectrum (Acetone-d6, 600 MHz) of compound 41

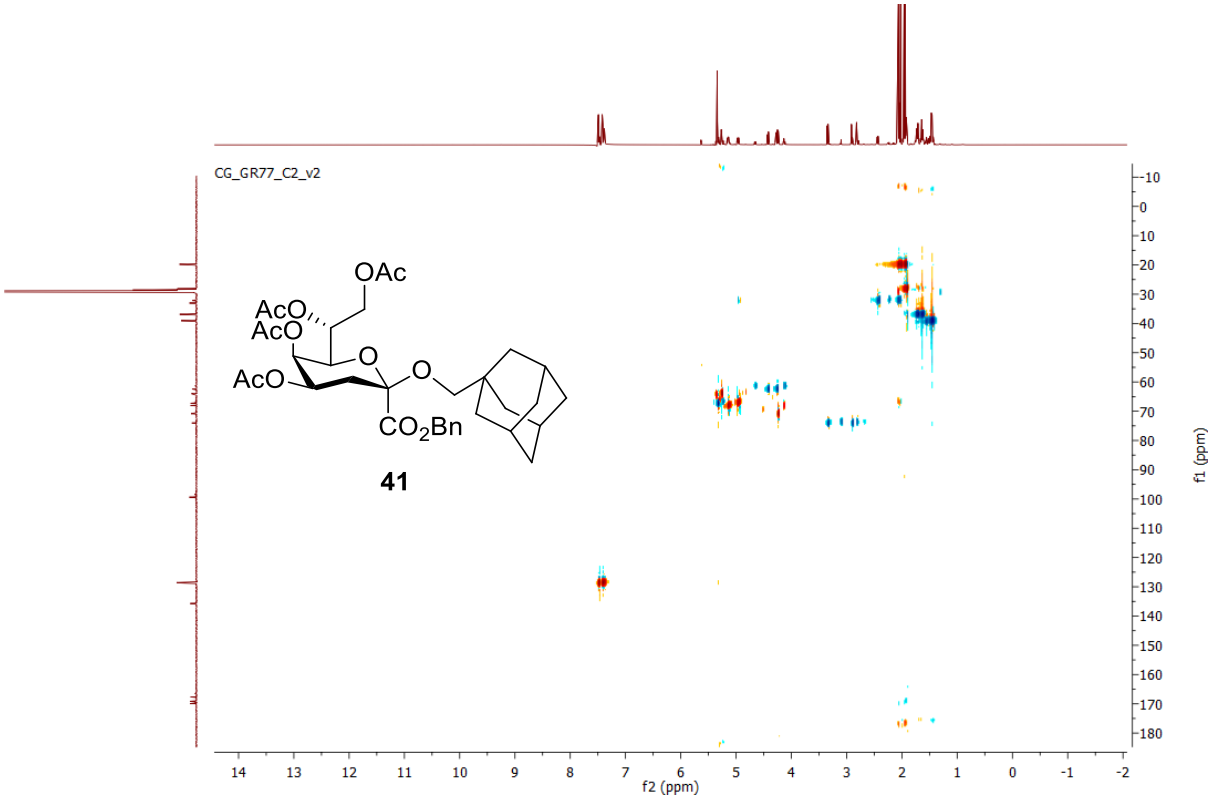

Supplementary Figure 16. ^{1}H NMR spectrum (Acetone-d6, 600 MHz) of compound 42

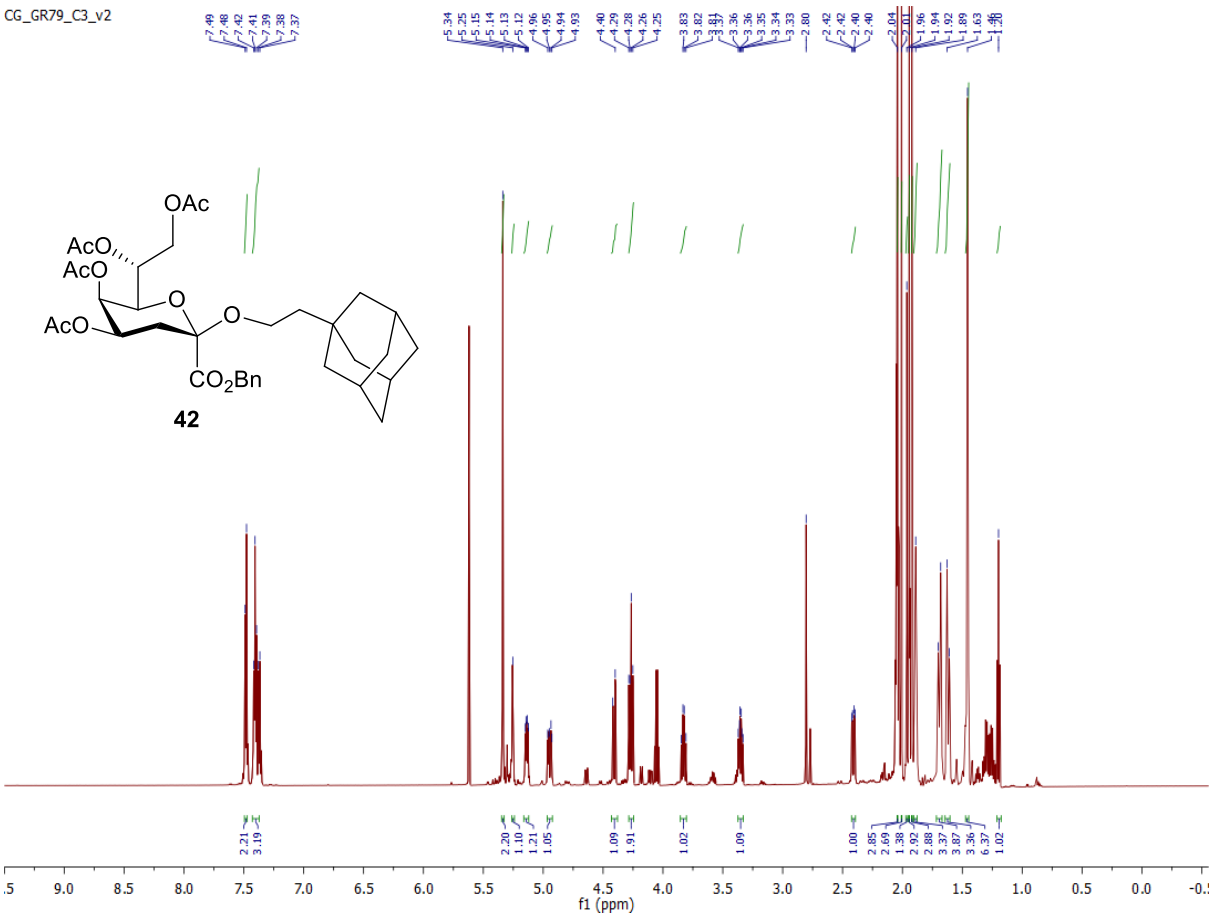

Supplementary Figure 17. ^{13}C NMR spectrum (Acetone-d6, 100 MHz) of compound 42

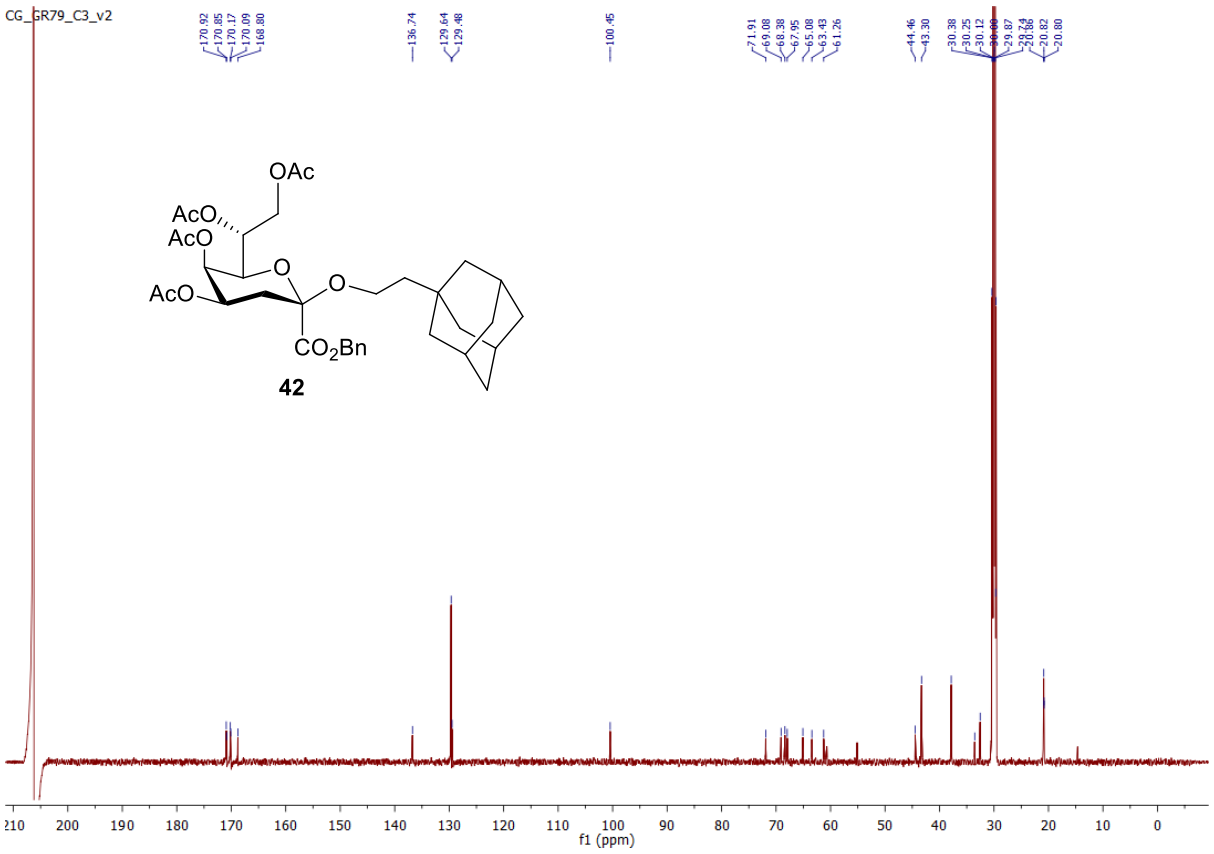

Supplementary Figure 18. COSY NMR spectrum (Acetone-d6, 600 MHz) of compound 42

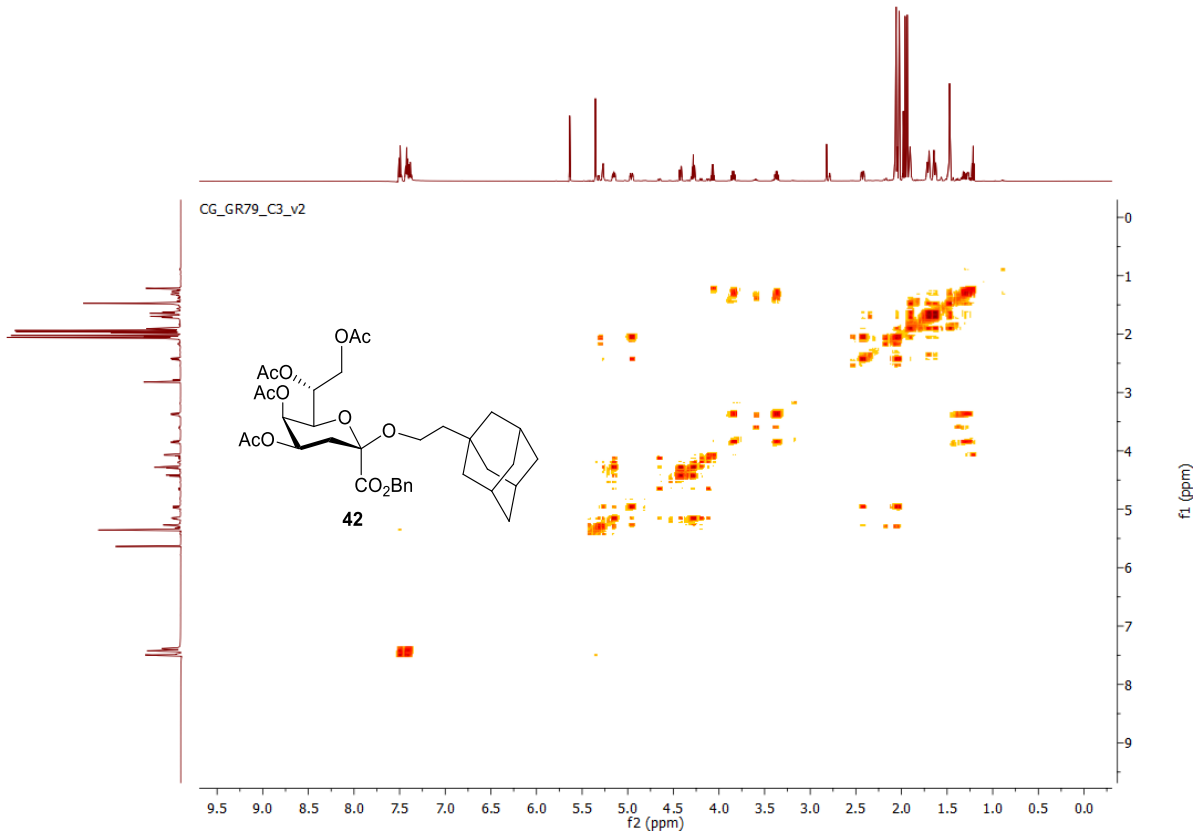

Supplementary Figure 19. HSQC NMR spectrum (Acetone-d6, 600 MHz) of compound 42

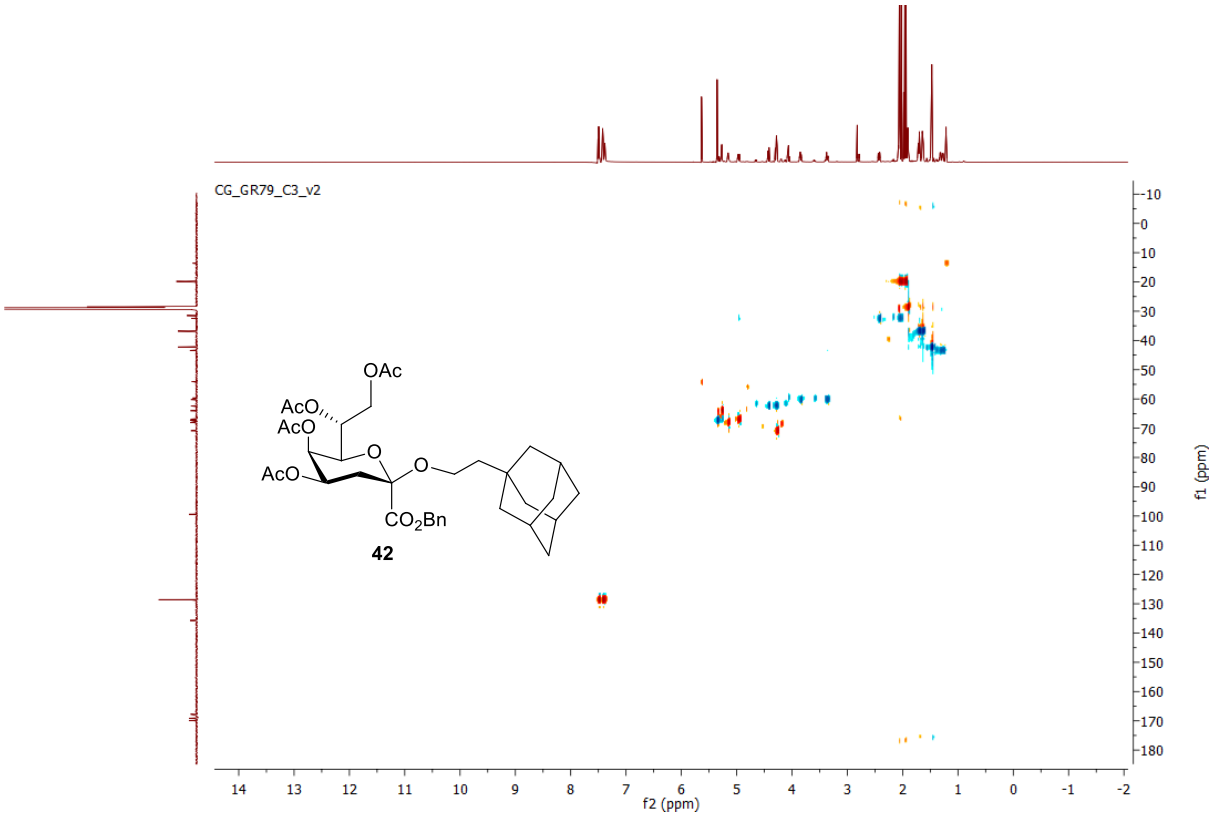

Supplementary Figure 20. ^{1}H NMR spectrum ($CDCl_3$, 600 MHz) of compound 46

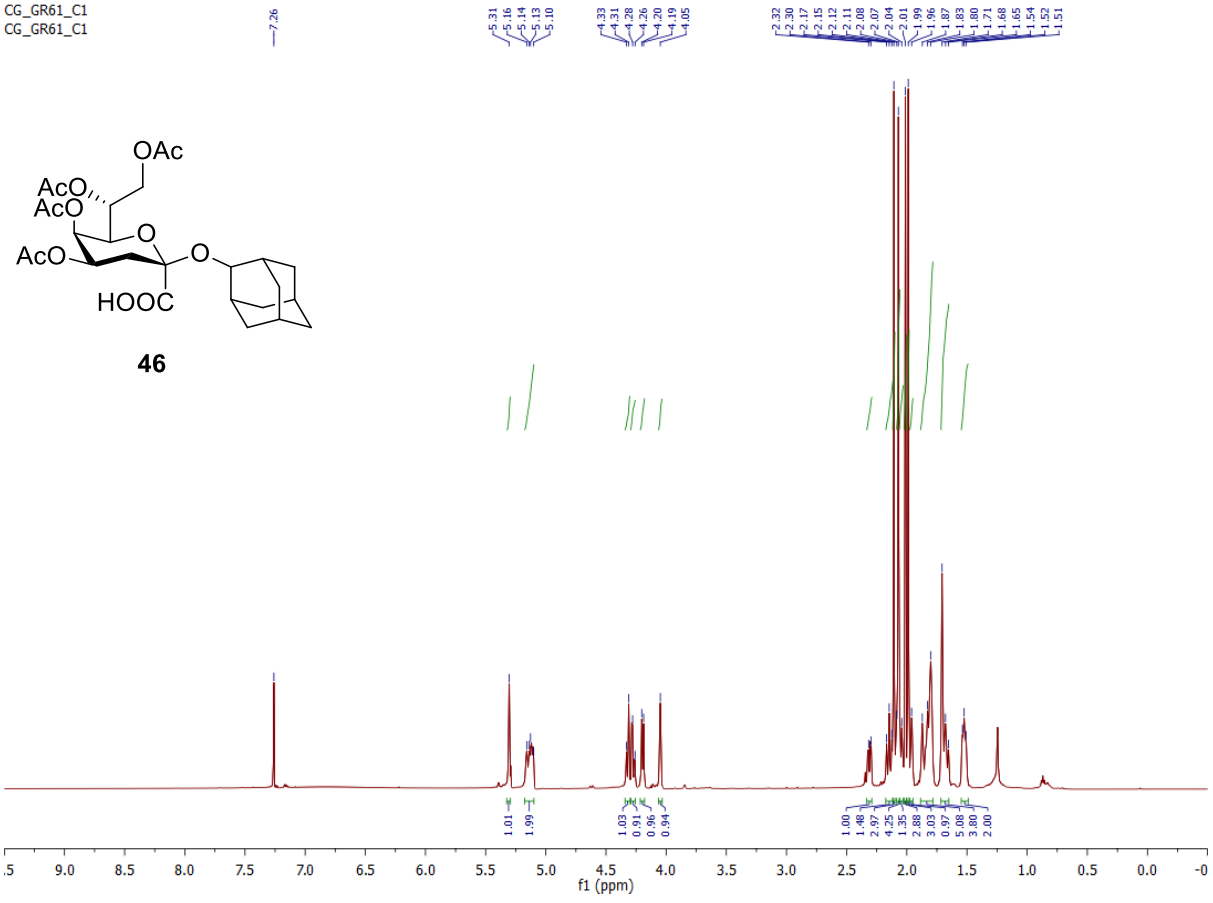

Supplementary Figure 21. ^{13}C NMR spectrum (CDCl3, 100 MHz) of compound 46

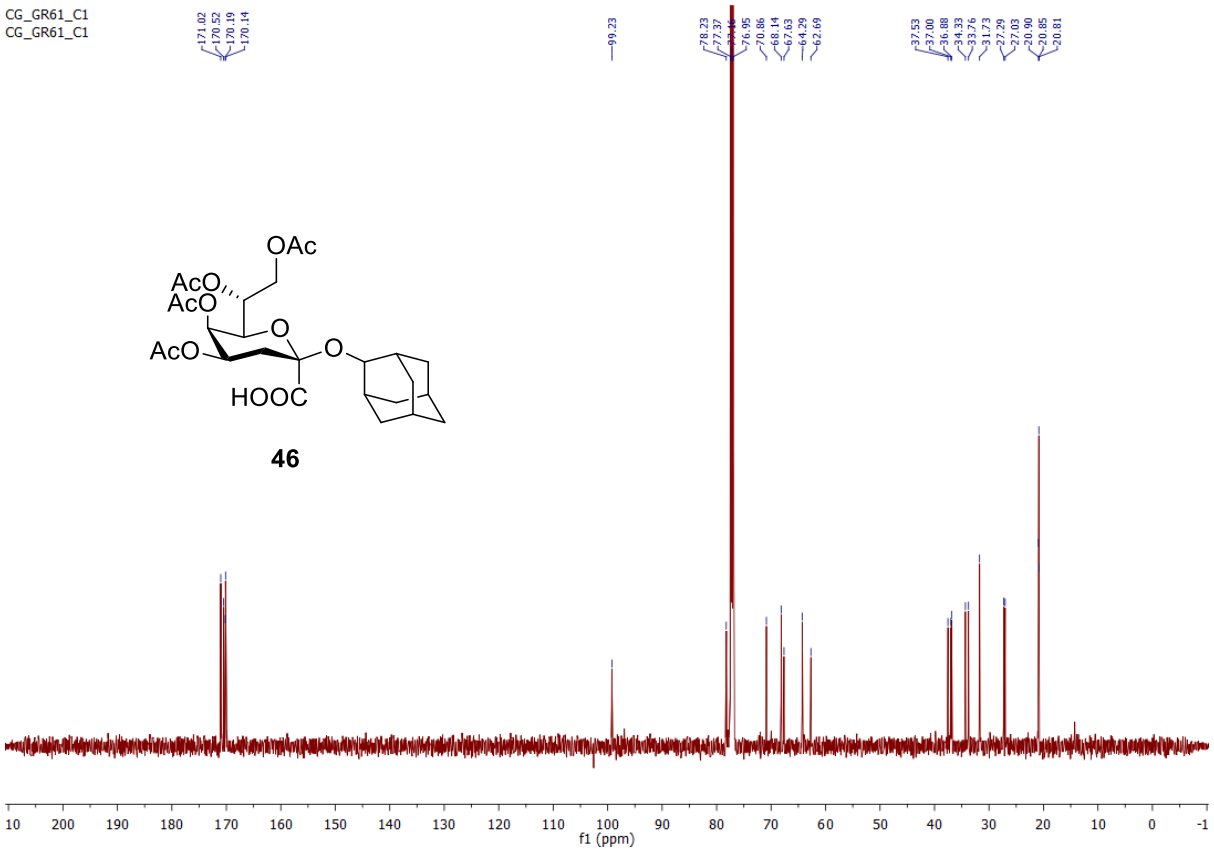

Supplementary Figure 22. COSY NMR spectrum (Acetone-d6, 600 MHz) of compound 46

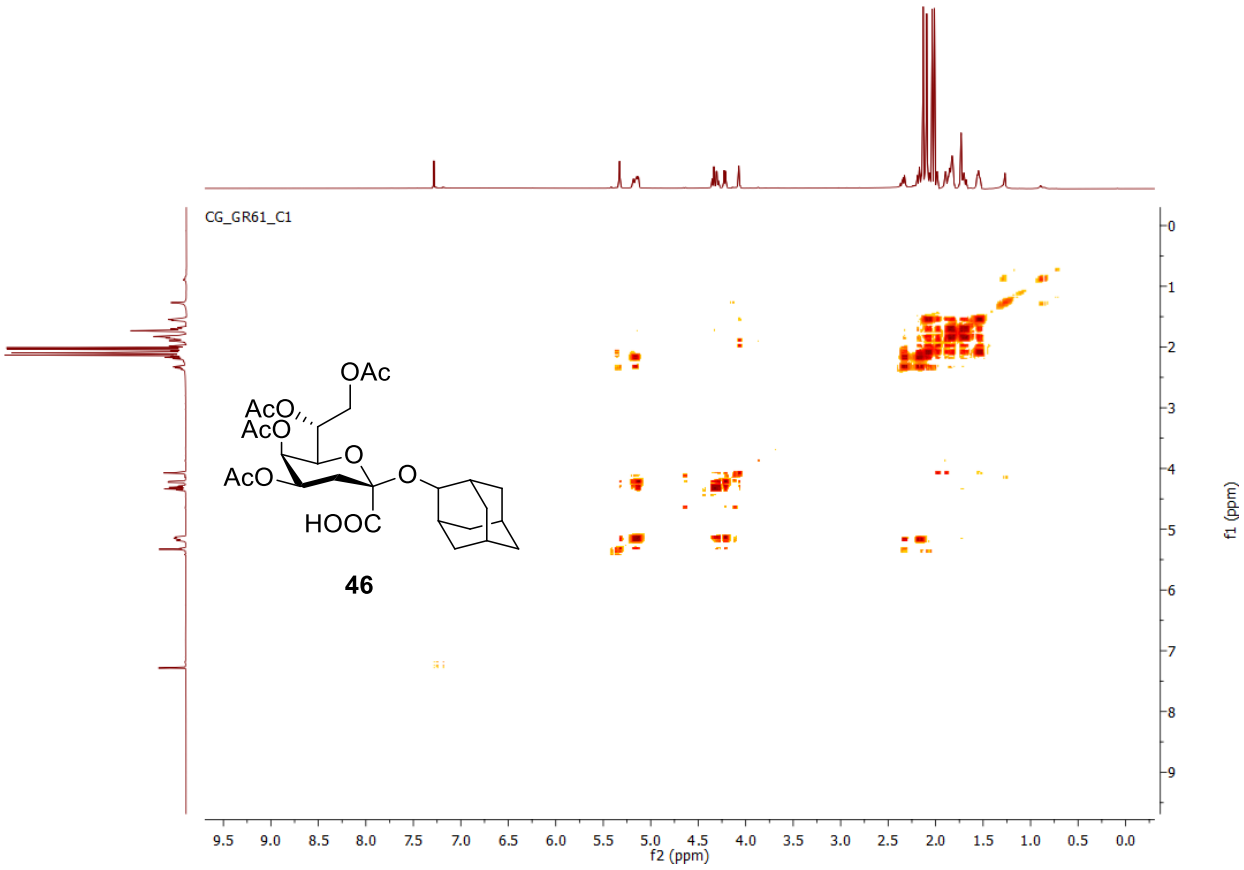

Supplementary Figure 23. HSQC NMR spectrum (Acetone-d6, 600 MHz) of compound 46

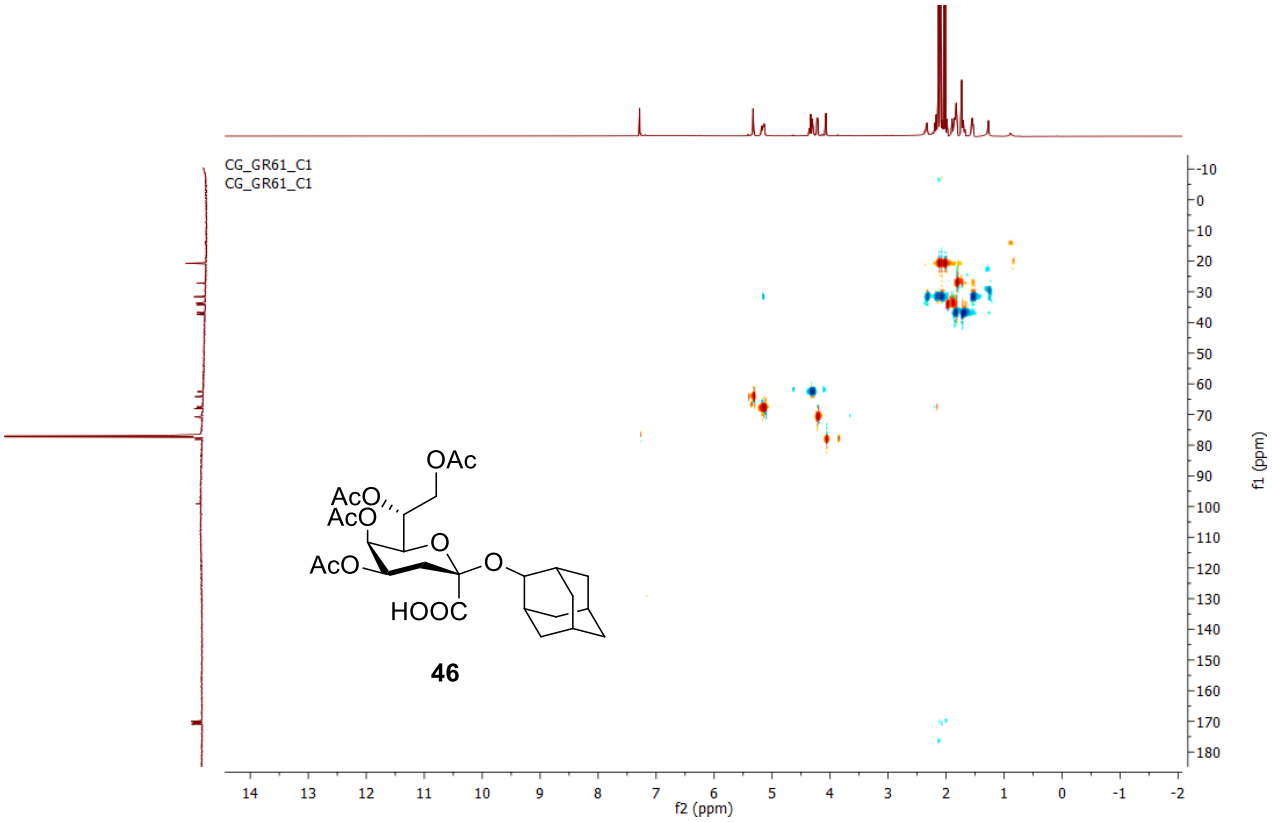

Supplementary Figure 24. ^{1}H NMR spectrum (Acetone-d6, 600 MHz) of compound 47

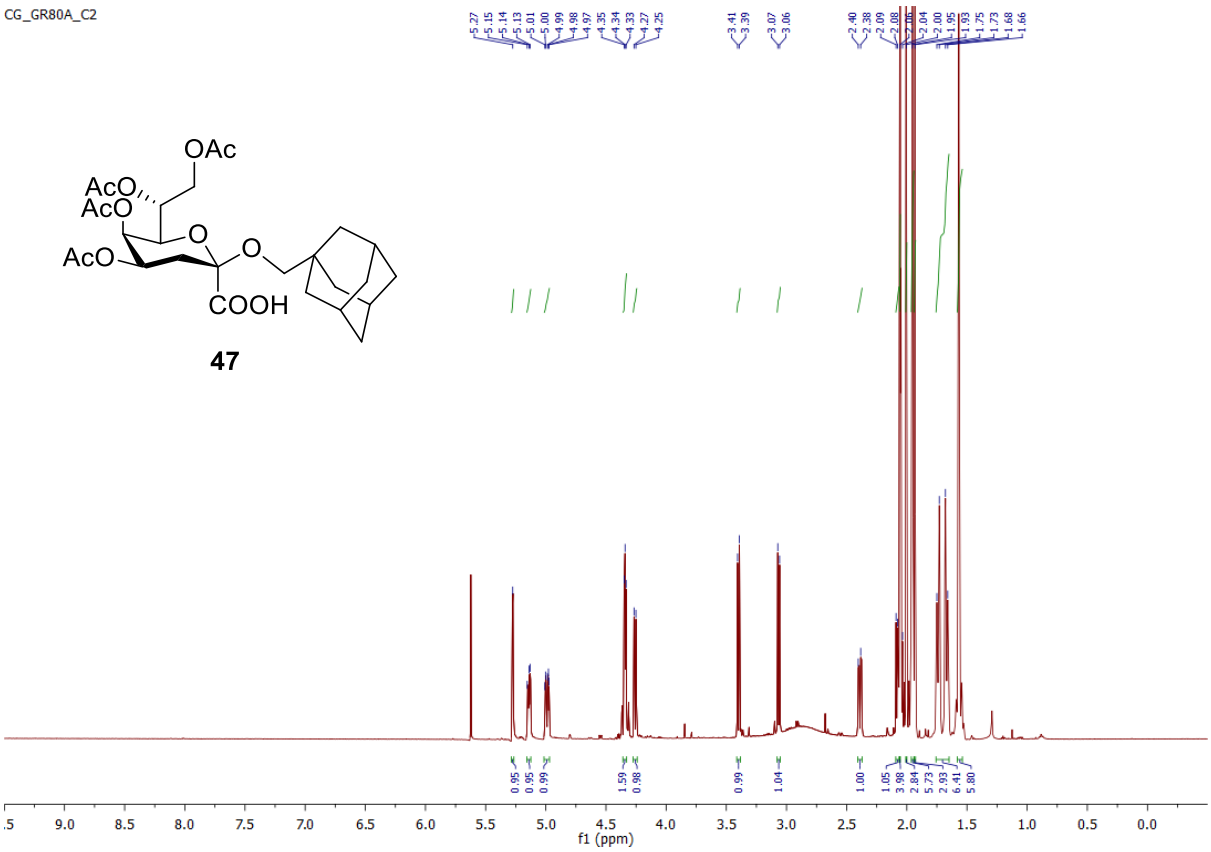

Supplementary Figure 25. ^{13}C NMR spectrum (Acetone-d6, 100 MHz) of compound 47

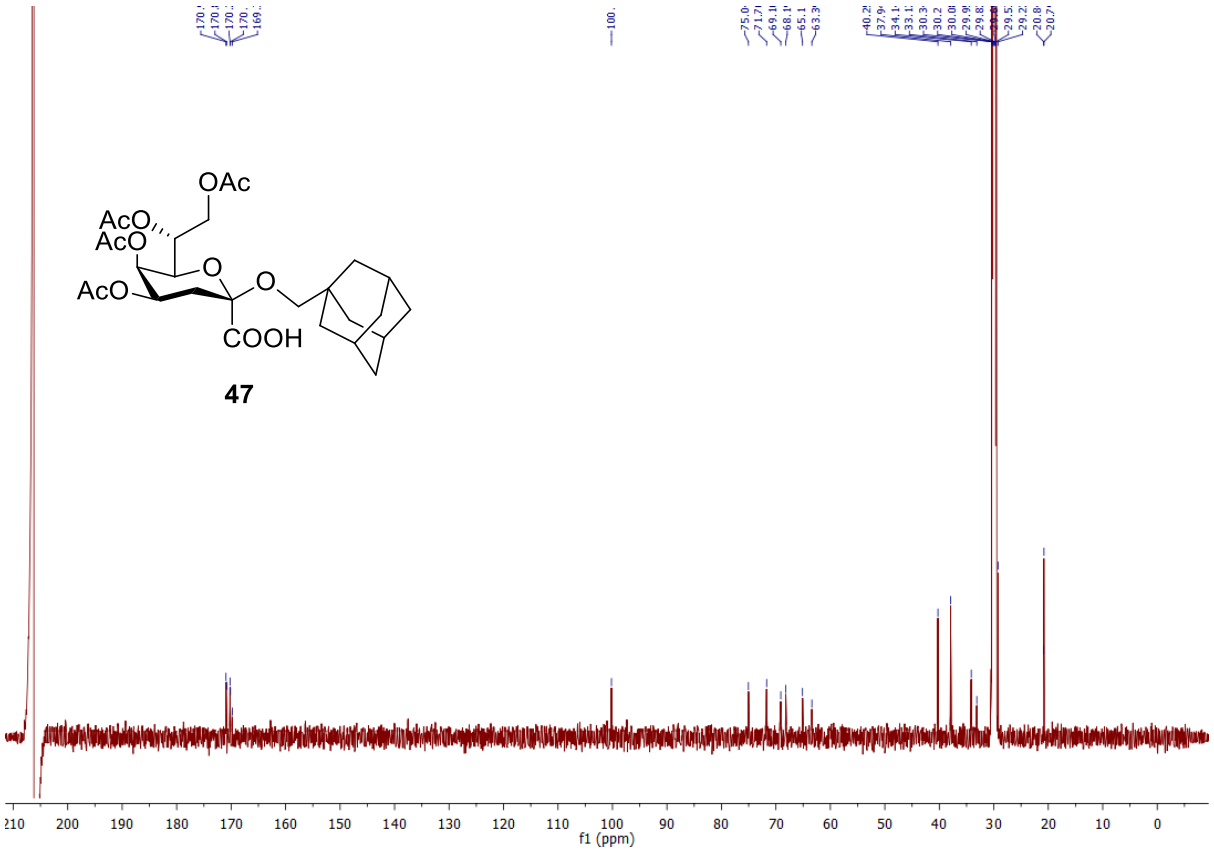

Supplementary Figure 26. COSY NMR spectrum (Acetone-d6, 600 MHz) of compound 47

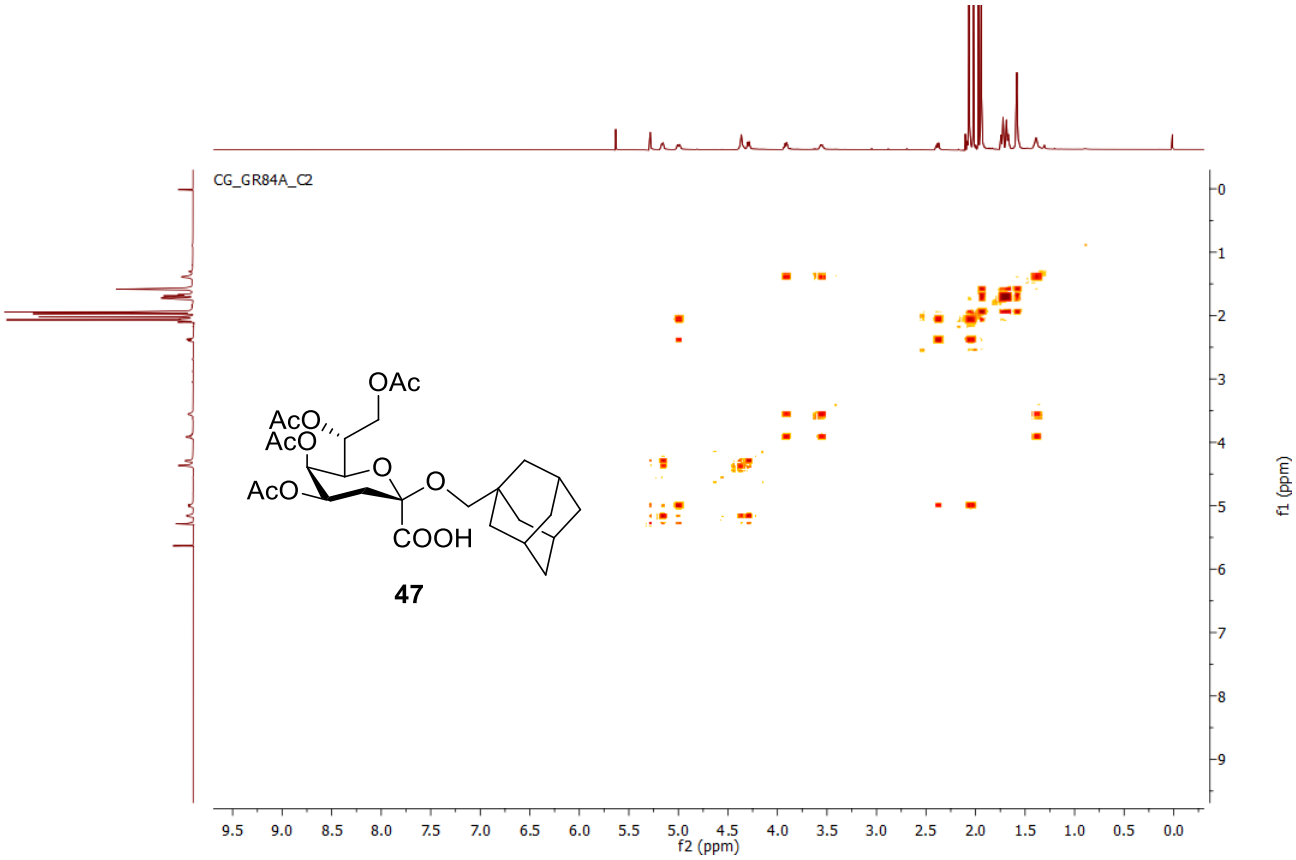

Supplementary Figure 27. HSQC NMR spectrum (Acetone-d6, 600 MHz) of compound 47

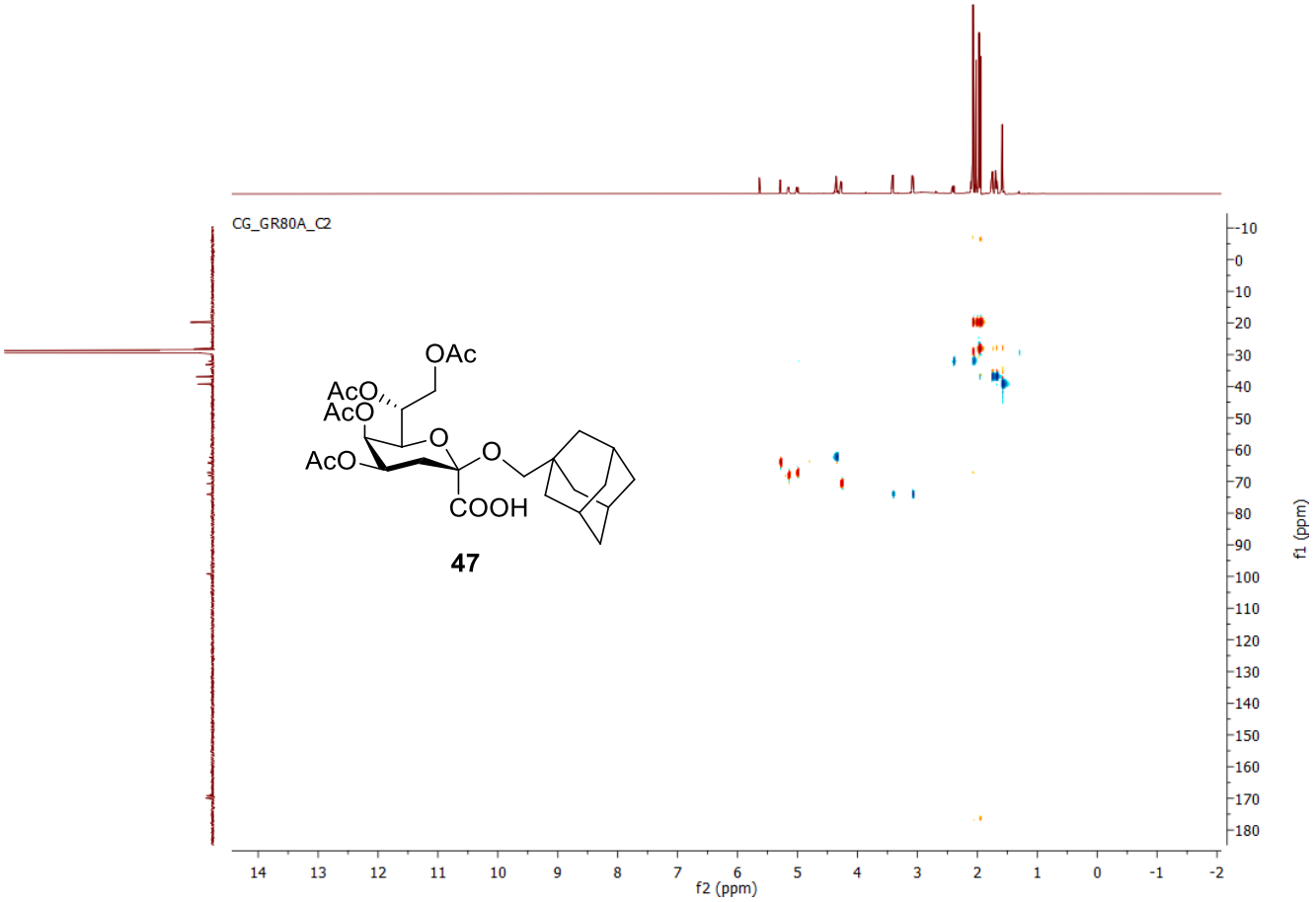

Supplementary Figure 28. ^{1}H NMR spectrum (Acetone-d6, 600 MHz) of compound 48

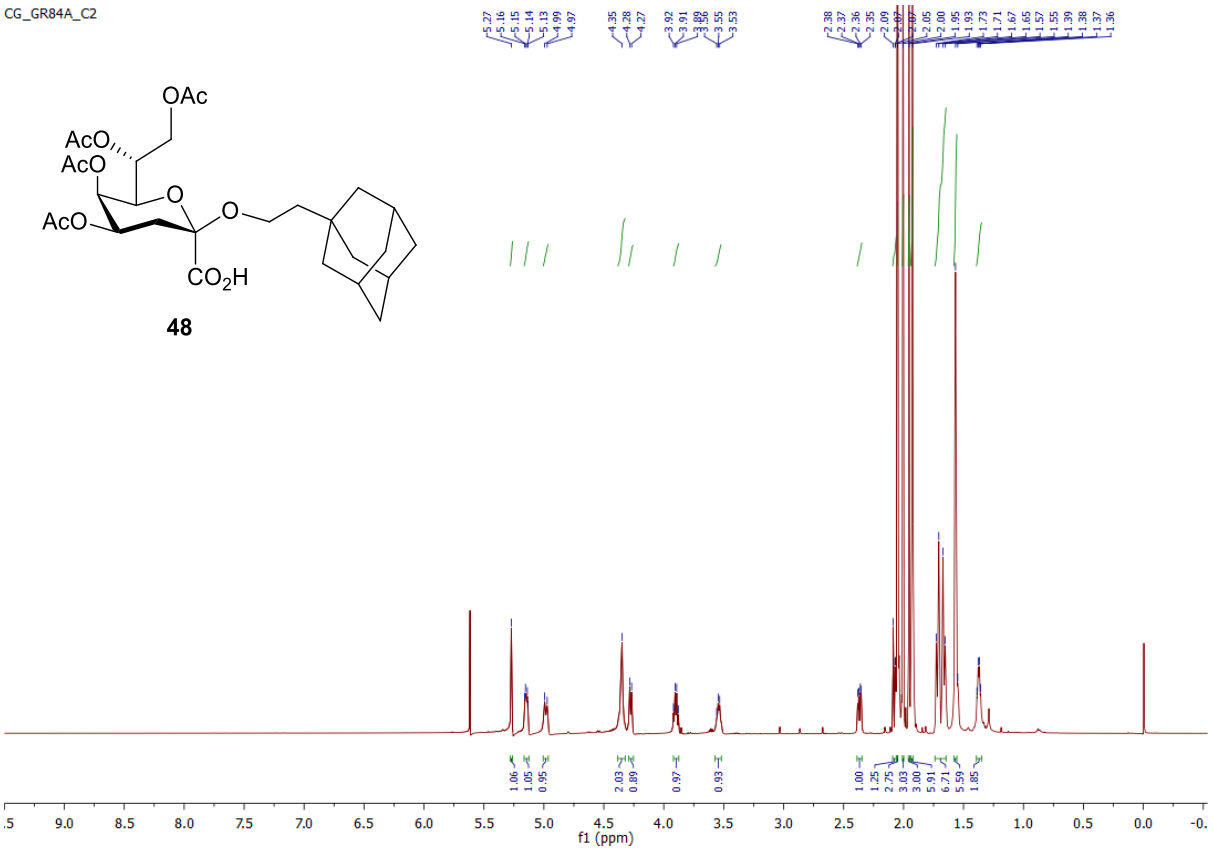

Supplementary Figure 29. ^{13}C NMR spectrum (Acetone-d6, 100 MHz) of compound 48

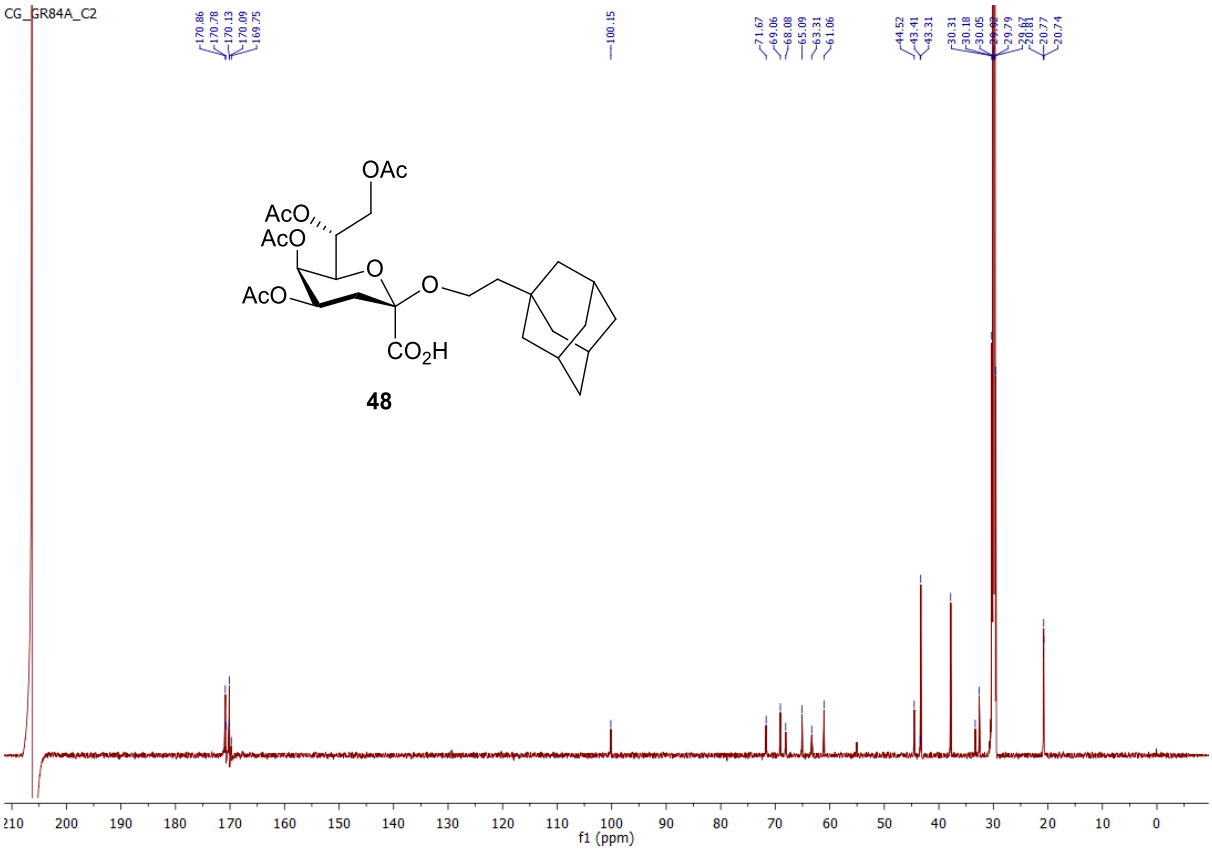

Supplementary Figure 30. COSY NMR spectrum (Acetone-d6, 600 MHz) of compound 48

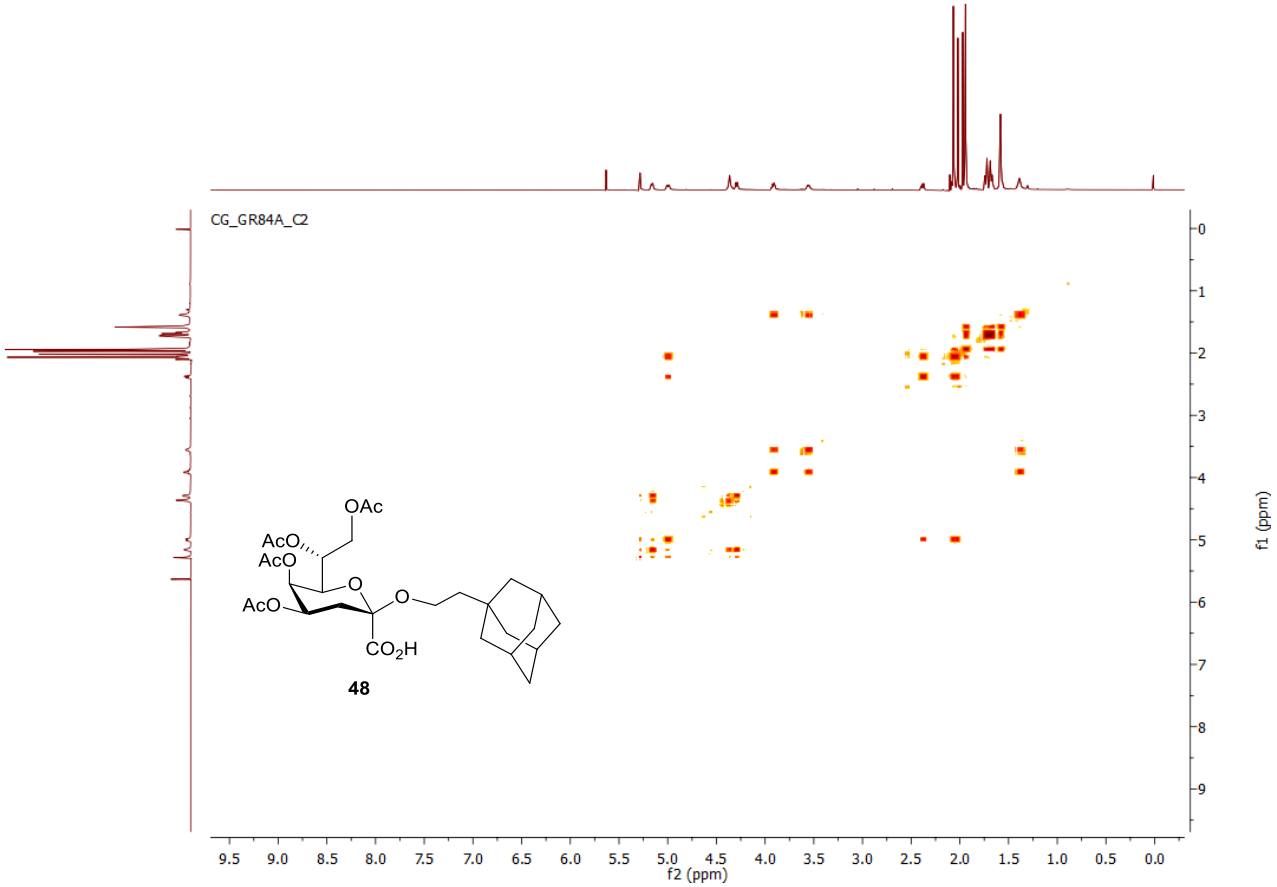

Supplementary Figure 31. HSQC NMR spectrum (Acetone-d6, 600 MHz) of compound 48

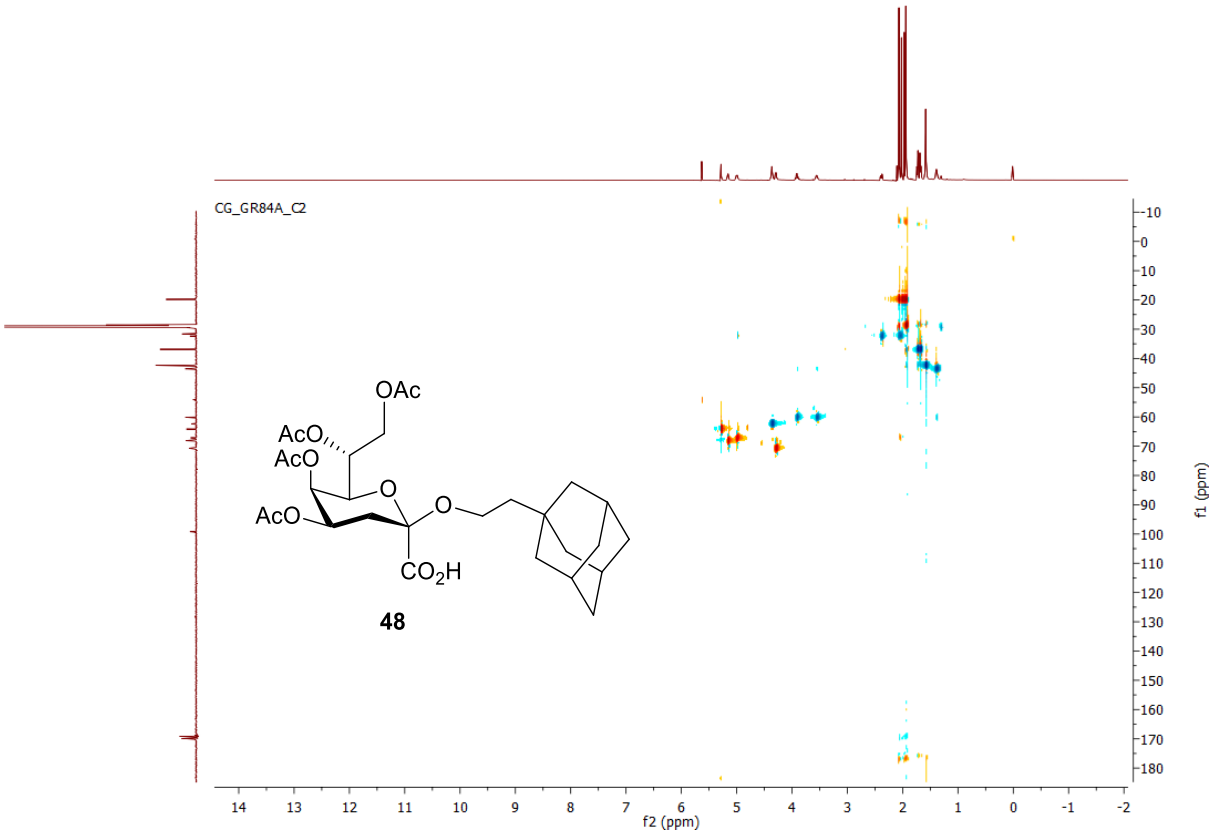

Supplementary Figure 32. ^{1}H NMR spectrum (MeOH-d4, 600 MHz) of compound 49

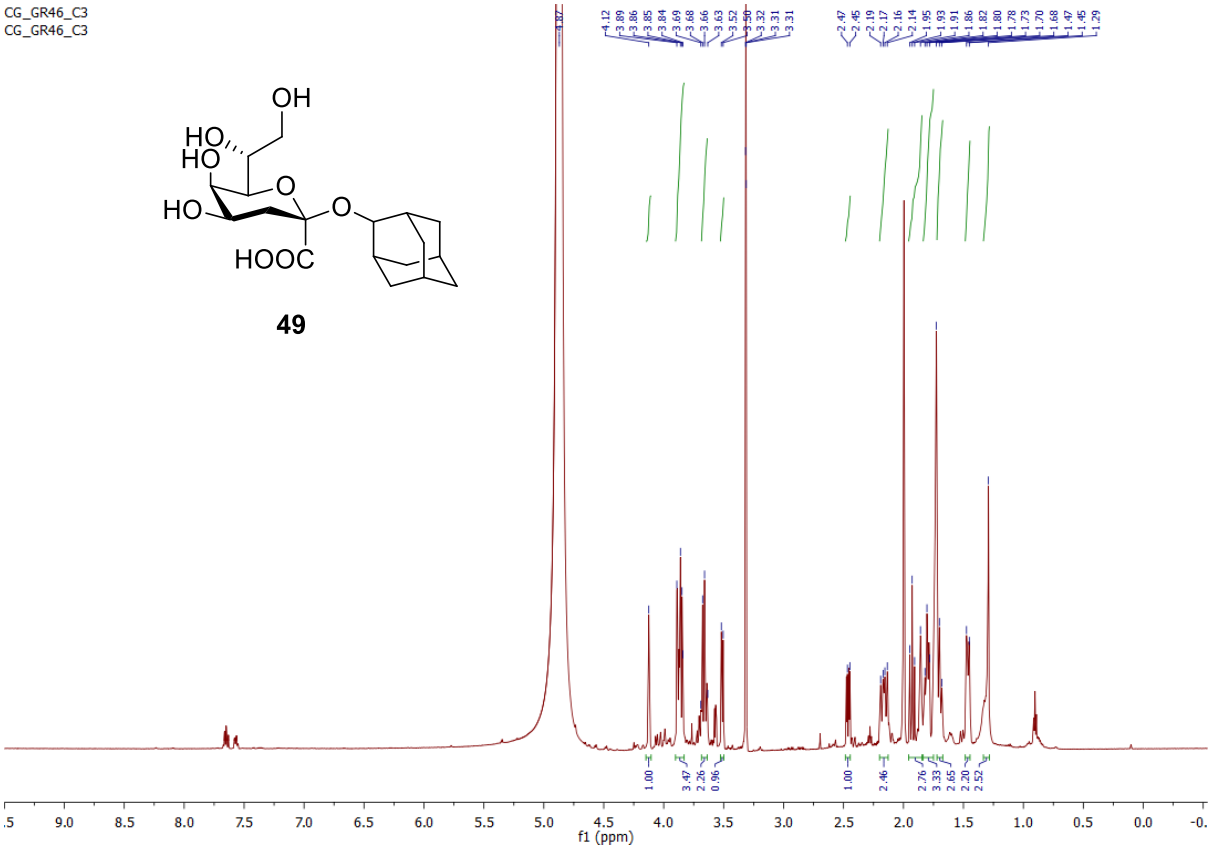

Supplementary Figure 33. ^{13}C NMR spectrum (MeOH-d4, 100 MHz) of compound 49

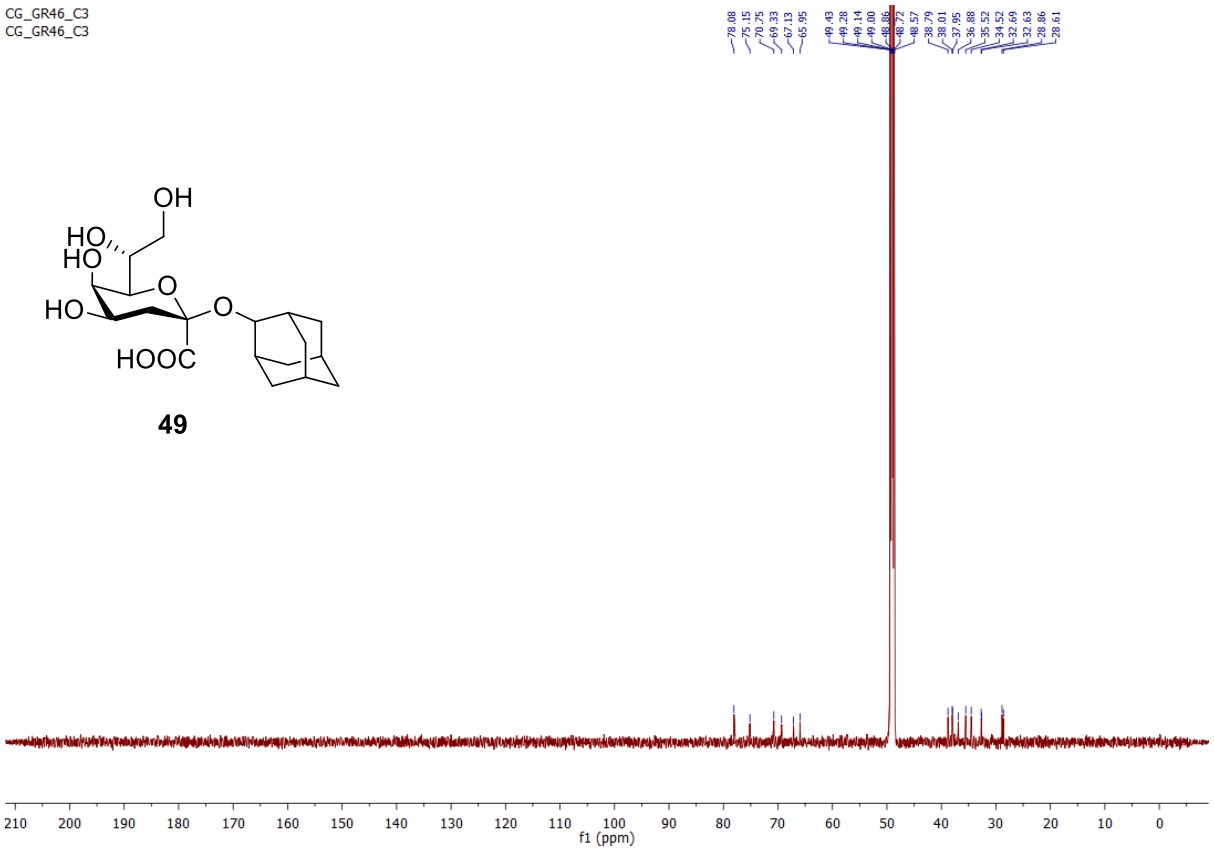

Supplementary Figure 34. COSY NMR spectrum (MeOH-d4, 600 MHz) of compound 49

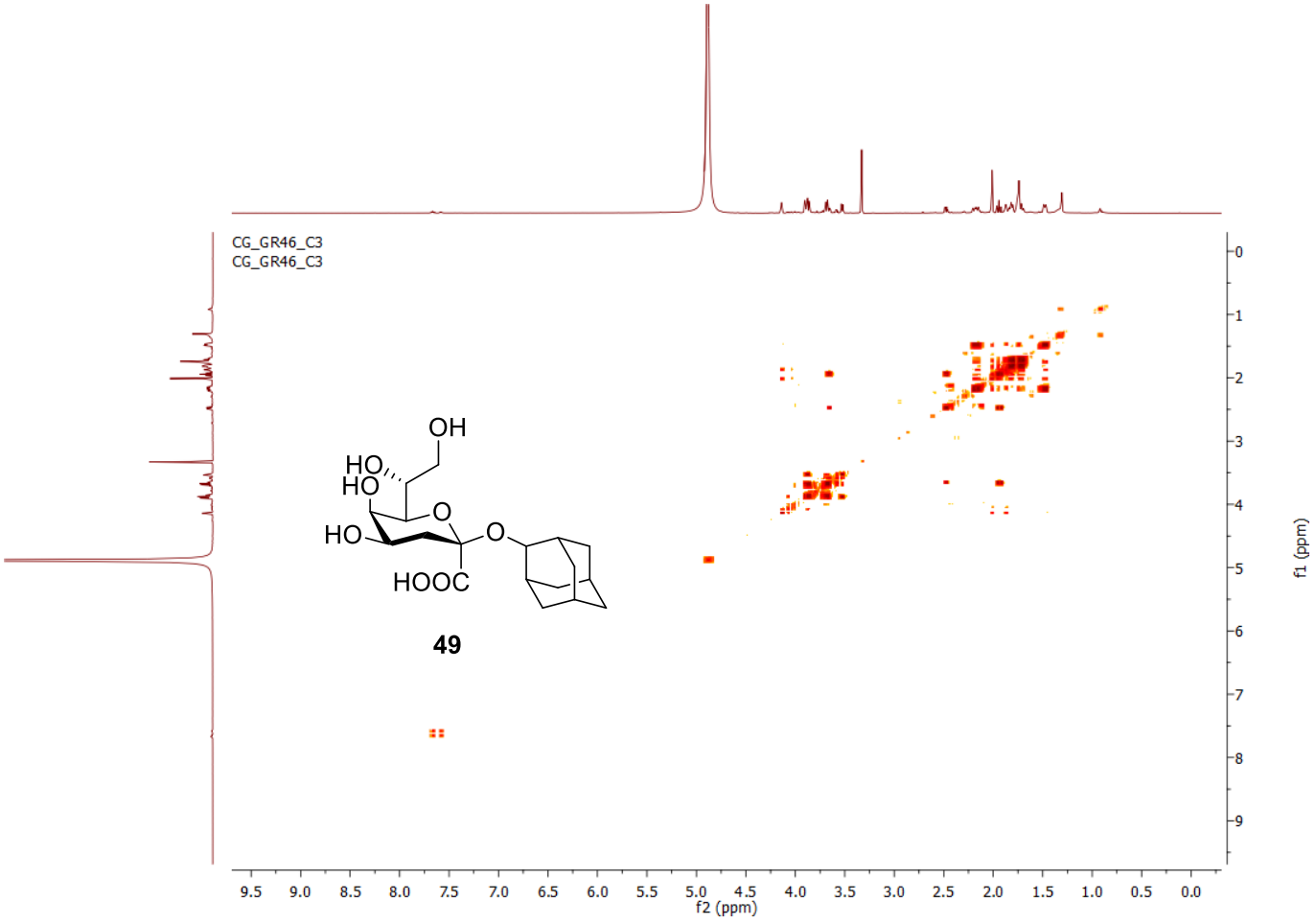

Supplementary Figure 35. HSQC NMR spectrum (MeOH-d4, 600 MHz) of compound 49

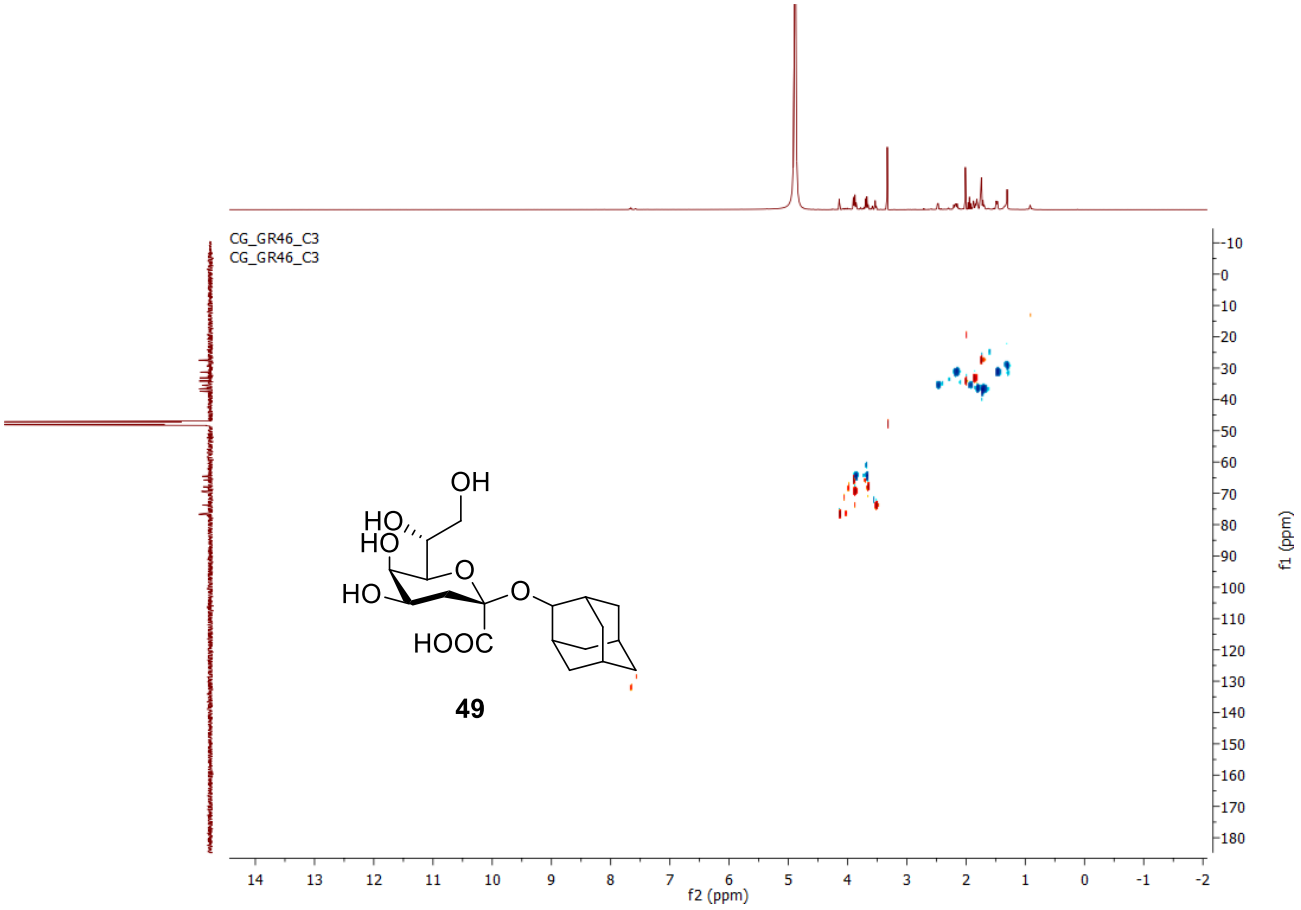

Supplementary Figure 36. ^{1}H NMR spectrum (MeOH-d4, 600 MHz) of compound 50

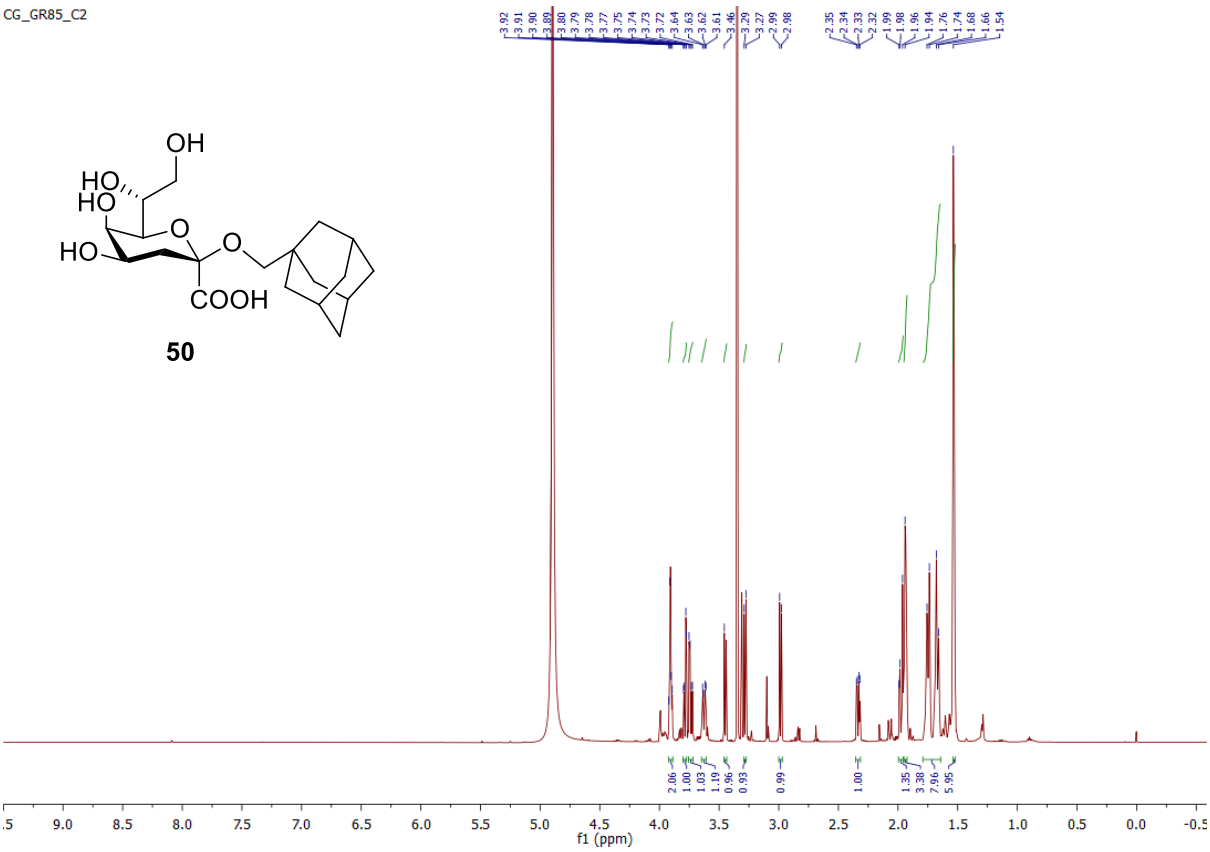

Supplementary Figure 37. ^{13}C NMR spectrum (MeOH-d4, 100 MHz) of compound 50

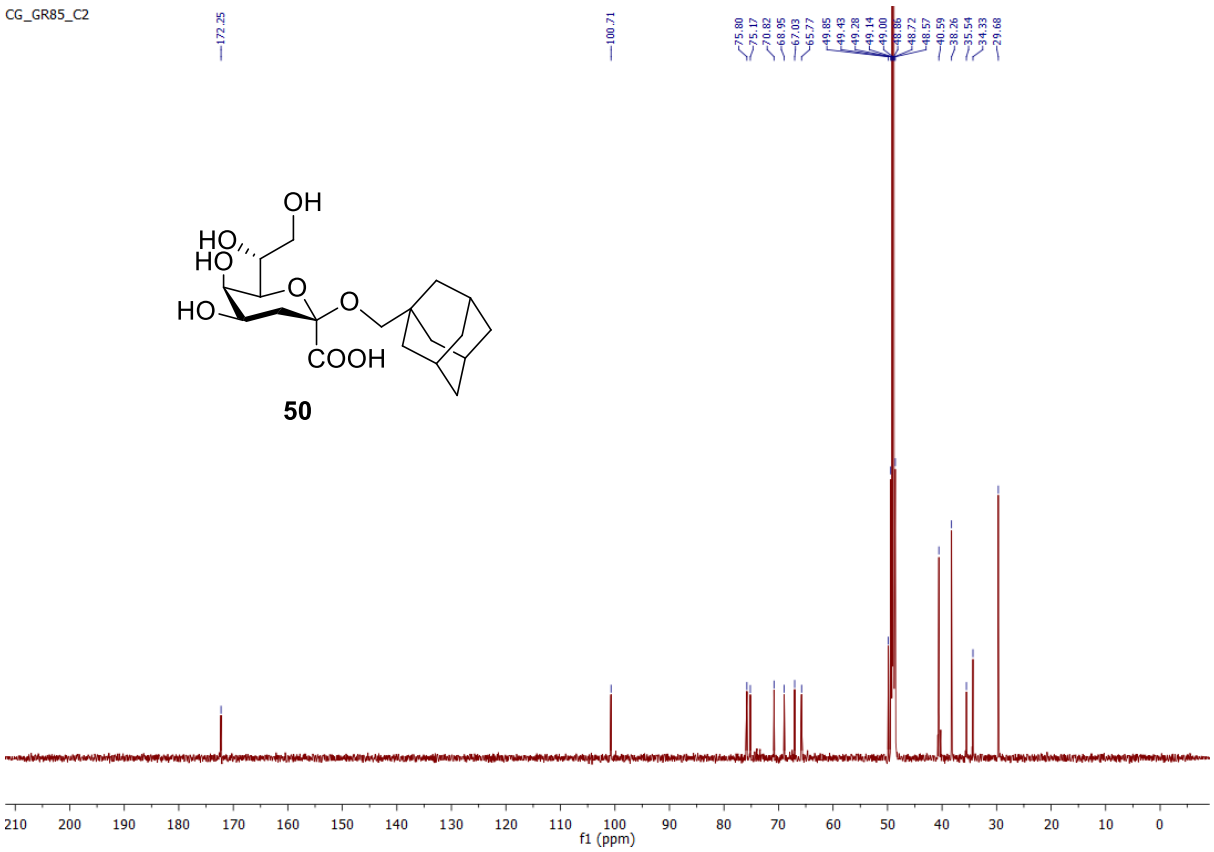

Supplementary Figure 38. COSY NMR spectrum (MeOH-d4, 600 MHz) of compound 50

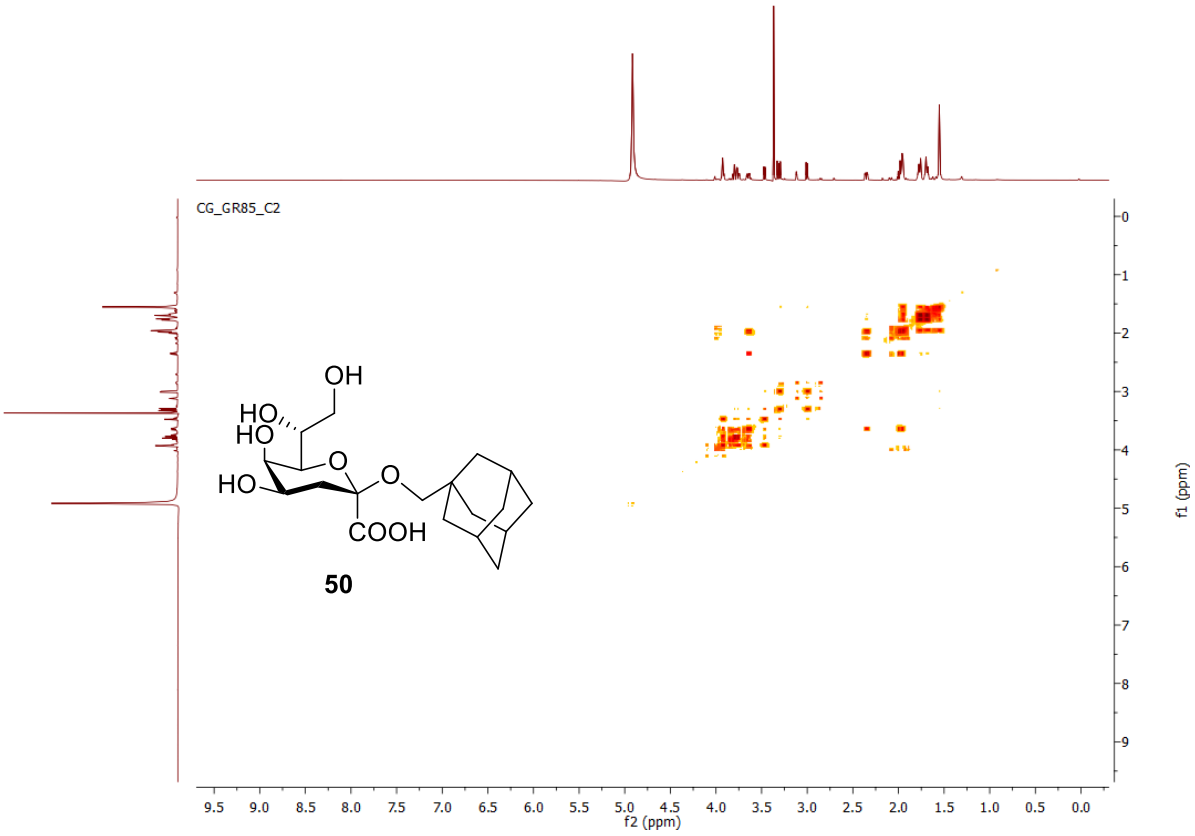

Supplementary Figure 39. HSQC NMR spectrum (MeOH-d4, 600 MHz) of compound 50

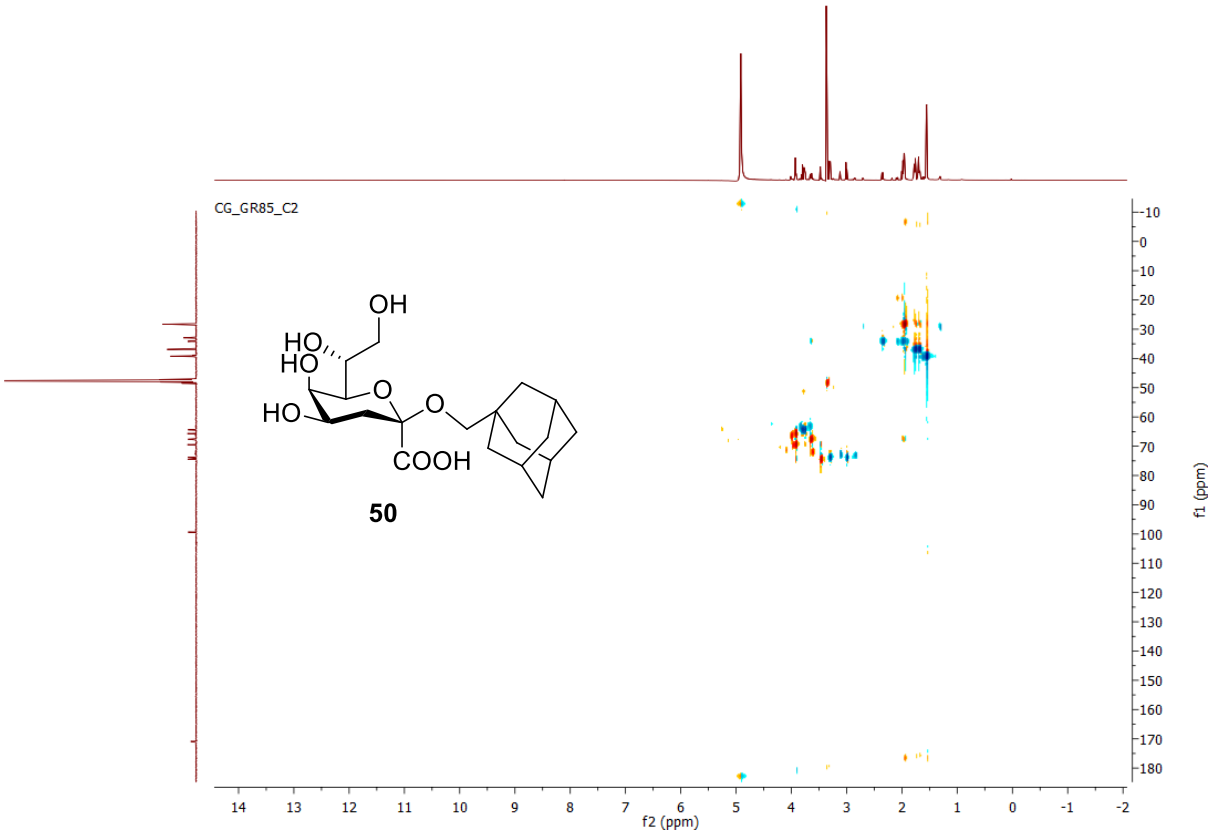

Supplementary Figure 40. ^{1}H NMR spectrum (MeOH-d4, 600 MHz) of compound 51

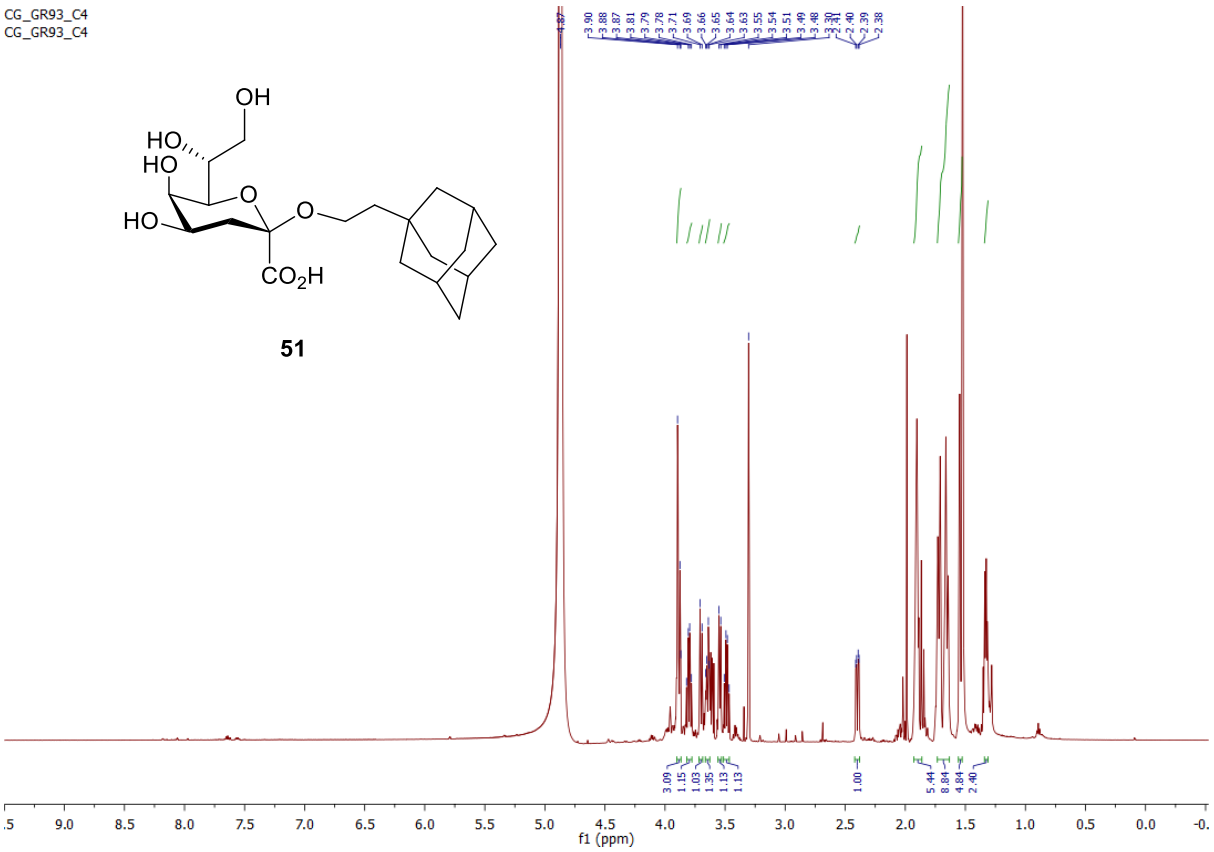

Supplementary Figure 41. ^{13}C NMR spectrum (MeOH-d4, 100 MHz) of compound 51

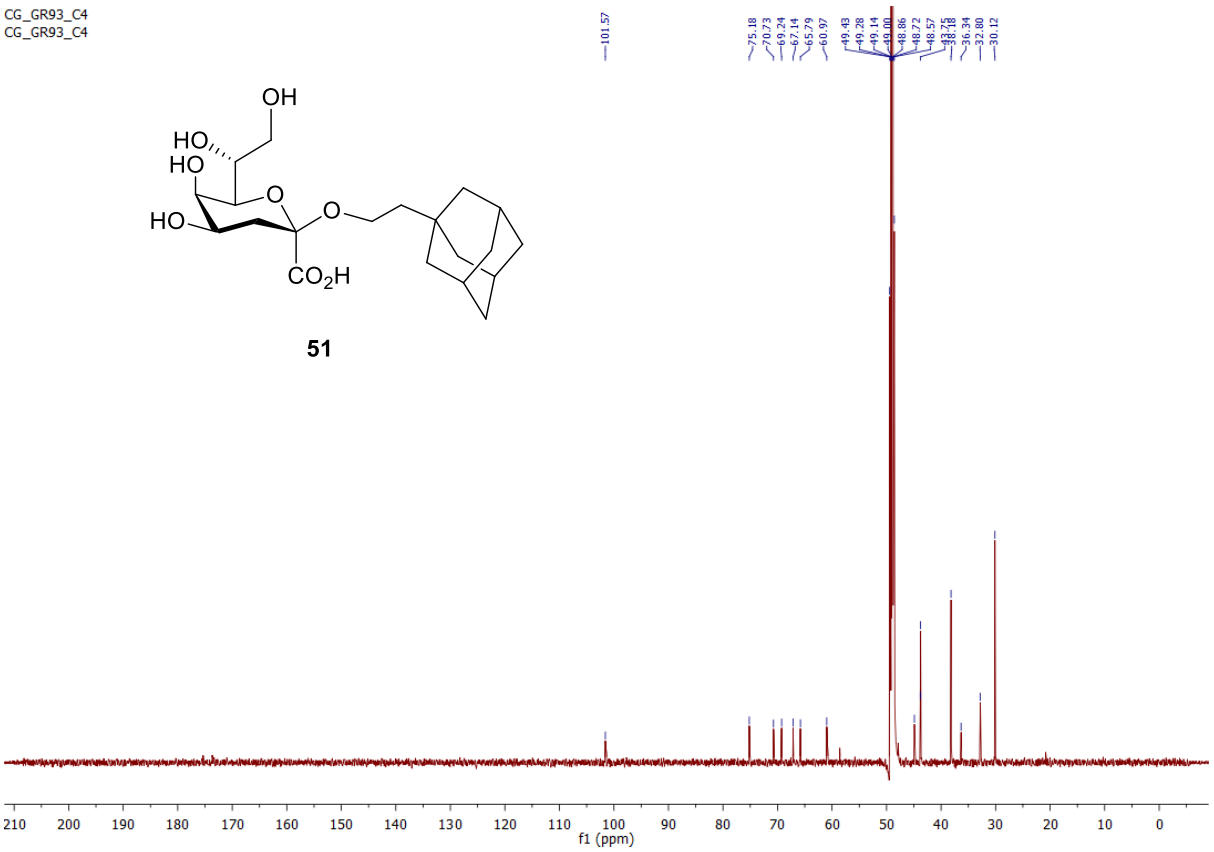

51

Supplementary Figure 42. COSY NMR spectrum (MeOH-d4, 600 MHz) of compound 51

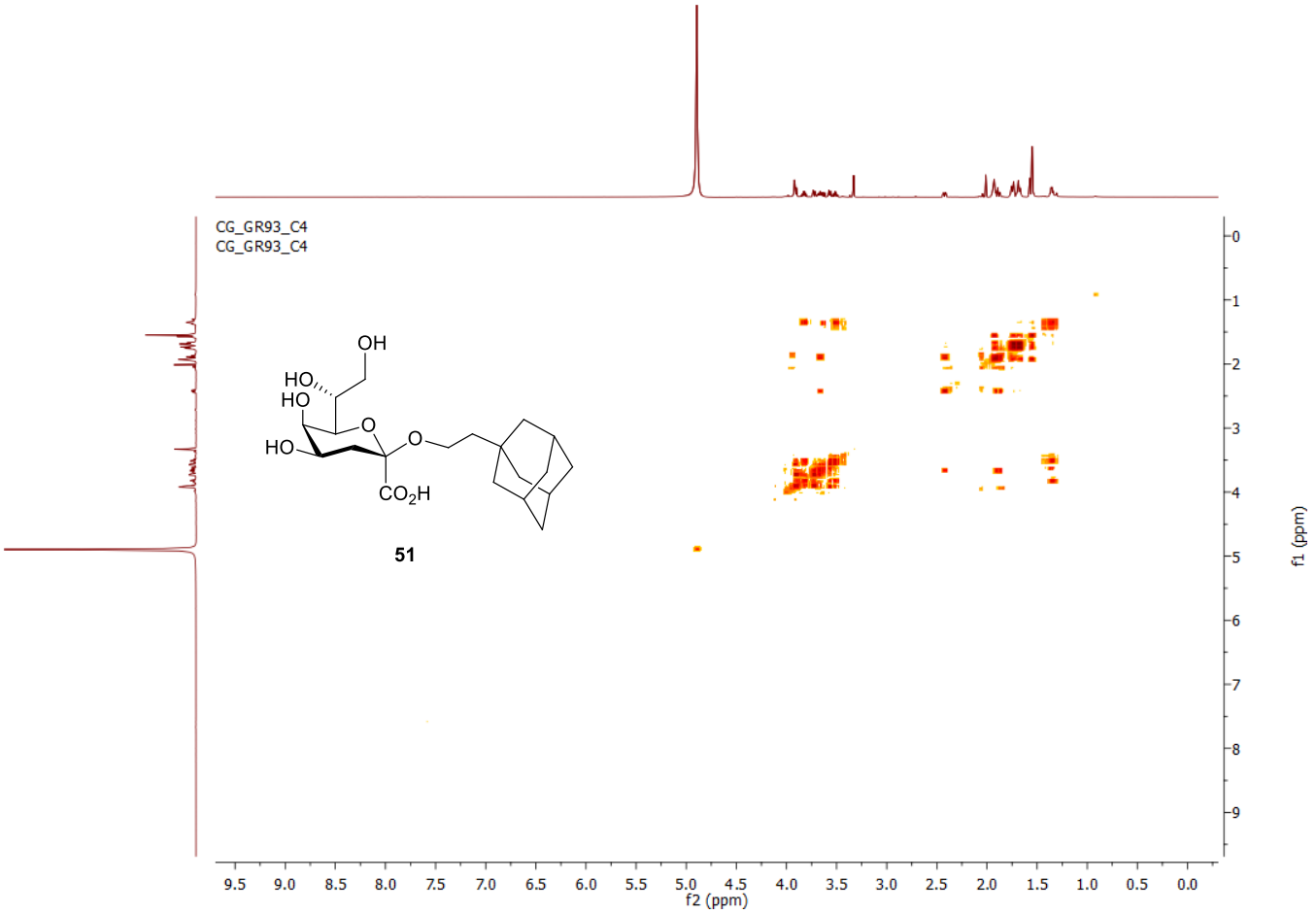

Supplementary Figure 43. HSQC NMR spectrum (MeOH-d4, 600 MHz) of compound 51

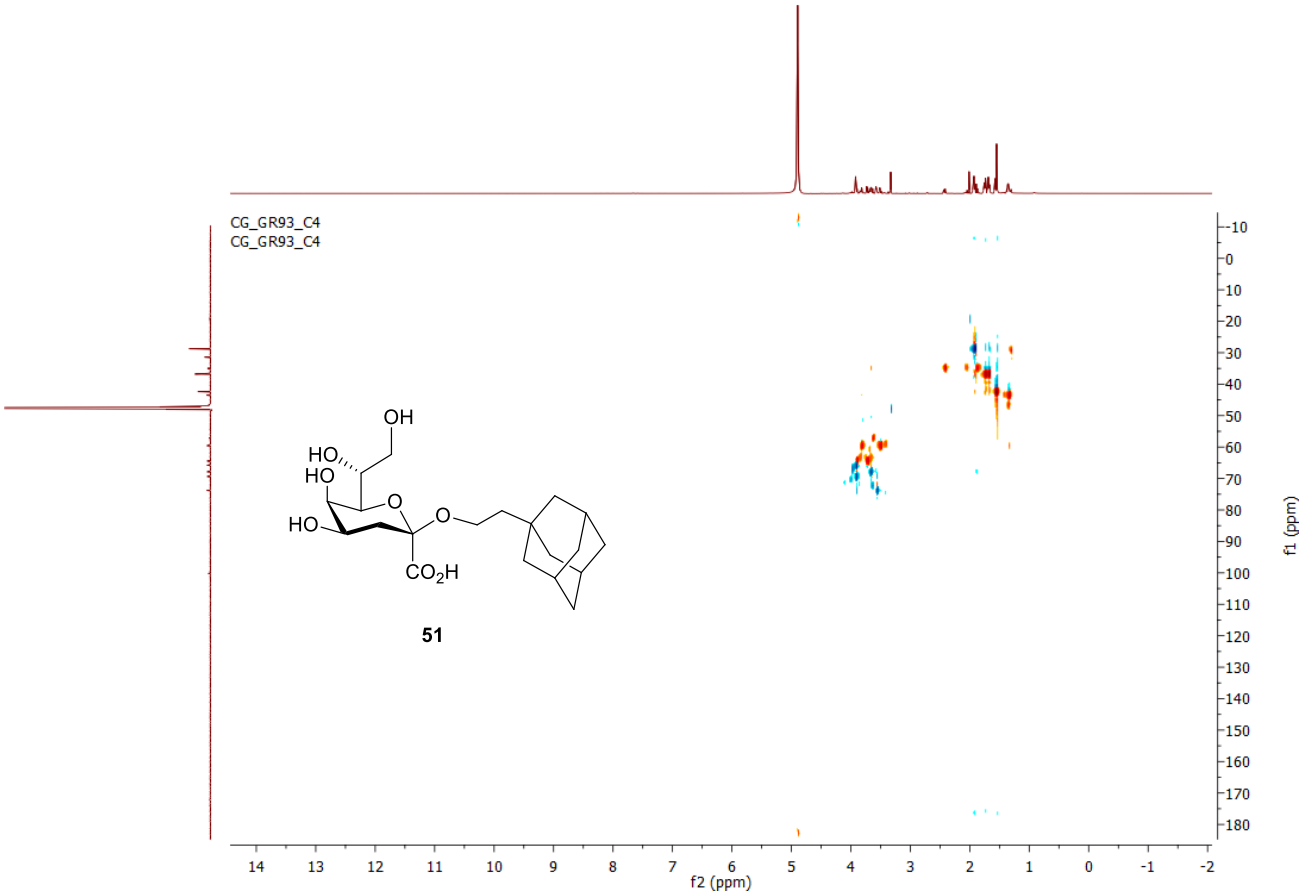

Supplementary Figure 44. ^{1}H NMR spectrum ($CDCl_3$, 600 MHz) of compound 62

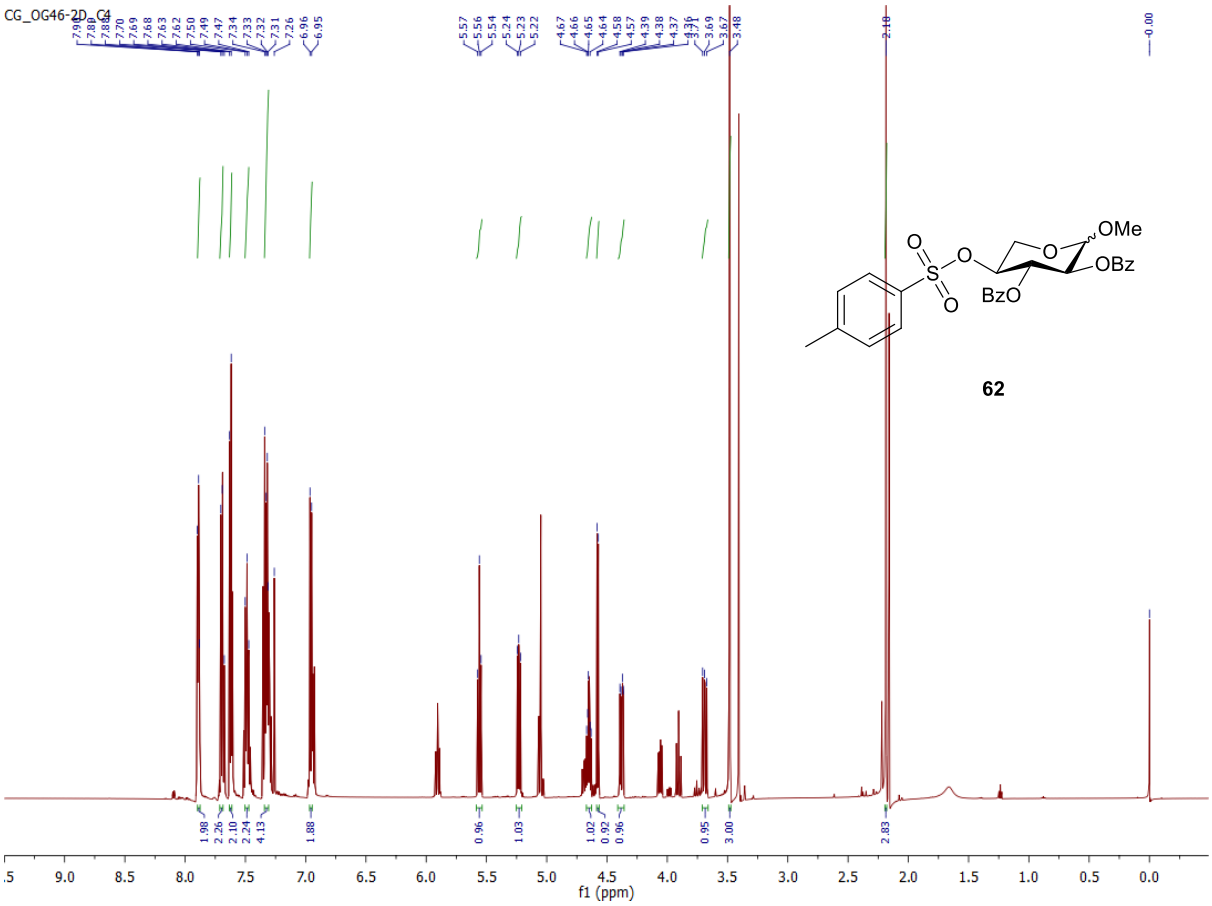

Supplementary Figure 45. ^{13}C NMR spectrum ($CDCl_3$, 100 MHz) of compound 62

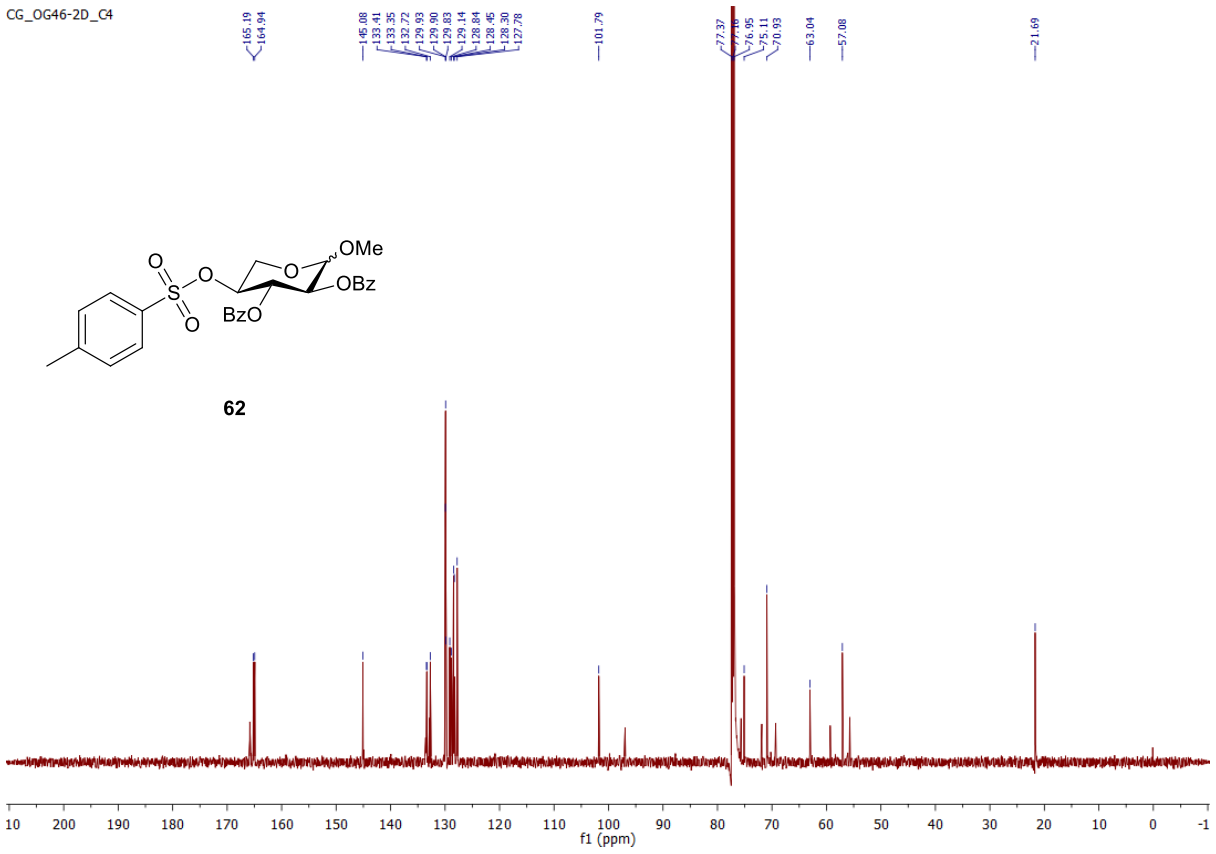

Supplementary Figure 46. COSY NMR spectrum ($CDCl_3$, 600 MHz) of compound 62

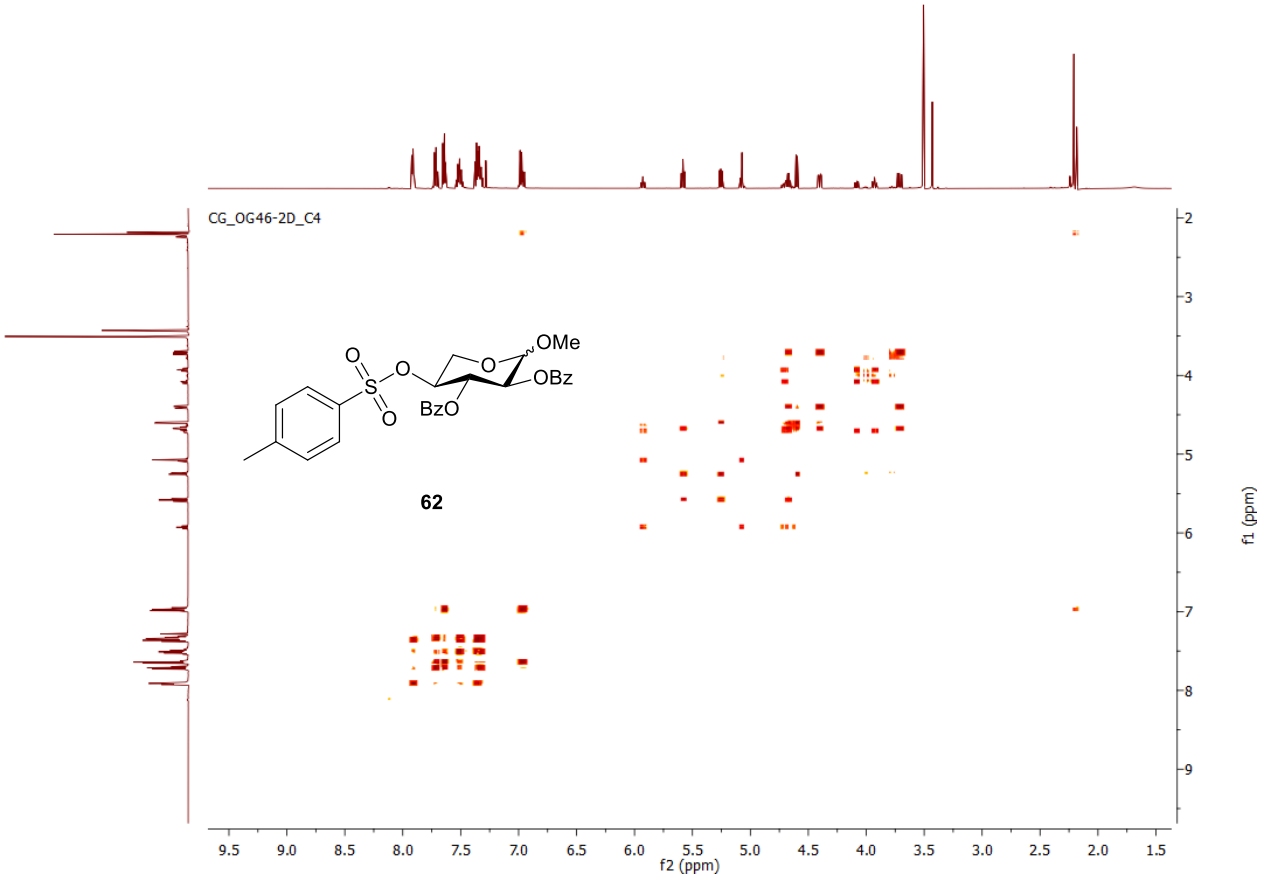

Supplementary Figure 47. HSQC NMR spectrum ($CDCl_3$, 600 MHz) of compound 62

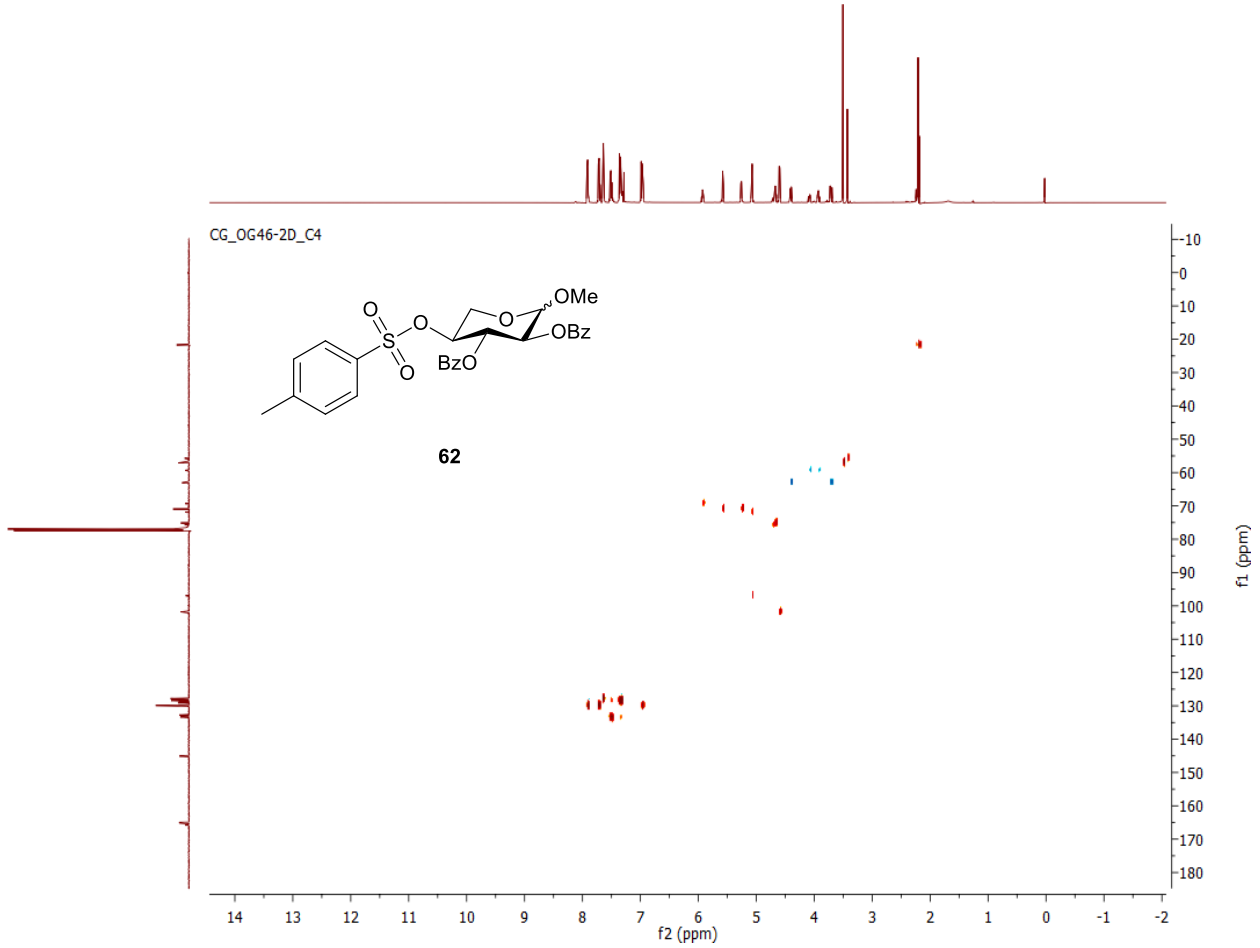

Supplementary Figure 48. ^{1}H NMR spectrum ($CDCl_3$, 600 MHz) of compound 63

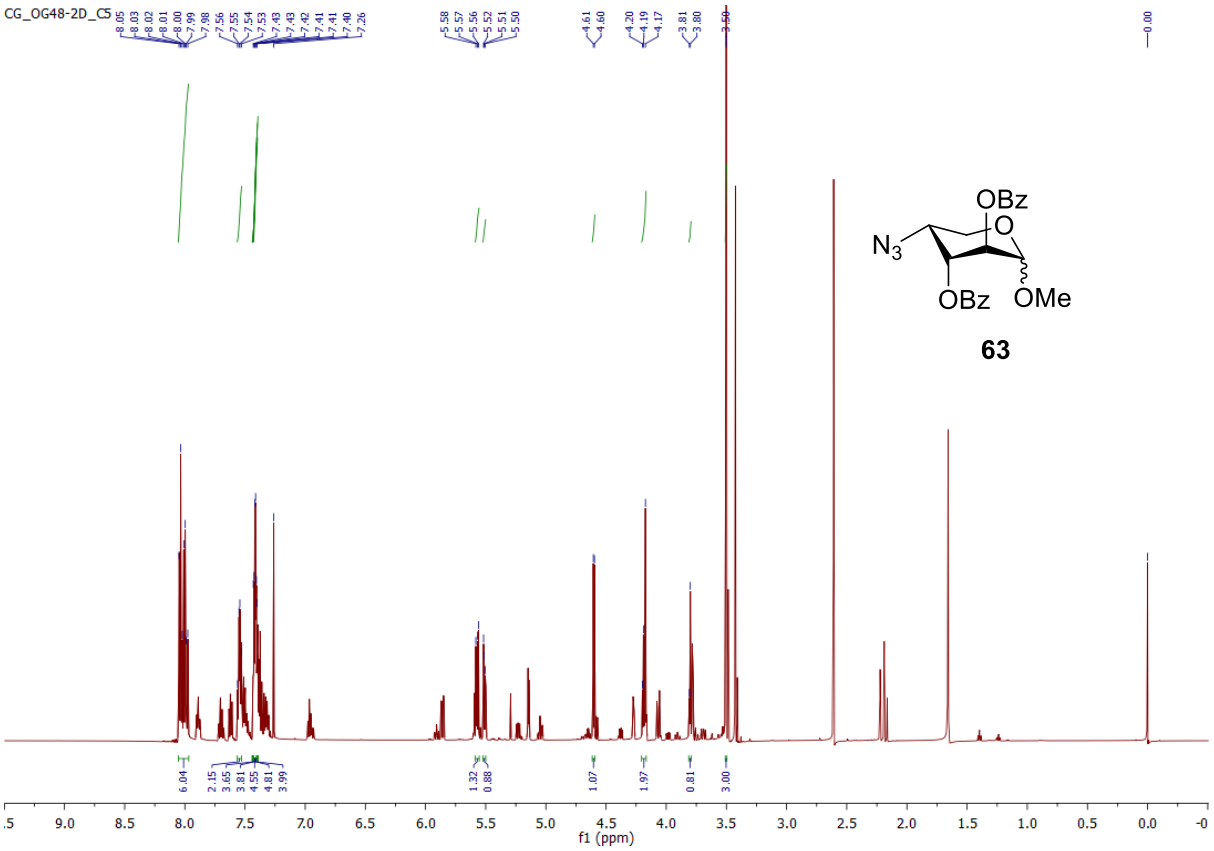

Supplementary Figure 49. ^{13}C NMR spectrum ($CDCl_3$, 100 MHz) of compound 63

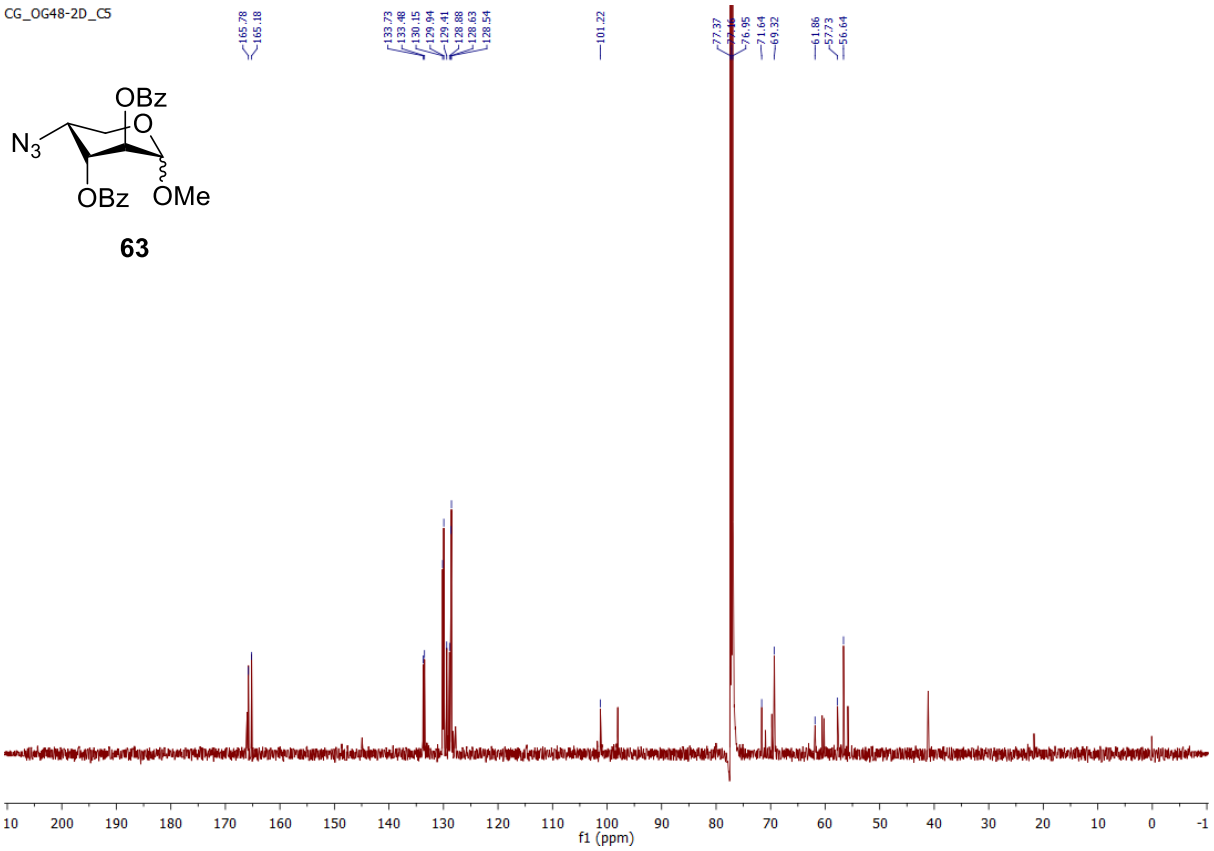

Supplementary Figure 50. COSY NMR spectrum ($CDCl_3$, 600 MHz) of compound 63

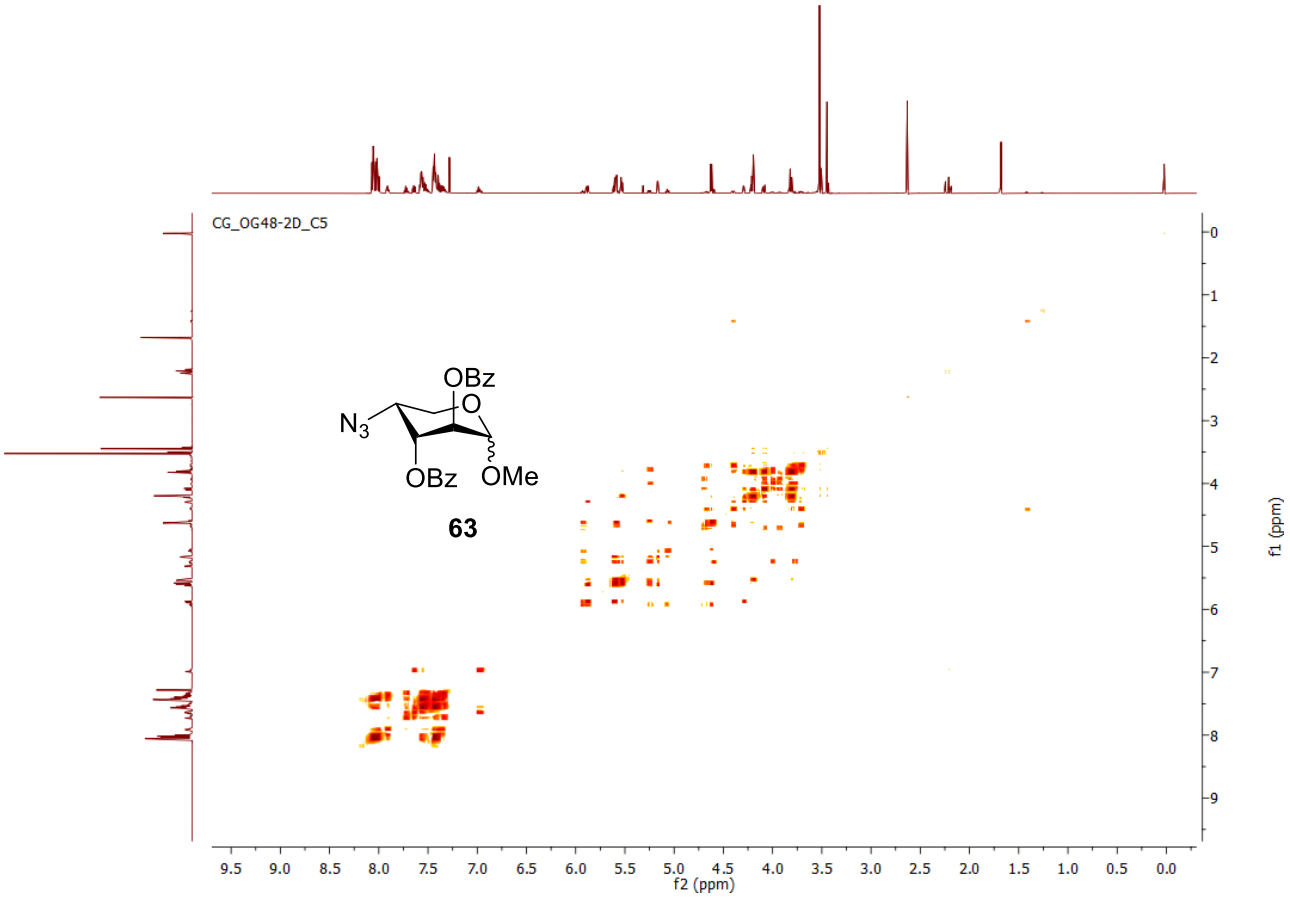

Supplementary Figure 51. HSQC NMR spectrum ($CDCl_3$, 600 MHz) of compound 63

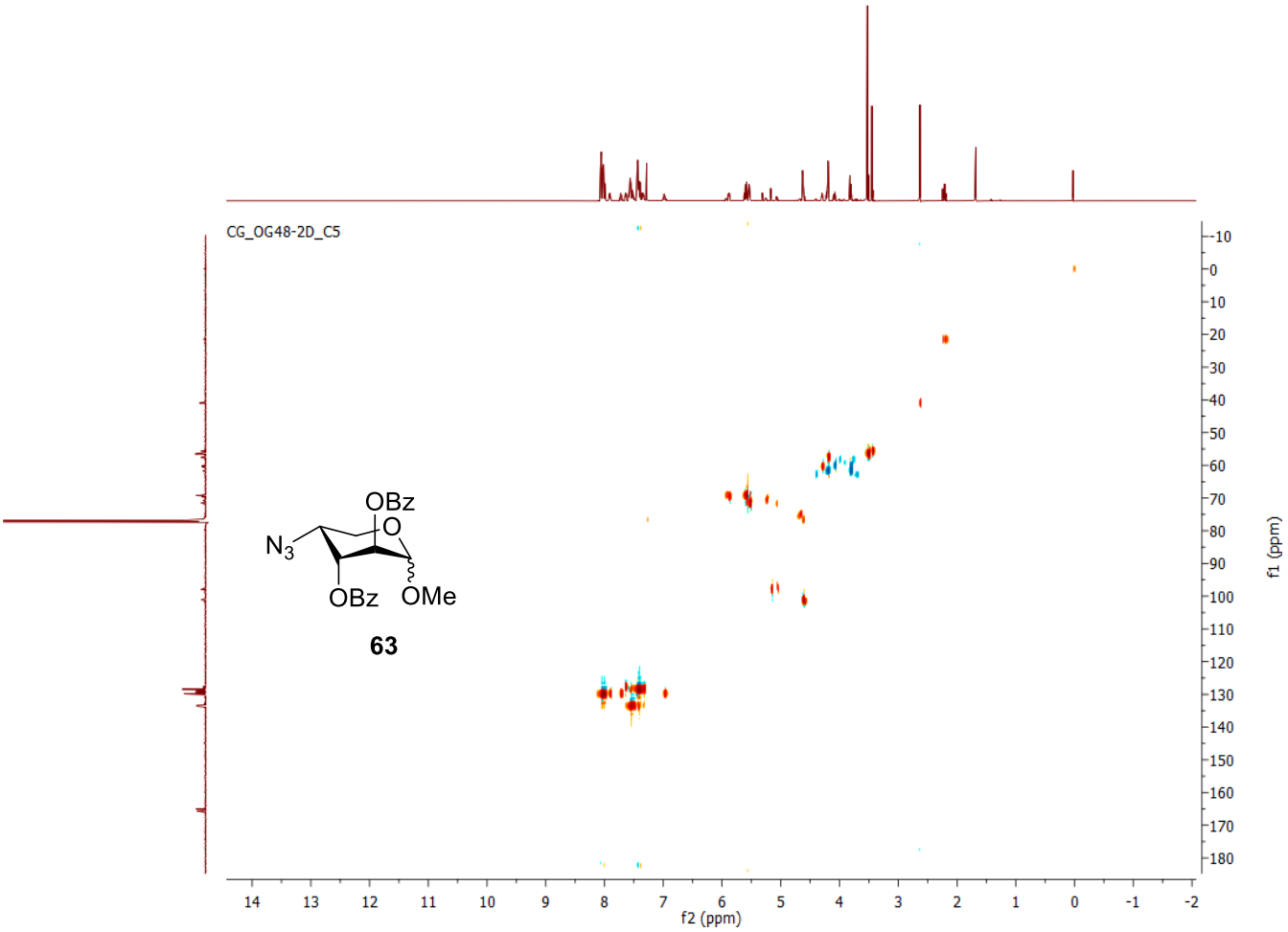

Supplementary Figure 52. ^{1}H NMR spectrum (D_2O, 600 MHz) of compound 64

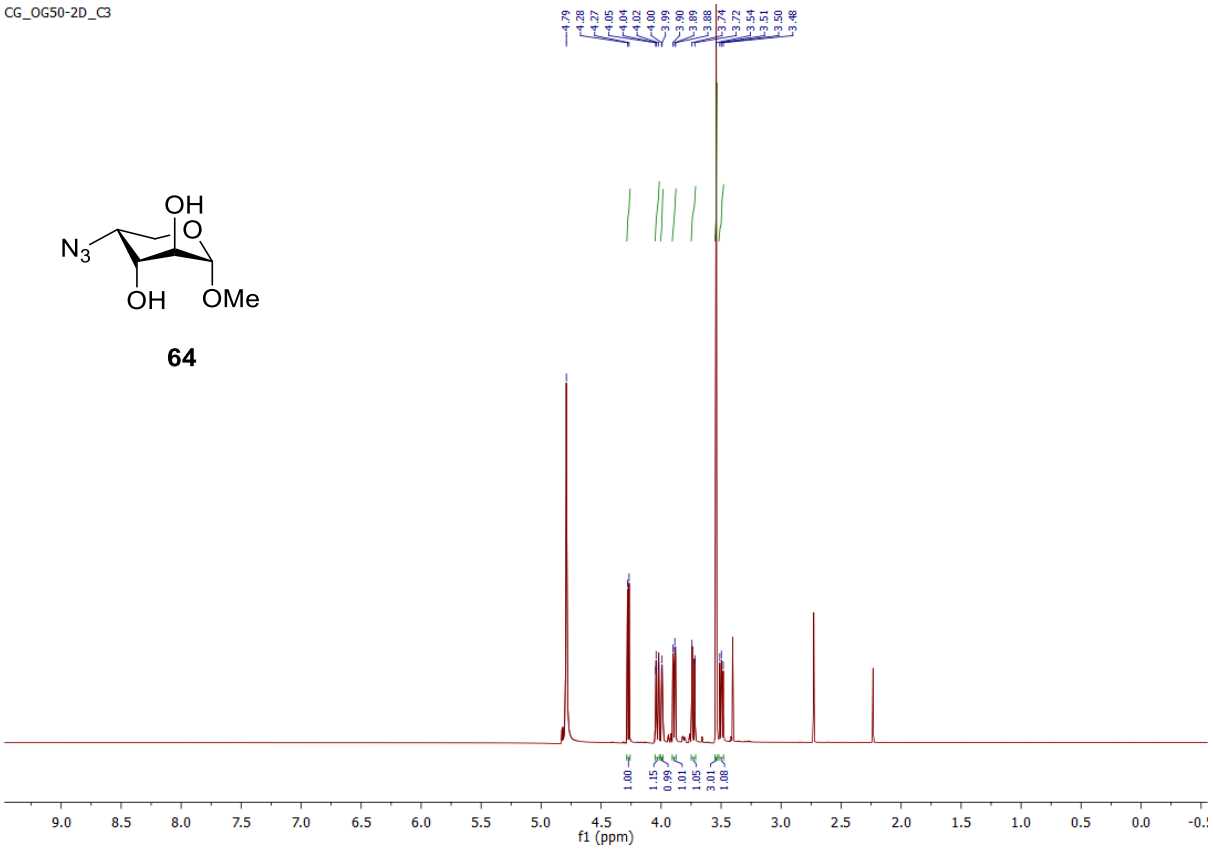

Supplementary Figure 53. ^{13}C NMR spectrum (D_2O, 100 MHz) of compound 64

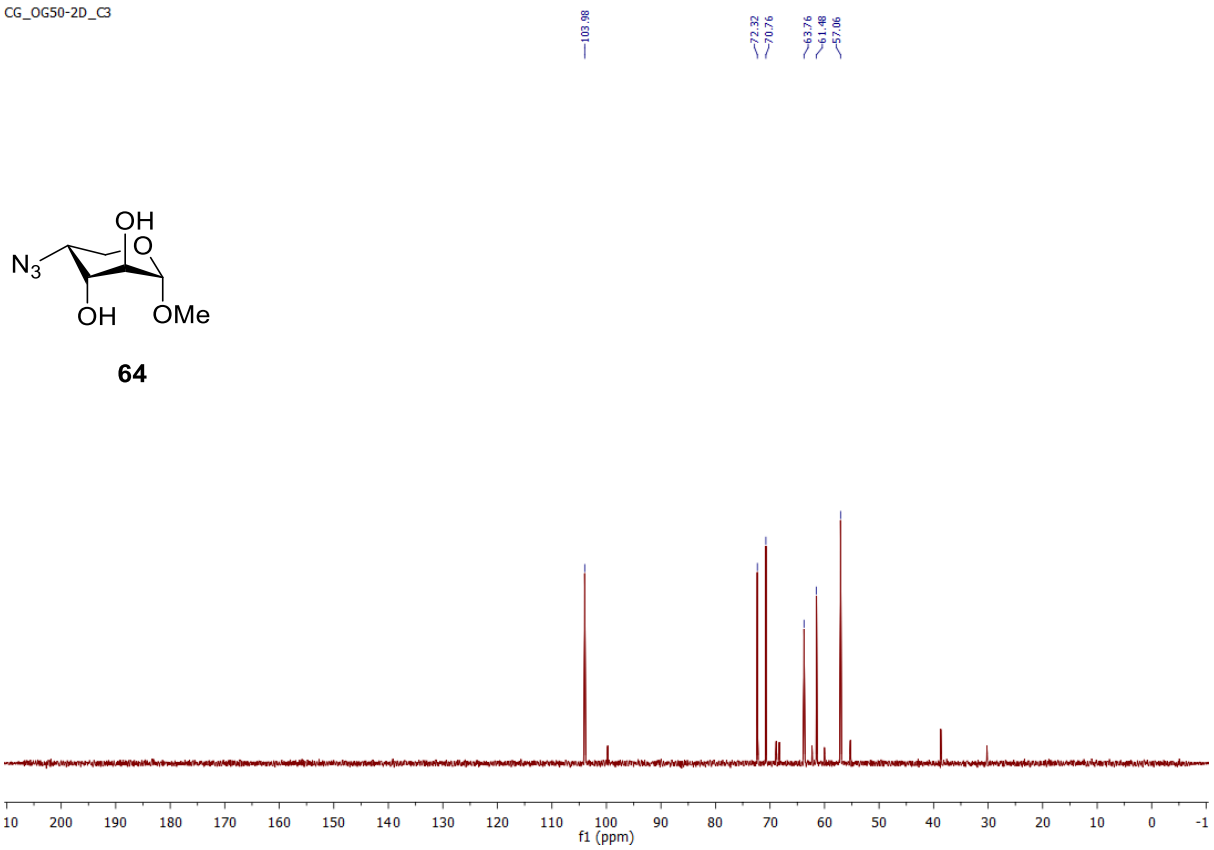

Supplementary Figure 54. COSY NMR spectrum (D_2O, 600 MHz) of compound 64

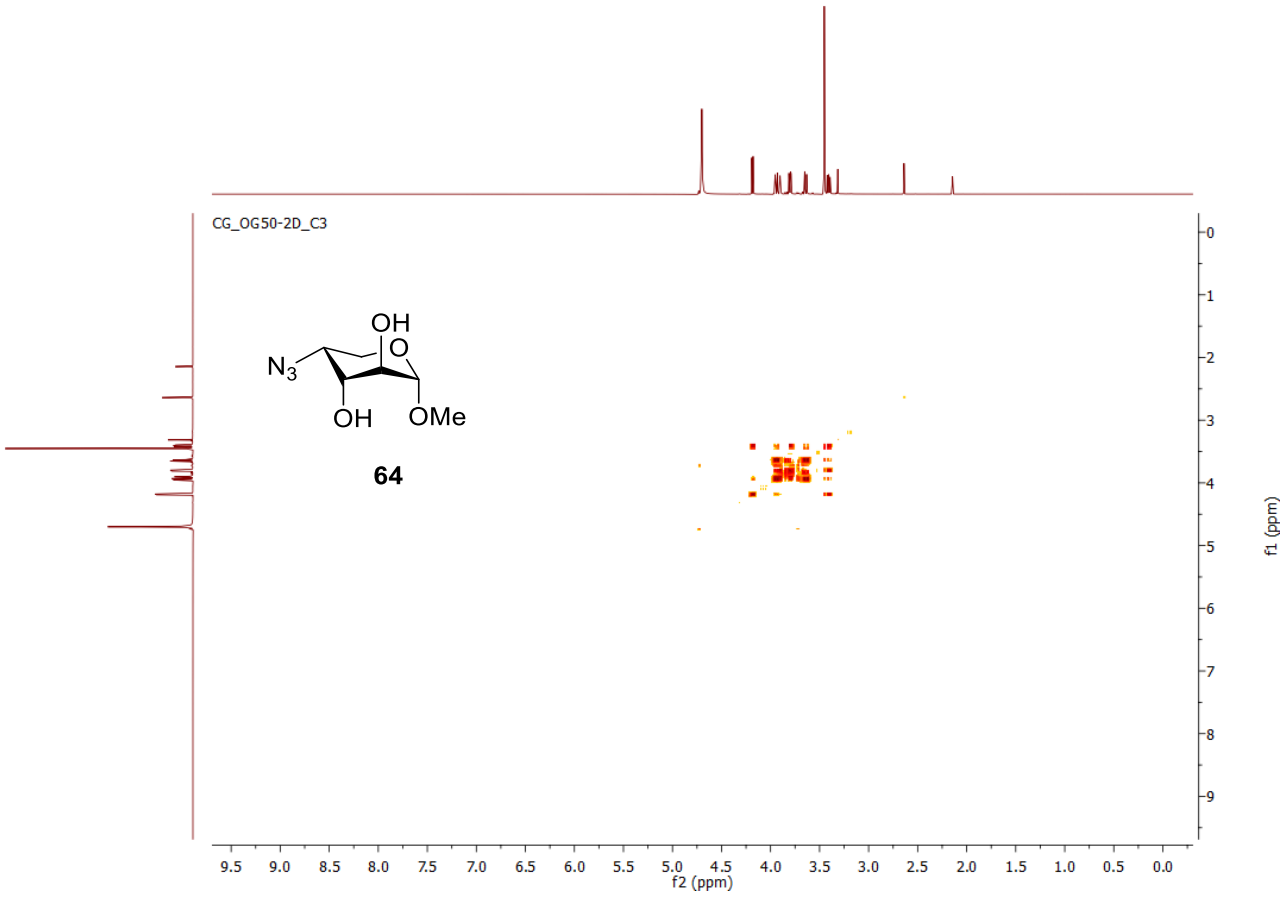

Supplementary Figure 55. HSQC NMR spectrum (D_2O, 600 MHz) of compound 64

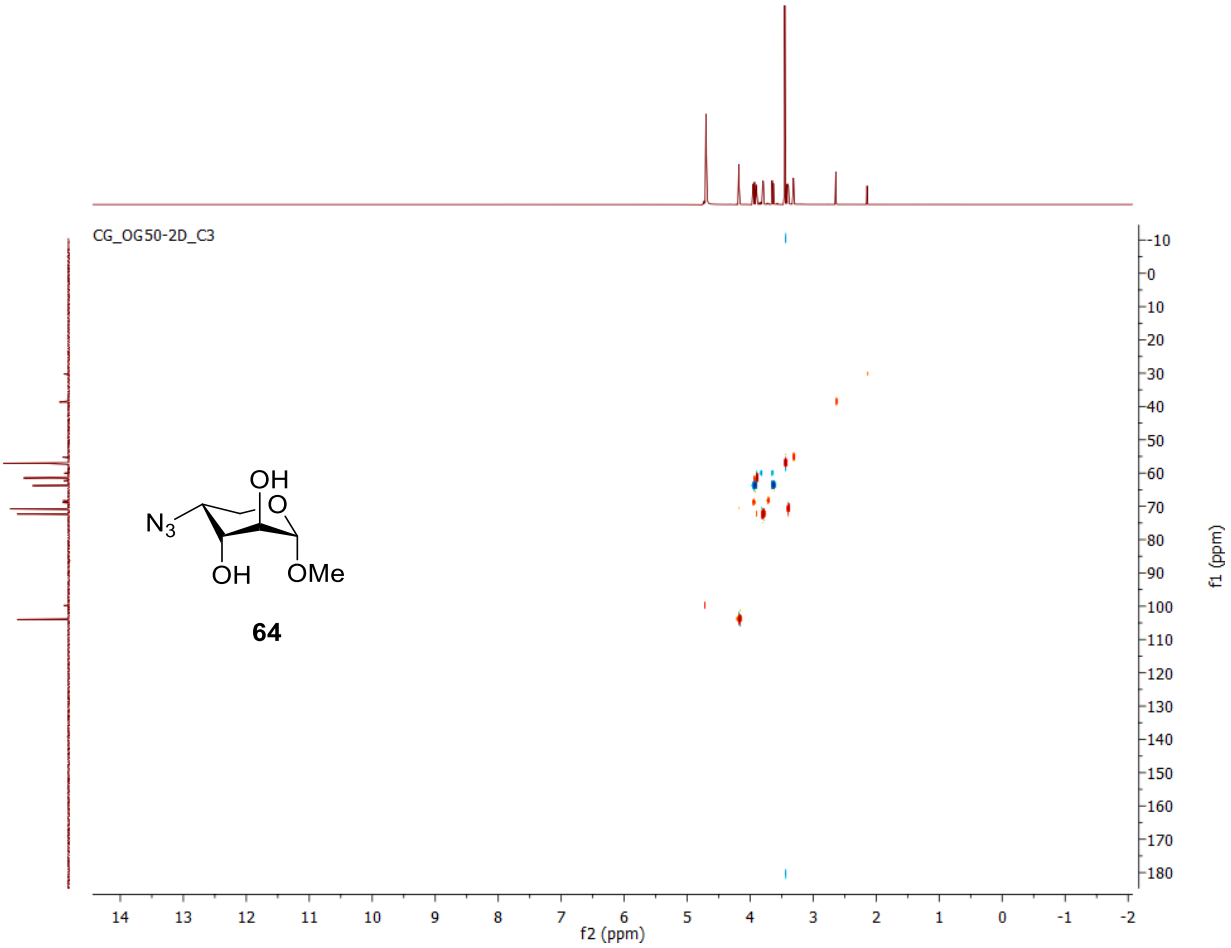

Supplementary Figure 56. ^{1}H NMR spectrum ($CDCl_3$, 600 MHz) of compound 65

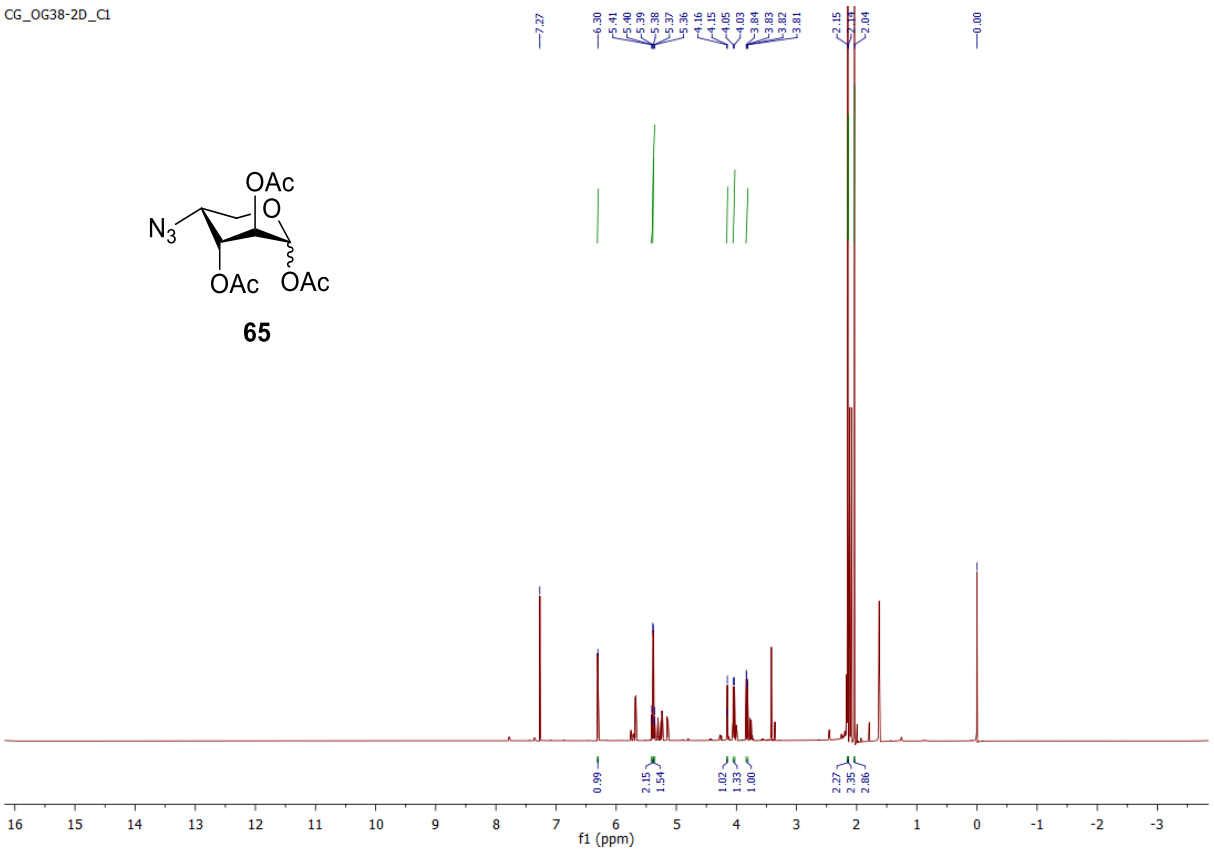

Supplementary Figure 57. ^{13}C NMR spectrum ($CDCl_3$, 100 MHz) of compound 65

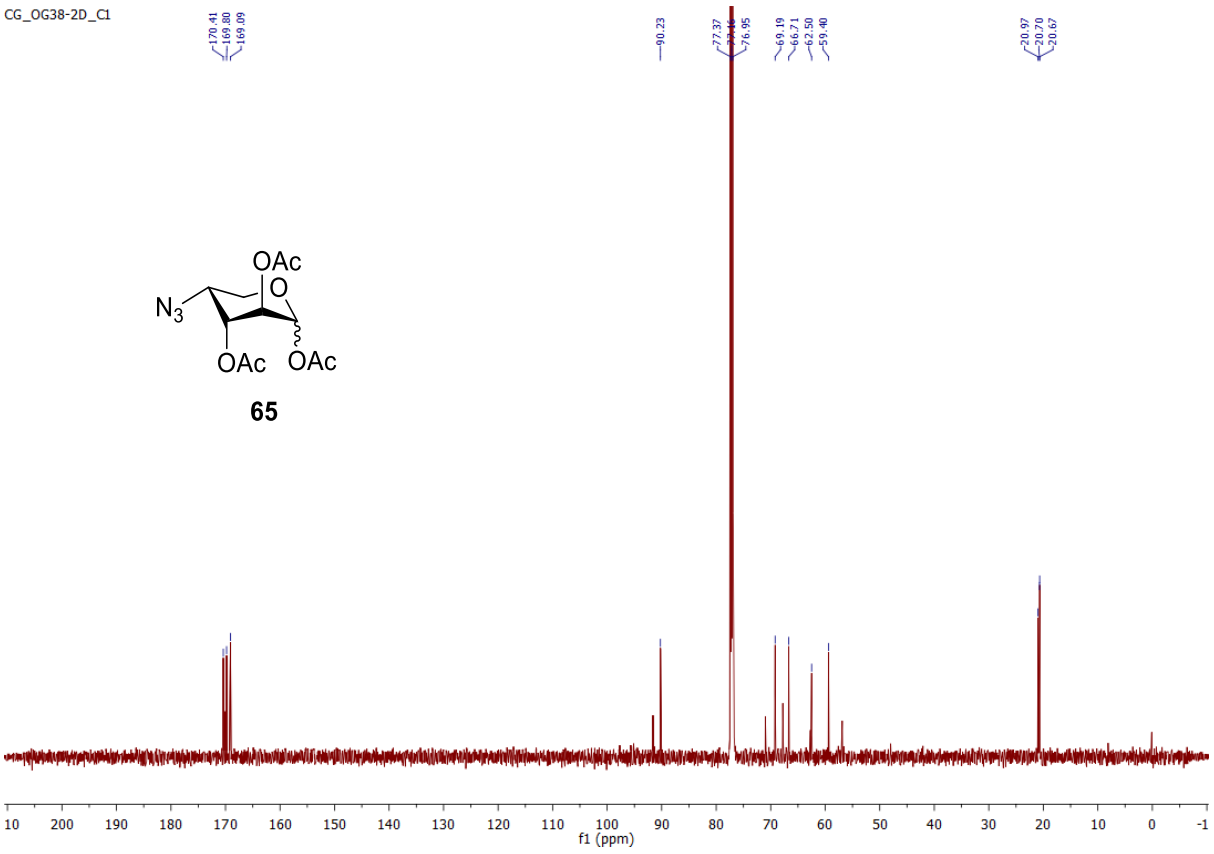

Supplementary Figure 58. COSY NMR spectrum ($CDCl_3$, 600 MHz) of compound 65

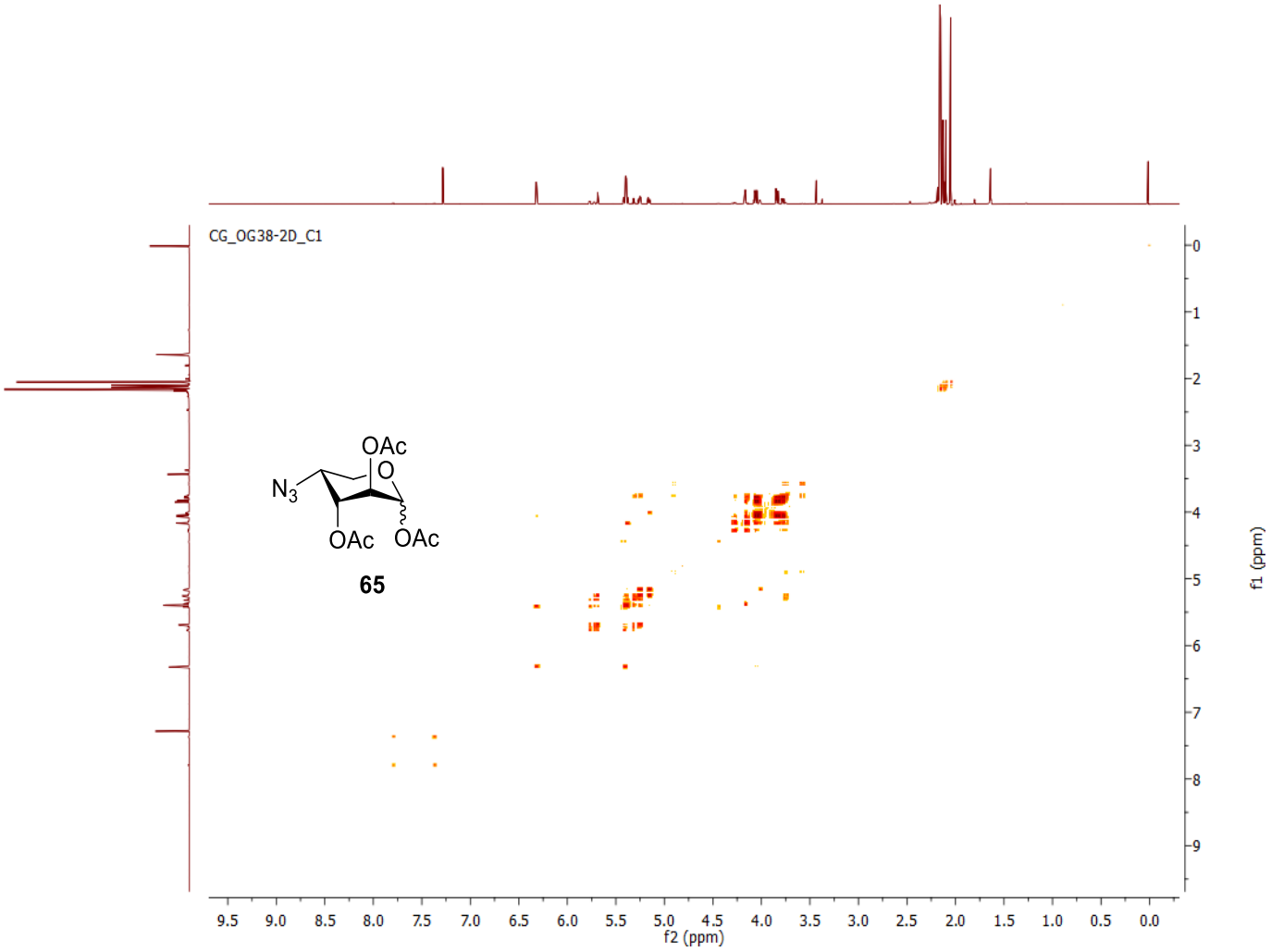

Supplementary Figure 59. HSQC NMR spectrum ($CDCl_3$, 600 MHz) of compound 65

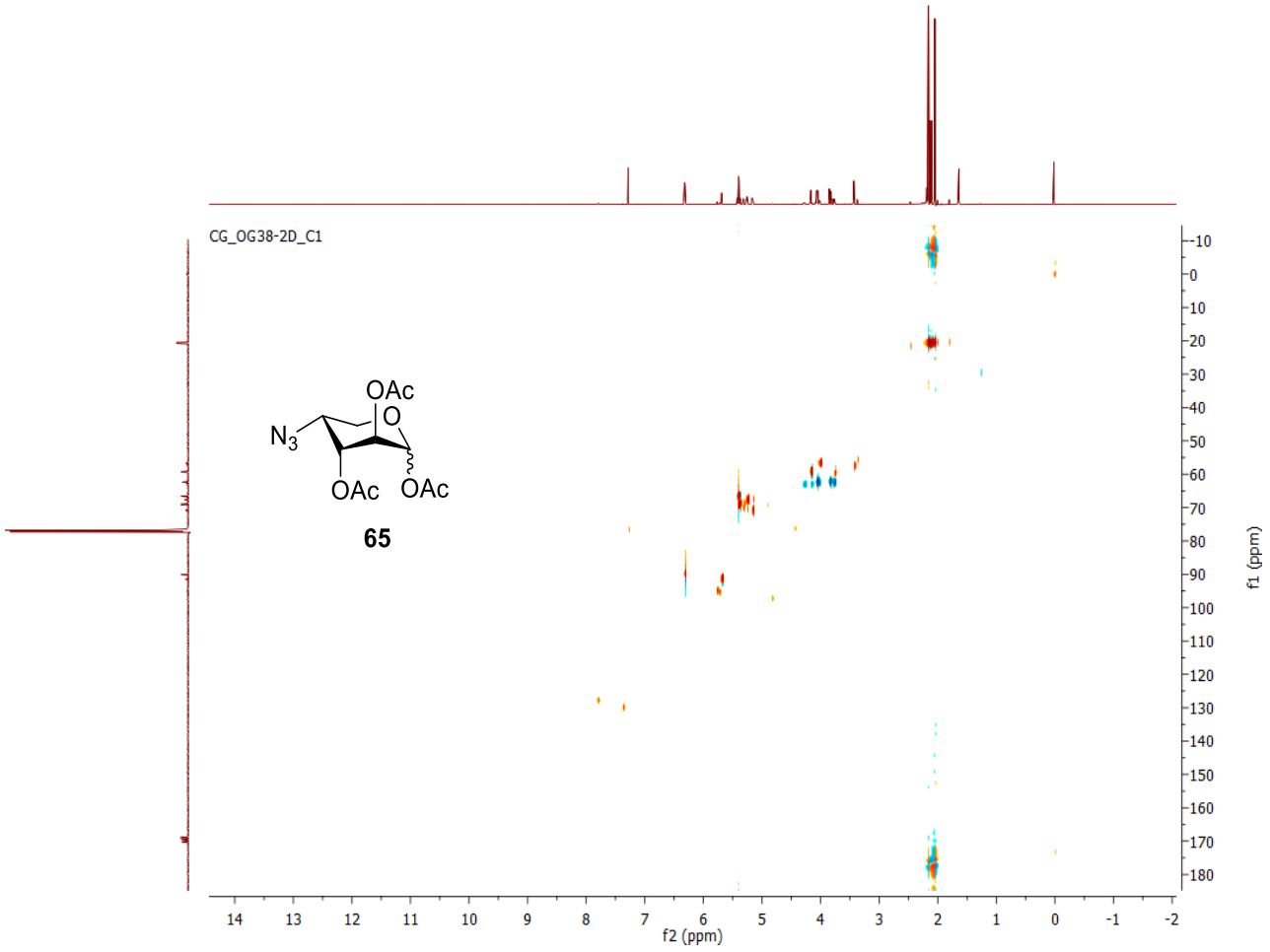

Supplementary Figure 60. ^{1}H NMR spectrum (D_2O, 600 MHz) of compound 66

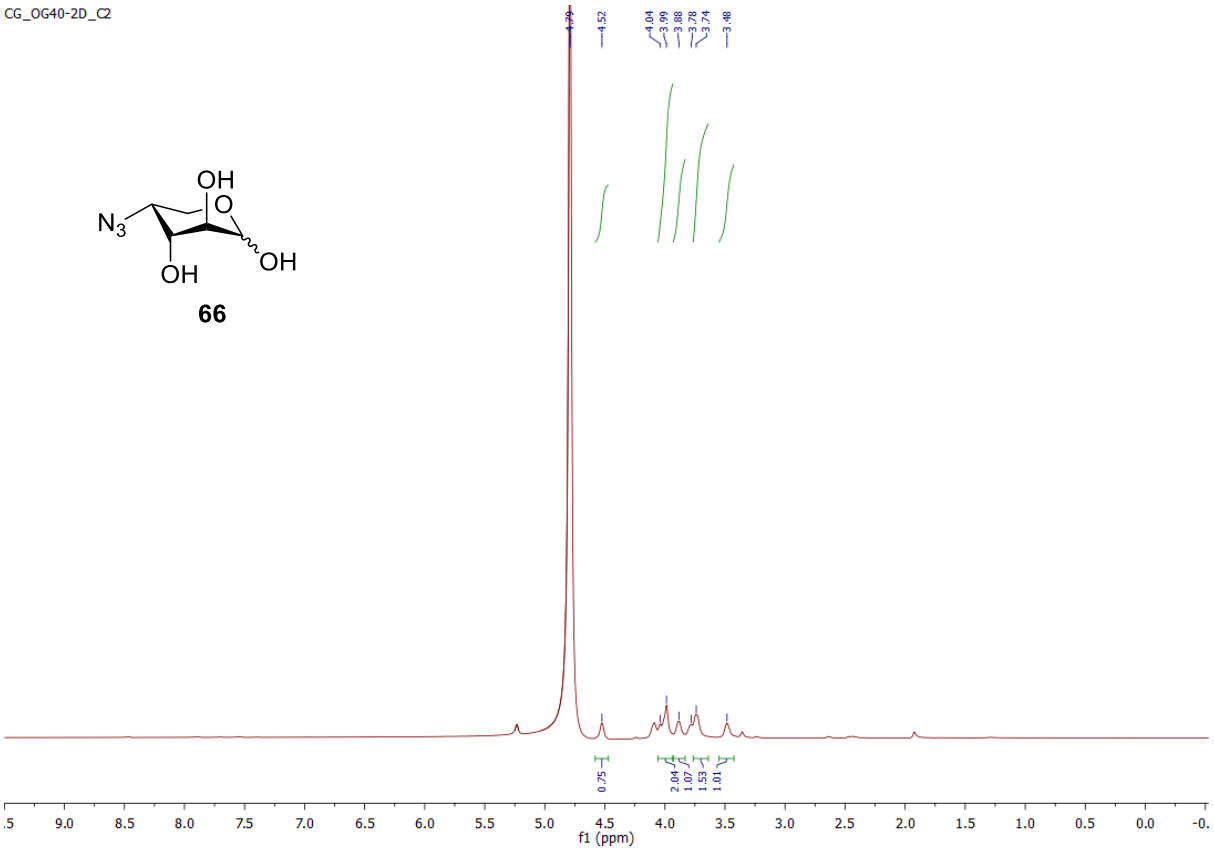

Supplementary Figure 61. ^{13}C NMR spectrum (D_2O, 100 MHz) of compound 66

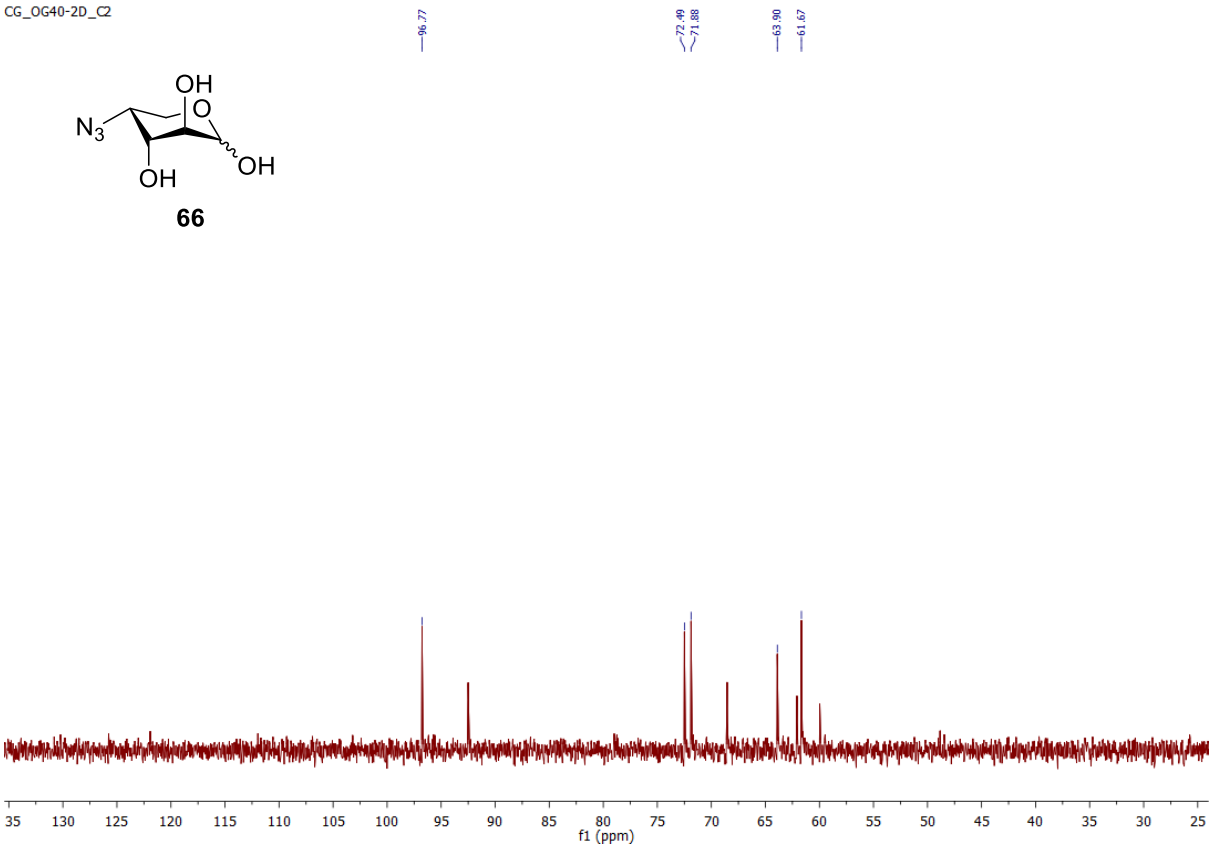

Supplementary Figure 62. COSY NMR spectrum (D_2O, 600 MHz) of compound 66

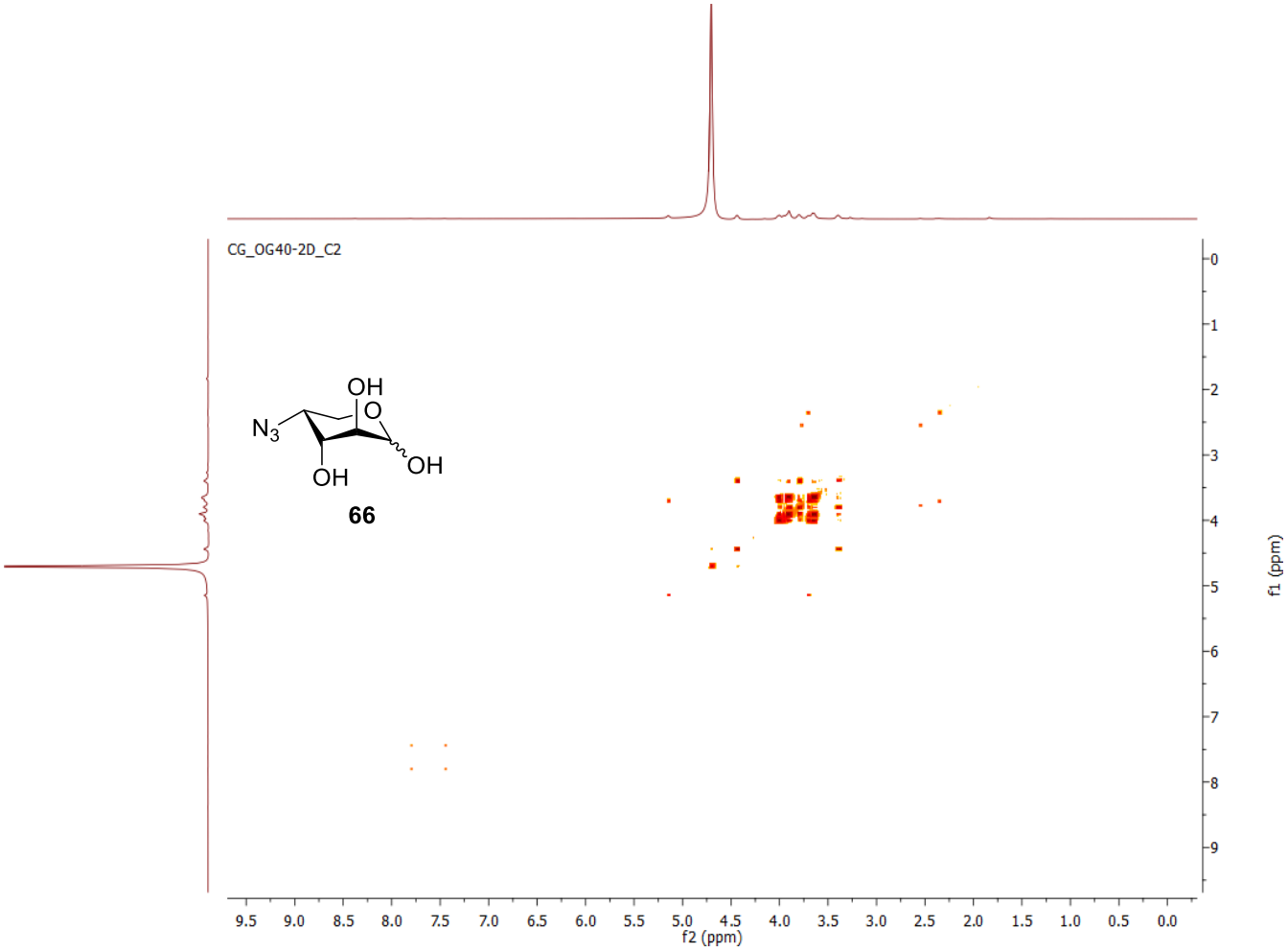

Supplementary Figure 63. HSQC NMR spectrum (D_2O, 600 MHz) of compound 66

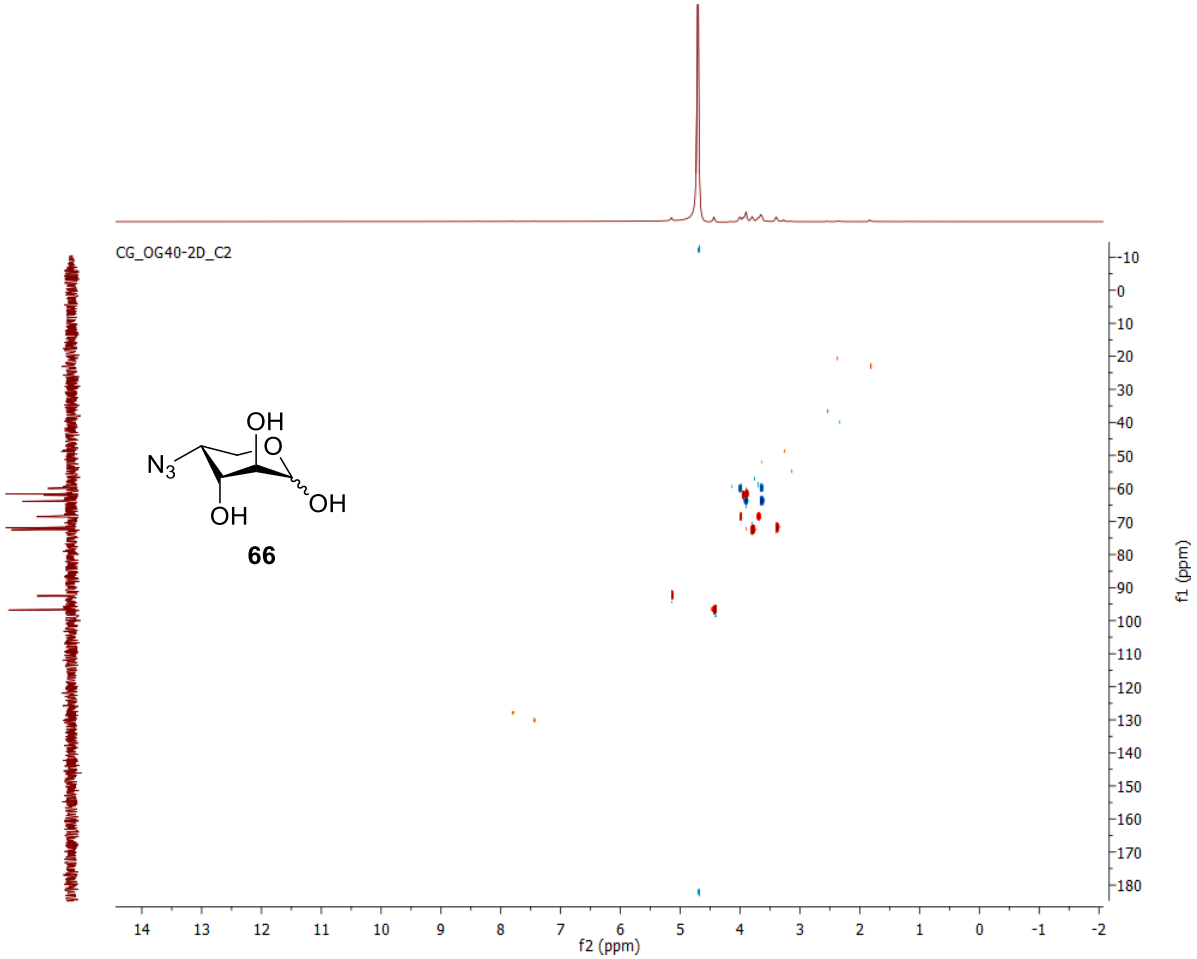

Supplementary Figure 64. ^{1}H NMR spectrum (D_2O, 600 MHz) of compound 67

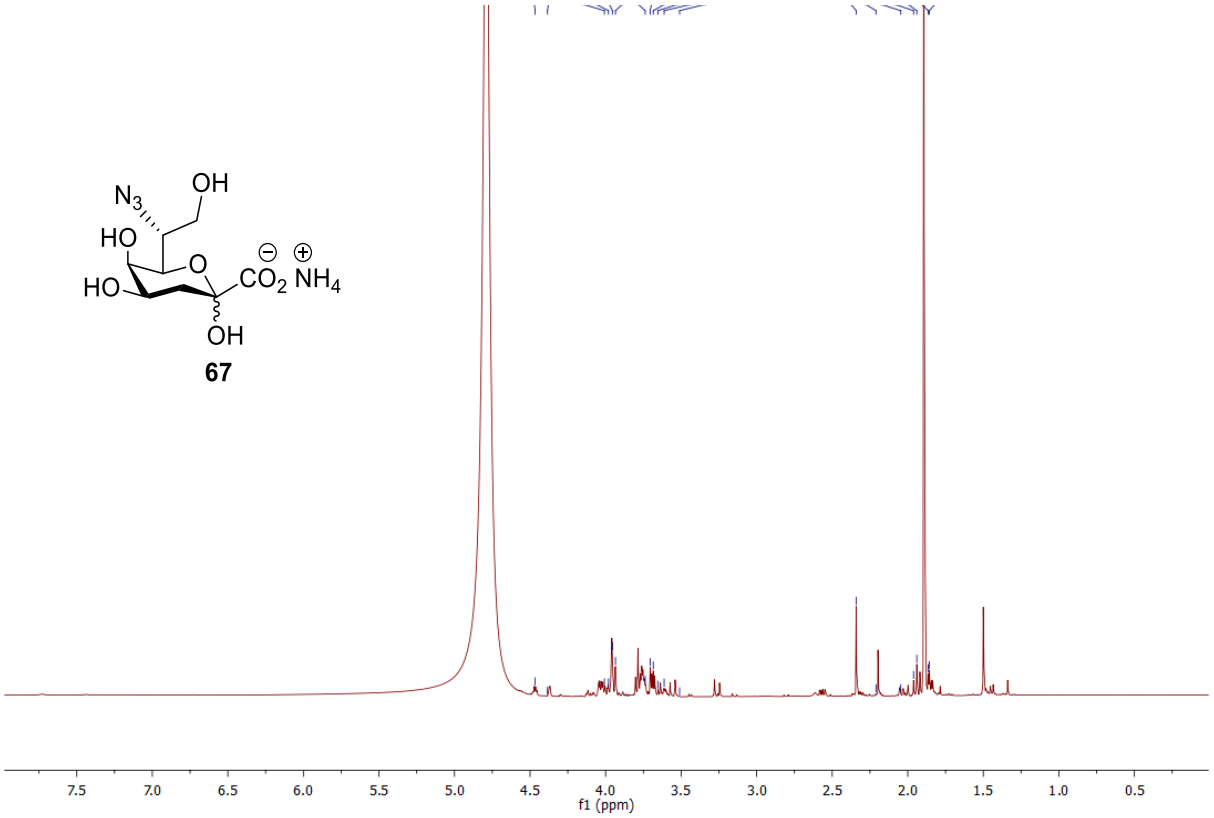

Supplementary Figure 65. ^{13}C NMR spectra (D_2O, 100 MHz) of compound 67

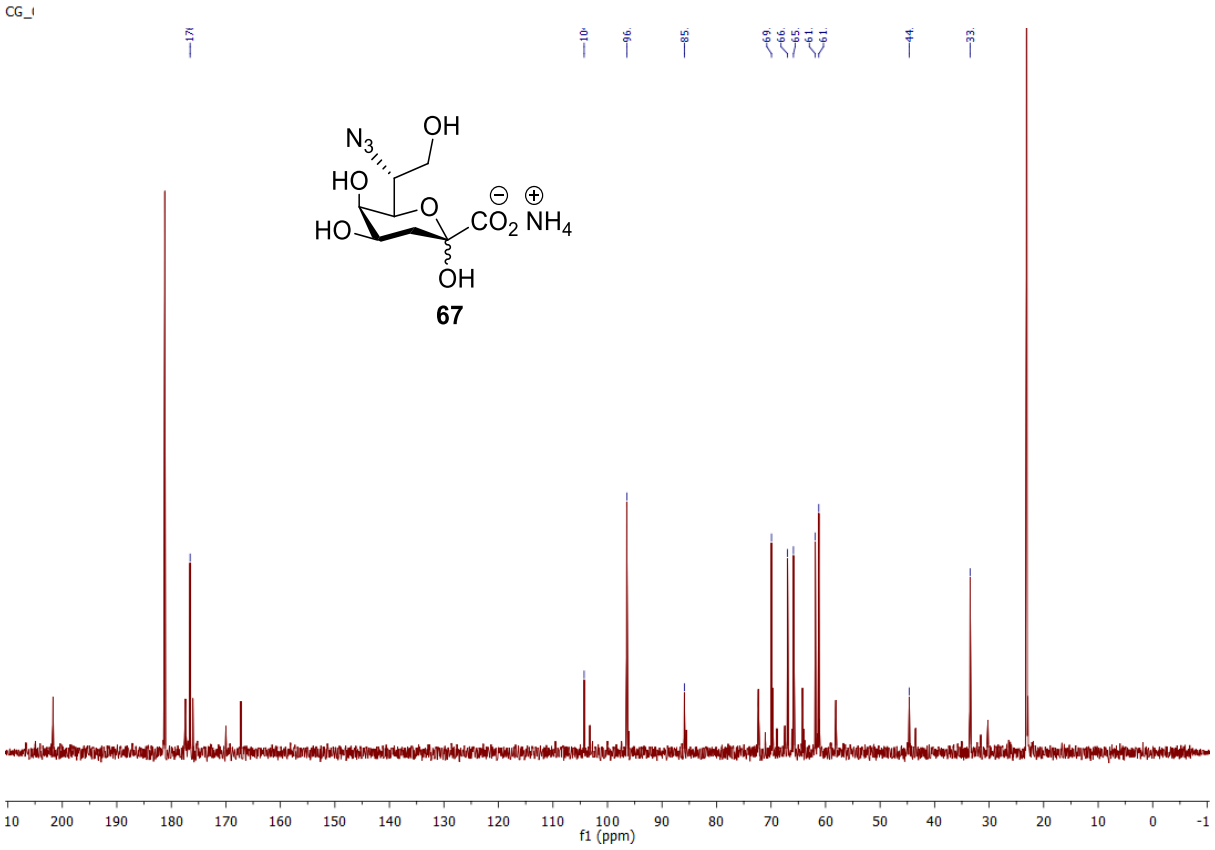

5. References

[1] C. R. Woese, O. Kandler and M. L. Wheelis, *Proc Natl Acad Sci U S A* **1990**, *87*, 4576-4579.

[2] J. H. Kavouras, *Journal of Microbiology & Biology Education* **2011**, *12*.

[3] N. R. Pace, *Science* **1997**, *276*, 734-740.

[4] C. R. Strachan and J. Davies, *J Ind Microbiol Biotechnol* **2016**, *43*, 149-153.

[5] H. Yoneyama and R. Katsumata, *Bioscience, Biotechnology, and Biochemistry* **2006**, *70*, 1060-1075.

[6] J. Davies, *Mol Microbiol* **1990**, *4*, 1227-1232.

[7] R. I. Aminov, *Frontiers in microbiology* **2010**, *1*, 134-134.

[8] R. I. Aminov, *Environ Microbiol* **2009**, *11*, 2970-2988.

[9] R. C. MacLean and A. San Millan, *Science* **2019**, *365*, 1082.

[10] E. Martens and A. L. Demain, *The Journal of Antibiotics* **2017**, *70*, 520-526.

[11] J. E. Davies, *Microbiologia* **1996**, *12 1*, 9-16.

[12] H. I. Zgurskaya, C. A. Lopez and S. Gnanakaran, *ACS Infect Dis* **2015**, *1*, 512-522.

[13] A. Dumont, A. Malleron, M. Awwad, S. Dukan and B. Vauzeilles, *Angewandte Chemie International Edition* **2012**, *51*, 3143-3146.

[14] W. Vollmer, D. Blanot and M. A. de Pedro, *FEMS Microbiol Rev* **2008**, *32*, 149-167.

[15] C. Whitfield and M. S. Trent, *Annu Rev Biochem* **2014**, *83*, 99-128.

[16] T. J. Silhavy, D. Kahne and S. Walker, *Cold Spring Harb Perspect Biol* **2010**, *2*, a000414.

[17] K. Luthman, M. Orbe, T. Waglund and A. Claesson, *The Journal of Organic Chemistry* **1987**, *52*, 3777-3784.

[18] C. R. H. Raetz and C. Whitfield, *Annual review of biochemistry* **2002**, *71*, 635-700.

[19] E. T. Rietschel, T. Kirikae, F. U. Schade, U. Mamat, G. Schmidt, H. Loppnow, A. J. Ulmer, U. Zahringer, U. Seydel, F. Di Padova and et al., *FASEB J* **1994**, *8*, 217-225.

[20] X. Li, Y. Gu, H. Dong, W. Wang and C. Dong, *Scientific Reports* **2015**, *5*, 11883.

[21] E. T. Rietschel, T. Kirikae, F. U. Schade, A. J. Ulmer, O. Holst, H. Brade, G. Schmidt, U. Mamat, H. D. Grimmecke, S. Kusumoto and et al., *Immunobiology* **1993**, *187*, 169-190.

[22] a) Y. Zhang, J. Gaekwad, M. A. Wolfert and G.-J. Boons, *Chemistry (Weinheim an der Bergstrasse, Germany)* **2008**, *14*, 558-569; b) J. P. van Putten, *The EMBO Journal* **1993**, *12*, 4043-4051; c) J. A. Yethon and C. Whitfield, *Curr Drug Targets Infect Disord* **2001**, *1*, 91-106.

[23] S. Müller-Loennies, B. Lindner and H. Brade, *The Journal of biological chemistry* **2003**, *278*, 34090-34101.

[24] a) S. Muller-Loennies, B. Lindner and H. Brade, *J Biol Chem* **2003**, *278*, 34090-34101; b) E. V. Vinogradov, K. van der Drift, J. E. Thomas-Oates, S. Meshkov, H. Brade and O. Holst, *European Journal of Biochemistry* **1999**, *261*, 629-639.

[25] a) O. Holst, A. J. Ulmer, H. Brade, H.-D. Flad and E. T. Rietschel, *Pathogens and Disease* **1996**, *16*, 83-104; b) S. Müller-Loennies, B. Lindner and H. Brade, *European Journal of Biochemistry* **2002**, *269*, 5982-5991.

[26] S. Fadel and A. Eley, *J Med Microbiol* **2008**, *57*, 261-266.

[27] S. G. Gattis, H. S. Chung, M. S. Trent and C. R. H. Raetz, *The Journal of biological chemistry* **2013**, *288*, 9216-9225.

[28] O. Holst, *FEMS Microbiology Letters* **2007**, *271*, 3-11.

[29] R. Vuorio and M. Vaara, *Antimicrobial agents and chemotherapy* **1992**, *36*, 826-829.

[30] U. Seydel, H. Labischinski, M. Kastowsky and K. Brandenburg, *Immunobiology* **1993**, *187*, 191-211.

[31] C. R. Raetz, *Journal of bacteriology* **1993**, *175*, 5745-5753.

[32] P. Plesiat and H. Nikaido, *Mol Microbiol* **1992**, *6*, 1323-1333.

[33] A. D. Elbein and E. C. Heath, *J Biol Chem* **1965**, *240*, 1926-1931.

[34] L. Cipolla, L. Gabrielli, D. Bini, L. Russo and N. Shaikh, *Natural Product Reports* **2010**, *27*, 1618-1629.

[35] A. M. Gil-Serrano, M. A. Í.-C. Rodr, P. Tejero-Mateo, J. L. Espartero, J. Thomas-Oates, J. E. Ruiz-Sainz and A. M. Í.-C. Buend, *Biochemical Journal* **1998**, *334*, 585-594.

[36] Y. A. Knirel, N. A. Kocharova, A. S. Shashkov, N. K. Kochetkov, V. A. Mamontova and T. F. Solov'eva, *Carbohydrate Research* **1989**, *188*, 145-155.

[37] T. Angata and A. Varki, *Chemical Reviews* **2002**, *102*, 439-470.

[38] a) N. Yuki, *Cellular and Molecular Life Sciences CMLS* **2000**, *57*, 527-533; b) M. P. Glode, A. Sutton, J. B. Robbins, G. H. McCracken, E. C. Gotschlich, B. Kaijser and L. A. Hanson, *J Infect Dis* **1977**, *136 Suppl*, S93-97.

[39] G. Reuter and H. J. Gabius, *Biol Chem Hoppe Seyler* **1996**, *377*, 325-342.

[40] L. Cipolla, A. Polissi, C. Airoldi, L. Gabrielli, S. Merlo and F. Nicotra, *Curr Med Chem* **2011**, *18*, 830-852.

[41] S.-S. Chng, L. S. Gronenberg and D. Kahne, *Biochemistry* **2010**, *49*, 4565-4567.

[42] L. M. Willis and C. Whitfield, *Proc Natl Acad Sci U S A* **2013**, *110*, 20753-20758.

[43] R. C. Goldman and E. M. Devine, *Journal of Bacteriology* **1987**, *169*, 5060.

[44] C. Laura, A. Cristina, G. Paolo, P. Alessandra and N. Francesco, *Current Organic Chemistry* **2008**, *12*, 576-600.

[45] P. H. Ray, J. E. Kelsey, E. C. Bigham, C. D. Benedict and T. A. Miller in *Synthesis and Use of 3-Deoxy-D-manno-2-octulosonate (KDO) in Escherichia coli*, *Vol. 231* AMERICAN CHEMICAL SOCIETY, **1983**, pp. 141-169.

[46] G. D. Dotson, R. K. Dua, J. C. Clemens, E. W. Wooten and R. W. Woodard, *Journal of Biological Chemistry* **1995**, *270*, 13698-13705.

[47] J. Wu and R. W. Woodard, *Journal of Biological Chemistry* **2003**, *278*, 18117-18123.

[48] R. C. Goldman, T. J. Bolling, W. E. Kohlbrenner, Y. Kim and J. L. Fox, *J Biol Chem* **1986**, *261*, 15831-15835.

[49] R. C. Goldman and W. E. Kohlbrenner, *Journal of bacteriology* **1985**, *163*, 256-261.

[50] R. C. Goldman, T. Bolling, W. Kohlbrenner, Y. Kim and J. L. Fox, *Journal of Biological Chemistry* **1986**, *261*, 15831-15835.

[51] A. Claesson, K. Luthman, K. Gustafsson and G. Bondesson, *Biochemical and biophysical research communications* **1987**, *143*, 1063-1068.

[52] a) S. M. Hammond, A. Claesson, A. M. Jansson, L.-G. Larsson, B. G. Pring, C. M. Town and B. Ekström, *Nature* **1987**, *327*, 730-732; b) R. Goldman, W. Kohlbrenner, P. Lartey and A. Pernet, *Nature* **1987**, *329*, 162-164.

[53] R. C. Hider and X. Kong, *Nat Prod Rep* **2010**, *27*, 637-657.

[54] J. B. Neilands, *Journal of Biological Chemistry* **1995**, *270*, 26723-26726.

[55] V. Braun and H. Killmann, *Trends in Biochemical Sciences* **1999**, *24*, 104-109.

[56] M. L. Guerinot, *Annu Rev Microbiol* **1994**, *48*, 743-772.

[57] G. Schwarzenbach and K. Schwarzenbach, *Helvetica Chimica Acta* **1963**, *46*, 1390-1400.

[58] K. N. Raymond and C. J. Carrano, *Accounts of Chemical Research* **1979**, *12*, 183-190.

[59] U. Möllmann, L. Heinisch, A. Bauernfeind, T. Köhler and D. Ankel-Fuchs, *BioMetals* **2009**, *22*, 615-624.

[60] S. C. Andrews, A. K. Robinson and F. Rodríguez-Quiñones, *FEMS Microbiology Reviews* **2003**, *27*, 215-237.

[61] A. Gorska, A. Sloderbach and M. P. Marszall, *Trends Pharmacol Sci* **2014**, *35*, 442-449.

[62] K. D. Krewulak and H. J. Vogel, *Biochimica et Biophysica Acta (BBA) - Biomembranes* **2008**, *1778*, 1781-1804.

[63] M. Miethke and M. A. Marahiel in *Siderophore-based iron acquisition and pathogen control. Microbiol Mol Biol Rev71: 413–451*, *Vol.* **2007**.

[64] A. D. Ferguson, J. W. Coulton, K. Diederichs, W. Welte, V. Braun and H.-P. Fiedler, *Protein Science* **2000**, *9*, 956-963.

[65] J. Lubelski, W. N. Konings and A. J. M. Driessen, *Microbiology and Molecular Biology Reviews* **2007**, *71*, 463.

[66] V. Braun, A. Pramanik, T. Gwinner, M. Köberle and E. Bohn, *BioMetals* **2009**, *22*, 3.

[67] K. Schauer, D. A. Rodionov and H. de Reuse, *Trends in Biochemical Sciences* **2008**, *33*, 330-338.

[68] B. Mathieu, C. Pierre and B. Christine, *Recent Patents on Anti-Infective Drug Discovery* **2009**, *4*, 190-205.

[69] a) C. C. C. R. de Carvalho and P. Fernandes, *Frontiers in microbiology* **2014**, *5*, 290-290; b) T. A. Wencewicz, U. Mollmann, T. E. Long and M. J. Miller, *Biometals* **2009**, *22*, 633-648.

[70] a) T. Aoki, H. Yoshizawa, K. Yamawaki, K. Yokoo, J. Sato, S. Hisakawa, Y. Hasegawa, H. Kusano, M. Sano, H. Sugimoto, Y. Nishitani, T. Sato, M. Tsuji, R. Nakamura, T. Nishikawa and Y. Yamano, *Eur J Med Chem* **2018**, *155*, 847-868; b) S. Portsmouth, D. van Veenhuyzen, R. Echols, M. Machida, J. C. A. Ferreira, M. Ariyasu, P. Tenke and T. D. Nagata, *The Lancet Infectious Diseases* **2018**, *18*, 1319-1328.

[71] P. Klahn and M. Bronstrup, *Nat Prod Rep* **2017**, *34*, 832-885.

[72] R. Codd, T. Richardson-Sanchez, T. J. Telfer and M. P. Gotsbacher, *ACS Chemical Biology* **2018**, *13*, 11-25.

[73] A. T. Butt and M. S. Thomas, *Front Cell Infect Microbiol* **2017**, *7*, 460.

[74] W. Neumann and E. M. Nolan, *J Biol Inorg Chem* **2018**, *23*, 1025-1036.

[75] A. Brezden, M. F. Mohamed, M. Nepal, J. S. Harwood, J. Kuriakose, M. N. Seleem and J. Chmielewski, *Journal of the American Chemical Society* **2016**, *138*, 10945-10949.

[76] C. F. Riber, A. A. A. Smith and A. N. Zelikin, *Advanced Healthcare Materials* **2015**, *4*, 1887-1890.

[77] A. K. Ghosh and M. Brindisi, *J Med Chem* **2015**, *58*, 2895-2940.

[78] T. Memanishvili, N. Zavradashvili, N. Kupatadze, D. Tugushi, M. Gverdtsiteli, V. P. Torchilin, C. Wandrey, L. Baldi, S. S. Manoli and R. Katsarava, *Biomacromolecules* **2014**, *15*, 2839-2848.

[79] Y. Amano, N. Umezawa, S. Sato, H. Watanabe, T. Umehara and T. Higuchi, *Bioorganic & Medicinal Chemistry* **2017**, *25*, 1227-1234.

[80] J. Liu, D. Obando, L. G. Schipanski, L. K. Groebler, P. K. Witting, D. S. Kalinowski, D. R. Richardson and R. Codd, *J Med Chem* **2010**, *53*, 1370-1382.

[81] M. B. Jones, H. Teng, J. K. Rhee, N. Lahar, G. Baskaran and K. J. Yarema, *Biotechnol Bioeng* **2004**, *85*, 394-405.

[82] G.-J. Boons and P. Wu, *Glycobiology* **2016**, *26*, 788-788.

[83] a) M. Nimtz, V. Wray, T. Domke, B. Brenneke, S. Häussler and I. Steinmetz, *European Journal of Biochemistry* **1997**, *250*, 608-616; b) P. Cescutti, G. Impallomeni, D. Garozzo, L. Sturiale, Y. Herasimenka, C. Lagatolla and R. Rizzo, *Carbohydr Res* **2003**, *338*, 2687-2695.

[84] A. Laroussarie, B. Barycza, H. Andriamboavonjy, M. Tamigney Kenfack, Y. Blériot and C. Gauthier, *The Journal of Organic Chemistry* **2015**, *80*, 10386-10396.

[85] B. Cuzzi, Y. Herasimenka, A. Silipo, R. Lanzetta, G. Liut, R. Rizzo and P. Cescutti, *PLoS One* **2014**, *9*, e94372.

[86] P. D. Anderson and G. Bokor, *Journal of Pharmacy Practice* **2012**, *25*, 521-529.

[87] a) W. J. Wiersinga, H. S. Virk, A. G. Torres, B. J. Currie, S. J. Peacock, D. A. B. Dance and D. Limmathurotsakul, *Nature Reviews Disease Primers* **2018**, *4*, 17107; b) B. J. Currie, *Semin Respir Crit Care Med* **2015**, *36*, 111-125.

[88] J. Gilad, I. Harary, T. Dushnitsky, D. Schwartz and Y. Amsalem, *Isr Med Assoc J* **2007**, *9*, 499-503.

[89] a) A. M. Jones, M. E. Dodd and A. K. Webb, *European Respiratory Journal* **2001**, *17*, 295; b) E. Mahenthiralingam, A. Baldwin and P. Vandamme, *J Med Microbiol* **2002**, *51*, 533-538.

[90] a) M. Cloutier, K. Muru, G. Ravicoularamin and C. Gauthier, *Natural Product Reports* **2018**, *35*, 1251-1293; b) E. Mahenthiralingam, T. A. Urban and J. B. Goldberg, *Nature Reviews Microbiology* **2005**, *3*, 144-156.

[91] P. Vandamme and P. Dawyndt, *Systematic and Applied Microbiology* **2011**, *34*, 87-95.

[92] M. Mazur, B. Barycza, H. Andriamboavonjy, S. Lavoie, M. Tamigney Kenfack, A. Laroussarie, Y. Blériot and C. Gauthier, *The Journal of Organic Chemistry* **2016**, *81*, 10585-10599.

[93] a) E. M. Sletten and C. R. Bertozzi, *Accounts of Chemical Research* **2011**, *44*, 666-676; b) M. Boyce and C. R. Bertozzi, *Nature Methods* **2011**, *8*, 638-642.

[94] a) S. T. Laughlin, J. M. Baskin, S. L. Amacher and C. R. Bertozzi, *Science* **2008**, *320*, 664; b) H. C. Hang, C. Yu, D. L. Kato and C. R. Bertozzi, *Proc. Natl. Acad. Sci. U.S.A.* **2003**, *100*, 14846.

[95] a) D. H. Dube, K. Champasa and B. Wang, *Chemical Communications* **2011**, *47*, 87-101; b) M. J. Hangauer and C. R. Bertozzi, *Angew. Chem., Int. Ed.* **2008**, *47*, 2394.

[96] E. M. Sletten and C. R. Bertozzi, *Angewandte Chemie International Edition* **2009**, *48*, 6974-6998.

[97] S. R. Hanson, W. A. Greenberg and C.-H. Wong, *QSAR & Combinatorial Science* **2007**, *26*, 1243-1252.

[98] F. M. Unger in *The Chemistry and Biological Significance of 3-Deoxy-d-manno-2-Octulosonic Acid (KDO)*, *Vol. 38* Eds.: R. S. Tipson and D. Horton), Academic Press, **1981**, pp. 323-388.

[99] R. Shirai and H. Ogura, *Tetrahedron Letters* **1989**, *30*, 2263-2264.

[100] R. Cherniak, R. G. Jones and D. S. Gupta, *Carbohydrate Research* **1979**, *75*, 39-49.

[101] D. W. Norbeck, J. B. Kramer and P. A. Lartey, *The Journal of Organic Chemistry* **1987**, *52*, 2174-2179.

[102] Y. Qian, J. Feng, M. Parvez and C.-C. Ling, *The Journal of Organic Chemistry* **2012**, *77*, 96-107.

[103] Y. Feng, J. Dong, F. Xu, A. Liu, L. Wang, Q. Zhang and Y. Chai, *Org Lett* **2015**, *17*, 2388-2391.

[104] T. K. Pradhan, C. C. Lin and K.-K. T. Mong, *Organic Letters* **2014**, *16*, 1474-1477.

[105] J. Yadav, M. C. Chander and K. K. Reddy, *Tetrahedron Letters* **1992**, *33*, 135-138.

[106] A. Claesson, A. M. Jansson, B. G. Pring, S. M. Hammond and B. Ekstroem, *Journal of Medicinal Chemistry* **1987**, *30*, 2309-2313.

[107] D. C. Akwaboah, D. Wu and C. J. Forsyth, *Organic Letters* **2017**, *19*, 1180-1183.

[108] M. Martinková, K. Pomikalová, J. Gonda and M. Vilková, *Tetrahedron* **2013**, *69*, 8228-8244.

[109] A. Claesson, *The Journal of Organic Chemistry* **1987**, *52*, 4414-4416.

[110] G. J. P. H. Boons, P. A. M. van der Klein, G. A. van der Marel and J. H. van Boom, *Recueil des Travaux Chimiques des Pays-Bas* **1990**, *109*, 273-276.

[111] R. Winzar, J. Philips and M. Kiefel, *Synlett* **2010**, *2010*.

[112] Y. Yu, K.-S. Ko, C. J. Zea and N. L. Pohl, *Organic Letters* **2004**, *6*, 2031-2033.

[113] B. Muller, M. Blaukopf, A. Hofinger, A. Zamyatina, H. Brade and P. Kosma, *Synthesis (Stuttg)* **2010**, *2010*, 3143-3151.

[114] M. B. Hannes Mikula, Georg Sixta, Christian Stanetty, Paul Kosma, *Carbohydrate chemistry: Proven Synthetic Methods* **2014**, *2*, 207-211.

[115] M. Dumont, A. Lehner, B. Vauzeilles, J. Malassis, A. Marchant, K. Smyth, B. Linclau, A. Baron, J. Mas Pons and C. T. Anderson, *The Plant Journal* **2016**, *85*, 437-447.

[116] H. Adachi, K. Kondo, F. Kojima, Y. Umezawa, K. Ishino, K. Hotta and Y. Nishimura, *Nat Prod Res* **2006**, *20*, 361-370.

[117] F. M. Unger, D. Stix and G. Schulz, *Carbohydrate Research* **1980**, *80*, 191-195.

[118] S.-I. Nakamoto and K. Achiwa, *CHEMICAL & PHARMACEUTICAL BULLETIN* **1987**, *35*, 4537-4543.

[119] I. A. Smellie, S. Bhakta, E. Sim and A. J. Fairbanks, *Organic & Biomolecular Chemistry* **2007**, *5*, 2257-2266.